Transfert de polluants inorganiques dans un technosol de brûlage d'armes organo-arséniées soumis à un apport de matière organique et à des cycles de saturation/désaturation : expérimentation en mésocosme

Hugues Thouin

▶ **To cite this version:**

Hugues Thouin. Transfert de polluants inorganiques dans un technosol de brûlage d'armes organo-arséniées soumis à un apport de matière organique et à des cycles de saturation/désaturation : expérimentation en mésocosme. Sciences de la Terre. Université d'Orléans, 2016. Français. NNT : 2016ORLE2069 . tel-01581323

HAL Id: tel-01581323
https://theses.hal.science/tel-01581323

Submitted on 4 Sep 2017

HAL is a multi-disciplinary open access archive for the deposit and dissemination of scientific research documents, whether they are published or not. The documents may come from teaching and research institutions in France or abroad, or from public or private research centers.

L'archive ouverte pluridisciplinaire **HAL**, est destinée au dépôt et à la diffusion de documents scientifiques de niveau recherche, publiés ou non, émanant des établissements d'enseignement et de recherche français ou étrangers, des laboratoires publics ou privés.

UNIVERSITÉ D'ORLÉANS

ÉCOLE DOCTORALE
ENERGIE, MATERIAUX, SCIENCES DE LA TERRE ET DE L'UNIVERS

Institut des Sciences de la Terre d'Orléans

THÈSE présentée par : **Hugues THOUIN**

Soutenue le : **15 décembre 2016**

pour obtenir le grade de : **Docteur de l'université d'Orléans**

Discipline/ Spécialité : Science de la Terre et de l'Univers

Transfert de polluants inorganiques dans un technosol de brûlage d'armes organo-arséniées soumis à un apport de matière organique et à des cycles de saturation/désaturation : Expérimentation en mésocosme

THÈSE dirigée par :

Fabienne BATTAGLIA-BRUNET	Chercheur, BRGM Orléans
Pascale GAUTRET	CR CNRS, ISTO Orléans

RAPPORTEURS :

Mélanie DAVRANCHE	Professeur, Université de Rennes
Jerome ROSE	DR CNRS, CEREGE Aix-en-Provence

JURY :

Mikael MOTELICA-HEINO	Professeur, Université d'Orléans, Président du jury
Mélanie DAVRANCHE	Professeur, Université de Rennes
Jerome ROSE	DR CNRS, CEREGE Aix-en-Provence
Georges ONA NGUEMA	Maître de conférences, UPMC Paris
Patrick BILLARD	Maître de conférences, Université de Lorraine
Fabienne BATTAGLIA-BRUNET	Chercheur, BRGM Orléans
Fatima LAGGOUN-DEFARGE	DR CNRS, ISTO Orléans
Lydie LE FORESTIER	Maître de conférences, Université d'Orléans

UNIVERSITÉ D'ORLÉANS

ÉCOLE DOCTORALE
ENERGIE, MATERIAUX, SCIENCES DE LA TERRE ET DE L'UNIVERS

Institut des Sciences de la Terre d'Orléans

THÈSE présentée par : **Hugues THOUIN**

Soutenue le : **15 décembre 2016**

pour obtenir le grade de : **Docteur de l'université d'Orléans**

Discipline/ Spécialité : Science de la Terre et de l'Univers

Transfert de polluants inorganiques dans un technosol de brûlage d'armes organo-arséniées soumis à un apport de matière organique et à des cycles de saturation/désaturation : Expérimentation en mésocosme

THÈSE dirigée par :

Fabienne BATTAGLIA-BRUNET	Chercheur, BRGM Orléans
Pascale GAUTRET	CR CNRS, ISTO Orléans

Co-encadrée par :

Lydie LE FORESTIER	Maître de conférences, Université d'Orléans
Sébastien DUPRAZ	Chercheur, BRGM Orléans

Remerciements

Ces travaux, effectués ces trois dernières années entre le Bureau de Recherche Géologique et Minière (BRGM) et l'Institut des Sciences de la Terre d'Orléans (ISTO), ont été l'occasion de faire la connaissance de nombreuses personnes. La liste est longue des personnes associées à cette tranche de vie et il sera difficile de n'oublier personne…

En premier lieu je souhaite remercier les membres du jury qui ont accepté d'évaluer ces travaux. Merci aux rapporteurs, Mélanie Davranche, Professeur à l'université de Rennes et Jerome Rose, Directeur de recherche CNRS au CEREGE à Aix-en-Provence. Je remercie également Georges Ona Nguema, Maître de conférences à l'IMPMC, Patrick Billard, Maître de conférences à l'université de Lorraine, et Mickaël Motellica, Professeur à l'université d'Orléans, d'avoir accepté d'examiner cette thèse.

Je remercie, le BRGM et la Région Centre-Val de Loire pour avoir co-financé cette thèse. Je remercie également le Labex VOLTAIRE qui a contribué à ces travaux.

Bien évidemment, je remercie amplement Fabienne Battaglia-Brunet qui a merveilleusement bien dirigé ces travaux. Ses qualités scientifiques et humaines m'ont parfaitement accompagné pendant ces trois années. Merci pour tout.

Je remercie également Pascale Gautret qui m'encadre maintenant depuis 5 ans, de m'avoir supporté si longtemps. Promis c'est bientôt fini ! Merci pour ce temps passé.

Je tiens aussi à exprimer ma gratitude à Lydie Le Forestier qui m'a apporté son aide dès les premiers instants de cette thèse et à Sébastien Dupraz pour m'avoir fait confiance quand il a fallu mettre en place le LABBIO et pour m'avoir toujours poussé à aller plus loin.

Par la même occasion je remercie Francis Garrido, prédécesseur de Sébastien au poste de responsable de l'unité Bio-géochimie environnementale et qualité de l'eau du BRGM, pour l'attention particulière qu'il a donné au bon déroulement de cette thèse. Merci à Fabienne Poiriez de m'avoir supporté, malgré tous les ennuis que je lui ai procurés. De manière générale je remercie l'ensemble des membres de l'unité BGE, et en particulier Catherine Joulian qui m'a formé à la biologie moléculaire, domaine qui m'était inconnu et que j'ai pu appréhender pendant ces travaux.

Je remercie Marie-Paule Norini, qui a collaboré à ces travaux pendant cette dernière année et qui a complètement pris en charge les expériences en cours pour que je puisse rédiger ce manuscrit dans les temps. Il nous reste du boulot pour publier ça.

Je remercie également les membres de l'unité LAB/EXP qui ont tous, à un moment, été associés à ces travaux et qui m'ont réservé un accueil chaleureux. J'ai passé de bons moments à tous vous côtoyer au café ou au self. Un merci particulier à tous ceux qui ont contribué au montage de la plateforme LABBIO, à la mise en place et au bon déroulement de l'expérience en colonne. Je remercie ainsi Pierre Galle, pour son expertise et sa bonne humeur, Mickaël Beaulieu pour le prélèvement et le transport du sol d'étude, et Mohamed Djemil qui a assuré l'intérim lorsque je ne pouvais pas effectuer le suivi de l'expérience. Je remercie également Dominique Breeze qui a analysé pendant un an, toujours dans la joie et

la bonne humeur, la multitude d'échantillons que je lui fournissais. Merci, à Mickaël Charron qui a également apporté son aide au fonctionnement de la plateforme et qui m'a formé aux bonnes pratiques de la BioMol, pas toujours évidentes à acquérir pour un géologue de formation. Je n'oublie pas non plus Noémie, Cindy et Hafida, trois belles personnes qui se sont succédées pour donner de la vie au laboratoire de microbiologie.

Je remercie Daniel Hube pour avoir facilité la greffe de ces travaux au diagnostic environnemental du site de La Place-à-Gaz réalisé par le BRGM et commandité par la Préfecture de la Meuse. Ces connaissances scientifiques et historiques sur l'impact environnemental de la Première Guerre Mondiale sont passionnantes.

Je remercie tous les membres de l'ISTO qui ont contribué à ces travaux. Particulièrement Claude Le Milbeau, qui a dû subir mon squattage de bureau trois ans de plus. Mais également Philippe Penhoud, Marielle Hatton, Rachel Boscardin et Nathalie Lottier qui m'ont permis d'avoir de beaux résultats.

Merci à Camille Jongy, qui dans le cadre de son stage, m'a été d'une aide importante pendant les premiers mois de l'expérience en mésocosme.

Merci à Adeline, mon ancienne co-bureau au BRGM, qui m'a montré comment réussir sa thèse ! La plante est sauvée, elle s'est même fait des copines. Egalement merci à tous les stagiaires qui se sont succédés dans le bureau.

Merci à tous les copains, copines, qui ont rendu ces années orléanaises mémorables. Merci d'abord aux VV : Valou, Le Nain, qui formeront le dernier maillon de la diaspora grenobloise. Aussi à La Praline et Maxou pour cette amitié qui est née. Bon courage à vous quatre pour la fin de thèse. Et sinon pêle-mêle, Sarah et Thomas (et leur chienne, et Hugo !) pour les nombreux V&B partagés, Armel et Eloïse pour les « porchouis », Nolwenn la (Grande) Bretonne, Adoum, Kévin, Chloé, Anaëlle et j'en oublie… Un grand merci à mon Groboul pour les escapades à Llandudno.

Je pense également aux membres des sections Handball, Ultimate et Volley-Ball du BRGM, avec qui j'ai pu me défouler et rire. Un merci particulier au couple de dingues, qu'on ira bientôt voir en Nouvelle-Calédonie, et à Alex (le hipster) et Emeline (la maman).

Merci à ma famille et particulièrement à mes parents qui m'ont donné la chance de faire ces longues études. Mes sœurs, Marie qui m'a de nombreuses fois nourri (avec du Saint-Nectaire de préférence) lors de mes passages par Saint-Pierre-des-Corps et Valentine que je pourrais enfin aller voir à Marseille. En tout cas, cette fois au niveau des études, on peut dire que j'ai gagné !

Enfin, je n'oublie bien évidemment pas (cette fois) Joana. Pour ces 6 merveilleuses années passées ensemble. Les parenthèses bordelaises ont été de parfaites échappatoires mais j'espère qu'on ne sera plus séparé aussi longtemps. Le meilleur est à venir, enfin une fois que tu auras aussi rendu ta thèse!

Bonne lecture.

Table des matières

Introduction générale

Les sols naturels sont des matériaux essentiels à la vie, structurellement poreux et biologiquement actifs, qui sont formés et continuent de se développer via des processus d'altération liés aux facteurs biogéochimiques, climatiques, géologiques, topologiques et chronologiques. A l'interface entre l'atmosphère, la biosphère, l'hydrosphère et la lithosphère, le sol est le lieu de nombreux processus physiques, chimiques et biologiques impactant profondément la durabilité des écosystèmes. L'équilibre entre ces processus peut être affecté par d'importantes concentrations en contaminants inorganiques liées à des activités anthropiques, telles que les activités industrielles, minières ou encore les pratiques agricoles. Les technosols souvent trouvés sur les lieux d'anciennes activités industrielles, minières et métallurgiques, peuvent être composés de déchets inorganiques, de stériles miniers, ou encore de résidus de traitements industriels, et sont généralement appauvris en matière organique (MO). Les contaminants inorganiques toxiques communément trouvés sur ces sites comprennent les métaux et métalloïdes suivants : As, Cd, Cu, Hg, Pb, Sb, Cr. Les microorganismes présents dans ces sols peuvent affecter la mobilité et la toxicité des polluants inorganiques en modifiant leur spéciation. Ils sont également capables d'affecter indirectement leur comportement, en modifiant les paramètres physico-chimiques de leur environnement aqueux et la nature des phases solides. La présence de contaminants inorganiques peut affecter la qualité du sol, conduisant dans certains cas à la perte de certaines de ses fonctions, dont celle d'être un support à la biodiversité et l'implantation d'espèces végétales. Les contaminants présents dans les sols peuvent aussi représenter une source de pollution pour les eaux souterraines et de surface.

Des amendements de matière organique sont maintenant régulièrement utilisés pour restituer aux sols pollués leurs propriétés physico-chimiques ainsi que leurs fonctions biologiques et, *in fine*, permettre leur revégétalisation (Park *et al*., 2011). Ces travaux s'inscrivent dans l'étude des mécanismes de mobilisation/immobilisation des contaminants inorganiques dans le sol en relation avec l'évolution biogéochimique et la maturation de la matière organique, au cours de la restauration des fonctions du sol et de la colonisation par les plantes. L'objectif de la présente thèse est de caractériser, (du mésocosme au site) les mécanismes de transfert de polluants des sols vers les eaux souterraines, à travers le couplage des cycles biogéochimiques du carbone et des polluants inorganiques dans un sol pollué. Afin d'atteindre cet objectif, il était nécessaire d'évaluer l'évolution biogéochimique d'un sol pollué par un cocktail de

substances inorganiques aux comportements chimiques distincts (métaux divalents comme Cd et Pb, oxy-anions tels que Cr et As), suite à un apport MO naturelle, dans des conditions d'oxydo-réduction imposées et variables.

Le site de la Place-à-Gaz, où ont été détruites des munitions chimiques de la Première Guerre Mondiale contenant de l'arsenic, a été sélectionné comme site d'étude. En effet, il répond aux trois critères (i) une contamination inorganique pluri-élémentaire avec des métaux divalents et des métalloïdes sous formes d'oxyanions comme l'As ; (ii) un sol pauvre en MO intrinsèque ; (iii) un sol nu, non végétalisé, permettant d'étudier la refonctionnalisation d'un sol contaminé. Au niveau de ce site, le sol présente une contamination très importante en As, Zn, Cu et Pb sur une zone d'environ 2000 m^2 (Bausinger *et al.*, 2007). Situé en forêt domaniale de Spincourt, à 20 km au nord-est de Verdun (Meuse), ce site est en partie dénudé et la biodiversité de la flore environnante se résume à trois espèces. Son sol pollué est riche en MO, dont l'origine est liée à la présence de charbons de bois formés pendant la destruction des armes chimiques.

Afin d'atteindre les objectifs du projet de thèse, le programme de travail a été organisé en plusieurs phases jointes à des observations de terrains, des expériences en laboratoire, et un suivi en mésocosme utilisant la plateforme expérimentale LABBIO, mise au point dans le cadre de ces travaux. Ces phases successives étaient les suivantes :

- La caractérisation biogéochimique complète de l'héritage complexe, et encore très peu étudié, de la destruction de ces munitions, au niveau du sol.
- Le suivi biogéochimique du transfert des contaminants et de leur spéciation, considérant les phases solides et dissoutes, dans une colonne de sol soumise à des cycles sec/humide, artificiellement créés en laboratoire à l'échelle du mésocosme et à un apport de MO biodisponible.
- L'évaluation de l'influence des interactions sol-matière organique-microorganismes et le suivi de l'effet des activités microbiennes sur le comportement des contaminants inorganiques.

Pour cela, une approche multi-analytique a été mise en place afin d'étudier le comportement des contaminants, de caractériser la MO et de suivre l'évolution du compartiment microbien dans ce sol.

Ce manuscrit s'organise en quatre chapitres et une partie présentant les conclusions générales et les perspectives de ces travaux.

Le **premier chapitre** décrit l'état de l'art concernant les processus biogéochimiques affectant la mobilité des contaminants inorganiques dans les sols. L'effet de la saturation des sols et de la matière organique est développé de façon plus étendue. Le comportement spécifique des contaminants étudiés pendant ces travaux, *i.e*. As, Zn, Cu et Pb, est également décrit dans ce chapitre. Enfin, il détaille la problématique des pollutions liées aux activités de destruction d'armes de la Première Guerre Mondiale.

Le **second chapitre** détaille la caractérisation du site de la Place-à-Gaz. Dans un premier temps, il présente les observations de terrain effectuées pendant les trois campagnes de prélèvements. Ensuite, la partie principale de ce chapitre décrit la caractérisation et la mobilité de l'arsenic et des autres métaux dans plusieurs échantillons de sol issus de ce site. Ces résultats ont été publiés dans *Science of the Total Environment* 550 (2016).

Le **troisième chapitre** présente les données géochimiques obtenues au cours de la réalisation d'une expérience en mésocosme, pendant laquelle le sol de la Place-a-Gaz a été soumis à des alternances de périodes sèches et humides, ainsi qu'à l'apport de MO biodisponible. Cette expérience avait pour but de comprendre l'impact de ces changements de conditions environnementales, par ailleurs observés sur le site, sur les processus biogéochimiques affectant la mobilité des métaux et de l'arsenic. L'évolution des compartiments eau et gaz au cours de cette expérience est présentée sous la forme d'un article soumis au journal *Science of the Total Environment*. Le chapitre est précédé d'une description de la plateforme expérimentale, appelée LABBIO, développée et mise en œuvre dans le cadre de ces travaux.

Le **quatrième chapitre** expose les résultats de l'étude des solides prélevés au cours de l'expérience en mésocosme. L'évolution du cortège minéralogique et les paramètres microbiens liés à la spéciation de l'As sont étudiés dans cette partie.

La dernière partie de ce manuscrit présente les **conclusions générales et perspectives** de ces travaux tant au niveau du site de la Place-à-Gaz que des autres sites riches en métaux et métalloïdes, contaminés par des opérations de destructions d'armes chimiques ou par d'autres activités anthropiques.

Chapitre I : Etude bibliographique

Fabienne Loodts@Paysagesenbataille.be

Introduction au chapitre I

Cette étude bibliographique a pour but de faire le point sur l'état des connaissances scientifiques actuelles concernant les processus biogéochimiques affectant la mobilité des métaux et métalloïdes dans les sols pollués et la problématique de la pollution issue de la destruction d'armes chimiques de la Première Guerre Mondiale. La première section de ce chapitre est consacrée aux éléments traces métalliques dans les sols, leur origine et leur localisation, et aux processus physico-chimiques pouvant modifier leur mobilité. L'effet de la saturation des sols et de la matière organique sur le comportement des contaminants inorganiques et leur interaction avec l'activité microbienne sont développés. La deuxième section est focalisée sur les différents contaminants inorganiques étudiés dans ce manuscrit : As, Zn, Cu et Pb. Des généralités sur les propriétés physico-chimiques, la spéciation et l'influence des bactéries sur la mobilité de chacun de ces éléments spécifiques y sont développées. Dans la troisième section, l'impact environnemental de la Première Guerre Mondiale est présenté. Les sources de pollutions, liées à la composition des armes et aux méthodes de destructions sont exposées. Une présentation du site de la Place-à-Gaz, où ont été détruits 200,000 obus chimiques contenant des agents organo-arséniés, choisi comme cas d'étude dans le cadre de la présente thèse, termine cette partie.

1. Processus affectant la mobilité des contaminants inorganiques dans les sols

1.1. Sources des métaux et métalloïdes dans les sols

Les métaux non ferreux et métalloïdes sont présents dans tous les compartiments du sol et plus globalement de l'environnement en quantité généralement très faible. Leur concentration étant généralement inférieure à 0.1 %, ils sont communément appelés éléments traces. Les éléments traces représentent 0.6 % de la masse totale de la croûte terrestre tandis que les éléments majeurs la constituent à 99.4 % en masse (Baize, 1997). Lorsque les éléments traces sont des métaux ou des métalloïdes (par exemple, As, Cd, Cu, Ni, Pb, Zn), ils sont appelés éléments traces métalliques (ETM).

Les ETM sont naturellement présents dans les sols. Ils sont alors issus de l'altération de minéraux primaires ou secondaires présents dans la roche mère (roches magmatiques, métamorphiques ou sédimentaires). Ces concentrations des ETM dans le sol, homogènes à l'échelle de la région, correspondent au fond géochimique naturel. Ce fond géochimique est globalement plus important pour les ETM dans les régions géologiques où le socle affleure, en raison de la plus grande quantité de métaux et métalloïdes dans les roches magmatiques et métamorphiques.

L'origine des ETM dans les sols peut également être anthropique. Les sources anthropiques des contaminations en ETM dans les sols peuvent être divisées en plusieurs catégories :

- Les activités minières : l'exploration, l'extraction et le traitement des minerais produisent de nombreux déchets (stériles, drainage minier acide, émissions de poussières) pouvant contenir des concentrations en ETM localement très importantes. L'exploitation de mines métallifères date de la révolution industrielle du début du 20ème siècle. Les méthodes de gestion des déchets miniers, non respectueuses de l'environnement à cette époque, ont impacté durablement la qualité des sols à proximité des mines.
- Les activités industrielles : de nombreuses industries (métallurgique, plasturgique, phytosanitaire…) produisent des déchets et/ou des fumées riches en ETM. Ces activités induisent des pollutions généralement localisées.

- L'agriculture : l'activité agricole entraîne des pollutions diffuses par épandages d'engrais chimiques et naturels et de produits phytosanitaires pouvant contenir des ETM.
- Friches industrielles et dépôts de déchets : les usines abandonnées, les décharges sauvages ou encore le stockage de produits dangereux peuvent être source de pollution chronique en métaux et métalloïdes.

En France, les contaminants inorganiques les plus fréquemment mis en évidence sur les sites pollués répertoriés dans la base de données BASOL sont les suivants : Pb (7.90 % des sites), Cr (6.04 %), Cu (5.85 %), As (5.70 %), Zn (4.49 %), Ni (4.29 %), Cd (2.70 %), Hg (2.36 %) et Ba (1.11 %)[(1)]. L'accumulation des ETM dans la pédosphère est d'autant plus préoccupante que, contrairement aux polluants organiques, les polluants inorganiques ne sont pas dégradables. Ce caractère persistant des ETM implique d'avoir une bonne connaissance des processus affectant leur comportement dans le sol, afin de pouvoir prédire leur mobilité et leur transfert vers d'autres compartiments.

1.2. Localisation des ETM dans les sols et processus affectant leur mobilité

1.2.1. Localisation des ETM

Les ETM peuvent se trouver associés à différents compartiments du sol (Fig.1.1). Ils peuvent être :

- inclus dans le réseau cristallin de minéraux primaires, hérités de la roche mère, ou de minéraux secondaires, issus de l'altération ou de la re-précipitation de constituants de la roche mère,
- adsorbés sur des oxydes / hydroxydes de fer et de manganèse, sur des carbonates ou encore des minéraux argileux,
- complexés à des molécules organiques,
- incorporés dans la pédofaune, la pédoflore et les microorganismes,
- sous une forme échangeable (cations ou anions), associés aux surfaces des minéraux argileux et aux matières organiques,
- sous forme soluble, colloïdale ou particulaire, dans la solution du sol.

[1] http://basol.developpement-durable.gouv.fr/tableaux/home.htm

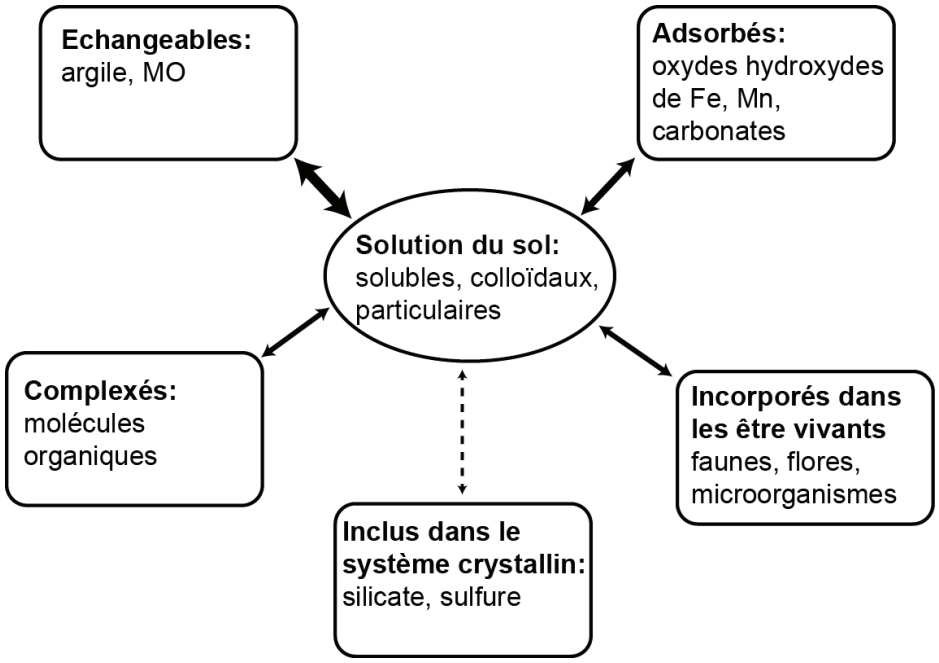

Figure 1.1 : *Spéciation et localisation des ETM dans les sols (d'après Baize, 1997).*

La forme chimique des métaux et métalloïdes, leur éventuel transfert d'un compartiment à un autre et leur transport potentiel dans les sols sont régis par les processus de précipitation/dissolution, d'adsorption/désorption, de complexation et de méthylation.

1.2.2. Processus affectant la mobilité des ETM

- **Contrôles par adsorption/désorption**

L'adsorption et la désorption des contaminants inorganiques à la surface de minéraux (oxydes/hydroxydes de Fe et Mn, carbonates, minéraux argileux) ou de composés organiques solides sont des processus ayant un contrôle important sur la mobilité des métaux dans les sols (Bradl, 2004). Ces processus sont principalement affectés par le pH qui va directement impacter la charge électrique des surfaces. Aux pH basiques, les sites de surface sont chargés négativement, et favorisent l'adsorption des cations, tandis qu'aux pH acides, les sites de surface sont chargés positivement et favorisent l'adsorption des anions. Pour les argiles, la charge électrique de surface peut également être impactée par des substitutions isomorphiques des ions Al^{3+} par des cations divalents ou des ions Si^{4+} par des ions trivalents. Ces substitutions résultent d'une charge de surface négative permanente, indépendamment du pH de la solution (Sposito *et al.*, 1999). La quantité de cations adsorbables est corrélée à la densité des sites de substitution ainsi qu'à la surface spécifique du matériau. Les ETM peuvent également être adsorbés ou inclus dans des nanoparticules et donc être mobiles

(Auffan, *et al*., 2009). Les nanoparticules sont des particules solides dont la taille varie de 1 nm à 100 nm. Le déplacement de solutions colloïdales par les pores du sol peut ainsi permettre à des éléments normalement insolubles d'être mobiles.

L'adsorption peut être physique ou chimique (Manceau *et al*., 2002, Andrieu et Muller, 2012). L'adsorption physique (physisorption) fait appel à des interactions électrostatiques de Van der Waals (Fig.1.2) entre les ions en solution et leur cortège de molécules d'eau et les charges de surface. Elle ne permet pas de décrire l'effet du pH. L'adsorption chimique (chimisorption) est caractérisée par une liaison chimique entre le cation et la surface de l'adsorbant après la perte du cortège de molécules d'eau (Fig.1.2). Ces liaisons, pouvant être covalentes, ioniques ou métalliques, sont fortes et peuvent jouer un rôle important sur la mobilité des métaux dans les sols.

- **Equilibre de précipitation/dissolution**

Lorsque les concentrations en ETM dans la phase aqueuse sont faibles, l'équilibre d'adsorption/désorption contrôle leur mobilité mais lorsque celles-ci sont supérieures à la limite de solubilité (Ks), les processus de précipitation/dissolution peuvent intervenir. La mobilité des contaminants peut être réduite par différent processus : i) la précipitation de phase minérale, lorsque les concentrations en solution induisent une sur-saturation, ii) l'inclusion du contaminant dans le système cristallin d'un minéral en remplacement d'un ion de charge et de taille similaire, iii) l'occlusion des contaminants dans une poche pendant la précipitation d'un minéral (Fig.1.2 ; Manceau *et al*., 2002). L'indice de saturation pour la majorité des minéraux est directement lié au pH et au potentiel d'oxydo-réduction.

Les minéraux qui jouent un rôle important sur la mobilité des contaminants, tels que les oxydes de fer et de manganèse, les oxy-hydroxydes de fer, les carbonates ou les sulfates, sont directement impactés par des processus de dissolution/précipitation lorsque les conditions environnementales changent. Par exemple, lorsque le milieu subit une oxydation, les sulfures porteurs potentiels de métaux (Fe, Pb, Zn, As) deviendront instables et leur dissolution va mobiliser des cations métalliques (Fe^{2+}, Fe^{3+}, Pb^{2+}, Zn^{2+}, As^{3+}). Les conditions oxydantes vont néanmoins favoriser la précipitation d'oxy-hydroxydes de fer et les autres métaux vont alors pouvoir être adsorbés à leur surface. Les métaux sont ainsi rapidement mobilisés par dissolution de la phase porteuse puis fixés par adsorption sur un solide néoformé (Scott Altmann et Bourg, 1997). Cet exemple met en évidence le couplage entre les équilibres de précipitation/dissolution et d'adsorption/désorption.

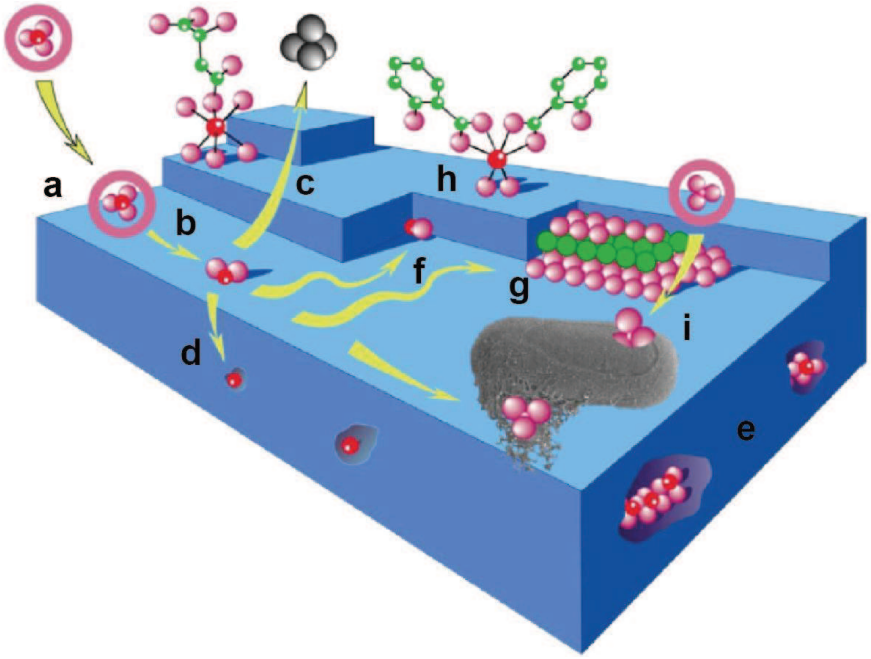

Figure 1.2 : *Processus affectant la mobilité des métaux et métalloïdes à l'interface eau-minéral. a) physisorption, b) chimisorption, c) désorption, d) inclusion, e) occlusion, f) fixation, g) nucléation, h) complexation organo-minérale, i) complexation à un biofilm. (Manceau et al., 2002).*

- **La complexation**

Un complexe est une espèce chimique dans laquelle un cation métallique est lié à un ou plusieurs anions ou molécules neutres, appelés ligands. Les ligands dans la solution des sols peuvent être des ions (hydroxyde, carbonate, sulfate) ou des molécules d'origines organiques (acide aminé, acide carboxylique ; Fig.1.2). Les complexes formés peuvent être solubles ou à l'inverse peuvent immobiliser les contaminants, soit par précipitation du complexe organique (agrégation, floculation), soit parce que le ligand est associé à une phase minérale (*e.g.* complexation sur un biofilm bactérie ; Fig.1.2). La présence de ligands dans la solution de sol peut créer une compétition avec les sites d'adsorption, en effet la présence de ligands entraîne un déplacement de l'équilibre d'adsorption/désorption en faveur de formes complexées du contaminant (Davis et Leckie, 1978).

1.2.3. Facteurs de contrôle de la mobilité des ETM

L'ensemble des processus décrits précédemment sont contrôlés par des facteurs physico-chimiques tel que le pH, le Eh ou la température.

- **Le pH**

Le pH est le facteur ayant le contrôle le plus important sur la mobilité et le comportement des ETM dans le sol. La modification du pH d'une solution va avoir un effet direct sur les ETM en modifiant l'équilibre de dissolution/précipitation. De plus, une acidification de la solution va augmenter la protonation des sites d'adsorption et ainsi favoriser la désorption des cations métalliques. A l'inverse, pour les ETM sous forme anionique comme pour l'arsenic, l'augmentation du pH (dans une zone de pH proche de la neutralité) va réduire leur solubilité. La modification du pH peut également induire une déstabilisation de minéraux porteurs de métaux (*e.g*. les carbonates) et ainsi libérer en solution les ETM qui leur sont associés.

- **Le potentiel d'oxydo-réduction**

Les conditions d'oxydo-réduction représentent le second facteur régissant le comportement des métaux et des métalloïdes dans les sols. Le potentiel redox (Eh) mesure l'aptitude du milieu à fournir des électrons à un agent oxydant ou à retirer des électrons à un agent réducteur. Il impacte donc directement la spéciation des éléments chimiques à plusieurs degrés de valence. Dans les sols, de nombreux éléments, tels que C, O, N, S, Mn ou Fe, sont affectés par des changements redox, mais de nombreux métaux et métalloïdes le sont aussi. L'As par exemple est affecté par les conditions d'oxydo-réduction, et cela affecte directement sa mobilité car l'As (III) est plus mobile que l'As (V). Les conditions d'oxydo-réduction peuvent également avoir un effet indirect sur la mobilité des métaux en provoquant des phénomènes de précipitation/dissolution de phases porteuses de métaux comme les oxy-hydroxydes de fer stables en milieu oxydant ou les sulfures stables en milieu réducteur. La solubilité des métaux et métalloïdes est donc directement corrélée avec le pH et le Eh. Le tableau 1.1 résume l'effet du pH et de Eh sur la mobilité des ETM.

Tableau 1.1 : *Effet du pH et du potentiel d'oxydo-réduction sur la mobilité des ETM du sol (d'après Förstner, 1985)*

Mobilité relative	**pH**		**Potentiel d'oxydo-réduction**	
	Neutre-alcalin	Acide	Oxydant	Réducteur
Haute	As, Se, Mo	Zn, Cd, Hg, Co, (Mn)	Se	-
Moyenne	Mn	Cu, Al, Pb, Cr	Cu, Hg, Zn, Cd	Mn
Basse	Pb, Fe, Zn, Cd	Fe III	Pb, Ti	Fe, Zn
Très basse	Al, Cr, Hg, Cu	Se, As	Al, Cr, Fe, Mn	Al, Cr, Hg, Cu, Se, Cd, Pb

- **La température**

La température du sol joue un rôle indirect sur la mobilité des métaux. En effet, elle peut influencer le pH en affectant la solubilité du CO_2 et des carbonates ou le potentiel d'oxydo-réduction en modifiant la solubilité de l'O_2. La température va également avoir un impact sur les cinétiques de réactions chimiques, mais également biologiques. Une augmentation de la température va favoriser la croissance et l'activité des microorganismes du sol et ainsi, accélérer les différents processus microbiologiques pouvant affecter la mobilité des métaux (modification d'états redox, production d'acide et de complexant organique, piégeage à la surface ou incorporation dans la cellule).

D'autres facteurs pouvant contrôler la mobilité des métaux tels que le niveau de saturation du sol ou la teneur en matière organique vont être développés ci-dessous.

1.3. Effet de la saturation du sol sur les processus d'oxydo-réduction

Le niveau de saturation du sol a un impact sur le comportement des métaux et métalloïdes dans les sols pollués en modifiant les conditions d'oxydo-réduction du milieu. Cette modification du milieu affecte le transport des gaz et particulièrement de l'oxygène, ainsi que des espèces en solution. Lorsque l'oxygène n'est pas présent, les métabolismes bactériens anaérobies vont affecter les couples redox permettant d'oxyder la matière organique du sol. Ces processus ainsi que l'effet de cycle de saturation/désaturation sur les ETM sont maintenant connus.

1.3.1. Diffusion et transport des gaz et solutés dans le sol.

L'humidité du sol, pendant les cycles épisodes secs/ épisodes humides, a un effet sur la diffusivité des gaz et des solutés. La diffusion, décrite par la loi de Fick, affecte le transport des gaz et des espèces solubles dans le sol. Lorsque la porosité est peu saturée (condition sèche), la diffusion des espèces solubles est moins importante en raison de la faible connectivité de l'eau porale. A l'inverse, la connectivité de pores non remplis par la solution du sol permettra une bonne diffusion des gaz. Comme ces changements se produisent simultanément, la diffusivité des gaz et celle des solutés ont un comportement complémentaire pendant le séchage et l'humidification du sol (Moldrup *et al*., 2001 ; Moyano *et al*., 2013).

L'oxygène du sol est le premier facteur contrôlant les conditions d'oxydo-réduction du milieu. La diffusion de l'O_2 dans le sol, contrôlée par l'humidité du sol mais également par la

structure du sol (taille des pores, connectivité des pores, distribution de la taille des particules), va avoir un impact direct sur les conditions redox du milieu. De plus, l'hétérogénéité de la structure du sol peut créer très localement des conditions redox très différentes du reste du milieu. Mais de manière générale, les concentrations en oxygène diminuent le long du profil de sol, en partie à cause de la baisse de la vitesse de diffusion mais également parce que l'oxygène est consommé. Dans la colonne de sol, les bactéries aérobies, les champignons ou la micro-faune consomment l'oxygène. L'effet combiné de la disponibilité de l'O_2 et des espèces solubles affecte la relation entre l'humidité du sol et l'activité bactérienne (Fig.1.3 ; Moyano *et al*., 2013).

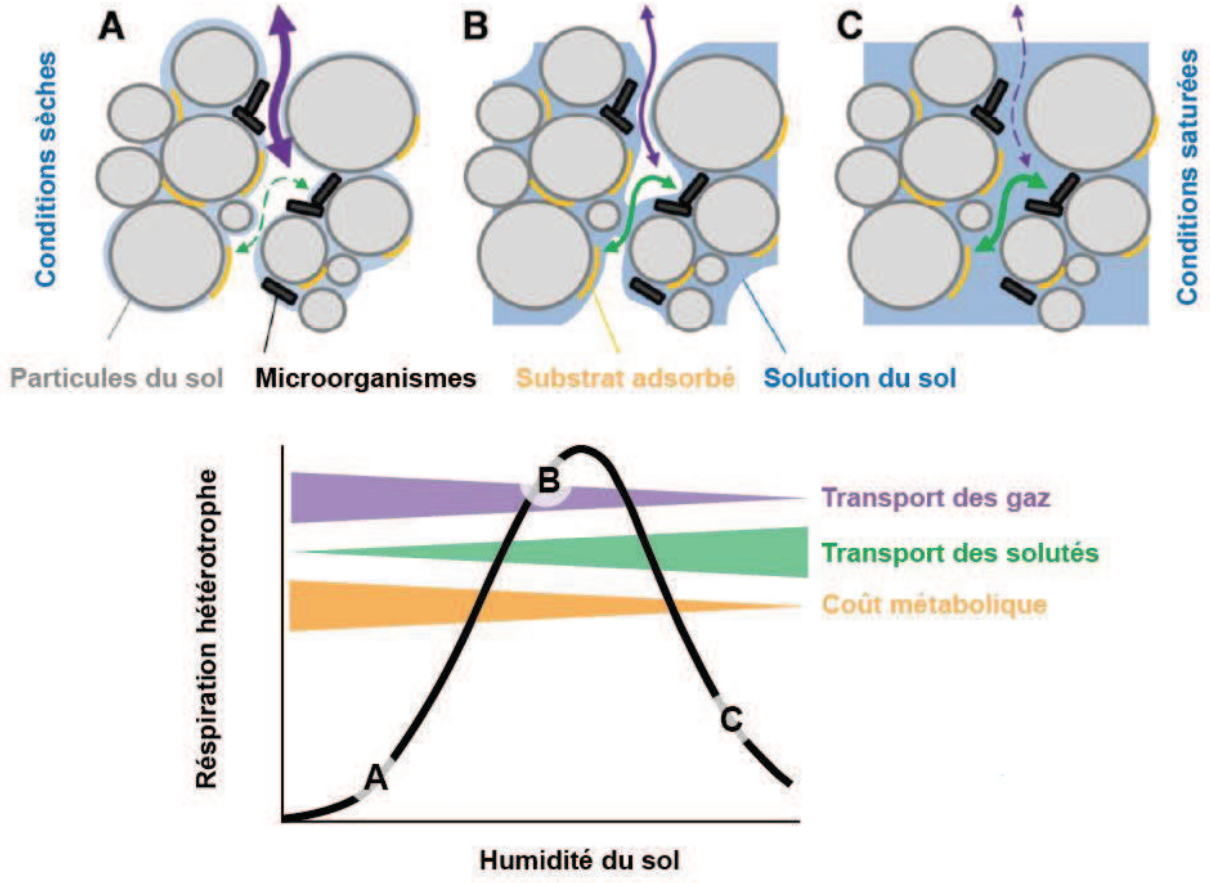

Figure 1.3 : *Illustration des effets de l'humidité du sol sur l'activité microbienne. La relation entre la respiration hétérotrophique et la disponibilité de l'eau dans les sols est le résultat de plusieurs processus (diffusion, biologique, écologique). Les effets agissent souvent dans des directions différentes ce qui induit un pic de respiration pour des valeurs intermédiaires d'humidité (d'après Moyano et al., 2013).*

1.3.2. Métabolismes microbiens anaérobies

En absence d'oxygène, la respiration anaérobie réalisée par des bactéries chimioorganotrophes, oxydant la matière organique en dioxyde de carbone pour utiliser divers autres accepteurs terminaux d'électrons, est un facteur de contrôle du potentiel d'oxydoréduction du milieu. Les microorganismes du sol ne sont pas contraints à sa zone oxique, de nombreuses espèces de bactéries, d'archées ou de champignons peuvent être présentes dans les zones suboxique et anoxique du sol. Les bactéries anaérobies facultatives ou anaérobies strictes sont capables de coupler l'oxydation la matière organique en dioxyde de carbone avec la réduction de molécules comme le nitrate, les oxydes de Mn et de Fe ou le sulfate pour tirer de l'énergie (Fig. 1.4). L'efficacité énergétique des couples redox, caractérisée par l'enthalpie libre de la réaction de réduction de l'accepteur terminal d'électrons, détermine l'ordre dans lequel ils peuvent être utilisés par une bactérie dans le cas idéal (Fig. 1.4). La respiration aérobie est le métabolisme bactérien le plus efficace et est donc privilégiée, tant que les concentrations en oxygène sont suffisamment importantes. Lorsque l'oxygène est absent ou en faible concentration, les bactéries utilisent des voies métaboliques alternatives, mieux adaptées aux conditions du milieu. Ainsi, des communautés bactériennes anaérobies vont pouvoir utiliser le nitrate ou le sulfate comme accepteurs d'électrons. La respiration aérobie, la dénitrification et les autres métabolismes énergétiques sont des processus qui peuvent consommer des protons. Il en résulterait alors une augmentation du pH et une diminution du potentiel d'oxydoréduction qui conduiraient à une évolution biogéochimique du milieu, suivant la séquence des réactions métaboliques présentée dans la figure 1.4.

Les bactéries sont également capables de catalyser les réactions d'oxydoréduction en utilisant des métaux et métalloïdes comme accepteurs terminaux d'électrons. Les bactéries chimiolithotrophes peuvent par exemple utiliser l'hydrogène moléculaire comme donneur d'électrons et coupler son oxydation avec la réduction de Fe(III) en Fe(II). Ce métabolisme respiratoire permet ainsi de modifier la spéciation du fer, mais également d'induire la solubilisation des oxydes et oxy-hydroxydes de fer. D'autres voies métaboliques permettent de modifier la spéciation de métaux et métalloïdes comme le chrome, l'arsenic, l'uranium, le sélénium, le molybdène,… (Tebo *et al*., 1998 ; Tucker *et al*., 1998). Prenons l'exemple de l'As. Certaines bactéries sont capables d'utiliser l'AsV comme accepteur terminal d'électron pour leur respiration anaérobie. Les bactéries qui réalisent la réduction dissimilatrice de l'As V produisent l'énergie nécessaire à leur croissance, en couplant la réduction de l'As V par le

système Arr à l'oxydation de composés organiques ou inorganiques (H_2 et H_2S). Ce mécanisme est d'une importance majeure d'un point de vue biogéochimique car il permet la réduction de l'As V associé à des phases solides et la libération d' As III dans les écosystèmes (Zobrist *et al*. 2000). Il est à noter que ce système, comme le système Ars (système de résistance à l'arsenic), permet aussi la réduction de l'As V soluble en condition anaérobie. La respiration de l'As V est une fonction bactérienne retrouvée dans des environnements variés : sédiments d'eaux douces (Ahmann *et al*. 1994), eaux de lacs salés (Blum *et al*. 2009), de points chauds (Gihring et Banfield 2001), de mines d'or (Macy *et al*. 1996). *Sulfurospirillum arsenophilum* MIT-13 est la première bactérie décrite pour sa capacité à réaliser ce processus (Ahmann *et al*. 1994). Ce type de respiration est maintenant connu chez plus de 20 bactéries incluant les genres *Desulfomaculum*, *Desulfitobacterium*, *Bacillus*, *Chrysiogenes*, *Shewanella*, *Wolinella*, *Thermus* et *Pyrobaculum*.

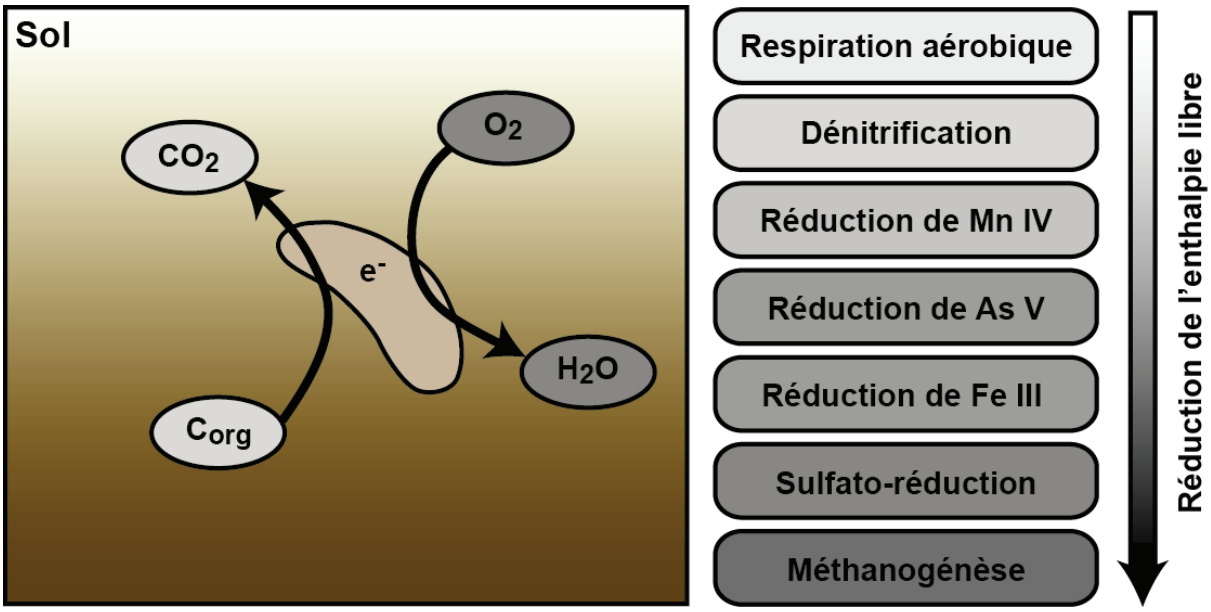

Figure 1.4 : *Métabolisme bactérien simplifié et ordre des réactions métaboliques utilisant successivement les accepteurs terminaux d'électrons les plus efficaces.*

Après l'épuisement de l'oxygène dans le sol, les modifications des conditions redox sont donc contrôlées par trois facteurs : la présence de communautés bactériennes anaérobies actives, la présence des accepteurs d'électrons appropriés et enfin, la présence de matière organique oxydable biodisponible. La modification de la concentration de l'un de ces facteurs, liée par exemple à des cycles secs et humides, peut conduire à des conditions redox oscillantes. L'effet de tels cycles sur le comportement du carbone et des métaux et métalloïdes va maintenant être discuté.

1.3.3. Le cas de cycles de saturation/désaturation

- **Effet sur le cycle du carbone**

De nombreux environnements sont affectés par des cycles de saturation et désaturation : plaines inondables, rizières, sol soumis à des fluctuations de la nappe phréatique ou à de fortes précipitations.

Ces environnements sont le lieu de processus affectant les cycles du carbone et de l'azote. De nombreuses études ont examiné l'effet de cycle sec et humide sur la production de carbone organique dissous (COD), la minéralisation du carbone ou sur l'activité des microorganismes dans différents environnements tels que des sols agricoles, des sols de forêts, des tourbières, ou des zones humides (Lundquist *et al*., 1999a ; Lundquist *et al*., 1999b ; Fierer et Schimel, 2002 ; Rey *et al*., 2005 ; Chow *et al*., 2006 ; Smith et Jacinthe, 2014).

L'effet des cycles sec/humide ne semble pas affecter directement le carbone organique dissous (COD). En effet, des effets antagonistes ont pu être observés dans différentes études. Lundquist *et al*. (1999a) montrent une augmentation de COD dans un sol agricole soumis à des cycles sec/humide, tandis que d'autres études ne montrent aucun effet (Chow *et al*., 2006) ou au contraire une diminution du COD après plusieurs cycles dans des conditions plus réductrices (Parsons *et al*., 2013 ; Fig.1.6). La minéralisation du carbone est plus clairement affectée par l'humidité du sol (Fierer et Schimel, 2002 ; Mikha *et al*., 2005 ; Chow *et al*., 2006) car, comme expliqué précédemment, cette humidité affecte directement le transport des gaz et des solutés nécessaires aux processus de respiration bactérienne (Fig.1.3). Néanmoins, Chow *et al*. (2006) observent des différences de vitesse de minéralisation du carbone en fonction de la profondeur du sol. A la surface du sol, les vitesses de minéralisation diminuent en fonction du nombre de périodes sèches et humides, tandis que dans le sol plus profond (< 3 m), la vitesse augmente avec les cycles sec/humide. Une diminution de la vitesse de minéralisation liée au nombre de cycles de ré-humidification du sol successifs a été observée dans d'autres études (Fierer et Schimel, 2002 ; Mikha *et al*., 2005 ; Fig.1.5). Ce phénomène peut être expliqué par une modification des communautés bactériennes subissant les cycles sec/humide (Lundquist *et al*., 1999b ; Fierer et Schimel, 2002 ; Fierer *et al*., 2003). Les microorganismes subissant ces cycles vont s'adapter. Par exemple, des bactéries anaérobies facultatives vont entrer en compétition avec les bactéries aérobies strictes et à termes, altérer la vitesse de minéralisation de la MO.

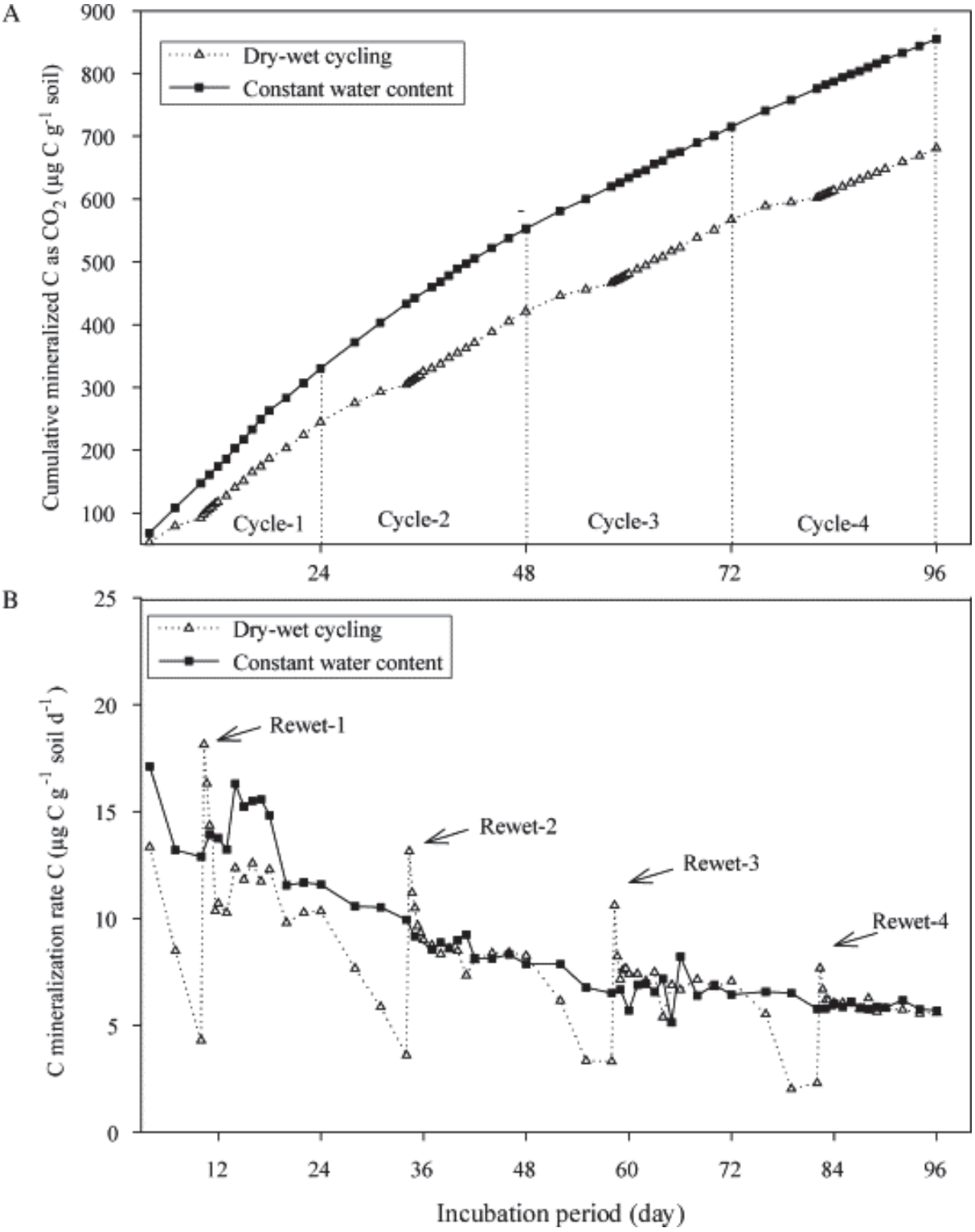

Figure 1.5 : *Minéralisation du carbone affecté par les cycles de séchage et de réhumidification du sol. A: Minéralisation cumulée du carbone. B : Vitesse de minéralisation. (d'après Mikha et al., 2005)*

- **Effet sur la mobilité des ETM**

Les cycles redox auxquels un sol pollué est soumis sont susceptibles de modifier la stabilité des ETM. Ils vont avoir un impact direct sur le potentiel d'oxydo-réduction et donc sur les processus biogéochimiques précédemment décrits. Par exemple, plusieurs auteurs observent que la saturation du sol augmente la mobilité de l'As par le biais de la dissolution des oxydes de fer et la réduction simultanée de l'As V en As III (Kumpiene *et al*., 2009 ; Weber *et al*., 2010 ; Parsons *et al*., 2013 ; Couture *et al*., 2015). Néanmoins, après plusieurs cycles, l'efficacité de ces processus peut être affectée et, ainsi, peut modifier le comportement à long terme des ETM. En effet, la répétition de périodes de saturation peut, par exemple, engendrer une dissolution progressive des oxydes de Mn et Fe et ainsi libérer les ETM qui leur étaient liés (Contin *et al*., 2007, Couture *et al*., 2015). La mobilité de l'arsenic peut également être affectée par l'effet cumulé de cycles redox (Parsons *et al*., 2013 ; Fig.1.6), avec une réduction de la mobilité de l'As observée par la formation progressive d'édifices minéraux plus stables.

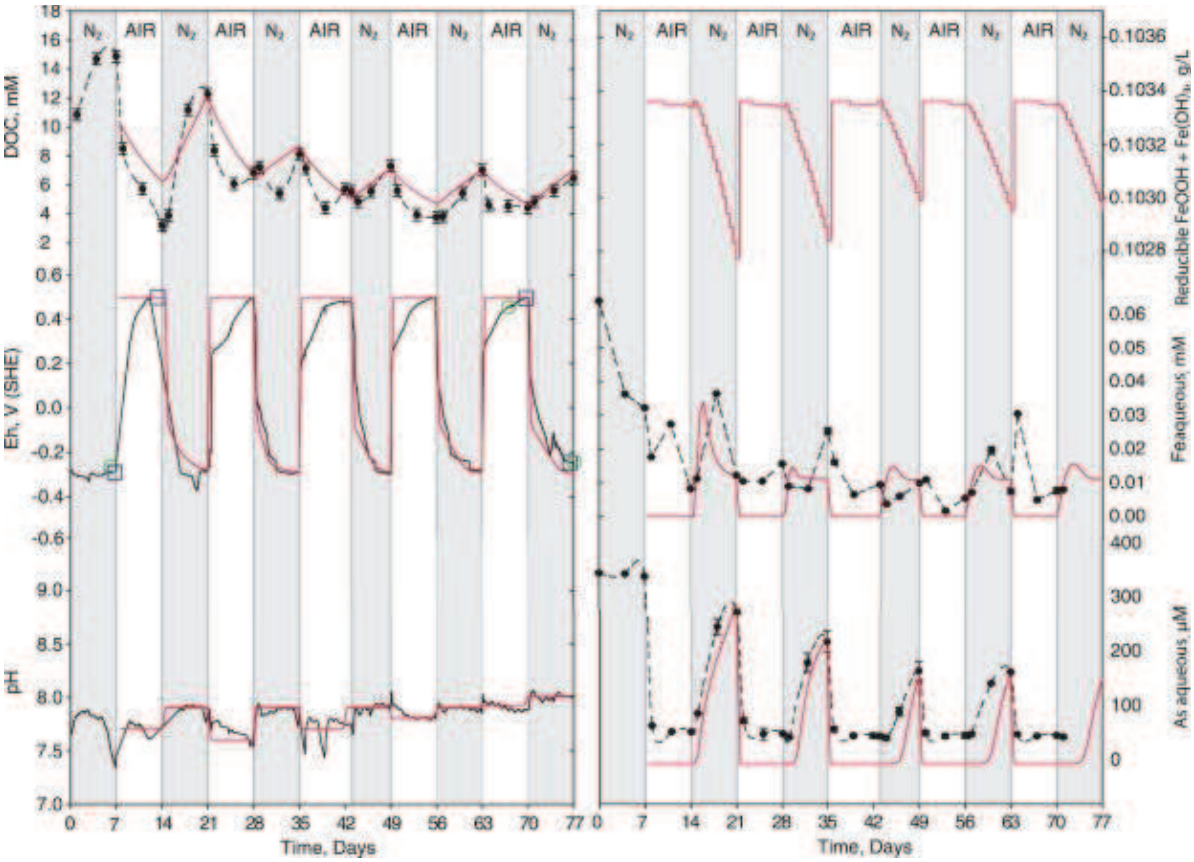

Figure 1.6 : *Impact de l'alternance de cycles redox sur différents paramètres chimiques (en noir : mesuré ; en rouge : modélisé). (d'après Parsons et al.,2013)*

Dans les sols saturés, la stabilité des ETM peut également être principalement contrôlée par la mobilité de la MO (Grybos *et al*., 2007).

1.4. Influence de la matière organique sur la mobilité des contaminants inorganiques dans le sol en relation avec l'activité bactérienne

1.4.1. La matière organique des sols

La matière organique naturelle des sols peut être définie comme l'ensemble des matières organiques vivantes et mortes d'origine végétale, animale ou microbienne. La composante vivante, qui comprend les racines, les macro-organismes et les microorganismes, peut représenter jusqu'à 4 % du carbone organique total (Shibu *et al*., 2006). La matière organique non-vivante peut représenter jusqu'à 98 % du carbone organique total. Elle est composée de matière organique non dégradée et de produits transformés.

La matière organique fraiche est principalement issue de débris végétaux (feuilles, racines), de restes et déjections d'animaux. Sa composition va orienter sa capacité à être biodégradée. Une matière organique riche en sucres, en acides aminés ou en protéines, avec un rapport C/N faible va favoriser la décomposition de la MO fraîche, tandis qu'une matière organique riche en lignine, cellulose avec un rapport C/N élevé sera moins biodégradable. Cette décomposition s'effectue par minéralisation des composés organique en composés inorganiques. La MO fraîche peut également subir un processus d'humification, transformant la MO fraîche en humus. L'humus contient des substances non humiques, comprenant des classes de composés organiques tels que les glucides, les lipides et les protéines. Les substances humiques sont formées par polymérisation et condensation des substances non humiques. Elles peuvent constituer 70 à 90% de la MO des sols (Griffith et Schnitzer, 1976) et sont divisées en trois groupes :

- Les acides fulviques, toujours solubles,
- Les acides humiques, solubles à pH alcalins,
- L'humine, rassemblant les composés les plus stables, insoluble à tous les pH.

Les molécules composant les substances humiques sont porteuses de groupements fonctionnels carboxyle, phénol, alcool, phénol, amine, thiol, etc… Les groupements carboxyliques et phénoliques présentent les proportions les plus importantes de ces sites actifs (Tsutsuki et Kuwatsuka, 1978). Ces groupes fonctionnels possèdent une forte polarité qui induit une forte affinité pour les ETM, ce qui peut affecter la mobilité de ces derniers.

1.4.2. Influence de la matière organique sur la mobilité des ETM

La matière organique du sol, de par sa surface spécifique importante et son nombre important de sites fonctionnels peut induire une bonne rétention des métaux et métalloïdes dans les sols. La déprotonation de ces groupes fonctionnels donne à la MO une charge globalement négative (Tipping, 1998). Les métaux sous forme cationique en solution sont naturellement adsorbés à la MO, cependant les métalloïdes comme l'As sont généralement sous forme d'oxyanions qui peuvent être neutres ou chargés négativement. D'autres mécanismes de complexation directs ou indirects ont été observés pour fixer ces éléments à la MO. L'As par exemple peut être complexé sur les groupements phénoliques, carboxyliques et thiols à la MO du sol (Buschmann *et al*., 2006 ; Catrouillet *et al*., 2015), ou former des complexes ternaires avec la MO par pont cationique du Fe (Hoffmann *et al*., 2013 ; Catrouillet *et al*., 2016).

Des amendements de MO peuvent être utilisés sur des sites pollués afin d'améliorer leur fertilité et aider la végétalisation (Schwab *et al*., 2007 ; Park *et al*., 2011). De par son pouvoir de complexation, la MO peut être utilisée comme amendement pour contribuer à la bioremédiation des sols contaminés par des métaux et métalloïdes. Park *et al*. (2011) dressent une liste des amendements organiques (compost, fumier, boue d'épuration,…) permettant une immobilisation des métaux et métalloïdes dans le sol. Par exemple, Farrell et Jones (2010) testent plusieurs amendements organiques qui ont tous pour effet de diminuer la présence en solution de Cu, Pb, Zn et As. Hattab *et al*, 2015 ont montré que des amendements de MO fraîche étaient plus efficaces pour réduire la mobilité des ETM que des amendements de MO plus matures.

L'un des problèmes lié à cette technique de bioremédiation des sols est la stabilité sur le long terme des complexes formés, car au fil du temps, la MO va être décomposée. Il a été mentionné à plusieurs reprises dans la littérature que lors de la dégradation de la MO, des contaminants inorganiques immobilisés sont remobilisés vers d'autres compartiments de l'environnement (McBride, 2003 ; Egli *et al*., 2010). Afin de réduire ce risque, le compostage peut être utilisé. Il permet de réduire les proportions de fractions facilement dégradables, telles que les glucides et les protéines, et d'augmenter l'humification. Le taux d'humification de la MO influence la stabilité de la MO et donc des ETM qui lui sont adsorbés (Merritt et Erich, 2003).

Ces amendements peuvent également apporter des composés organiques solubles susceptibles d'augmenter la mobilité des ETM à cause de (i) leur complexation avec les ligands

organiques, (ii) la modification du pH du sol par les acides organiques (Schwab *et al*., 2007). La matière organique dissoute, mesurée par le COD, est la fraction soluble de la MO. Tout comme la matière organique insoluble, elle est composée de molécules contenant des groupes fonctionnels capables de complexer les métaux. La complexation des ETM à la matière organique dissoute est un processus qui induit la diminution de l'adsorption et l'augmentation de la mobilité des contaminants inorganiques dans le sol (Davis, 1984 ; Ashworth et Alloway, 2008). Cela est dû à la formation de complexes organo-métalliques solubles dont la stabilité s'oppose à la (ré)-adsorption des ETM à la phase solide du sol. La décomposition de la litière et le compostage produisent des molécules de poids moléculaire plus faible et de polarité croissante (Wershaw *et al*., 1996), favorisant la formations de tels complexes.

De par sa composition, ses groupes fonctionnels, sa maturité, et sa forte affinité pour les métaux, la complexité de la MO du sol va donc avoir des effets différents sur la mobilité des polluants inorganiques. De plus, la matière organique joue un rôle central dans l'interaction métaux/microorganismes en fournissant une source de donneur d'électrons et un substrat carboné pour les microorganismes.

1.4.3. Effet de la MO dans les interactions microorganismes/ETM

Les microorganismes présents dans les sols pollués peuvent affecter le comportement des ETM par transformation directe ou indirecte en modifiant leur environnement et la nature des phases porteuses (cf. paragraphes 1.3). L'activité de minéralisation de la MO est le processus le plus important dans la relation MO/activité microbienne. L'utilisation d'accepteurs d'électrons, pendant la métabolisation de la MO (décrite dans la partie précedente), peut correspondre à la réduction de l'As V en As III (Macy *et al*., 2000) ou à la mobilisation indirecte d'ETM pendant la réduction d'oxydes de Fe ou de Mn (Fig.1.4). La quantité, la disponibilité, la qualité de la MO vont influencer directement la biomasse et la diversité de la microflore des sols. Ainsi, l'apport de MO fraîche va entraîner une minéralisation importante associée à une augmentation de la biomasse bactérienne.

D'autres processus bactériens peuvent être influencés par la nature et la concentration de la MO. Lescure *et al*. (2016) ont étudié l'effet de la MO sur la spéciation de l'As par la microflore des sols. Les auteurs ont démontré l'influence de la MO sur les cinétiques d'oxydation bactérienne de l'As III. Dans un sol pauvre en nutriments, l'oxydation bactérienne d'As III est limitée par la biodisponibilité des substrats organiques. Cette limitation est levée par un apport de MO soluble à une concentration de 0,08 $g.L^{-1}$.

Néanmoins, un apport de carbone excédant cette concentration induit une plus forte mobilité de l'As. Ces résultats sont expliqués par une diminution de la vitesse d'oxydation bactérienne de l'As III (Bachate *et al*., 2012 ; Lescure *et al*., 2016) associée à une stimulation de l'activité de réduction de l'As V, elle-même liée au processus de résistance de type ARS (Yamamura *et al*., 2009).

2. Description des processus de mobilité spécifiques aux polluants considérés

2.1. Arsenic

2.1.1. Généralités

L'As est un métalloïde analogue du P, présent à des concentrations moyennes de 1.8 $mg.kg^{-1}$ dans la croûte terrestre (Kabata-Pendias, 2010). L'As est connu pour ses propriétés toxiques et carcinogènes (Smith *et al*., 1992 ; Wang *et al*., 2007). L'arsenic inorganique est à l'origine, en Asie (Inde et Bengladesh, mais aussi Taïwan, ViêtNam, Mongolie…), de la plus importante catastrophe épidémiologique d'origine environnementale connue jusqu'à présent, liée à la consommation d'eau contenant ce métalloïde. La toxicité aigüe et sub-aigüe de l'arsenic touche de nombreux organes tels que les systèmes gastro-intestinal, dermique, neural, rénal, hépatique, hématologique, cardio-vasculaire, respiratoire et ophtalmique. De nombreux effets chroniques, cardio-vasculaires et carcinogènes ont également été décrits. La présence d'arsenic dans les nappes phréatiques peut avoir pour origine des transformations biogéochimiques des minéraux constituant l'aquifère.

Cependant, la pollution des sols, des eaux et des sédiments par des activités humaines contribue de façon non négligeable à la dispersion de l'arsenic et à la contamination des ressources en eau. Les activités minières, industrielles, ainsi que l'utilisation de pesticides et herbicides à base d'arsenic ont généré des problèmes de pollution des milieux par le métalloïde toxique dans de nombreuses régions et sur une multitude de sites en France (Juillot, 1998 ; Bodénan *et al*., 2004 ; Morin et Calas, 2006 ; Mamindy-Pajany *et al*., 2013).

2.1.2. Spéciation et mobilité de l'arsenic

L'As appartient au groupe 15 du tableau périodique des éléments. Sa masse atomique est de 75 $g.mol^{-1}$. L'As possède 4 degrés d'oxydation (-III, 0, III et V). Les formes III et V sont les plus couramment retrouvées dans l'environnement. Dans la zone non saturée des sols l'As est principalement sous forme d'arséniate, As V, tandis que l'As III et l'As 0 sont caractéristiques de milieux réducteurs. L'As V, chargé négativement à pH environnemental (proche de la neutralité) est adsorbé plus efficacement que l'arsénite ou As III, qui est non chargé dans ces conditions, et donc beaucoup plus mobile (Fig.1.7) (Smedley and Kinniburgh, 2002).

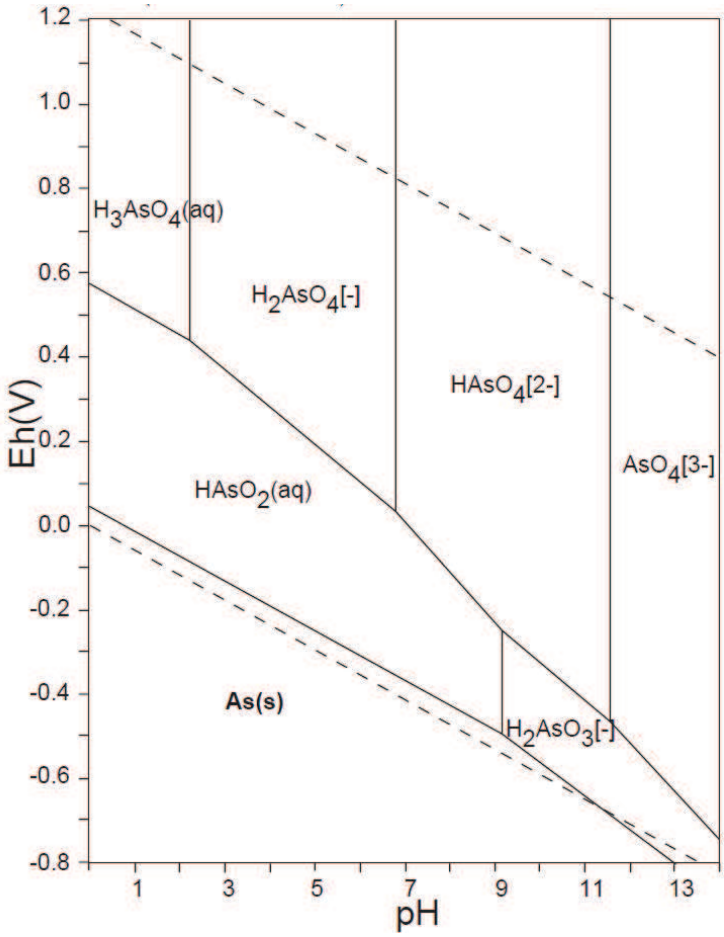

Figure 1.7 : *Diagramme Eh-pH du système As-O-H. ∑ As = 10^{-10} mol.kg^{-1}, 298.15 K, 10^{5} Pa (d'après Takeno, 2005).*

L'arsenic peut s'adsorber, dans les sols, sur les argiles, les carbonates et surtout sur les oxydes de Fe, Mn et Al (Dixit et Hering, 2003 ; Gupta *et al*., 2005 ; Ona-Nguema *et al*., 2005). Les oxydes et hydroxydes de Fe, Mn et Al sont considérés comme les principaux composés contrôlant l'adsorption de l'As dans les sols. Néanmoins, cette adsorption sur les oxydes et hydroxydes est plus ou moins efficace selon la spéciation de l'As et selon le pH. Par exemple, l'adsorption de l'As V à la surface des oxyhydroxydes de Fe est optimale à pH = 4-6, alors que pour l'As III, elle est optimale à pH = 6-9 (Dixit et Hering, 2003).

Le phénomène d'adsorption de l'As en solution peut également être impacté par la présence d'ions phosphates et, dans une moindre mesure, carbonates (Violante et Pigna, 2002; Radu *et al*., 2005). Cette compétition due à un comportement chimique voisin des arséniates peut provoquer une saturation des sites d'adsorption et donc une plus forte mobilité de l'As.

La MO joue également un rôle sur la mobilité de l'As dans le sol, tout d'abord parce qu'elle est une source de carbone pour les métabolismes microbiens affectant la spéciation de l'As (décrit dans la suite du manuscrit), ensuite parce qu'elle peut s'adsorber aux oxydes et oxyhydroxydes de Fe et donc entrer en compétition avec l'As (Redman *et al*., 2002; Catrouillet *et al*., 2014). Enfin l'As peut également être lié à la MO principalement par les groupements carboxyliques, phénoliques et thiols (Buschmann *et al*., 2006 ; Preuβ ouillet *et al*., 2015).

2.1.3. Effet des microorganismes du sol sur la mobilité de l'arsenic

De nombreux travaux ont montré que les microorganismes jouent un rôle très important dans la bio-géochimie de l'arsenic, à travers la réduction de l'As V, l'oxydation de l'As III, mais aussi la méthylation. Ces processus jouent un rôle-clef dans la stabilisation ou la mobilisation de l'arsenic dans les sols, les sédiments ou les aquifères.

De nombreuses études ont mis en évidence la capacité de certaines bactéries à oxyder ou réduire l'arsenic (Stolz *et al*., 2002 ; Battaglia-Brunet *et al*. 2002 ; Battaglia-Brunet *et al*., 2006). L'oxydation de l'As III en As V par l'arsénite oxydase, en condition aérobie, peut avoir un rôle de détoxification du milieu, car l'As V est d'une part moins toxique que l'As III, et d'autre part moins mobile donc moins biodisponible. Certaines bactéries peuvent également utiliser la réaction d'oxydation de l'arsenic comme source d'énergie (Santini *et al*., 2004 ; Battaglia-Brunet *et al*., 2006). L'oxydation anaérobie de l'As III en condition anaérobie de dénitrification a également été mise en évidence chez certaines bactéries (Hoeft *et al*., 2007).

En conditions anaérobies, l'As V peut être réduit par des bactéries qui « respirent » l'arsenic, c'est-à-dire qui l'utilisent comme accepteur terminal d'électrons grâce à une arsénate réductase (Malasarn *et al*., 2008). Cette réduction dissimilatrice est énergétiquement favorable lorsque le potentiel redox est négatif, au-dessous de -90 mV (Tufano *et al*., 2008). Les gènes *aioA* et *arrA* codant pour des sous-unités de l'arsénite oxydase et de l'arsénate réductase respiratoire, respectivement, ont été proposés comme bio-indicateurs de la présence et de la biodisponibilité de l'arsenic dans l'environnement (Quéméneur *et al*., 2010).

Par ailleurs, de très nombreuses bactéries possèdent un ou plusieurs systèmes de résistance à l'arsenic, les opérons *ars* (Achour-Rokbani *et al*., 2007). Ils confèrent aux microorganismes la capacité d'expulser l'arsenic qui a pénétré dans les cellules par le dispositif de transport du phosphate. Cependant, seul l'As III est expulsé des cellules. L'As V est réduit par une

arsénate réductase avant d'être pris en charge par le système de transport (Silver, 1996 ; Achour-Rokbani *et al*., 2010). Ce système de détoxification de la cellule consomme de l'énergie. Il est susceptible d'induire une transformation de l'As V en As III, plus mobile dans les sols.

En condition réductrice, les formes inorganiques d'As peuvent être méthylées par des bactéries anaérobies. La méthylation met en jeu plusieurs étapes, dont la réduction de l'As V en As III et l'addition oxydative d'un groupement méthyl (Dombrowski *et al*., 2005 ; Fig.1.8)

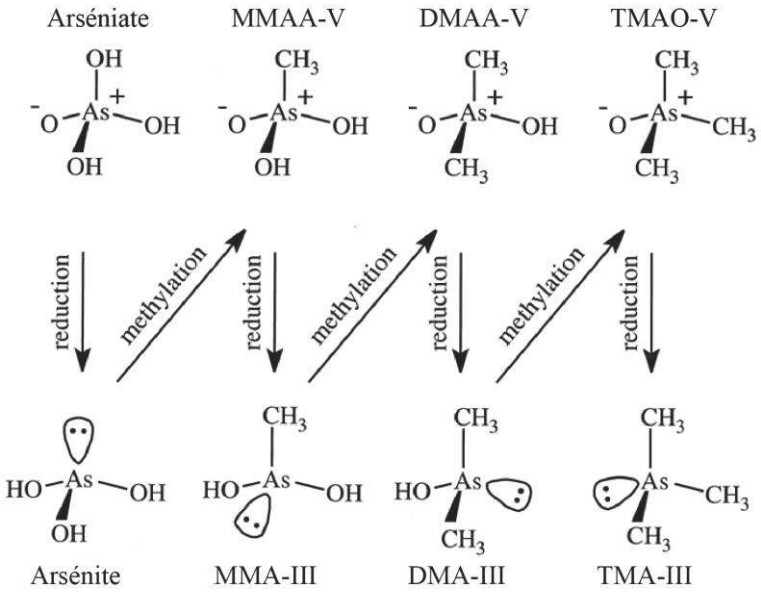

Figure 1.8 : *Schéma de la voie de biométhylation avec la séquence de réduction et de méthylation oxydante de l'As. MMAA-V : acide mono-méthylarsénique ; DMAA-V : acide diméthylarsénique ; TMAO-V : oxyde triméthylarsenic ; MMA-III : mono-méthylarsine ; DMA-III : diméthylarsine ; TMA-III : triméthylarsine. (d'après Bentley et Chasteen, 2002).*

Ce mécanisme conduit à la formation de composés gazeux (MMA, DMA et TMA) et de composés organométalliques dont les plus fréquents sont l'acide mono-méthylarsénique (MMAA-V) et l'acide diméthylarsénique (DMAA-V).

2.2. Zinc

2.2.1. Généralités

La concentration moyenne de Zn dans la croûte terrestre et le sol mondiale est estimée à 70 $mg.kg^{-1}$ (Kabata-Pendias, 2010). En France, les teneurs en zinc dans les sols naturels varient entre 10 et 100 $mg.kg^{-1}$ (Baize, 1997). Les minéraux communs composés de Zn sont la

sphalérite (ZnS), la zincite (ZnO), la smithsonite ($ZnCO_3$), la willemite ($ZnSiO_4$) et l' hemimorphite ($Zn_4Si_2O_7(OH)_2\ H_2O$ (Vodyanistkii, 2010).

Les sources anthropogéniques de Zn sont liées essentiellement à l'industrie et aux pratiques agricoles. Le zinc est utilisé dans de nombreuses industries, principalement comme protection contre la corrosion de l'acier. Il est également un composant important de divers alliages et est largement utilisé comme catalyseur dans différents processus chimiques (*e.g.* production de caoutchouc, plastique, pigments).

Le Zn est un oligo-élément qui semble être nécessaire pour toute forme de vie car il se trouve dans les protéines et les enzymes du métabolisme des acides nucléiques. Les concentrations élevées de zinc le rendent toxique, car le zinc interagit avec les groupements thiols et peut bloquer des réactions essentielles dans la cellule.

2.2.2. Spéciation et mobilité du zinc

Le Zn a une masse atomique de 65.4 $g.mol^{-1}$ et appartient au groupe 12 du tableau périodique des éléments. On le trouve généralement à l'état d'oxydation II et en solution, sa forme prédominante, à pH < 8, est Zn^{2+} (Fig.1.9).

Le Zn est très mobile pendant les processus d'altération et ses composés sont très solubles. Le Zn peut également se complexer en solution avec les anions chlorures, phosphates, nitrates et sulfates. Bien que le Zn soit très mobile dans la plupart des sols, les argiles, les oxydes de Fe, Al et Mn, ainsi que la MO, sont susceptibles de l'adsorber, en particulier à des pH neutres et alcalins. De plus, il semble qu'il y ait deux mécanismes différents affectant les processus d'adsorption du Zn : dans les milieux acides, une adsorption physique liée aux sites d'échange de cations et en milieux alcalins, la chimisorption, qui va être très fortement influencée par les ligands organiques (Vodyanistkii, 2010).

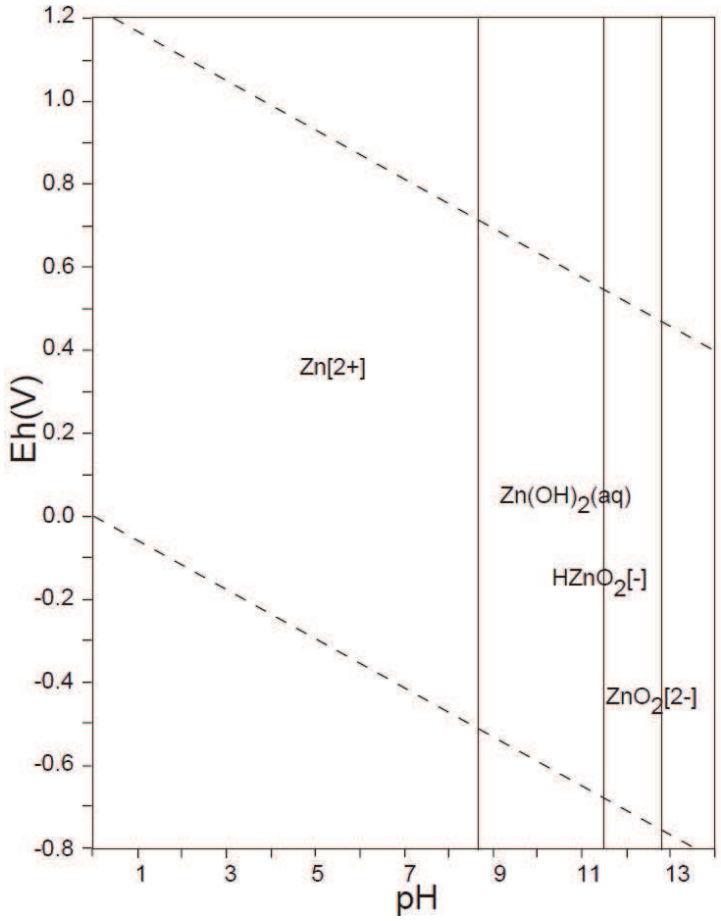

Figure 1.9 : *Diagramme Eh-pH du système Zn-O-H.* $\sum Zn = 10^{-10}$ *mol.kg*$^{-1}$*, 298.15 K,* 10^{5} *Pa (d'après Takeno, 2005).*

2.2.3. Effet des microorganismes du sol sur la mobilité du zinc

Comme pour de nombreux oligo-éléments métalliques, les microorganismes peuvent contrôler la concentration en Zn dans leur cellule afin qu'elle n'atteigne pas un seuil toxique. Plusieurs mécanismes, décrits par Hantke (2005), permettent de réguler cet équilibre entre le besoin et la toxicité en Zn. Néanmoins, la microflore des sols intervient principalement de façon indirecte sur la mobilité du Zn. La production microbienne d'acide citrique, par exemple, permet de solubiliser le Zn à partir d'oxyde de Zn insoluble (Frantz *et al.*, 1991). Des processus similaires de dissolution de minéraux porteurs de Zn par des microorganismes hétérotrophes ou autotrophes peuvent engendrer une solubilisation du Zn. La microflore peut également promouvoir la séquestration du Zn dans le sol. Le Zn peut être retenu à la surface des cellules ou par des biofilms bactériens composés essentiellement de substances polymériques extracellulaires (EPS). Il peut également être adsorbé à la surface de minéraux biogéniques comme les sulfures ou les oxydes et hydroxydes.

2.3. Cuivre

2.3.1. Généralités

Les concentrations en Cu dans la croûte terrestre sont comprises entre 25 et 75 $mg.kg^{-1}$ avec une moyenne de 55 $mg.kg^{-1}$ (Kabata-Pendias, 2010). Dans les sols mondiaux ces concentrations varient entre 14 et 109 $mg.kg^{-1}$, en France elles sont comprises entre 5 et 60 $mg.kg^{-1}$ (Baize, 1997). Le cuivre a une forte affinité pour les sulfures, par conséquent ses principaux minéraux sont la chalcopyrite ($CuFeS_2$), la bornite (Cu_5FeS_4), la chalcocite (Cu_2S) et la covellite (CuS).

Le cuivre est largement utilisé dans l'industrie car il offre une bonne conductivité thermique et électrique et résiste à la corrosion. Grâce à ces caractéristiques, il est utilisé dans les réseaux électriques, dans la télécommunication ou encore l'électronique. Il a également longtemps été utilisé en architecture, essentiellement pour les toitures et gouttières. Le cuivre est aussi utilisé par les activités agricoles où ses propriétés fongicides et bactéricides sont recherchées. L'utilisation de sulfate de cuivre dans la bouillie bordelaise en viticulture pour lutter contre le mildiou en est un exemple.

2.3.2. Spéciation et mobilité du cuivre

Le Cu appartient au groupe 11 du tableau périodique des éléments, et a une masse atomique de 63.5 $g.mol^{-1}$. Il se trouve généralement à l'état d'oxydation II et en solution sa forme prédominante, à pH < 7, est Cu^{2+} (Fig.1.10).

Le comportement du cuivre est assez semblable à celui du Zn. Il peut être complexé à la matière organique, aux oxydes et hydroxydes de Fe, de Mn ou d'Al. Néanmoins, il a une meilleure affinité avec la matière organique et particulièrement avec les groupements carboxyliques et phénoliques. Des concentrations importantes en Cu peuvent ainsi favoriser la lixiviation des autres ETM en saturant les sites d'échanges.

En solution, le Cu peut être sous forme ionique libre (Cu^{2+} à pH acide), complexé à des ligands inorganiques (OH^-, HCO_3^-, $H_2PO_4^-$, Cl^-, …), chélaté à la matière organique dissoute (acides aminés, acides phénoliques, protéines,…) ou sorbé sur des colloïdes. Ses complexes avec des ligands organiques solubles peuvent représenter une proportion importante du cuivre soluble total (Vulkan *et al*., 2000).

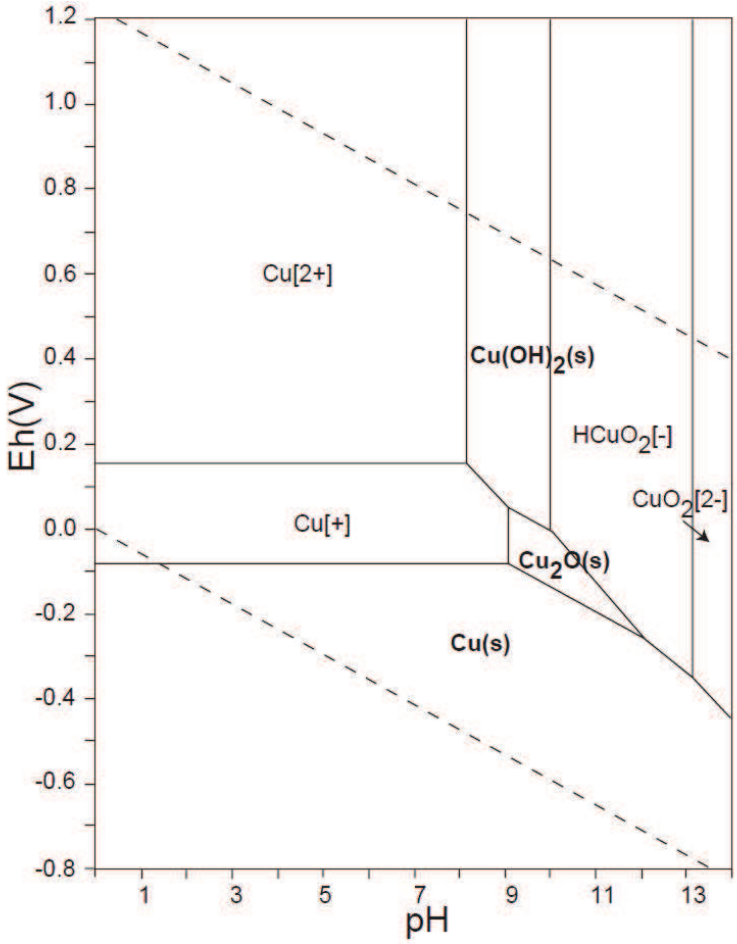

Figure 1.10 : *Diagramme Eh-pH du système Cu-O-H. ∑ Cu = 10^{-10} mol.kg^{-1}, 298.15 K, 10^5 Pa (d'après Takeno, 2005).*

2.3.3. Effet des microorganismes du sol sur la mobilité du cuivre

Le cuivre est un oligo-élément, mais en raison de son caractère fongicide et antibactérien, des concentrations élevées dans les sols peuvent affecter la biomasse microbienne (Flemming and Trevors, 1989). Cependant, divers microorganismes sont connus pour leur résistance à des concentrations élevées en Cu. Des champignons comme *Penicillium ochron-chloron* peuvent adsorber des quantités élevées de Cu (Gadd et White, 1985). La fixation du Cu à la surface des cellules microbiennes ou des biofilms peut être très important (Kabata-Pendias, 2010).

Les bactéries peuvent également induire une mobilisation indirecte de Cu en solubilisant le composé porteur de cet élément. Les bactéries acidophiles sulfo-oxydantes peuvent libérer des quantités importantes de Cu en solution par l'oxydation des sulfures, sur des sites miniers ou des formations géologiques riches en sulfure (Jonhson *et al*. 1993; de la même façon que pour le Zn, le Pb et l'As). La précipitation de minéraux biogéniques peut à contrario immobiliser le Cu dans le compartiment solide du sol. Les bactéries sulfato-réductrices (*e.g*. *Desulfovibrio*)

vont, en réduisant les sulfates en sulfure, favoriser la précipitation de sulfure de Cu (Jong et Parry, 2003).

2.4. Plomb

2.4.1. Généralités

La concentration moyenne en plomb de la croûte terrestre est estimée à 15 $mg.kg^{-1}$, dans les sols elle est estimée à 27 $mg.kg^{-1}$ (Kabata-Pendias, 2010). En France, le fond pédogéochimique naturel de Pb est compris entre 9 et 50 $mg.kg^{-1}$ (Baize, 1997). A l'état naturel, le Pb se trouve dans divers minéraux sous forme de sulfure PbS (galène), de sulfates $PbSO_4$ (anglésite) et de carbonates $PbCO_3$ (cérusite) pour les plus répandus.

Tout comme le Zn et le Cu, le plomb est utilisé dans l'industrie. Sa grande malléabilité et ductilité, ainsi que son point de fusion très bas, ont influencé son usage. Il a ainsi été utilisé pour la plomberie, la soudure, ou encore les fusibles. Le Pb est également utilisé dans des alliages avec l'étain et l'antimoine. Il a également longtemps été utilisé comme pigment dans les peintures ou comme anti-détonnant dans les moteurs à explosion (jusque dans les années 2000). L'utilisation du plomb dans l'essence a provoqué une pollution importante des sols à proximité des réseaux routiers, par retombées atmosphériques. A la fin du siècle dernier, cette source anthropique représente jusqu'à 95 % du Pb contaminant les sols.

Le Pb est une substance toxique qui agit principalement sur le cerveau et le système nerveux, affectant les facultés mentales. Il est également cause d'anémie, hypertension et déficience rénale.

2.4.2. Spéciation et mobilité du plomb

Le Pb a une masse atomique 207 $g.mol^{-1}$ de et appartient au groupe 14 de tableau périodique des éléments. Par conséquent, il possède trois états de valence (0, +II et +IV), mais il est soluble seulement dans sa forme divalente (Fig.1.11). A pH < 6, sa forme dominante est Pb^{2+}.

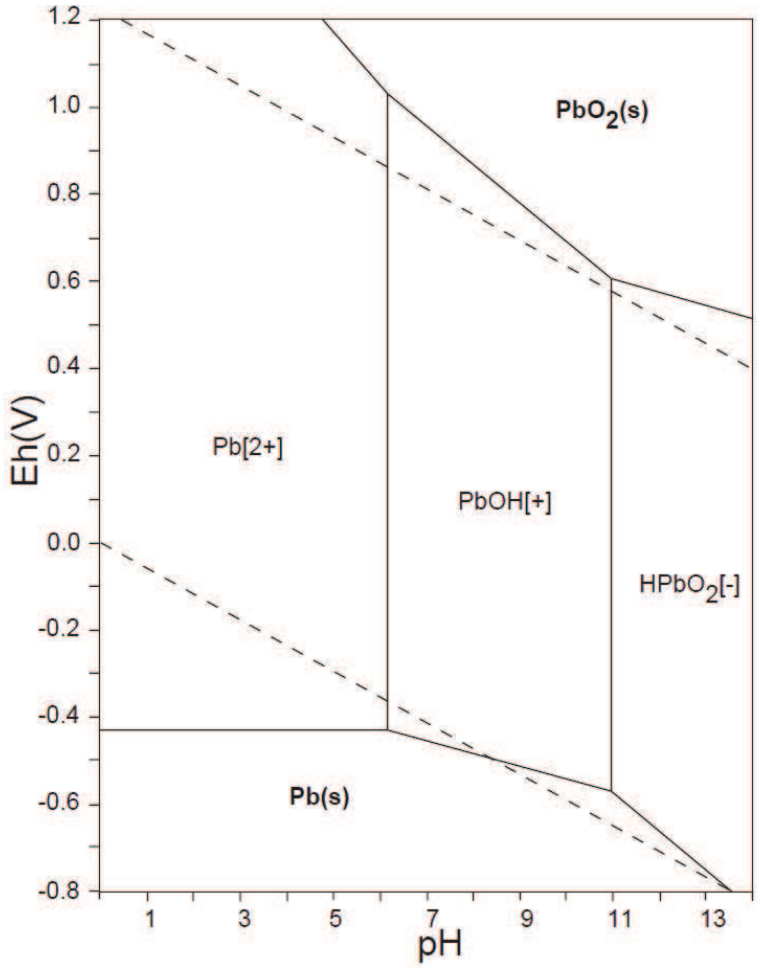

Figure 1.11 : *Diagramme Eh-pH du système Pb-O-H. ∑ Pb = 10^{-10} mol.kg^{-1}, 298.15 K, 10^{5} Pa (d'après Takeno, 2005).*

Le Pb serait l'élément trace métallique le moins mobile dans les sols, bien que sa capacité d'adsorption soit inférieure à celle du Cu et du Zn (Vega *et al*., 2007). Tout comme pour le Zn et Cu, ses proportions de Pb immobilisés dans les sols dépendent du pH du sol et de sa CEC, et font intervenir les processus de physi- et chimisorption. Le Pb a également une bonne propension à se complexer à la surface des oxydes et oxyhydroxydes de Fe et Mn (Swallow *et al*., 1980 ; Morin *et al*., 2001).

La forte capacité du Pb à se fixer avec la MO, principalement par complexation, contribue à son importante rétention dans les sols. Le Pb exogène a ainsi tendance à s'accumuler dans les horizons superficiels des sols où les teneurs en MO sont les plus fortes (Baize, 1997). Néanmoins, sa complexation avec des ligands organiques solubles peut entrainer sa mobilisation. A de fortes concentrations, des ligands organiques comme l'acide citrique ou acétique augmentent fortement la désorption du Pb (Yang *et al*., 2006). A des pH neutres,

Sauvé *et al*. (1997) estiment que 60-80 % du Pb dissous est présent sous forme de complexes organo-métalliques, et que ce pourcentage diminue pour des pH plus faibles.

2.4.3. Effet des microorganismes du sol sur la mobilité du plomb

Contrairement à d'autres ETM, le Pb n'est nécessaire à aucun organisme vivant. Comme pour le Cu et le Zn, les microorganismes du sol n'interviennent pas directement sur la mobilité du Pb, en modifiant sa spéciation par exemple. Ils agissent de façon indirecte par des phénomènes de solubilisation des phases porteuses de Pb et de séquestration. L'excrétion d'acides organiques peut permettre de changer localement les conditions de pH et par exemple solubiliser le Pb par le biais de la dissolution d'oxyde de Pb ou de Fe et Mn porteur de Pb. La pyromorphite ($Pb_5(PO_4)_3Cl$) est un minéral très stable, qui peut se former dans des sols contaminés. Sa précipitation est utilisée comme technique de remédiation, sur les sites pollués au Pb, par ajout, si nécessaire de phosphate. Cependant, la pyromorphite peut être solubilisée par des champignons solubilisant le phosphate *e.g*. *Aspergillus niger*. Cette transformation de la pyromorphite, peut entrainer la libération d'oxalate de Pb dans l'environnement (Sayer *et al*., 1999).

La minéralisation de MO complexée au Pb par les microorganismes est également susceptible le libérer cet élément toxique dans l'environnement. L'activité microbienne peut également entrainer une immobilisation du Pb, essentiellement par des processus de biosorption, directement sur la paroi cellulaire, sur des biofilms bactériens.

3. La pollution héritée de la Grande Guerre

3.1. L'impact environnemental de la Première Guerre Mondiale

Nous célébrons actuellement le centenaire de La Première Guerre Mondiale. Pendant plus de 4 ans, de 1914 à 1918, elle a opposé la Triple-Entente composée de la France, du Royaume-Uni et de la Russie et de leurs empires coloniaux à la Triple-Alliance composée de l'Allemagne, de l'empire Austro-Hongrois et plus tard de l'Empire ottoman. Les Etats Unis d'Amérique rejoindront la Triple-Entente en 1917. Les combats atteignent une échelle et une intensité inconnues jusqu'alors. Elle a impliqué sur les différents fronts près de 60 millions de soldats et causé la perte de près de 9 millions de vies humaines.

La Première Guerre Mondiale marque un tournant dans la façon de mener et d'organiser la guerre. Elle est la première guerre « industrielle », utilisant l'artillerie de façon intensive sur tous les fronts. Grâce à la révolution industrielle, les grandes nations sont capables de produire des quantités importantes d'armes et de matériel de guerre. Les avancées technologiques permettent de produire des armes plus puissantes, avec des cadences de tir et des portées plus élevées. En France, au cœur de la guerre, la production d'obus atteint 100 000 unités par jours.

Le nombre de munitions lancées sur le front ouest est estimé pour être compris entre 856 000 000 [(2)] et 1 400 000 000 [(3)] obus. Le front ouest s'étend du Nord de la France (Somme et Pas de Calais) à l'Alsace. Il a très peu évolué pendant les quatre ans de conflit, embourbant les belligérants dans une guerre de positions. Cette guerre de tranchées a eu un impact environnemental très important. A la fin du conflit, des millions d'hectares de terre ont été complètement dévastée sur près de 700 km, de la Belgique à la Suisse. Ces sols, maintes fois retournés et dénudés de toute végétation ont été classés « zone rouge » (Fig.1.12) et inaptes à l'agriculture en 1919.

[2] Prentiss A.M., 1937 : Chemicals in war McGraw-Hill, p.739.
[3] Linnenkohll H., 1996 : Vom Einzelschuss zur Feuerwalze. Bonn, Bernard & GrA.E.Fe, p. 304.

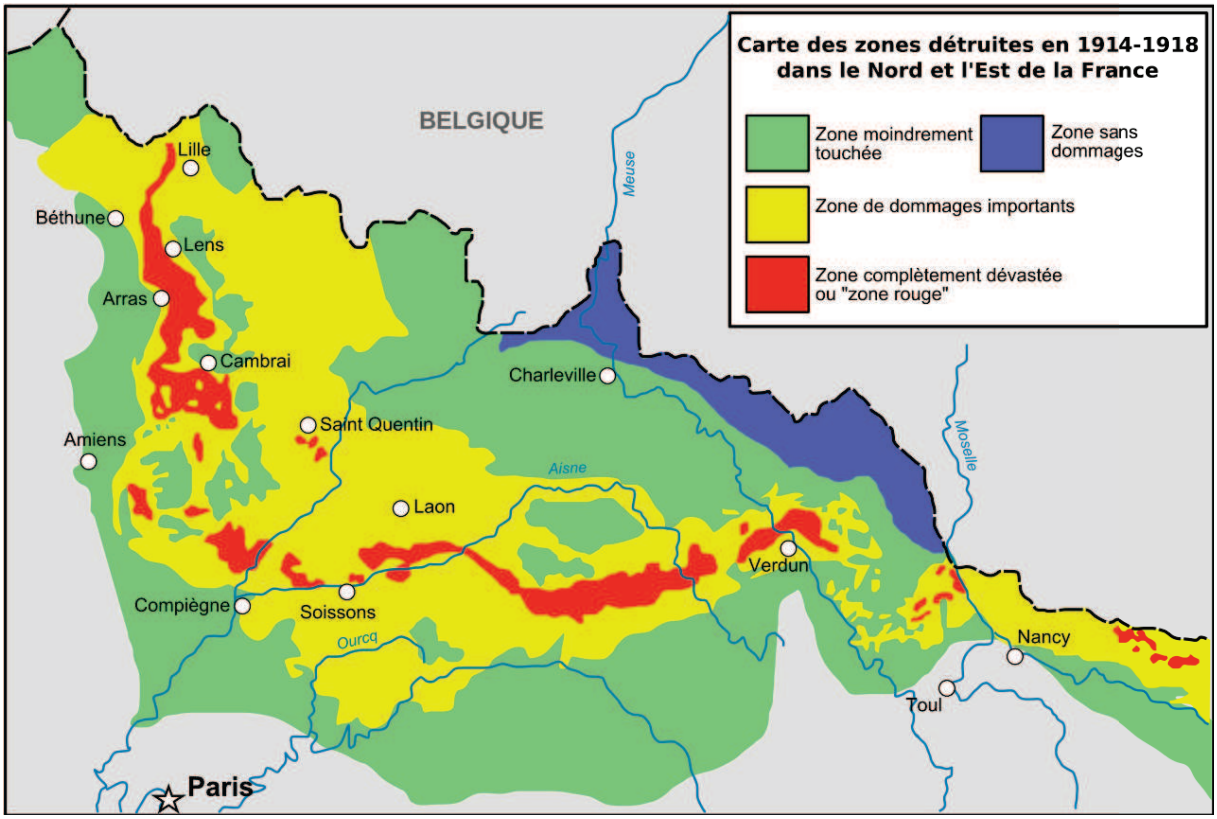

Figure 1.12 : *Localisation de la zone rouge de destruction suite aux combats de la Première Guerre Mondiale sur le front ouest (Source wikipedia.org d'après Guicherd, J., et Matriot, C., 1921[4]).*

Les cicatrices de ces batailles sur l'environnement sont encore très visibles un siècle après la fin du conflit. A Verdun, lieu d'une des batailles les plus violentes de la guerre, les combats et les tirs d'artillerie ont modelé le paysage (Fig.1.13). Pendant les 300 jours de combats de la bataille de Verdun, 60 millions d'obus ont été tirés sur une ligne de front de 20 km et d'une largeur de quelques centaines de mètres. Au plus fort du combat, 2000 tonnes de munitions pouvaient être lancées par jour. Par endroit, le sol a subi une érosion de 7 m et 9 villages ont été rasés de la carte. Les explosions répétées ont complétement déstructuré le sol et modifié le réseau hydrographique, d'après Hupy and Schaetzl (2008). Ainsi, ces auteurs parlent de « bombturbation » pour qualifier l'impact des bombardements sur la structure des sols.

La Première Guerre Mondiale est le premier conflit utilisant massivement des armes chimiques. Néanmoins, très peu d'études inspectent l'impact chimique de cette guerre, malgré les quantités incommensurables de fragments d'explosifs riches en métaux, de composés explosifs et d'agents toxiques littéralement déversés à la surface des champs de batailles.

[4] Guicherd, J., et Matriot, C., 1921. *La terre des régions dévastées*. *Journal d'Agriculture Pratique*, 34, 154-6.

Figure 1.13 : *Photo du champ de bataille du fort de Douaumont après la fin des combats et un siècle plus tard (photo d'époque provenant du site lesfrancaisaverdun-1916.fr).*

3.2. Les munitions de la Grande Guerre : source de pollution

3.2.1. Description des munitions

- **Organisation des projectiles d'artillerie**

Une munition d'artillerie de la Première Guerre Mondiale était constituée d'un obus, d'une douille avec une amorce, d'une ceinture et d'une fusée. Tous ces éléments sont composés d'une variété de métaux et d'alliages. Le corps de l'obus était généralement fabriqué en acier ou en fonte, il contenait la charge offensive qui pouvait être de différents types (à fragmentation, explosive, ou chimique ; développé par la suite). La douille contenait la charge propulsive qui impulse l'énergie nécessaire à l'obus afin qu'il atteigne sa cible. Elle est généralement en Cu ou en laiton. La nitrocellulose ($C_6H_8N_2O_9$) était le plus souvent utilisée comme charge de propulsion, elle était appelée poudre B ou coton-poudre. La ceinture, le plus souvent située à la base des obus, permettait d'imposer aux projectiles une rotation autour de leur axe lors de leur passage dans le canon, afin d'avoir une trajectoire stable pendant le vol. Elle est constituée de métal mou (Cu ou Zn). Enfin, la fusée qui permettait d'amorcer la détonation, était fabriquée en Zn, acier, laiton et/ou Al selon le modèle de l'obus.

Les obus sont selon leur chargement de trois types différents :

- **Les obus à fragmentation**

Les obus à fragmentations étaient les principales munitions d'artillerie utilisées au début de la guerre. Ils étaient destinés à exploser au-dessus des troupes ennemies, en dispersant leurs fragments et balles. Le chargement de l'obus à fragmentation était rempli de balles en Pb (Fig.1.14.A). Un obus à fragmentation pouvait contenir jusqu'à 3 kg de Pb. Entre les balles,

un liant constitué de soufre était souvent utilisé. Au centre de l'obus, se situait la charge explosive, composée de poudre noire ou de poudre B. A la fin du conflit, ces obus n'ont plus été utilisés car leur système de détonation était trop coûteux et plus difficile à utiliser que celui des obus explosifs.

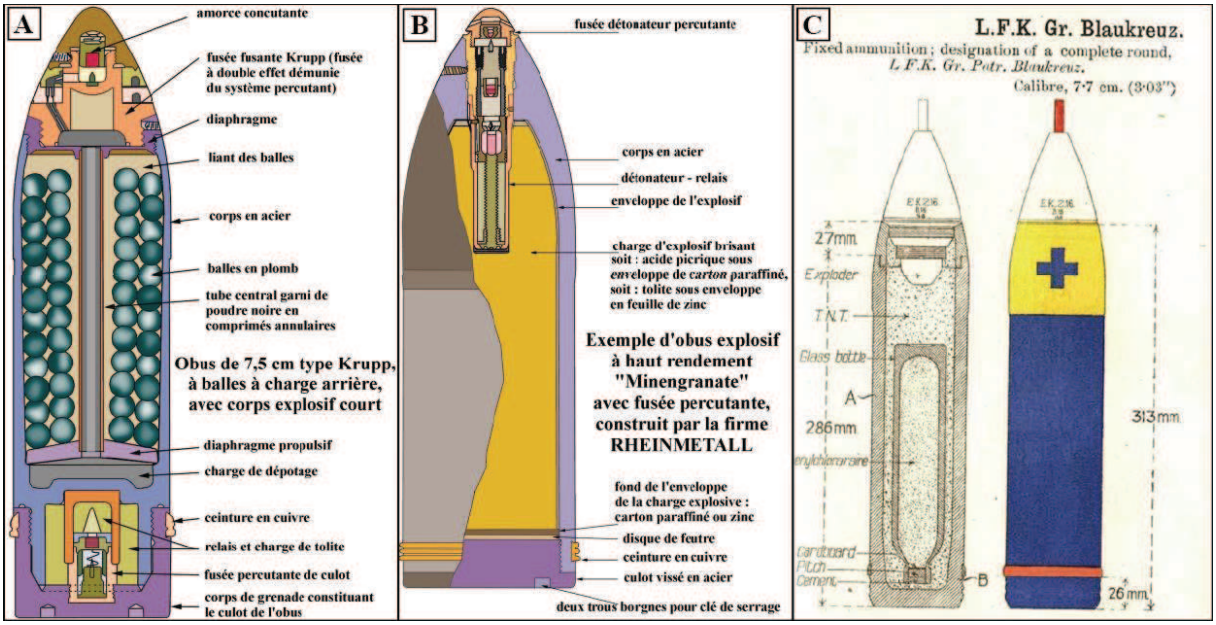

***Figure 1.14 : A** : Schéma d'un obus à fragmentation de 75 mm de type Krupp. **B** : Schéma d'un obus à charge explosive (« mélinite »). **C** : Obus de 77 mm à « Croix Bleue » contenant dans une bouteille en verre les agents toxiques Clark I ou Clark II (Illustration H. et M. Bélot).*

- **Les munitions explosives**

La majorité des obus utilisés pendant la Première Guerre Mondiale était de types explosifs. Les obus explosifs ont été conçus pour exploser au contact de la cible. Ils étaient remplis de matériel explosifs destinés à libérer de fortes quantités d'énergie pendant la détonation (Fig.1.14.B). Les composés explosifs se présentaient sous de très nombreuses variantes mais étaient le plus souvent constitués de composés azotés. Les molécules les plus utilisées pendant la guerre étaient la « mélinite » (ou acide picritique, 2,4,6-trinitrophénol), la « Schneiderite » (nitrates d'ammonium et nitronaphtralène), la « crésylite » (Trinitro-2,4,6 m-crésol). Les « cheddites » composées d'un mélange d'hydrocarbures et de chlorate de potassium ou de perchlorate d'ammonium étaient également utilisées.

La production de ces composés explosifs pendant la guerre fut très importante comme en témoigne le tableau 1.2.

Tableau 1.2 : *Production française des poudres et explosifs durant la guerre (Hubé, 2016).*

Produit	**Composition**	**Usages**	**Tonnage utilisé et exporté (1914-18) en tonnes**
Poudre B, coton-poudre	Nitrocellulose ± nitroglycérine	Propulseurs dans les douilles de munitions. Dynamite dans certaines mines	445 845
Acide picrique (« mélinite »)	2,4,6-Trinitrophénol	Explosifs binaires / ternaires (avec TNT et nitronaphtalène), amorces	306 300
« Schneiderite »	Nitrates d'ammonium + nitronaphtalènes + TNT	Explosifs de munitions d'artillerie	135 700
Explosifs (chloratés)	$KClO_3$, $KClO_4$, NH_4ClO_4, avec matrice paraffinée et éventuellement $NaNO_3$	Grenades, artillerie de tranchées et mines de sapes	130 905
Autres explosifs azotés	TNT (Tolite), nitrobenzènes, « crésylite », etc.	Explosifs de munitions d'artillerie	84 849
Total			**1 103 599**

- **Les munitions chimiques**

Les munitions de la Grande Guerre ne contenaient pas que des explosifs, certaines avaient des chargements incendiaires, d'autres des chargements fumigènes ou encore traçants, et des armes chimiques. Ces dernières devaient permettre d'ouvrir des brèches dans le front, mais leur efficacité fut toute relative. Elles ont été utilisées dans des proportions très faibles en comparaison des obus explosifs.

Une grande variété d'agents toxiques de guerre a été utilisée. Plusieurs effets étaient recherchés chez les agents toxiques :

- Les agents suffocants attaquant les tissus plumonaires et empêchant les échanges d'oxygène avec le sang (Phosgène ($COCl_2$), diphosgène ($C_2O_2Cl_4$), chloropicrine (CCl_3NO_2), sulfure d'hydrogène(H_2S)).
- Les agents vésicants produisant des brûlures douloureuses, aveuglement et difficulté respiratoire (« Ypérite » ou gaz moutarde($C_4H_8Cl_2S$)).

- Les agents sternutatoires et lacrymogènes provoquant éternuements, larmes et nausées qui contraignent les soldats à retirer leur masque à gaz (produits organoarséniés, et organobromés).

Le groupe des produits organo-arséniés utilisés comme agents sternutatoires, vomitifs et lacrymogènes est composé du diphénylchloroarsine (Clark I), du diphénylcyanoarsine (Clark II), du phényldichloroarsine (Fiffikus), des Lewisites (3 Isomères) et du diphénylamine-chloroarsine (Adamsite). Les obus allemands à « Croix bleue », présentés sur la figure 1.14.C, étaient remplis de Clark I ou de Clark II.

3.2.2. Les processus de stockage et de destruction du surplus d'armements

A la cessation des hostilités, les différents belligérants ont eu à traiter un surplus très important de munitions. Ce surplus est estimé à environ 1 700 000 tonnes de munitions en tout genre, stockées dans d'importants dépôts de part et d'autre de la ligne de front. Environ 1 100 000 tonnes de ces munitions ont été détruites pendant l'entre-deux-guerres (Hubé, 2016). La destruction des déchets des munitions chimiques et la gestion de ces composés toxiques après des conflits a fait l'objet de différentes stratégies (Fig.1.15).

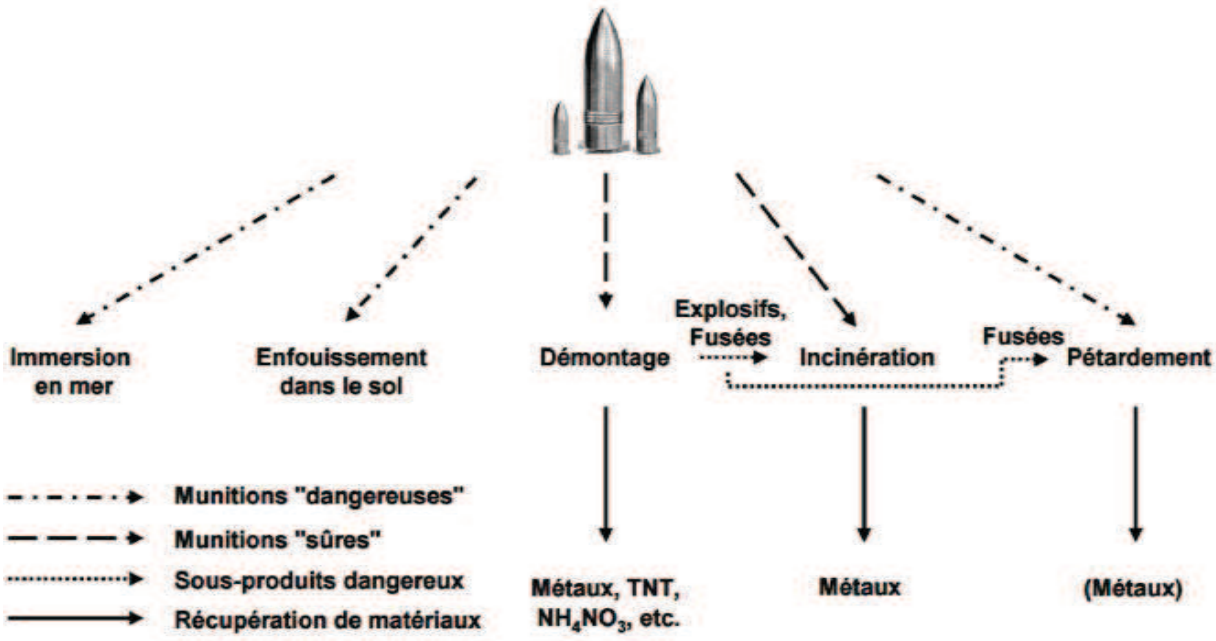

Figure 1.15 : *Stratégies employées pour se débarrasser du surplus de munitions de la Première Guerre Mondiale (d'après Bausinger, 2014).*

- **Stockage et enfouissement**

L'immersion dans les étangs et lacs (lac Bleu, Avrillé) et en milieu marin (par ex. en Golfe de Gascogne ou en Mer Baltique ou du Nord, etc.), et l'enfouissement en milieu terrestre (dans des cavités ou le sol) (Matousek, 1997 ; Bunnett *et al*., 1998) ont été appliqués dans un premier temps, dès la fin du conflit. Ces méthodes de gestion des déchets posent un problème différé. Tout d'abord, l'ennoyage ou l'enfouissement ont souvent été effectués à la hâte, entraînant une perte d'information pour les générations suivantes sur la localisation de ces dépôts. Egalement, et surtout, l'enfouissement dans le sol et la submersion ont favorisé la corrosion de l'enveloppe des munitions. Avec le temps, cette enveloppe devient poreuse, pouvant libérer à terme le contenu des obus dans l'environnement. Ces munitions sont de véritables bombes à retardement pour l'environnement. Il n'existe pas d'étude de ce phénomène sur les dépôts de munitions de la Première Guerre Mondiale. Néanmoins, des teneurs anormalement élevées d'As dans les sédiments de la mer Baltique, à proximité de munitions chimiques ennoyées de la Deuxième Guerre Mondiale (Garnada *et al*., 2006), témoignent de ce problème de stabilité dans le temps.

- **Recyclage des obus**

L'ennoyage ou l'enfouissement des obus impliquent une perte définitive des matières premières, souvent onéreuses, composant ces munitions. Une autre filière, le recyclage, avait pour but de récupérer la matière valorisable des obus, ceux-ci étant démontés avant la destruction du reste de l'obus non valorisable. Les ceintures et les fusées riches en métaux (Cu, Zn, Sn, Cd,…) étaient récupérées. La charge des obus explosifs était fondue afin de séparer le nitrate d'ammonium des autres substances explosives non valorisables (TNT, nitronaphtalènes, …). Le nitrate d'ammonium était valorisé comme engrais pour l'agriculture. Cependant, de nombreuses substances non valorisables ou dangereuses et des obus instables ont été détruits, par pétardement ou par brûlage.

- **Destruction par pétardement**

Le pétardement, ou l'éclatement des obus pouvait être nécessaire pour des obus dangereux comme les obus chargés d'ypérite et intransportables. Le pétardement de masse a également été utilisé afin d'éliminer des stocks importants de munitions, essentiellement explosives. Les munitions à détruire étaient disposées en tas au fond d'un entonnoir puis mises à feu par une charge explosive. L'opération était reconduite jusqu'à ce que l'entonnoir d'éclatement devienne inutilisable, soit parce qu'il était trop profond, soit parce qu'il avait atteint la nappe

phréatique. Pour les plus gros centres d'éclatement, ces entonnoirs, d'une dimension de 5-7 m de profondeur pour 10-15 m de diamètre pouvaient être agglomérés formant un « trou » très important (Fig.1.16.A), ou être alignés (Fig.1.16.B).

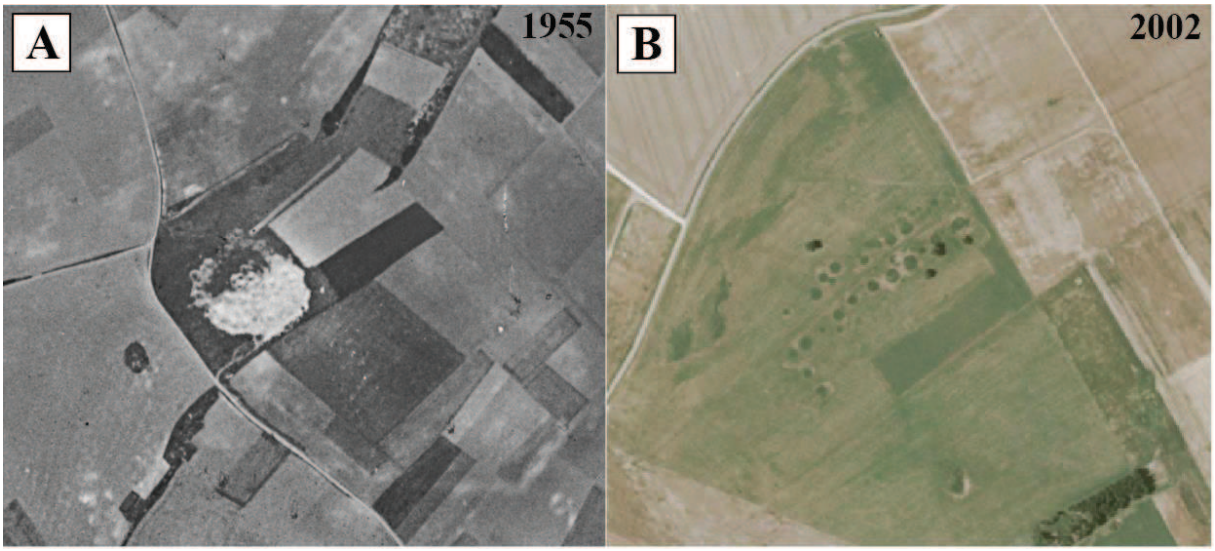

***Figure 1.16 : A** : Photo aérienne (IGN) du cône d'éclatement du champ d'explosion de Mochy-le-Preux (Pas-de-Calais) en 1955. **B** : Orthophoto (IGN, 2002) du champ d'explosion de Vaudoncourt (Meuse) (geoportail.fr).*

Le pétardement ne détruit que partiellement le contenu des obus. Il est donc susceptible de relâcher dans l'environnement, en plus des métaux liés aux fragments d'obus, des composés nitro-aromatiques ou perchloratés. Les sites concernés sont encore visibles aujourd'hui, particulièrement par photo aérienne. Environ 250 sites de pétardements ont été identifiés sur le seul territoire français.

- **Destruction par brûlage**

Les composés les plus dangereux, et en particulier les composés organo-arséniés de type Clark I et II, ont été détruits par traitement thermique sur plusieurs sites répartis le long du front Ouest, en Belgique, en Allemagne, et en France dans le Nord, en Meuse, et en Alsace. Deux de ces sites ont fait l'objet d'études au début des années 2000 (Bausinger et Preuβ, 2005 ; Bausinger *et al.*, 2007) et sont connus du public, les autres ne le sont pas et leur localisation reste confidentielle. Les sites étudiés sont ceux de Poeklapellen (Belgique) et de la Place-à-Gaz (Meuse), qui est notre site d'étude.

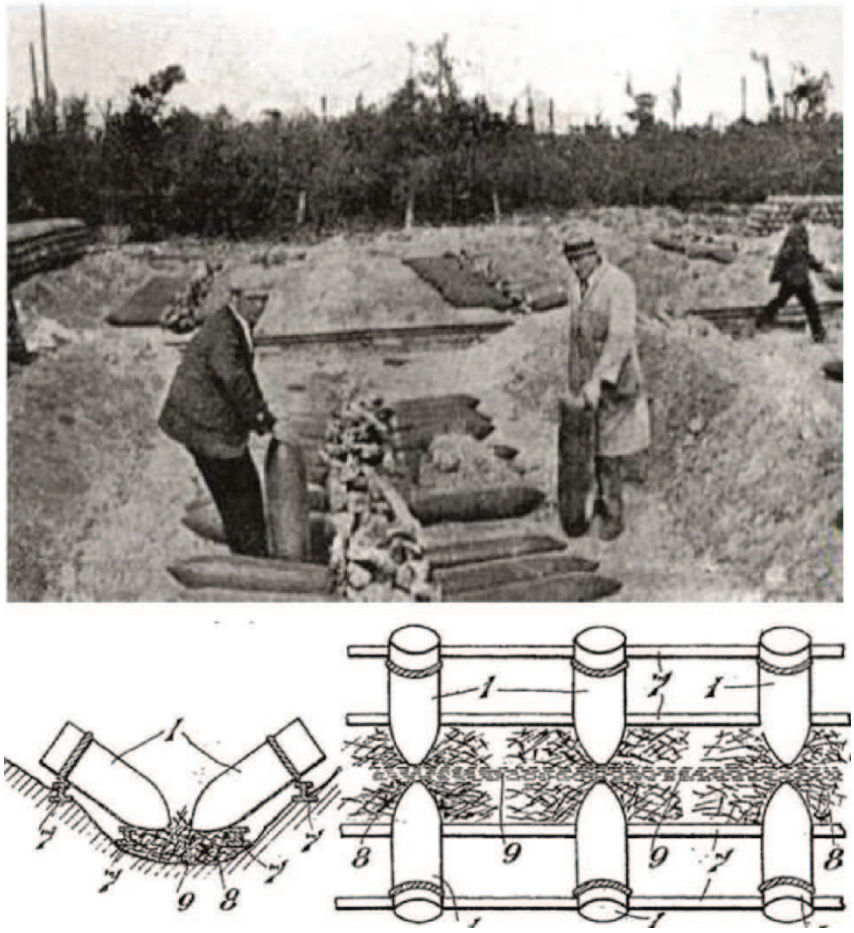

Figure 1.17 : *Photo de préparation d'une opération de brûlage d'obus et croquis du protocole de destruction d'obus chimiques (Archives Nationales, Londres)*

Sur ces sites, les obus étaient ouverts (retrait de la fusée), puis alignés la tête en bas dans des fossés (Fig.1.17). De la poudre et du bois de chauffe recouvraient les obus afin d'entretenir le feu. Ce système de brûlage permettait de se débarrasser de la charge toxique tout en permettant de récupérer l'enveloppe métallique. Néanmoins les niveaux de pollution observés sur ces sites démontrent l'empreinte environnementale de ces processus de brûlage sur les sols (Bausinger et Preuβ, 2005 ; Bausinger *et al*., 2007).

3.2.3. Pollution du sol de la Grande Guerre

Au vu de la composition des munitions en métaux et composés organiques et du nombre de munitions tirées pendant le conflit, on peut légitimement se poser la question de l'impact chimique de la Grande Guerre. D'autant qu'il est estimé qu'environ 20 à 30 % de tirs n'auraient pas fonctionné, soit 200 à 300 millions d'obus inexplosés répartis dans les sols des champs de batailles. De plus, les sites d'enfouissement, d'explosion et brûlage sont autant de

sources potentielles de pollutions aux métaux lourds et aux polluants organiques issus des explosifs et agents chimiques de guerre.

- **Pollution du sol par les métaux**

Très peu d'informations existent sur la potentielle contamination des sols par les conflits de la Grande Guerre. En 2011, Meerschmann *et al*. s'intéressent à l'effet de la guerre sur la répartition spatiale des métaux lourds dans les sols. Cette étude fait suite à la découverte d'un enrichissement en Cu de 6 $mg.kg^{-1}$ dans la partie superficielle de la zone de combat de Ypres (Belgique), attribué à la corrosion de fragments d'obus (Van Meirvenne *et al*., 2008). Les auteurs ont effectué un échantillonnage complet de la zone d'Ypres, et ont analysé les teneurs en As, Cd, Cr, Cu, Hg, Ni, Pb et Zn des sols. Leurs résultats montrent qu'il n'y a pas de pollution des sols à l'échelle régionale. Néanmoins, localement les concentrations en Pb, Cu et Zn associées à des fragments de munitions de la Première Guerre Mondiale dépassent les seuils sanitaires.

Les sites de destructions d'obus par brûlage ou pétardement sont aussi des sources, cette fois plus localisées, mais également plus intenses, de pollution aux métaux. Le site de destruction d'obus Clere and Schwander de Muzeray-Vaudoncourt-Spincourt, récemment « redécouvert » fut l'un des plus importants complexes de destruction connus. Environ 40 000 tonnes d'obus chimiques et hautement explosifs y ont été détruites. Tout comme pour les aires de brûlage de Poeklapellen et de la Place-à-Gaz, les teneurs en métaux dans les sols des champs de destruction et des aires de brûlage de ce site sont localement très importantes (source interne BRGM).

- **Devenir des explosifs et agents toxiques dans les sols**

La dégradation des munitions enfouies dans les sols des anciens champs de batailles ou ennoyées dans les lacs, tout comme les processus de destruction des obus, sont susceptibles de libérer dans l'environnement les composés explosifs ou les agents toxiques. Leur stabilité dans l'environnement, qui va déterminer leur impact environnemental, dépend alors de plusieurs facteurs.

La solubilité des composés est le premier facteur. Les chlorates et les perchlorates, par exemple, en raison de leur très forte solubilité vont être très rapidement transportés par l'eau porale du sol vers l'aquifère. Les teneurs anormalement élevées en perchlorate (jusqu'à 15 $\mu g.L^{-1}$), observées dans l'eau potable du Nord-Est de la France par l'Agence Régionale de la

Santé, sont associées par Hubé (2013) aux perchlorates libérés dans l'environnement par les combats et les sites de destructions de munitions.

D'autres composés beaucoup moins solubles, comme les nitro-aromatiques ou les organo-arséniés, qui ne sont pas forcément stables dans l'environnement, vont avoir le temps d'être dégradés. L'introduction et la dégradation des composés organo-arséniés (Clark I et II, Adamsite, ... ; Fig.1.18) dans l'environnement conduisent par exemple à la dispersion de sous-produits de réactions qui représentent des contaminants environnementaux plus mobiles (et souvent aussi toxiques) que les molécules initiales, comme l'acide diphénylarsenique (DPAA), l'acide phénylarsonique (PAA), ou l'oxyde de phénylarsine (PAO). Le DPAA est le produit de dégradation des composés organo-arséniés par hydrolyse et oxydation le plus couramment détecté sur les sites pollués par les munitions de type Clark (Daus *et al*., 2010 ; Certini *et al*., 2013).

Contrairement à d'autres molécules polluantes de la chimie militaire, essentiellement organiques (comme les composés nitro-aromatiques), les molécules organo-arséniées contiennent un élément toxique inorganique qui sera libéré au cours de leur hydrolyse et/ou de leur biodégradation. Le devenir de l'arsenic inorganique sur le sol de la Place-à-Gaz, libéré lors de la combustion des composés Clark I et II, sera l'un des enjeux de cette thèse.

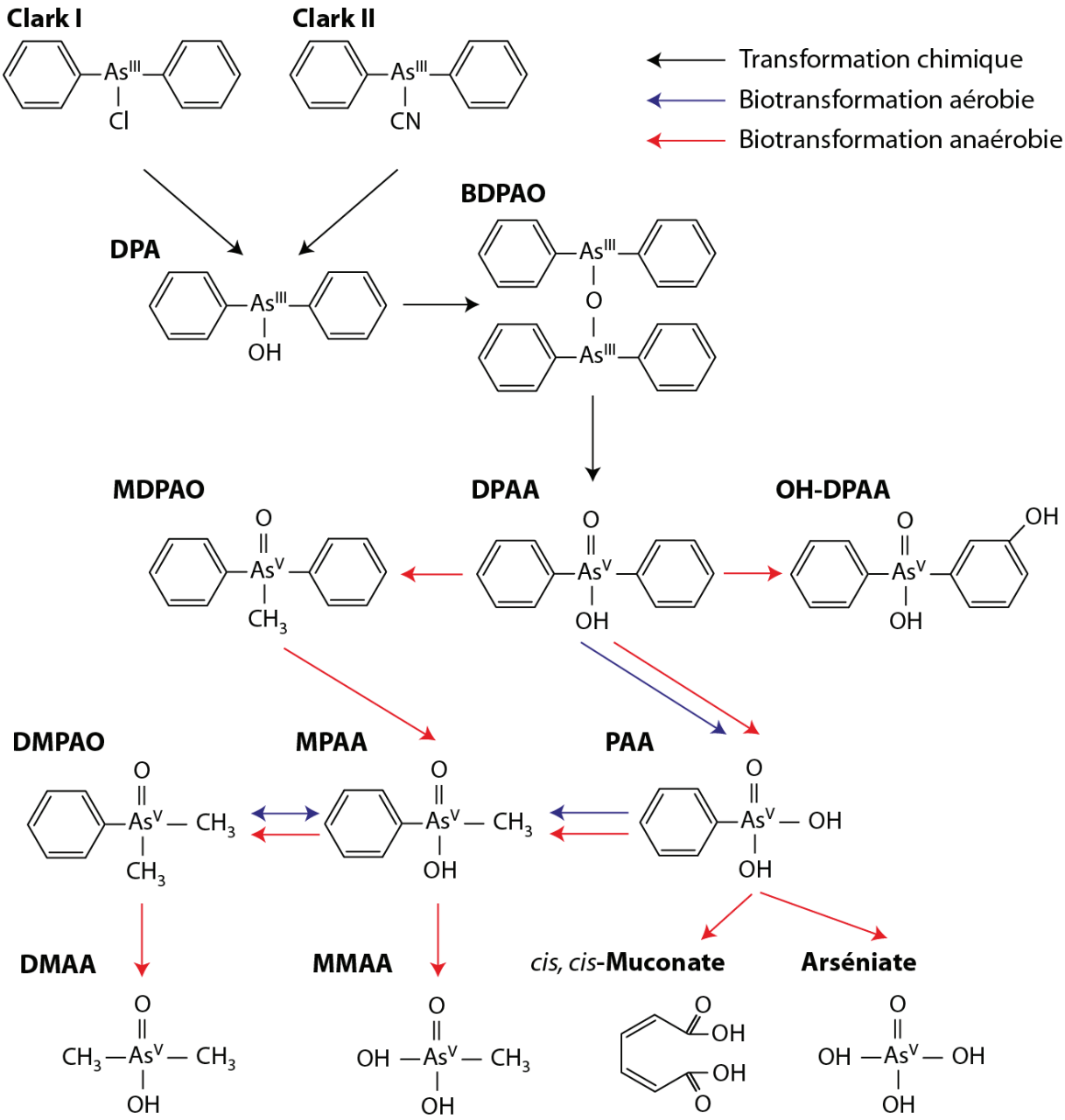

Figure 1.18 : *Voie de dégradation des agents organo-arséniés Clark I et II. Clark I: diphénylchloroarsine ; Clark II: diphénylcyanoarsine; DPA: hydroxyde de diphénylarsine ; BDPAO: Bis-(diphénylarsine) oxyde ; DPAA: acide diphénylarsénique OH-DPAA: Acide diphénylarsénique monohydroxylé ; MDPAO: diphénylméthylarsonique oxyde; PAA: acide phénylarsonique ; MPAA : acide méthylphénylarsénique ; DMPAO: diméthylphénylarsonique oxyde ; MMAA: acide mono-méthylarsénique; DMAA: acide diméthylarsénique (d'après Nakamiya et al., 2007 ; Harada et al., 2010 ; Maejima et al., 2011).*

3.3. Le site de la Place-à-Gaz

3.3.1. Historique du site

Le site de la Place-à-Gaz (Fig.1.19), se situe en forêt domaniale de Spincourt, sur la commune de Grémilly, au Nord-Est de Verdun. La Place-à-Gaz fait partie du complexe de désobusage de la Gélinerie (du nom de la ferme où ont été stockées et détruites les munitions) exploité par la société Clere & Schwander entre 1920 et 1926. La société a entrepris la destruction d'un stock de munitions allemandes de 400 000 unités. Un second exploitant, la société Pickett & fils, a pris le relai en 1926 afin de détruire les obus à Croix bleue (Fig.1.14.C). Cet exploitant, ayant déjà procédé à la destruction de munitions chimiques en France et en Belgique (site de brûlage de Poeklapellen), possédait les méthodes, les moyens et le savoir-faire pour détruire ce type d'obus. Sa société Pickett & Fils détruisit selon ces procédés (Fig.1.17) 200 000 obus à Croix bleue ainsi que des obus à ypérite et des munitions lacrymogènes. Ces activités sur le site de la Place-à-Gaz prirent fin en 1928.

Figure 1.19 : *Photo du site de la Place-à-Gaz (Le républicain Lorrain, photo Pascal Brocard).*

En 2004, l'Office National des Forêts (gestionnaire du site) alerte la préfecture de la Meuse qui demande au BRGM de procéder à des analyses de sol. Celles-ci révèlent une pollution importante du sol du site en As (11 %), Zn (9 %), Pb (0.65 %) et Cu (0.38 %) (Baubron, 2004). Le rapport préconise de cartographier l'étendue de la contamination du site, d'évaluer la dispersion possible des contaminants dans l'environnement et d'interdire son accès. En

2005, l'accès au site est empêché par un grillage. En 2007, une étude effectuée par des universitaires allemands permet de mieux caractériser la pollution et son étendue (Bausinger *et al*., 2007). Dès lors, le site a été médiatisé [(5)]. Les préoccupations socio politiques poussent la Préfecture de la Meuse à agir. En 2012 un arrêté préfectoral interdit l'accès au site et, en 2014, le BRGM est mandaté pour réaliser un diagnostic environnemental du site de la Place-à-Gaz. Quatre campagnes d'échantillonnages seront effectuées entre avril 2014 et mars 2015. C'est à cette étude que se sont greffés les travaux présentés dans ce manuscrit.

3.3.2. Pollution du site

Les études effectuées depuis 2004 ont révélé des concentrations très élevées en As (17.5 %), en Zn (13.3 %), en Cu (1.7 %) et en Pb (2.6 %) dans la partie superficielle du sol correspondant aux résidus de l'incinération (Bausinger *et al*., 2007). Des teneurs assez élevées dans les sols sous-jacents (1,2-1,8 m de profondeur) et dans les eaux interstitielles (Baubron, 2004 ; Bausinger *et al*., 2007) ont été mises en évidence. Les sols contiennent également des composés nitro-aromatiques et des chlorates provenant d'explosifs et des dioxines et furannes chlorées et bromées. Deux autres informations importantes sur ce site sont à prendre en considération : l'arsenic semble se trouver principalement sous la forme inorganique As V et le pH du profil de sol est assez bas, entre 4,8 et 5,8 en subsurface au centre de la zone d'incinération.

La nature polluée de ce sol est mise en évidence par l'absence de végétation sur sa partie centrale. Seules trois espèces végétales se développent sur le reste du site, une mousse *Pohlia nutans* (Hedw.), un lichen *Cladonia fimbriata* (L.) et une herbacée *Holcus lanatus* (L.), toutes trois présentant des signes de tolérances à l'arsenic (Bausinger *et al*., 2007). L'extension de la pollution est marquée par la lisière de la forêt, le site forme ainsi une clairière de 1000 m^2 (Fig.1.19)

[5] La Destruction d'armes chimiques de la guerre de 14 a laissé des traces, Yves Miserey, Le Figaro, 2007
Arsenic et vieux obus : casse-tête en Meuse, Pascal Brocard, Le Républicain Lorrain, 2013.
Le poison de la Guerre coule toujours à Verdun, Benoît Hopquin, Le Monde, 2014.
14-18 : Le scandale enterré, Pierre Belet et Romain Fleury, Canal+, 2014.
Paysage en Bataille, RTBF, 2014

Chapitre II : Caractérisation et mobilité de l'arsenic et des métaux dans le sol de la Place-à-Gaz

Mesures de terrain et échantillonnage sur le site de la Place-à-Gaz

Introduction au chapitre II

Caractérisation et mobilité de l'arsenic et des métaux dans le sol de la Place-à-Gaz

Ce chapitre est rédigé sous la forme d'un article publié dans le journal *Science of the Total Environment* (STOTEN) en avril 2016. Il décrit la spéciation et la mobilité de l'arsenic et des métaux dans le sol de la « Place-à-Gaz ». Cet article est précédé d'une description de l'environnement de la Place-à-Gaz effectuée pendant les campagnes de terrains. Il a également fait l'objet d'une communication orale au congrès As2016, dont le résumé étendu est fourni en annexe 2.

Résumé graphique :

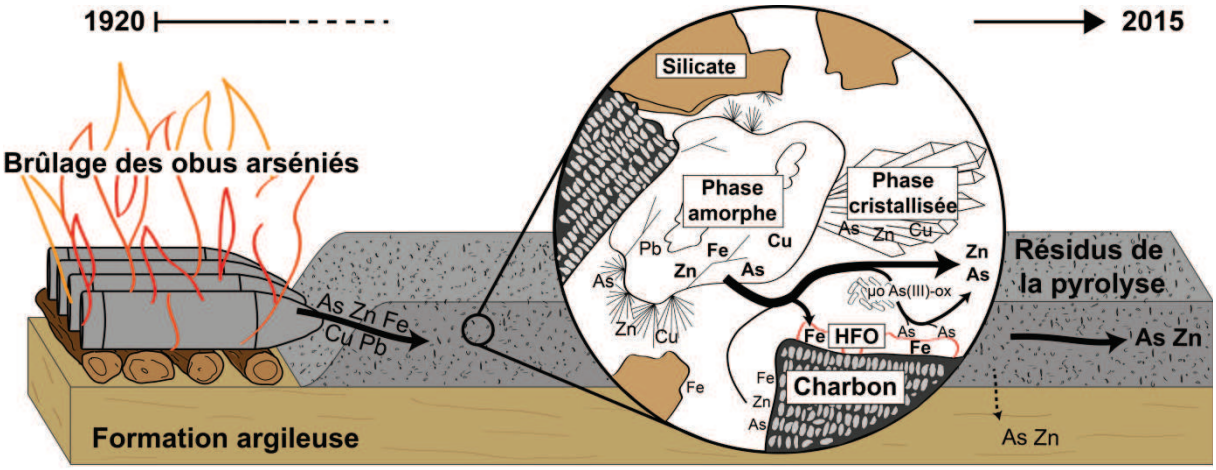

Résumé :

La destruction de munitions chimiques de la Première Guerre Mondiale a provoqué une contamination importante de la partie supérieure du sol de la Place-à-Gaz par l'arsenic et les métaux lourds. Le comportement biogéochimique de ces éléments est mal documenté dans ce type d'environnement. Quatre échantillons de sol présentant différents niveaux de contamination ont été prélevés. Le niveau de concentrations en As des échantillons était compris entre 1937 et 72820 $mg.kg^{-1}$. Les concentrations de Zn, Cu et Pb ont respectivement atteint 90190 $mg.kg^{-1}$, 9113 $mg.kg^{-1}$ et 5777 $mg.kg^{-1}$. Les concentrations importantes en argiles, héritées de la formation géologique sous-jacente et les quantités importantes de charbon de bois, liées à l'utilisation de bois de chauffage pendant la combustion, constituent un vaste réservoir de sites d'adsorption pour les métaux et l'arsenic. Cependant, les observations MEB-EDS ont montré que l'As et les métaux n'étaient pas, pour l'essentiel, liés

à ces phases mais associés entre eux dans des grains. Parmi ces grains riches en métaux, plusieurs phases ont été identifiées: des phases cristallisées, principalement des arséniates secondaires, et une phase amorphe riche en Fe, Zn, Cu et As. Les arséniates secondaires, identifiés par diffraction des rayons X, sont l'adamite et l'olivenite (respectivement des arséniates de zinc et de cuivre) et deux pharmacosidérites. Dans la partie centrale du site, le matériel amorphe est la principale phase porteuse de l'As et des métaux. Cet assemblage minéral singulier résulte probablement du traitement thermique des obus contenant des agents arsenio-arséniés. La caractérisation microbienne inclut des dénombrements de cellules totales, des tests de respiration, et la détermination de l'activité d'oxydation de l'As III. Les résultats ont montré la présence de microorganismes contribuant activement au métabolisme du carbone et de l'arsenic, même dans le sol le plus pollué, influençant ainsi le comportement de l'As biodisponible sur le site. Cependant, la mobilité de l'As est principalement corrélée à la disponibilité des sites d'adsorption des oxy-hydroxydes de fer.

Observations de terrain

Trois campagnes de terrain ont été réalisées pendant cette thèse sur le site de la Place-à-Gaz. La première campagne a eu lieu en juin 2014, elle a permis d'effectuer une première observation du site, une cartographie de l'étendue de la pollution et de prélever des échantillons de la surface du sol du site. Les résultats présentés dans cette partie du manuscrit proviennent de cette campagne de terrain La seconde campagne s'est déroulée en octobre 2014. Elle a permis, à l'aide d'une pelle mécanique, de creuser des fosses pédologiques afin d'établir des profils de sols, au droit et en dehors de la Place-à-Gaz. Un gros volume de la couche contaminée a été prélevé sur la partie centrale du site, afin d'effectuer une étude en mésocome (décrite dans la suite du manuscrit). Une dernière campagne a eu lieu en septembre 2015, pendant laquelle un échantillonnage de la litière organique forestière a été réalisé.

A. Description de la zone d'étude

La Place-à-Gaz est une clairière située en forêt domaniale de Spincourt, sur la commune de Gremilly à 20 km au nord-est de Verdun (Meuse, France). Le site est isolé en milieu forestier et ne fait actuellement l'objet d'aucun usage, cependant un cabanon témoigne de son utilisation passée par les gardes forestiers de l'ONF et par les chasseurs. La clairière a une superficie d'environ 2000 m^2 et correspond à la zone où ont été détruites les munitions (Fig.2.1.a). Des dépôts satellites ont également été observés dans la périphérie proche de cette « place ». Ceux-ci correspondent à d'anciennes fosses de combustion des imbrûlés. Ils sont riches en fioles contenant les arsines, en bouchons et en déchets divers issus des obus (Fig.2.2.b). Ces dépôts satellites font environ 50 à 70 cm de profondeur. Une deuxième zone peut être établie, à environ 40 m au nord de la clairière, où des éléments métalliques ont été retrouvés. Le sol de cette zone, recouvert par la litière, a une texture sablo graveleuse, et présente une couleur noire. Cette zone, d'une surface d'environ 400 m^2, peut correspondre à une aire de démontage et de brûlage de fusées.

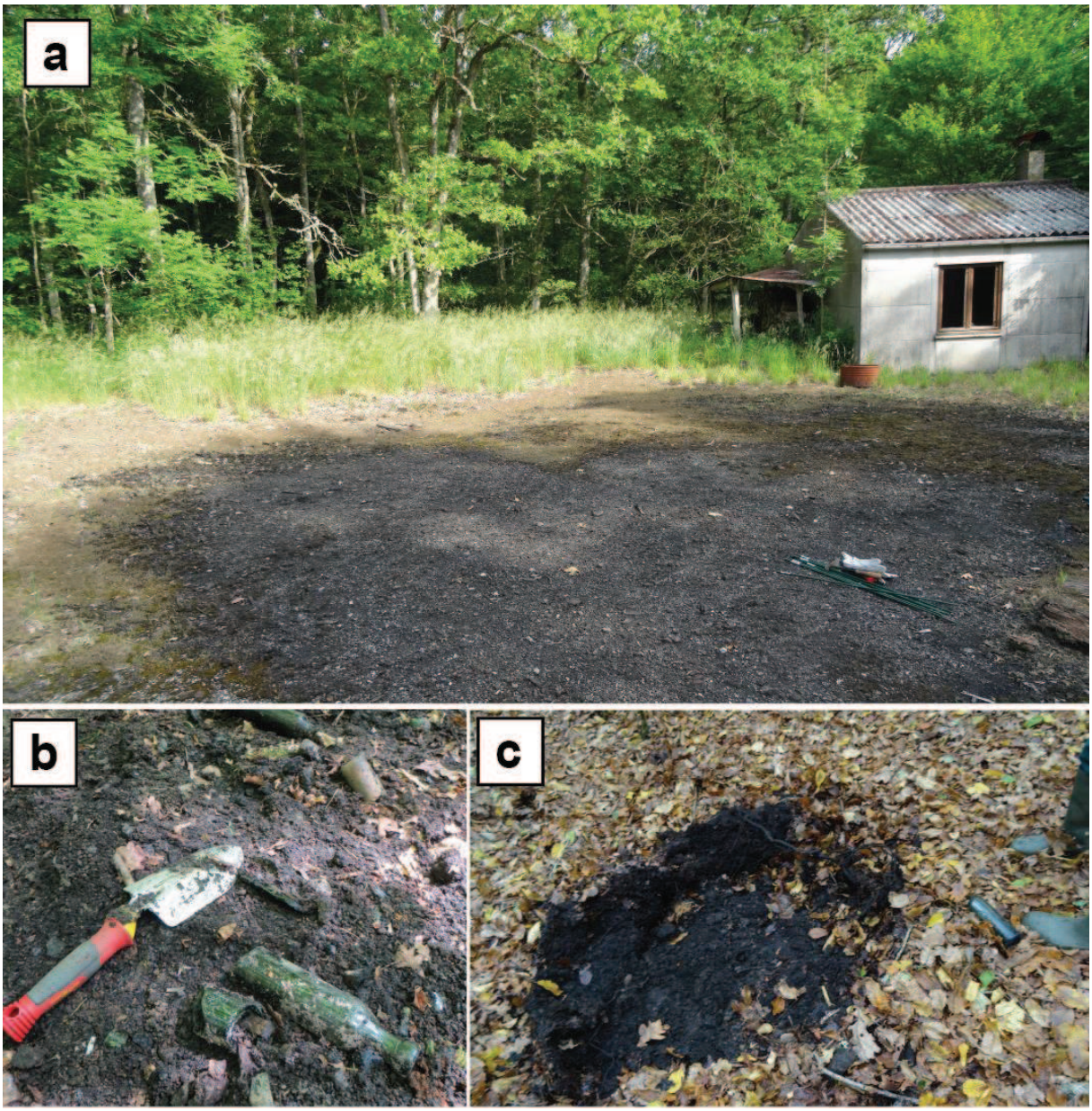

Figure 2.1 : *Photos a : de la clairière de la Place-à-Gaz (juin 2014). b : de fioles d'arsine retrouvées dans l'un des dépôts satellites (juin 2014). c : du sol de la zone nord, recouvert par la litière.*

B. Profil de sol

Cinq fosses pédologiques, effectuées à la pelle mécanique, ont permis d'étudier le profil de sol sur la place centrale (Fig.2.2). La surface du sol est recouverte par une couche noire composée de scories, charbons, cendres, éléments d'obus. Cette couche correspond aux résidus de brûlage. Elle s'étend sur toute la superficie de la clairière mais son épaisseur est variable. Au centre de la place, l'épaisseur de la couche est la plus importante et dépasse 40

centimètres (Fig.2.3.c). Son épaisseur diminue progressivement en s'éloignant du centre pour atteindre environ 5 cm. Le volume total de ces résidus est estimé à environ 1500 m^3.

Sous cette couche, un horizon gris compact, d'une épaisseur constante d'environ 5-10 cm, montre une structure en plaquettes centimétriques horizontales et contient des inclusions charbonneuses ainsi que des traces de racines. Cette couche était en contact direct avec le feu, et on peut se demander si son débit en plaquettes et son aspect compact sont liés à une « cuisson » du matériel d'origine.

En dessous, on retrouve le substrat argileux du sol appartenant à la formation des argiles de la Woëvre (Callovien). L'épaisseur de cette formation peut atteindre 200 m, au droit de la Place-à-Gaz, elle est estimée à environ 50 m. Ici, cette formation est de couleur brun orangé avec des zones grises, et présente une texture grumeleuse. De nombreuses traces de racines, d'aspect noir, et centrées sur les zones grises ont été observées (Fig.2.2)

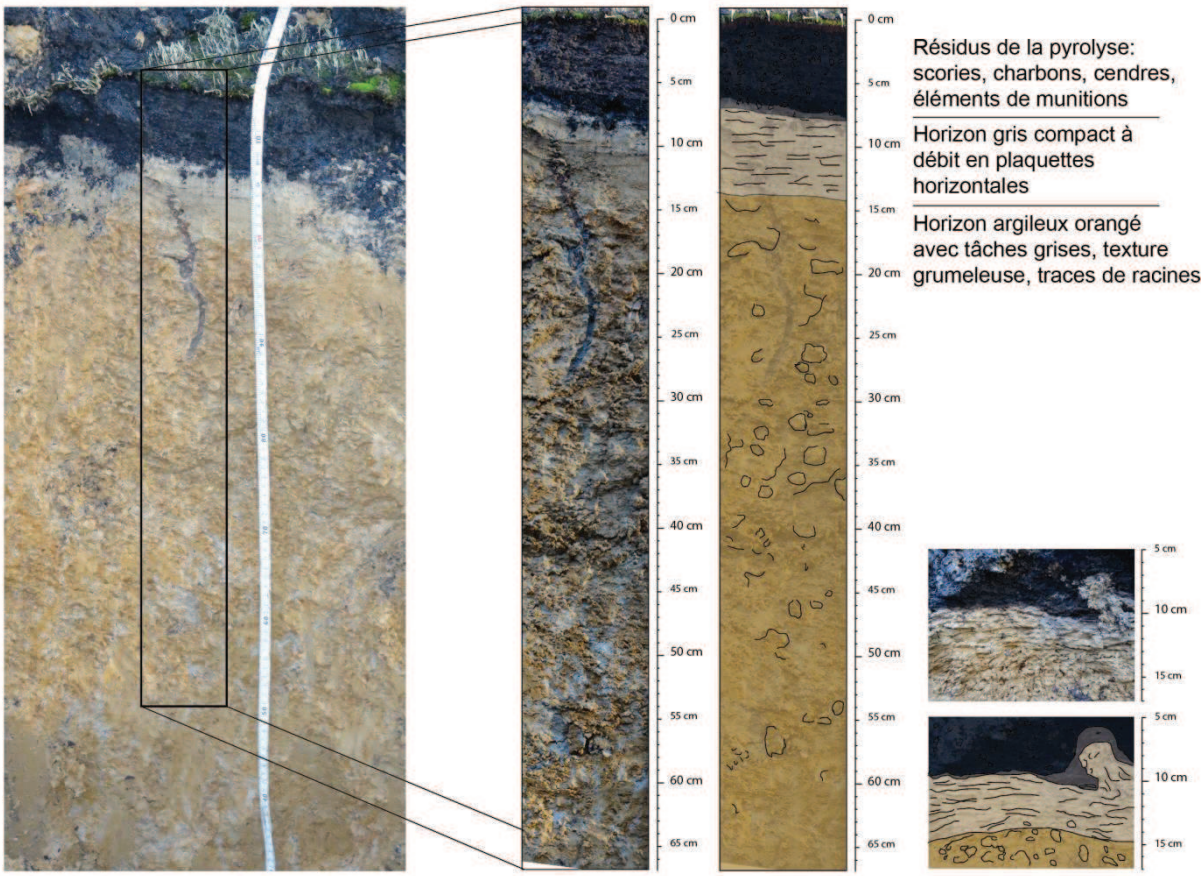

Figure 2.2 : *Profil de sol du site de la Place-à-Gaz.*

C. Zones humides et saturation du sol

La nature imperméable du substrat argileux, associée à la topographie du site, contribue à la formation de zones humides aux pourtours de la Place-à-Gaz. En juin 2014, pendant une période assez sèche, deux zones humides ont été observées au nord et au sud de la clairière, à la lisière de la forêt. Dans ces zones, la surface de l'eau était affleurante ou située à moins de 5 centimètres de la surface du sol (Fig.2.3.a). Pendant les périodes de fortes précipitations, la couche noire, correspondant aux résidus de la pyrolyse, se sature en eau. Cette saturation peut être totale, formant ainsi des flaques à la surface de la Place-à-Gaz (Fig.2.3.b). L'imperméabilité des argiles de la Woëvre a été vérifiée pendant notre deuxième campagne de terrain en octobre 2014. En effet, en l'espace de quelques heures de précipitations, les fosses pédologiques se sont remplies d'eau, et après une nuit, le niveau d'eau dans celles-ci n'avait pas varié (Fig.2.3.c).

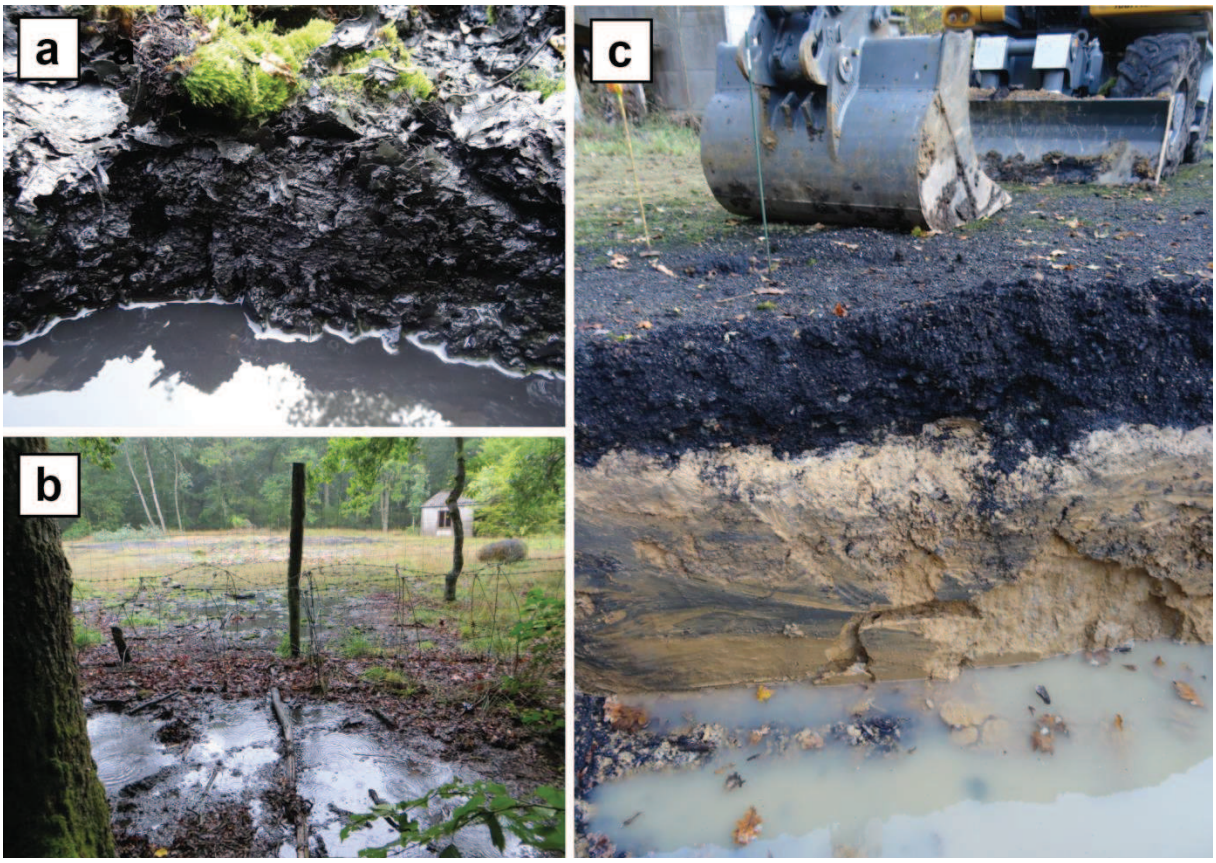

Figure 2.3 : *a: Niveau saturé dans la zone humide situé au sud de la clairière (juin 2014). A noter l'accumulation de litière organique. b : Vue du site pendant un épisode de précipitation intense en septembre 2015. c : Accumulation d'eau dans une fosse pédologique liée au caractère imperméable des argiles de la Woëvre (octobre 2014).*

D. Végétation et apports de litière organique

La Place-à-Gaz n'est pas entièrement colonisée par la végétation, sa partie centrale restant nue depuis la destruction des obus. Les espèces végétales observées sur le site sont les mêmes que celles décrites par Baussinger *et al*. (2007), c'est-à-dire : une mousse *Pohlia nutans* (Hedw.), un lichen *Cladonia fimbriata* (L.) et une herbacée *Holcus lanatus* (L.). Entre 2007 et 2014, l'implantation de ces espèces semble avoir évolué, avec une végétalisation progressive de la clairière de sa périphérie vers son centre. Cette fermeture du milieu est accélérée par la formation de litière, déposée par les arbres entourant la zone. L'accumulation de litière peut être importante (Fig.2.3.a et b), mais impacte seulement la circonférence de la clairière. La forêt domaniale de Spincourt, au droit du site, est essentiellement composée de chênes et de hêtres, la litière est donc principalement issue de ces arbres feuillus.

Chapitre II: Characterization and mobility of arsenic and heavy metals in soils polluted by the destruction of arsenic-containing shells from the Great War.

Hugues Thouin [a,b], Lydie Le Forestier [b], Pascale Gautret [b], Daniel Hube [a], Valérie Laperche [a], Sebastien Dupraz [a], Fabienne Battaglia-Brunet [a,b].

[a] BRGM, 3 avenue Claude Guillemin, 45060 Orléans, France

[b] Université d'Orléans, ISTO, UMR 7327, 45071 Orléans, France, and CNRS, ISTO, UMR 7327, 45071 Orléans, France, and BRGM, ISTO, UMR 7327, BP 36009, 45060 Orléans, France

Abstract

Destruction of chemical munitions from World War I has caused extensive local top soil contamination by arsenic and heavy metals. The biogeochemical behavior of toxic elements is poorly documented in this type of environment. Four soils were sampled presenting different levels of contamination. The range of As concentrations in the samples was 1,937–72,820 mg.kg^{-1}. Concentrations of Zn, Cu and Pb reached 90,190 mg.kg^{-1}, 9,113 mg.kg^{-1} and 5,777 mg.kg^{-1}, respectively. The high clay content of the subsoil and large amounts of charcoal from the use of firewood during the burning process constitute an ample reservoir of metals and As- binding materials. However, SEM-EDS observations showed different forms of association for metals and As. In metal-rich grains, several phases were identified: crystalline phases, where arsenate secondary minerals were detected, and an amorphous phase rich in Fe, Zn, Cu, and As. The secondary arsenate minerals, identified by XRD, were adamite and olivenite (zinc and copper arsenates, respectively) and two pharmacosiderites. The amorphous material was the principal carrier of As and metals in the central part of the site. This singular mineral assemblage probably resulted from the heat treatment of arsenic-containing shells. Microbial characterization included total cell counts, respiration, and determination of As III-oxidizing activities. Results showed the presence of microorganisms actively contributing to metabolism of carbon and arsenic, even in the most polluted soil, thereby influencing the fate of bioavailable As on the site. However, the mobility of As correlated mainly with the availability of iron sinks.

Keywords: Chemical ammunition destruction, Soil contamination, Metals, Arsenates, Microbial As III-oxidation

1. Introduction

Almost 100 years after the end of the First World War the scars of battle can still be observed along the front line. Hupy and Schaetzl (2008) have studied the effect of shelling on soil structure and landscape recovery after the conflict. The First World War was the first incidence of major warfare that made massive use of chemical weapons. However, very little information is available on the chemical impacts of the conflict on soil, groundwater or wildlife. High concentrations of metals in living organisms and the presence of perchlorate in groundwater along the red zone nevertheless reflect a real impact of this war on the environment (Hube, 2013; Prefectoral decree, Pas de Calais, 25 October 2012).

In the early 2000s, several sites where First World War chemical weapons were destroyed were found to be contaminated by inorganic pollutants. Only two of these were investigated: the first is located in Belgium (Bausinger and Preuβ, 2005), the second is northeast of Verdun, in France (Bausinger *et al*., 2007). Chemical shells were disposed of by burning on both of these sites during the 1920s. The munitions destroyed were mainly "blue cross shells" containing organoarsenic warfare agents. The Belgian burning ground has since been used for agriculture (Bausinger and Preuβ, 2005) but the French site, named "Place-à-Gaz", has been unaffected by human activities and undisturbed since destruction of the shells.

Bausinger *et al*. (2007) showed that the "Place-à-Gaz" had locally limited but severe soil contamination by arsenic, zinc, copper and lead, with concentrations reaching respectively 150 g/kg, 130 g/kg, 15 g/kg and 25 g/kg. The metals came from various parts of the munitions. Shells contained mainly iron, while fuses, driving bands and shell casings were made from copper or zinc. Lead was used for shrapnel balls, primary explosives and chemical warfare equipment. "Blue cross shells" were filled with diphenylchloroarsine (Clark I) and diphenylcyanoarsine (Clark II). These organoarsenic molecules were probably oxidized during the combustion, releasing huge amounts of inorganic arsenic into the surrounding environment. Bausinger *et al*. (2007) estimated that, over a century, most of the arsenic oxides have been transformed into arsenates or sorbed onto iron oxides or clays, abundant in the inherited soil.

The primary factor influencing mobility of heavy metals in these soils appeared to be pH (Bausinger *et al*., 2007). Under the site conditions, the soil pH varied from 5 to 6, which favored Cu and Pb fixation in soil, while Zn was more mobile and leached. Arsenic was less affected by pH and behaved differently from metals. However, As concentrations in

interstitial waters (c_{mean}=838 µg/L) were significantly higher than the maximum contaminant level (MCL) of arsenic in drinking water as recommended by the World Health Organization (WHO) in 1993, i.e. 10 µg/L. The mobility of As on the site thus required further investigation.

Arsenic is mainly found in the environment as inorganic species, arsenate As V and arsenite As III (Cullen and Reimer, 1989). Microbial activities play a major role in As speciation in soil. Different bacterial mechanisms are responsible for As III oxidation or As V reduction (Santini *et al*., 2000, Stolz *et al*., 2002), thus altering As mobility, toxicity and bioavailability (Pierce and Moore, 1982, Masscheleyn *et al*., 1991). The bacterial activity on former ammunition destruction sites has not been documented to date, but biogeochemistry may explain As speciation and mobility in such environments.

Organic matter, which can have high concentrations in soil (up to 25%), may drive the mobility of metals and arsenic on the site (Bausinger *et al*., 2007). Indeed, the organic compounds may contain adsorption or complexation sites or induce methylation of metals and metalloids (Saada *et al*., 2003, Park *et al*., 2011, Huang *et al*., 2012). The presence of organic matter also affects bacterial activity. A recent study has shown that As III-oxidizing activity in polluted soil can be influenced by the amount of bioavailable organic matter (Lescure *et al*., 2016).

Bausinger *et al*. (2007) explored the mobility of inorganic pollutants in the "Place-à-Gaz" ground material by sequential extractions. These experiments provided indirect information on the carrier phases but no direct information was available on the mineralogy of soil materials. Moreover, arsenic speciation was not directly determined and no data were available on the activity of microorganisms in this type of heavily polluted soil. Our work focused on the mineralogy, particle size and the geochemistry of the "Place-à-Gaz" surface soils, in order to better understand the behavior of inorganic pollutants on sites polluted by the destruction of chemical weapons. These data were also linked with the mobility of pollutants and biogeochemical parameters.

2. Materials and methods

2.1. Study site

The study site, known as "Place-à-Gaz", is located in the Spincourt forest, 20 km northeast of Verdun, France (Bausinger *et al*., 2007). At the end of the First World War large amounts of shells and ammunition were stored in the region. In 1920, the Pickett and Fils company was commissioned by the French Ministry of War to destroy these munitions. 200,000 German chemical shells were opened and burned in piles at the center of this area in 1928. The fire was fueled by wood covered with explosive materials.

2.2. Chemical characterization and soil sampling

Total concentrations of As, Cu, Zn and Pb were determined in situ using XL3t800 NITON© portable X-ray fluorescence field apparatus (pXRF), in order to defined the metal(loid)s distribution and to targeted the soil sampling. The signals were calibrated with the chemical analyzes of the soil samples and considered the soil moisture. Maps of As, Cu, Zn and Pb concentrations were drawn by interpolating data by kriging (ArcGIS©).

Four soils were sampled in the surface, non-saturated black layer (0–10 cm) in zones with contrasting vegetation cover. The soils were sieved at 2 mm through sterile sieves, placed in in sterile glass jars and stored at 5°C. Their water content was determined by drying at 105°C for 24h. In order to study the chemical composition of different particle size fractions, soil sub-samples were separated into three fractions by mechanical sieve shaker: coarse sand (>200 µm), fine sand (50–200 µm) and loam and clay (<50 µm).

2.3. Soil chemistry and mineralogy

For chemical and mineralogical analyses, the raw soils and particle fractions were ground to 70 µm. Major elements were determined by inductively coupled plasma (ICP) atomic emission spectroscopy (AES) using a Thermo Fischer ICap 6500; trace elements were determined by ICP-mass spectrometry (MS) on a Siex Perkin-Elmer Elan 5000a, both analyses being conducted at the *Service d'Analyses des Roches et des Minéraux* (*SARM* – rock and minerals analysis unit of the *CRPG-CNRS* national research institutes). Prior to analysis, the samples were fused with $LiBO_2$ and dissolved in a mixture of 1 N HNO_3, H_2O_2 and glycerol. Organic carbon (C_{org}) and total S were also determined at the SARM center, by carbon and sulfur determination on a Leco SC144 DRPC (SARM, CRPG-CNRS). The mineralogical composition was determined by X-ray diffraction (XRD). XRD patterns were

recorded between 0° and 90° (2θ) at a scan rate of 0.3° 2θ cm^{-1} using an INEL CPS120 diffractometer equipped with a Co anode (Co $K\alpha_1$ = 1.78897 Å).

Scanning electron microscopy (SEM) and energy dispersive X-ray spectroscopy (EDS) were performed to explore the composition and distribution of metals and As in the four soils. SEM was performed on a TM 3000 accompanied by a SwiftED3000 X-Stream module (Hitachi), and operated at 15 kV accelerating voltage. The acquisition time of EDS analyses was 300 s per sample.

2.4. Leaching and percolation tests

Leaching tests provide information about the mobility of metal and As from soil towards the water phase. The four wet soil samples were mixed with ultrapure water, with a solid/liquid ratio of 1 to 10 (wet soil equivalent to 25 g dry soil, 250 mL of ultrapure water), and the tubes were rotated on a roller mixer for 24 h. The leaching solutions were filtered at 0.45 µm then acidified with 10% of HNO_3. Fe, Cu, Zn and Pb concentrations were determined using an atomic absorption spectrophotometer (AAS, Varian, Palo Alto, CA, USA).

The leaching test was not suitable for evaluation of the speciation of soluble As, because some As III may be oxidized during the 24 h leaching test. A percolation test was performed to determine the speciation of soluble As in conditions close to those of the site. The soil (as wet soil equivalent to 1 g dry soil) was placed in a 5 mL syringe (diameter 13 mm) equipped with a rock wool stopper, without packing. Percolation experiments were performed in triplicate for each soil. 25 mL of a weakly mineralized spring water (Mont Roucous, pH 5.85; 3.1 $mg.L^{-1}$ Na^+; 2.4 Ca^{2+}; 0.5 Mg^{2+}; 2.0 SO_4^{2-}; 6.3 HCO_3^-; 3 NO_3^-), used to simulate rain water, was fed in drops onto the surface of the soil in the syringe. Percolation water was recovered and filtered at 0.2 µm. As III and As V were immediately separated using an ion exchange method (Kim, 2001). Separation was performed on anionic resin (AG 1-X8©, Biorad, Hercules, CA, USA). A sample of percolation water filtered at 0.2 µm was acidified for total As determination. Arsenic was quantified with an AAS oven (Varian, Palo Alto, CA, USA).

A specific leaching test was applied to particles coated with materials in the amorphous phase. Soil particles, previously observed by SEM, were incubated in 0.25 M hydroxylammonium chloride and 0.25 M HCl for 10 minutes. The particles were observed again by SEM after the leaching step.

2.5. Bacterial enumeration

Total bacteria were extracted from soils using a Nycodenz gradient separation method (Bertrand *et al*., 2005) and enumerated after fluorescent DAPI staining, as described in Kumar *et al*. (2013).

As III-oxidizing bacteria were enumerated by the Most Probable Number method. The soil (as wet soil, equivalent to 0.2 g dry soil) was placed in a sterile, glass Erlenmeyer flask with 10 mL of sterile physiological saline (9 $g.L^{-1}$ NaCl in demineralized water), agitated for 30 min at 25°C, then sonicated 2 x 20 s at 45 kHz. Triplicate suspensions were prepared for each soil. The soil suspension was diluted in stages in sterile physiological saline to a dilution of 10^{-7}. CAsO1 mineral medium (Battaglia-Brunet *et al*., 2002) containing 100 $mg.l^{-1}$ As III was distributed over Microtest TM Tissue culture plates (96 wells), 250 µL per well. Each well was inoculated with 25 µL of diluted soil suspension. Five wells were inoculated with each dilution. Culture plates were incubated at 25°C for 10 days. The presence of As III in the wells was revealed by the formation of As III-PyrrolidineDithioCarbamate (PDC), an insoluble white complex: 150 µL of 0.1 M acetate buffer (pH 5) and 100 µL PDC solution (5 g L^{-1}) were added to each cell. A white precipitate appeared when As III was present, i.e. when As III-oxidizing bacteria were absent (negative well). Non-inoculated wells served as negative blanks while wells containing CAsO1 medium with 100 $mg.L^{-1}$ As V provided a positive reference. The number of positive wells for each dilution was determined, and the most probable number of bacteria in dilutions was given by Mc Grady table for five tubes.

2.6. As III-oxidizing activity tests

The four samples were incubated at 25°C for 72 h before starting the tests. The As III oxidizing tests were performed in 250 mL Erlenmeyer flasks filled with 100 mL of CAsO1 medium (Battaglia-Brunet *et al*., 2002) supplemented with 1 mM As III and inoculated with a mass of material equivalent to 0.2 g of dry weight. Flasks were plugged with cotton to retain oxidizing conditions and were incubated at 25° under agitation (100 rpm). The flasks were sampled each day, and twice a day during As III oxidation. Samples were filtered at 45 µm and frozen at -20°C until As III/As V separation was performed. Tests were performed in triplicate. As V was quantified by flame AAS (Varian, Palo Alto, CA, USA), after As III/As V separation with the PDC/MIBK method (Battaglia-Brunet *et al*., 2002). First order As III oxidizing rate constants were determined by linear regression fitting of the As V versus time line, during the reaction.

2.7. Mineralization of biological carbon

The biodegradability of intrinsic organic matter was studied via CO_2 emission (soil respiration), as per Rey *et al*. (2005). The equivalent of 100 g of dry weight, adjusted to 80% of water holding capacity, was placed in 250 mL serum flasks. Samples were incubated at 25°C. After one week of stabilization, flasks were sealed hermetically with rubber stoppers and gas samples were taken weekly for 5 weeks via the septum with a double-needle blood collection tube and a vacuum tube (Vacuette®, Greiner Bio-one). The soil moisture was kept constant by adjusting the water content to the initial mass each week. CO_2 concentration in the gas phase was analyzed with a Varian 3400 gas chromatograph using thermal conductivity detection.

Carbon mineralization rates were calculated from the linear increase of CO_2 concentration in flasks over time. The specific carbon mineralization rate was calculated as the carbon mineralization rate / total soil organic carbon ratio.

2.8. Statistical tests

Statistical analyses were performed using the XLSTAT (Addinsoft) software. Data were tested for homogeneity of variance and normal distribution. One-way analysis of variance (ANOVA) and Tukey HSD (Honestly Significantly Different) tests were carried out to test for any significant differences between the means. Differences between means at the 5% level ($P<0.05$) were considered significant.

3. Results

3.1. Site characterization

The "Place-à-Gaz" has a surface area of 2000 m (Fig.2.4.a.1). The soil surface is covered by a black layer containing slag, coal, ash and residues from the pyrolysis of munitions (Fig.2.4.a.2). The thickness of this layer varies from a few centimeters at the edge of the zone to around 40 cm at the center of the site (Fig.2.4.a.3). The substrate beneath the black layer is a clayey Woëvre formation (Callovian age) with a thickness of around 200 m. These clays seriously limit the infiltration of rainwater, which will tend to run off to wetlands in low-lying areas at the periphery of the site (Fig.2.4.a). The height of annual precipitation in the study area is 758 mm and the annual average temperature is 10.7 °C (data from Météo France, Metz station).

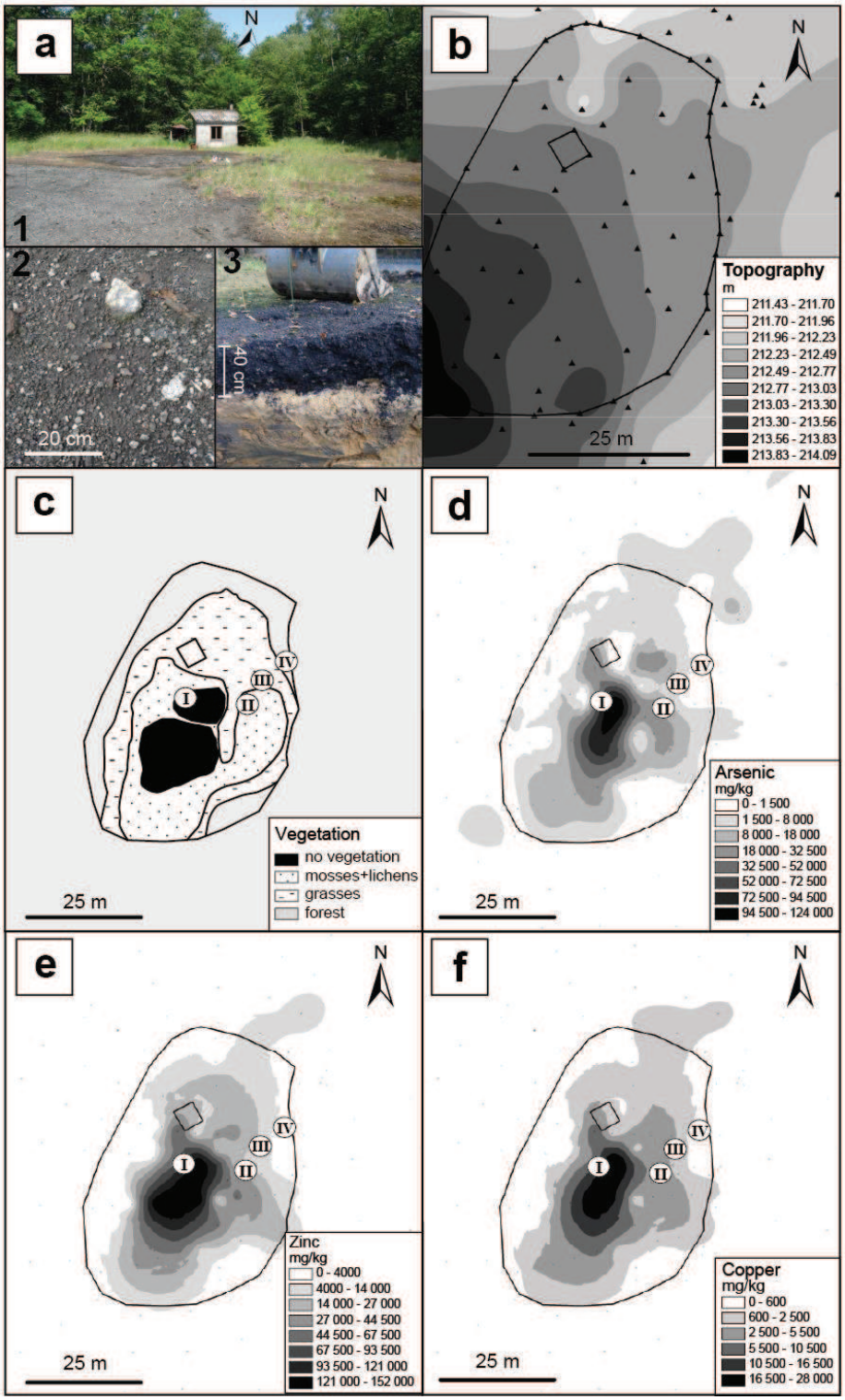

Figure 2.4 : *Situation and contamination of the study site. a.(1): overview of the "Place-à-Gaz"; a(2): black layer surface; and a(3): soil profile with black layer overlying Woëvre formation clays. b: topography of the study area. c: implantation of vegetation. Roman numerals represent soil sample locations. d,e,f: maps of concentrations of As, Zn and Cu at the soil surface, measured with pXRF.*

The central part of the site has not been colonized by plants (Fig.2.4.a and c). The first colonizing species was *Pohlia nutans* mosses. A species of lichen, *Cladonia fimbriata*, and an herbaceous plant, *Holcus lanatus*, are implanted on the outer areas, growing on mosses. The surface area of the bare zone seems to have declined since the Bausinger *et al*. (2007) study, indicating progressive revegetation of the site.

The central part of the burned area was heavily contaminated by zinc, copper and arsenic. Intensity of contamination decreased progressively towards the edge of the forest, as shown by As, Cu and Zn maps (Fig.2.4.d, e and f). For Pb mapping (given in SM 2.1) the interpolating kriging was conducted with five high-Pb-concentration measuring points in the northeast of the site, at the extremity of the sampling fields, which induced a nugget effect. These high Pb concentrations were measured in a peripheral deposit of shell fragments; however, the pollution gradient was still observable in the burned ground.

3.2. General soil characteristics and elemental composition

The four soil samples studied were taken from zones with contrasting pollution levels and different vegetation cover (Fig.2.4.c, d, e and f): soil I, with no vegetation, was the most contaminated; soil II, covered by mosses and lichens, was less contaminated; soil III was covered by grasses; and soil IV, covered by forest vegetation and humus, was the least contaminated.

All four soils contained 25–40% of fine sand (SM 2.2) but soil IV had a different texture with a lower proportion of coarse sand and a higher proportion of fine particles (clay and loam). The lowest proportion of fine particles was found in soil I. Electrical conductivity was similar for all soils (around 10 $mS.cm^{-1}$) but the pH of soil I (5.3) was lower than that of the others (5.8–5.9).

Concentrations of elements in the surface material samples are given in Table 2.1. Contamination of the soils by As, Zn and Cu decreased in the following order: sample I < sample II < sample III < sample IV. Concentrations of As vary between 72,820 and 1,937 mg/kg, Zn concentrations between 90,190 and 10,660 mg/kg and Cu concentrations between 9,113 and 1,451 mg/kg. Lead behaved differently, with a greater concentration in sample II: 5,777 mg/kg. Metals and arsenic were found mainly in the coarse and fine sand fractions, while Si, Al and K were most present in the loam and clay fraction. An important concentration of organic carbon was measured in sample I: 25.87%.

Table 2.1 : *Chemical analyses of the four soil samples.*

Sample	Particle size fractions	Major (%)										Trace (mg/kg)							
		SiO_2	Al_2O_3	Fe_2O_3	CaO	K_2O	P_2O_5	MnO	MgO	Corg	S total	As	Cu	Pb	Zn	Ba	Cd	Cr	Sn
I	Bulk	13.62	2.29	11.13	0.61	0.42	0.38	0.10	0.15	25.87	0.13	72820	9113	3830	90190	743.4	158.9	57.6	308.1
	CS	6.65	1.86	14.87	0.51	0.23	0.35	0.09	0.11	21.58	0.14	74870	12680	4331	152200	448.4	224	40.6	324.3
	FS	16.16	2.64	11.97	0.6	0.5	0.44	0.10	0.18	21.12	0.12	83090	8929	4526	84520	779.1	127.3	56.3	318
	L&C	26.06	3.09	10.17	0.59	0.71	0.39	0.09	0.20	19.89	0.1	67270	7331	3661	68330	993.4	109.1	104.6	323.6
II	Bulk	50.15	4.83	6.19	0.64	1.22	0.29	0.06	0.28	12.26	0.11	30840	5082	5777	37310	453.4	76.8	77.1	138.8
	CS	18.24	3.39	12.26	1.1	0.56	0.4	0.09	0.29	23.33	0.21	57840	8736	9325	61730	477.8	136	58.5	219.7
	FS	42.57	4.54	6.92	0.72	1.11	0.34	0.08	0.29	14.39	0.14	41900	6501	8012	40210	502.9	95.9	69.5	175.5
	L&C	66.17	5.48	4.08	0.49	1.52	0.21	0.04	0.29	5.63	0.07	21310	3106	3927	23610	465.1	48.1	98.7	109.1
III	Bulk	69.61	6.72	4.99	0.45	1.75	0.18	0.07	0.42	3.69	0.04	6253	1591	2528	10660	296.1	18	84.4	45.9
	CS	61.11	6.7	10.66	0.79	1.64	0.21	0.12	0.46	4.03	0.06	9793	3009	4379	19550	395.2	30.5	94.5	71.9
	FS	69.19	6.52	4.53	0.44	1.76	0.2	0.07	0.41	4.26	0.05	8480	1863	3620	12610	380.2	23.9	97.1	56.6
	L&C	75.85	6.8	2.9	0.38	1.83	0.15	0.04	0.40	2.55	0.03	4055	1078	2102	7257	345.3	12.9	120.1	34.9
IV	Bulk	58.85	7.2	4.08	0.62	1.73	0.27	0.15	0.53	8.44	0.07	1937	1451	968	13270	312.5	26.2	97.3	43.6
	CS	36.41	5.77	7.63	0.88	1.2	0.4	0.32	0.47	17.3	0.1	3612	2795	2007	24540	262.9	49.7	79.8	59.7
	FS	52.89	7.13	4.34	0.64	1.65	0.33	0.22	0.55	10.64	0.08	8469	2042	1427	12670	354.3	30.1	89.7	48.4
	L&C	67.57	7.5	3.42	0.47	1.88	0.21	0.07	0.52	5.3	0.05	1436	991.8	646	9284	321.8	17.6	111.8	39.2

CS: coarse sand. FS: fine sand. L&C: loam and clay.

3.3. Textural characterization, microscopic observation and EDS analysis

Several types of grains were observed in the four soils. Millimetrics to micrometric grains with tabular structure were observed in all soils, as well as aggregates of the smallest grains (Fig.2.5.a). These grains, present in greater proportions in soils III and IV, were identified as potassic and sodic aluminosilicate phases. No traces of metal(loid)s, except Fe, were detected by EDS analyses. Black grains, mainly in soils I and II, presented a wood structure with cell porosity, and high carbon contents (Fig.2.5.b). These grains were indentified as charcoals. Many micrometric particles were present at the charcoal surfaces, and may be composed by a mixture of Si, Al and Cl, associated with small amounts of metal(loid)s (Fe, Zn, As).

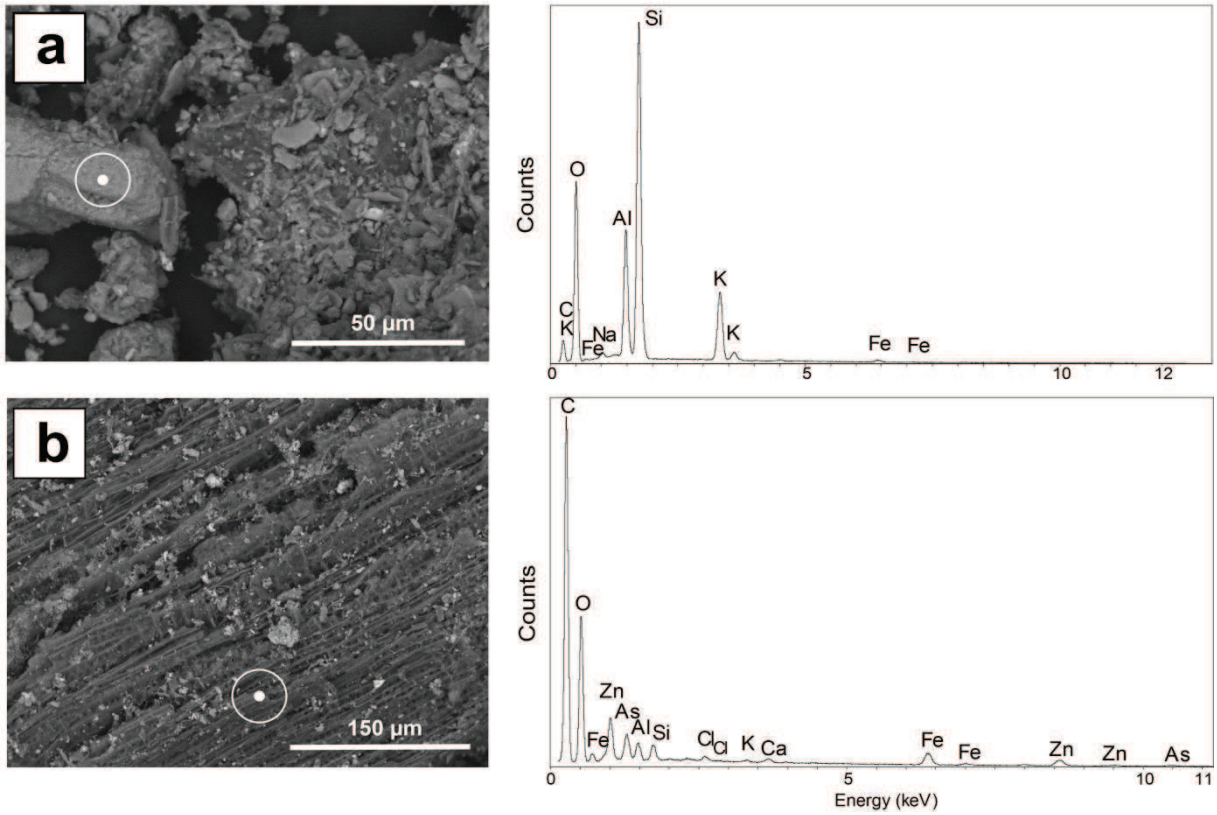

Figure 2.5: *Observation and composition of inherited silicates and charcoals from black layer. a: backscattered electron images and EDS spectrum of a silicate mineral from soil sample IV. This grain was mainly composed of Si, Al and O. K and Na were also detected. The only metal(loid) detected was Fe. b: SEM picture and EDS analysis of a charcoal grain from soil sample I. These grains were identifiable by their woody structure, and contain carbon associated with. The EDS spectrum indicated charcoal containing many small quantities of elements, particularly Fe, Zn and As. The targets correspond to the location of EDS elemental analysis.*

White and/or green-blue crystalline materials were observed in the macroporosity of soil I, and were characterized by a prismatic texture (Fig.2.6.a and b), on an acicular texture (Fig.2.6.c and d). As revealed by SEM/EDS analyses, the prismatic crystals mainly contained O, Zn and As (Fig.2.7.a), whereas acicular minerals were composed of an assemblage of O with Zn, As and Cu (Fig.2.7.b). The soil I was also characterized by large amorphous phases (Fig.2.6.e, f, g and h), with contrasting colors (yellow, red, white), covering diverse soil particles (charcoal, silicates, metallic fragments of shells), and forming aggregates. The surface of the amorphous phases presented semi-spherical nodules and micro-cracks (Fig.2.6.f).

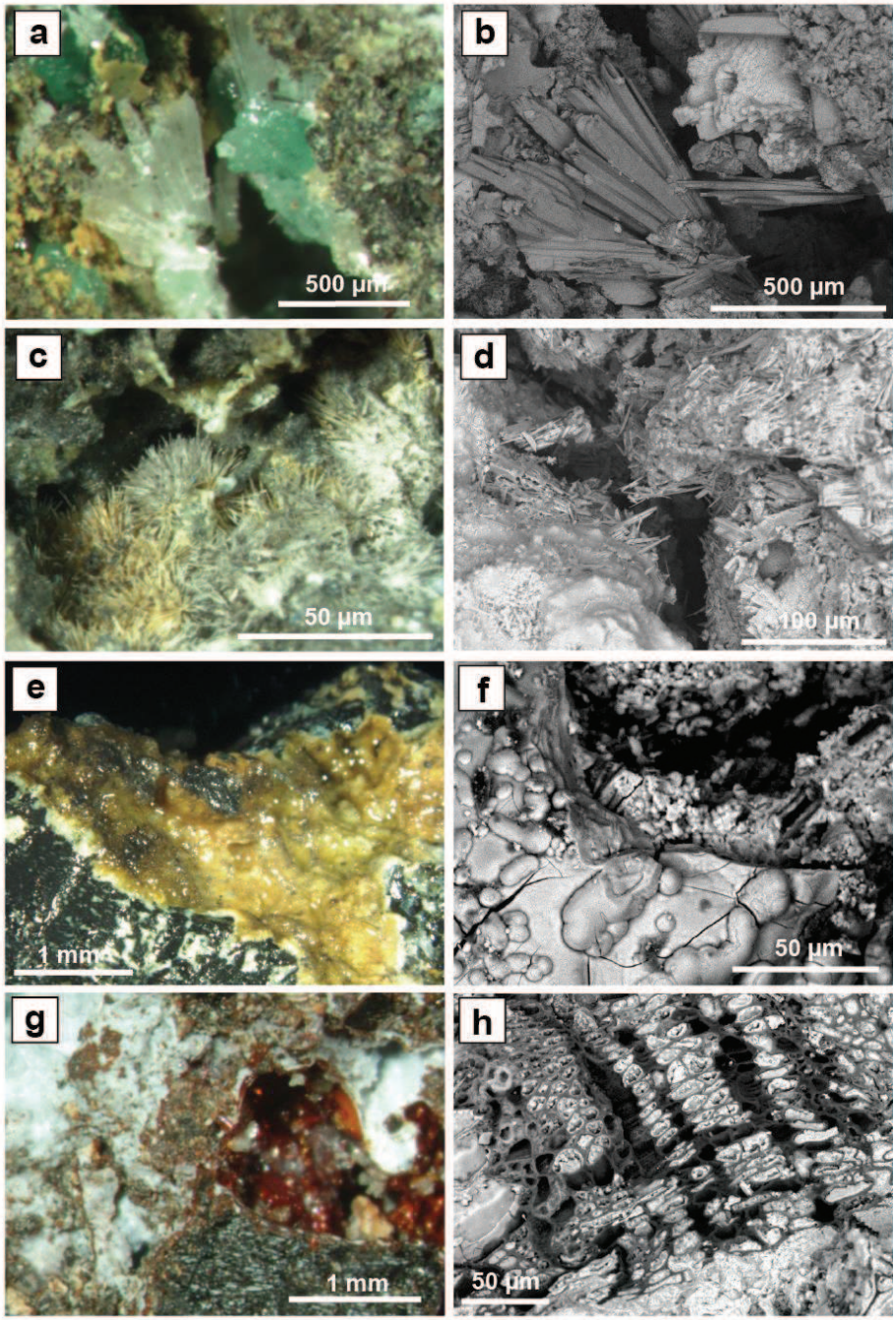

Figure 2.6: *Microscopic pictures of crystalline and amorphous phases of soil sample I. On the left, (a,c,e and g) binocular magnifier pictures, and on the right (b,d,f and h) SEM pictures. a and b: white prismatic crystals and green-blue crystals formed in the porosity. c and d: white acicular crystals with radial intergrowth. e: grain of charcoal covered with yellow amorphous phase. Its surface was smooth. f: SEM view of surface of the amorphous phases. This one is covered by semi-spherical nodules and micro-cracks. g: white and red amorphous phases close to a charcoal grain whose porosity was filled by white amorphous phases. h: high-resolution image of this wood charcoal.*

The agglomerates of micrometric spheres were also observed in the porosity (Fig.2.7.c), and are composed by a blend of Fe, As, Zn, Cu and Al (Fig.2.7.c). Incubation of grains, from soil sample I, in hydroxylammonium chloride and HCl resulted in the total or partial dissolution of the amorphous material (Fig.2.8).

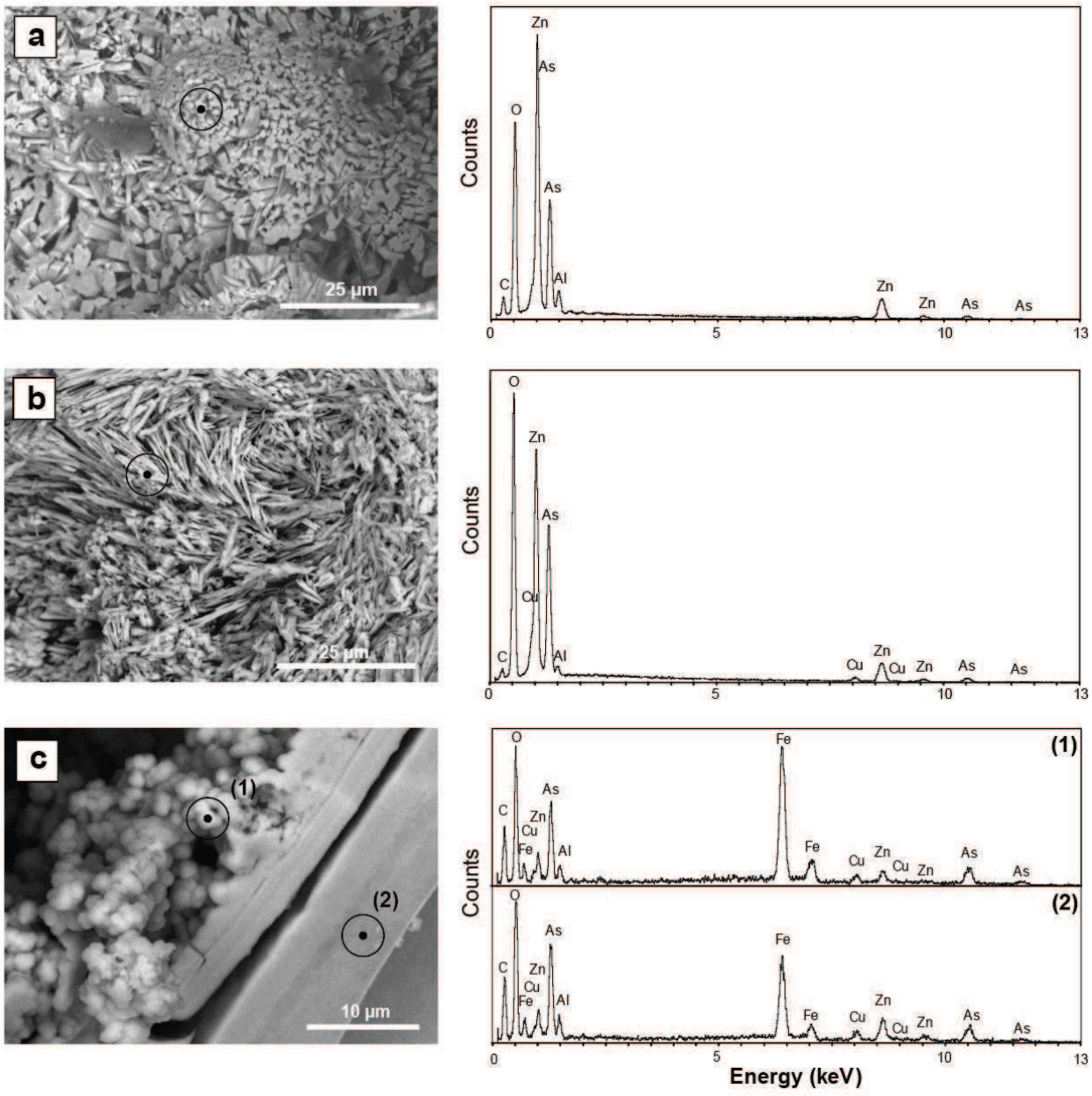

Figure 2.7: *Observation and composition of crystallized mineral and amorphous phase carriers of metal(loid)s. Soil sample I SEM images with elemental spectra of As carrier crystallized minerals with Zn (a) and Zn + Cu (b). c: iron-rich amorphous phases with spheres, carrier of As, Cu and Zn. The targets correspond to the location of EDS elemental analysis.*

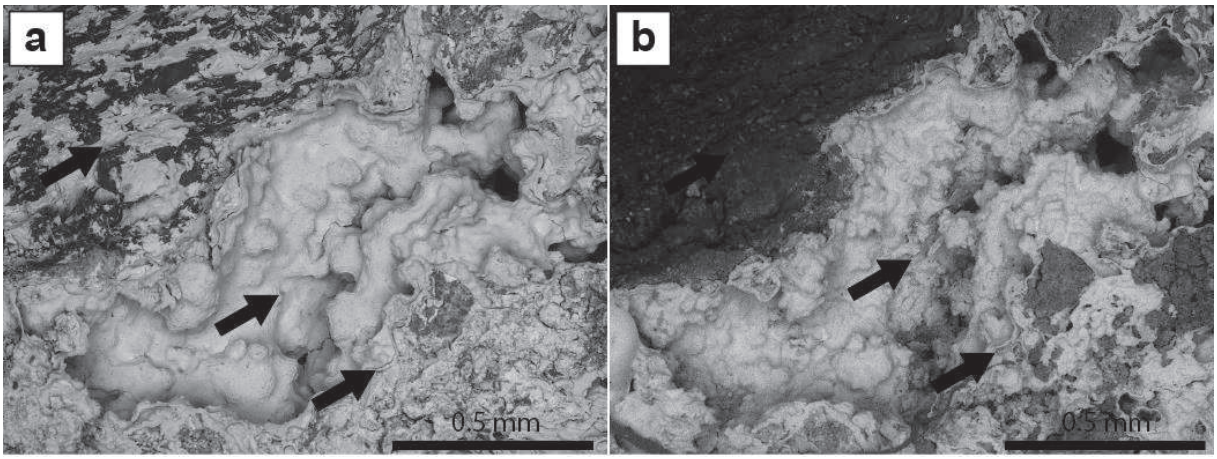

Figure 2.8: *SEM pictures showing effect of hydroxylammonium chloride and HCl on amorphous phases of soil sample I. a: grain of soil covered by amorphous phase. b: the same sample after 10 minutes in 0.25 M hydroxylammonuim chloride + 0.25 HCl solution. The amorphous phases that covered charcoal (top arrow) and silicate grains (bottom arrow) were totally dissolved. The surface of the thicker amorphous phase covering the cavity (middle arrow) was partially dissolved.*

3.4. Soil mineralogy

The crystallized phases from the four samples were investigated by XRD analysis for the different size fractions (Fig.2.9). Quartz, a ubiquitous mineral, was present in the four soils. Potassium and sodium feldspars were detected in samples from soils II, III and IV. Clays were detected in soil IV, particularly in its fine fraction, however the mineralogy of the clay could not be defined. In soil I, four secondary arsenic minerals were identified: adamite ($Zn_2AsO_4(OH)$), olivenite ($Cu_2AsO_4(OH)$), Na-pharmacosiderite ($NaFe_4(AsO_4)_3$ $(OH)_5$ 5H2O) and Ba-pharmacosiderite ($BaFe_4(AsO_4)_3(OH)_5$ $5H_2O$). The zinc and copper arsenates were more abundant in the coarse sands fraction. The pharmacosiderite minerals were mainly present in the silts and clays fraction. A zinc oxide, zincite (ZnO), was also identified in the bulk and coarse sand fraction. Soil I also gave a significant XRD background signal, suggesting an important amorphous phase.

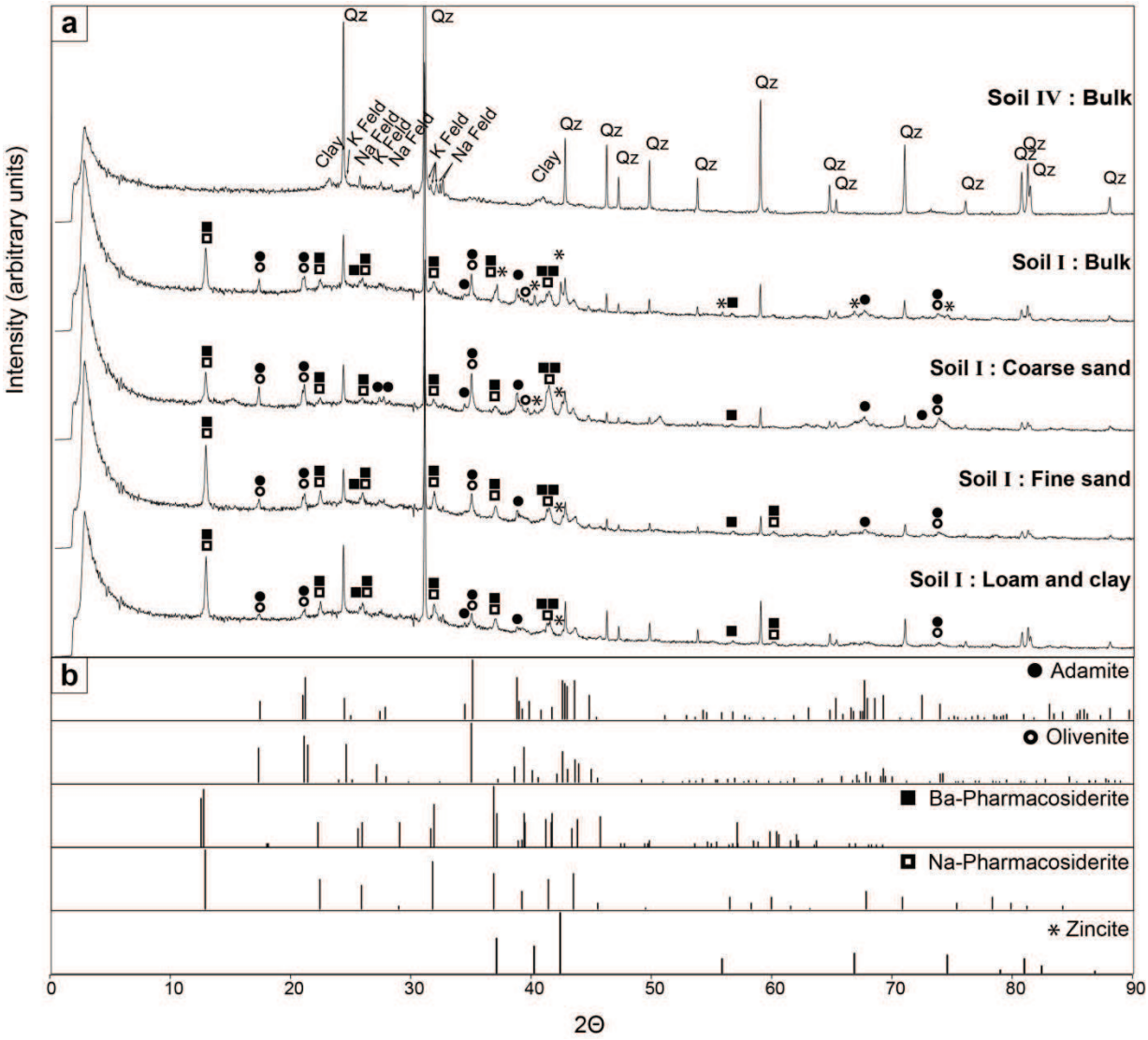

Figure 2.9: *Mineralogy of soils sample I and IV. a: X-ray diffractograms of bulk sample of soil IV and of each particle size fraction of soil sample I: Qz = quartz (ICDD 46-1045); Na Feld = sodium feldspar (ICDD 19-1184); K Feld = potassium feldspar (ICDD 31-0966). b: standard XRD patterns of the five reference mineral carriers of metals and As detected in soil I: Adamite (ICDD 39-1354); Olivenite (ICDD 42-1353); Ba-Pharmacosiderite (ICDD 34-0154); Na-Pharmacosiderite (ICDD 38-0388); Zincite (ICDD 36-1451).*

3.5. Mobility of contaminants

The mobility of As, Zn, Cu, Pb and Fe was assessed by leaching with water in batch systems (Tab.2.2). Concerning the absolute quantities of leached elements, As solubility was significantly higher in soil I than in the other soils and As was less leachable in soils III and IV. The concentrations of soluble Cu and Pb were similar in all soils and the mobility of Zn was higher in soil I than in the other soils. Focusing on the proportion (%) of each leached element compared to its total concentration in the solids, the mobility in closed (batch)

systems was overall low (<1.5%), however it was higher in all cases for soils III and IV than for soils I and II.

Table 2.2 : *Leaching test. Solubility of metal(loid) contaminants of samples after 24h batch leaching tests with ultrapure water. Amounts of leached elements were expressed as milligrams per kilogram of dry soil. The proportion of leached pollutants was expressed as percentage of total pollutant concentrations in the soils.*

	As		Fe		Cu		Pb		Zn	
Sample	mg/kg	%	mg/kg	%	mg/kg	%	mg/kg	%	mg/kg	%
I	77.2 a	0.11	39.1 a	0.04	3.0 a	0.03	2.9 a	0.08	103.9 a	0.12
II	40.5 b	0.13	27.2 b	0.04	2.8 a	0.05	4.6 a	0.08	70.8 ab	0.19
III	21.8 c	0.35	35.1 ab	0.07	2.8 a	0.17	4.2 a	0.17	59.9 b	0.56
IV	26.3 c	1.36	30.6 ab	0.07	3.0 a	0.21	2.2 a	0.22	74.5 ab	0.56

Values are the means (n=3). Values with different letters are significantly different (P<0.05, ANOVA, Tukey-HSD)

Table 2.3 : *Parameters related to As speciation. Arsenic speciation in the solid phases of the four bulk soils (solid), speciation in water from percolation tests (liquid), and enumeration of specific As III-oxidizing microorganisms (µo) (bacteria).*

			I	II	III	IV
Solid	**As III_{total}**	mg/kg	1577 a	852 b	191 c	29 c
	As V_{total}	mg/kg	70178 a	36846 b	7355 c	1954 c
	Ratio of As III_{total}	%	2.25 a	2.33 a	2.41 a	1.48 a
	As_{total}/Fe_{total}	mol As/mol Fe	0.48	0.37	0.09	0.04
Liquid*	**As_p**	µg/L	2202 a	1627 b	141 c	28 c
	As III_p	µg/L	97 a	39 b	<10	<10
	As V_p	µg/L	2106 a	1588 b	134 c	25 c
	Ratio of As total $_p$	%	0.075	0.13	0.056	0.036
	Ratio of As III_p	%	4.5 a	2.5 b	-	-
	pH		5.34	5.95	5.84	5.92
Bacteria**	**As III-ox *µo***	Bact/g dry soil $\times 10^3$	1.93 a	1.47 a	10.35 a	5.92 a
	Ratio of As III-ox *µo****	‰	0.165 a	0.049 ab	0.043 ab	0.012 b

Values are the means (n=3). Values with different letters are significantly different (P<0.05, ANOVA, Tukey-HSD). (*) percolation tests. (**) in the bulk soils, (***) ratio specific As III-oxidizing µo/total µo.

A different tendency was revealed by the percolation experiment (Tab.2.3): with this open and short-term system, mobile As concentration decreased from 2,202 µ/L in soil I to 28 µg/L in soil IV; the proportion of mobile As was highest in soil II and lowest in soil IV. As V was the main As species in all soils (Tab.2.3). Despite significant differences in absolute As III and As V concentrations in the four soils, the proportion of As III was constant at around 2%. Another species of arsenic was detected in all soils but did not correspond to monomethylarsonate, dimethylarsinate or arsenobetaine. As V was also the dominant form (Tab.2.3) in aqueous phases of percolation tests. The proportion of mobile As III was low (less than 5%), but significantly higher in soil I compared to soil II.

3.6. Biogeochemical parameters

Although microbial As III oxidation began earlier in the less polluted soils III and IV (Fig.2.10.a), the As III-oxidation rate was significantly higher in the most polluted soils I and II (Fig.2.10.b). The total bacterial concentration was significantly higher in soils III and IV than in soils I and II. Whereas the absolute concentration in As III-oxidizing bacteria was in the same range for the four soils, the percentage of active As III-oxidizing bacteria, in the whole bacterial community, was higher in the most polluted soil I (Tab.2.3).

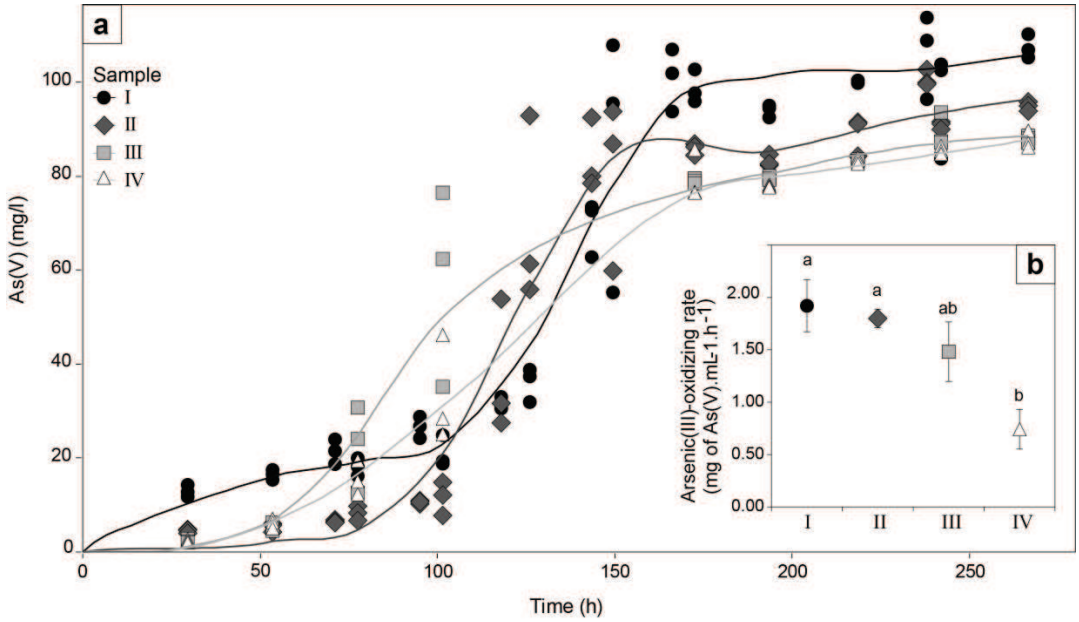

Figure 2.10: *Bacterial As-III oxidizing activities. a: evolution of As V concentration during the As III–oxidizing activity tests performed with triplicates on the four soils. b: As III oxidation rates corresponding to the previous activity tests. Error bars represent the standard deviation of the mean of three replicates. Different letters denote significant difference between samples (P < 0.05, ANOVA, Tukey-HSD).*

Carbon mineralization was significantly more rapid in soil IV (25.17 ± 2.07 µg C-CO_2 g^{-1}dry mass day^{-1}) and in soil I (19.01 ± 0.52 µg CO_2 g^{-1}dry mass day^{-1}) than in the two other samples (Fig.2.11a). Rates measured for II and III soils were about five times lower. However, as the intrinsic carbon content varied greatly from one soil to another, the data were also expressed as specific mineralization rates (Fig.2.11b). The specific carbon mineralization rate was therefore not significantly different in soils I and II (73 ± 2 µg CO_2 g^{-1}Corg day^{-1} and 58 ± 1 µg CO_2 g^{-1}Corg day^{-1}, respectively). Specific carbon mineralization of soil IV remained the highest.

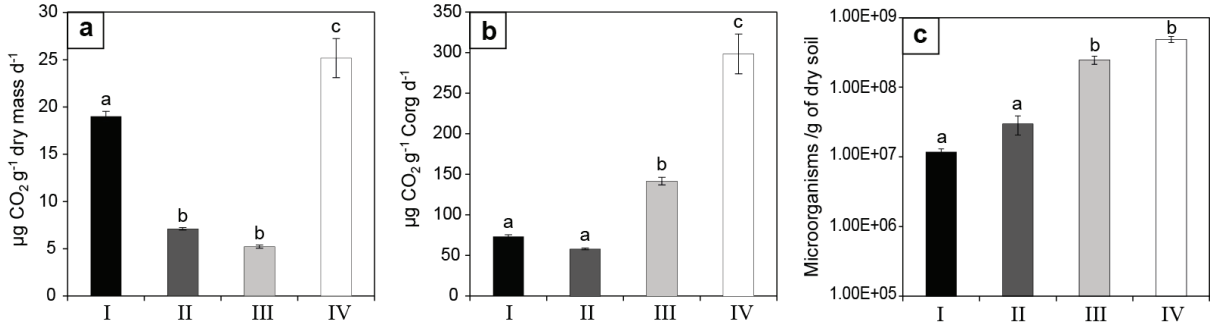

Figure 2.11 : *Biological carbon mineralization. a: carbon mineralization rates of the four contaminated soils. b: specific carbon mineralization rates (carbon mineralization rate / organic carbon concentration ratio). (c): total microorganisms concentration. Error bars represent the standard deviation of the mean of three replicates; Letters denote significant difference between samples (P < 0.05, ANOVA, Tukey-HSD).*

4. Discussion

4.1. Environmental contamination caused specifically by the thermal treatment of gas shells

The "Place-à-Gaz" was mainly contaminated by arsenic, copper, zinc and lead. The different parts of the containers of chemical shells probably constitute the sources of the heavy metals Cu, Zn and Pb. As contamination, on the other hand, was derived from the oxidation of diphenylarsines contained in "blue cross shells" during the combustion process. Besides the considerable amount of contaminants, the samples of the surface black layer contained high concentrations of organic carbon (Tab.2.1). Bausinger *et al*. (2007) have suggested that organic carbon had two origins; the humic matter provided by the forest and the charcoal resulting from the use of firewood during the thermal treatment. Here, the carbon mineralization rates confirm the presence of two types of organic matter (Fig.2.11):

bioavailable organic matter in the less polluted soil, which can be attributed to humic matter; and less bioavailable organic matter in the central part, corresponding to charcoal.

The subsoil of the Woëvre-plain (Fig.1.a.3) is formed from clay and other silicates. The concentrations of Si, Al and K, mainly present in the fine fraction of the four soils (Tab.2.1), and the detection of Na and K feldspars and clays in soil V (Fig.2.9) confirmed the presence of inherited silicates in the black layer. During and after the incineration treatment, metals and metalloids were released into an environment rich in iron, clay and charcoal, three substances known for their capacity to bind inorganic contaminants (Bradl, 2004). The spatial and mineralogical relationships between these substances and contaminants were investigated in the four soils.

Traces of As, Zn and Fe were detected in the charcoal fragments (Fig.2.5.b). However, the results of SEM-EDS analyses performed on different grains of the four soils attested that As and heavy metals were not principally bound to charcoals or silicates. The observations of crystalline and amorphous materials containing large quantities of metals and arsenic suggested common carriers for inorganic contaminants. The white and blue crystallized materials with prismatic structures with radial intergrowths (Fig.2.6,a-d and Fig.2.7.a,b) certainly correspond to minerals of the Adamite-Olivenite series ($(Zn\text{-}Cu)_2AsO_4$ (OH)) detected by XRD (Fig.2.9). Two other arsenates were identified in the most contaminated soil: Na-pharmacosiderite ($NaFe_4(AsO_4)_3(OH)_5$, 5H2O) and the Ba-pharmacosiderite ($BaFe_4(AsO_4)_3(OH)_5$ $5H_2O$). These arsenic carrier minerals are usually found as secondary minerals resulting from the alteration of primary minerals such as arsenopyrite and have been observed most frequently in post-mining environments (Morin *et al*., 2002, Drahota and Filippi, 2009, Haffert *et al*., 2010). To our knowledge, the present study is the first to reveal such a mineral association in a context of incineration of hazardous materials. However, the sequential extraction performed by Bausinger *et al*. (2007) showed that most of the As, Zn, Cu and Pb were not hosted by crystallized fractions yet, in the central part of the site, the majority of As, Cu, Pb and Zn were leached by hydroxylammonium chloride and HCl. This leached fraction was attributed to species bound to amorphous Fe-oxyhydroxides (Hall *et al*., 1996). DRX and SEM-EDS results highlighted the presence of amorphous material composed mainly of Fe but also containing important amounts of As, Cu and Zn. Moreover, this amorphous phase was leached by hydroxylammonium chloride and HCl (Fig.2.8) and can thus be attributed to the amorphous Fe-oxyhydroxides fraction mentioned by Bausinger *et al*. (2007) as a major carrier of pollutants, detected indirectly by a selective extraction procedure.

Consequently, the amorphous phase observed directly here was probably the principal carrier of arsenic and metals in the central parts of the "Place-à-Gaz".

Several indices suggested that the nature of the carrier phases was directly related to the incineration of chemical shells. The structure of the amorphous phase was the first sign that a significant high temperature was reached during destruction. The micro-cracks, observed on the surface (Fig.2.5.f), were certainly formed as the material cooled. Moreover, the small spherical particles in soil pores (Fig.2.7.c) present similar morphology as particles observed in fly ashes produced by incenerators (Fisher *et al*., 1978, Le Forestier *et al*., 1998). In addition, pharmacosiderite has a zeolite structure (Baur *et al*., 2012) and many authors have detected zeolite forms in incineration ashes (Shigemoto *et al*., 1993, Murayama *et al*., 2002, Querol *et al*., 2002). Zincite (ZnO) indentified in the soil I is a synthetic mineral found typically in metallurgical furnace residues. Sidenko *et al*. (2001) have observed the presence of zincite in the self-combusting waste heaps of a zinc smelting plant. The presence of amorphous materials, small spherical particles, zeolite-like structures of pharmacosiderite and zincite therefore suggested that the mineralogical associations in the polluted soil were driven by the incineration of shells. First, the combustion oxidized organoarsenic molecules and smelted metals from shell containers, resulting in the formation of an iron and oxygen-rich amorphous phase covering grains of the inherited soil. These amorphous material was the main carrier of As, Cu, and Zn. Then, during cooling, the secondary arsenate minerals (Adamite, Olivenite and pharmacosiderite) and zincite crystallized in the material pores. Furthermore, the presence of iron in the amorphous phase can be used to estimate that the maximum combustion temperature was above the melting point of iron, i.e. 1,538°C. Such an amorphous mineral phase, mainly composed of iron, oxygen, arsenic and heavy metals, had never been observed before this study.

4.2. Mobility of contaminants

Contamination of the site by As, Cu, Pb and Zn was significant but very localized. As, Cu and Zn (and to a lesser extent Pb) were distributed along a concentration gradient from the center of the site, devoid of vegetation, towards the forest (Fig.2.4.c-f). In June 2014, during the sampling campaign, wetland zones were observed in the periphery of the "Place-à-Gaz", resulting from meteoritic water accumulation at low topographic points, because of the very low permeability of the Woëvre formation clays. This formation, beneath the heavily contaminated black layer, limited the vertical transfer of metals and As, forming a natural barrier to infiltration of rainwater. The higher pH (above pH 7), in the clay horizon also

formed a chemical barrier to the mobility of metals, especially Zn (Bausinger *et al*., 2007). Transfer of contaminants on the site was therefore mainly driven by runoff water at the base of the highly permeable black layer. The contaminated area at the northern low topographic point of the site, outside the burning zone, showed this horizontal transfer (Fig.2.4.b and Fig.2.4.d-f).

The solubility of the main carrier phases of metals and arsenic was difficult to predict since, while the solubility constants of adamite and olivenite are documented (K_{sp} equal to 5.71 for adamite and 2.39 for olivenite, Magalhães *et al*., 1988), no solubility or thermodynamic data are available for pharmacosiderite minerals (Drahota and Filippi, 2009). Moreover, the stability of the amorphous phase was unknown. The potential mobility of metals and arsenic was first evaluated by leaching tests (Tab.2.2). Leached Cu and Pb values seemed to reach a threshold independently of the original ground level pollution (Tab.2.2). The percentage of leached pollutants were very low (below 2%), however they revealed that a higher proportion of pollutants were mobilized from the less contaminated soil. These observations can be explained by the saturation of these elements in the aqueous phase of the leaching batch systems, which would induce their re-precipitation. In order to evaluate the mobility of metals and arsenic in these conditions, the geochemical PHREEQCi 3.0.6.7757 code together with the minteq.v4 thermodynamic database was used by integrating the complete chemistry of the leached water (SM 2.3). In these acid ($5<pH<6$) and oxidizing conditions, the PHREEQCi simulation, integrating the chemical parameters and concentrations of major and trace chemical species of the leached water, highlighted that hydroxides and oxides containing Cu, Pb and Fe should precipitate (SM 2.3). This could explain the low mobility of Cu and Pb in the environmental conditions of the site. Conversely, according to the PHREEQCi simulation, no mineral containing arsenic or zinc should precipitate but iron minerals known to efficiently adsorb As (ferrihydrite, goethite) should precipitate. Where the behavior of zinc, is concerned, these results are consistent with the Bausinger *et al*. (2007) study concluding that the moderately acidic soil pH allowed mobilization of considerable amounts of Zn. However, Bausinger *et al*. 2007 did not explain the behavior of arsenic, as no simple correlation between As mobility and pH could be found.

Arsenic concentrations in water obtained with the percolation test (Tab.2.3) were in the same range than those measured by Bausinger *et al*. (2007) in soil interstitial water samples (mean value of 838 µg/L and maximum value of 2377 µg/L). The proportion of As III in the percolation water of the most polluted soil was greater than the proportion of As III in the

corresponding solid. This can be explained by the high mobility of arsenite which has no charge at this pH range, unlike the arsenate (Smedley and Kinniburgh, 2002). However, in soil II the proportion of As III in the percolating water was not higher than in the solid phase. This result can be explained by the difference of pH between soils I (5.3) and soil II (5.9), as differential As III and As V adsorption behavior is very sensitive to pH in this range. At pH 5–6, As V sorbs more readily to amorphous hydrous ferric oxides (HFO) than does As III (Dixit and Hering, 2003) and thus tends to immobilize As. However, adsorption of As III increases with pH, while adsorption of As V shows an opposing trend This may explain why more As III was released by soil I than by soil II.

Biological As III oxidation may decrease the proportion of As III. As III-oxidizing tests (Fig.2.10) and enumeration of specific As III-oxidizing organisms (Tab.2.2) revealed the potential for bacterial As III oxidation in all soils. However, the longer time lapse in As III-oxidizing activity tests in soil I than in other soils shows that this activity may be inhibited because of the high concentrations of toxic elements. This toxicity clearly influenced the total bacterial concentration and microbial activities (i.e. organic matter mineralization; Fig.2.11) that were significantly lower in soils I and II than in soils III and IV. The High Cu concentration in soil I may explain the lower microbial numbers and the lower microbial activities involved in C-mineralization process (Flemming and Trevors, 1989). Thus, the relative inhibition of microbial As III oxidizing activity may have contributed to the higher proportion of As III released from soil I compared to soil II.

However, the elevated toxic element concentrations seemed to have exerted a selective pressure on the microbial communities, as suggested by the high As III-oxidizing rates observed with microbial populations from soils I and II (Fig.2.10) and by the highest proportion of As III-oxidizing microorganisms compared to the total bacterial concentration in soil I (Tab.2.2).

Concerning total As mobility, the batch leaching test (Tab.2.2) resulted in a higher mobility from soils III and IV, contrary to the percolation experiment (Tab.2.3), which indicated a maximum As mobility in soil II. This apparent contradiction can be explained by the difference in experimental procedure. In the batch leaching test, the contact time between water and soils allowed the leaching and re-precipitation of iron that induced As removal through adsorption on fresh HFO, the absolute iron concentration being higher in soils I and II than in soils III and IV (Tab.2.1). This phenomenon explains why in batch leaching tests the

percentage of final soluble As was higher with soils III and IV. Conversely, the percolation test was rapid (less than 1 hour), and the percolating water was immediately filtered and acidified; re-precipitation of solubilized iron was, therefore, probably limited. In the percolation conditions, the mobility of As was most probably governed by the molar ratio As/Fe and pH of the soils.

Dixit and Hering, (2003) gave values of site density for As adsorption on HFO : between 0.2 and 0.3 mol sites per mol Fe. The molar ratio As/Fe in the center of the "Place-à-Gaz" was greater than 0.3 (Tab.2.3), suggesting that the adsorption sites for As in the soils I and II were saturated. Thus, As should be more mobile in soils I and II than in soils III and IV. Lastly, the higher mobility of As from soil II than from soil I in percolation tests may be explained by soil pH: soil I was more acidic than soil II, yet As V adsorption onto iron oxides continuously decreases when pH increases between 3.5 and 10 (Dixit and Hering, 2003). Thus, As V was less strongly adsorbed onto Fe-rich particles in soil II than in soil I.

Then, the adsorption of As onto the HFO in the most contaminated part of the site was not enough to immobilize the whole amount of arsenic. At the periphery of the site, where the As/Fe ratio was less than 0.2, a significant decrease of mobile arsenic was detected in the percolating water. Batch leaching and percolation experiments yielded different and complementary information concerning As mobility in the soils: percolation testing represents the short-term mobility occurring when rainwater passes rapidly through the permeable surface soil, whereas the leaching test mimics the phenomena that probably occur in the stagnant water retained in the saturated areas. On the whole, these results suggest that bacterial As III oxidation contributes to reduce the proportion of As III in soil pore water but that the adsorption of As onto HFO was the major phenomenon driving the short-term mobility of As.

5. Conclusion

The present study has provided new information about the carriers of arsenic and heavy metals in soils strongly polluted by the historical incineration of chemical weapons.

Nearly one century after the polluting event, arsenic speciation shown by SEM-EDS and XRD was proven to be directly linked to the incineration of shells. Indeed, the two main As-carriers were identified as amorphous materials composed of a blend of metals and secondary arsenate minerals that were formed in the pores of the material as it cooled. Such amorphous carriers of arsenic and heavy metals, with high iron content and no silica but presenting a glass-like morphology, were observed here for the first time.

The soils of the "Place-à-Gaz" site were strongly contaminated by As, Zn, Cu and Pb, the more mobile of these pollutants being Zn and As. The mobility of Zn was probably governed primarily by pH, whereas As behavior seems to be related to pH, As/Fe ratio, Fe dissolution / precipitation processes and microbial activities.

The long-term exposure to high levels of toxicity in soils I and II, and particularly in soil I, exerted a selective pressure on the microbial communities that probably tended to select organisms with high As III-oxidizing efficiency and increased the proportion of As III-oxidizing bacteria in the global community. Thus, microbes can contribute to maintaining of a high proportion of As V on site. However, the microbial activity studied, i.e. organic matter mineralization and As III oxidation, are less active in the most polluted soils compared to those with lower concentrations in inorganic pollutants, suggesting that the inorganic pollutants still exert an inhibiting effect on biogeochemical cycles in the most polluted part of the site.

Acknowledgements

This work was supported by the Région Centre Val de Loire (convention 00087485) and the Labex Vol-taire (ANR-10-LABX-100-01).

Supplementary Material

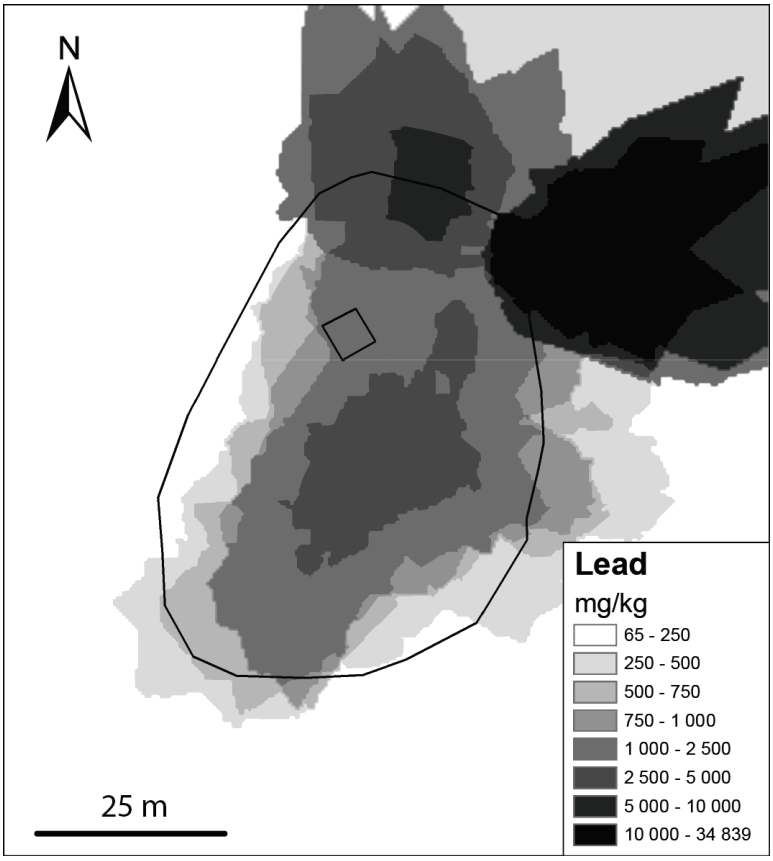

SM 2.1: *Map representing the Pb concentration at the soil surface, measured with NITON©. The square represents the hut and the line represents the boundary of the site.*

SM 2.2: *Particle size fractions and physical parameters determined for the four soils.*

	Particle size fractions			Physical parameters		
Sample	**Coarse sand (%)**	**Fine sand (%)**	**Loam and clay (%)**	**pH**	**Conductivity (mS/cm)**	**Water content**
I	37.0	39.9	23.2	5.34	10.1	0.87
II	18.7	27.5	53.8	5.95	9.2	0.58
III	36.8	26.3	36.9	5.84	10.4	0.31
IV	9.4	36.7	54.0	5.92	10.9	0.91

Coarse sand 2000–200 µm. Fine sand 200–50 µm. Loam and clay <50 µm.

SM 2.3: *Phreeqc simulation, integrating the chemistry of solution at the end of the leaching tests. The input data were pH and major and trace concentrations. The calculated saturation indexes are given.*

Sample	**I**	**II**	**III**	**IV**
pH	5.34	5.95	5.84	5.92
Water data in mg.L^{-1} (PHREEQC input data)				
As	7.67	4.07	2.18	2.64
Ca	0.83	2.14	2.09	3.62
Cl	1.16	1.82	0.40	0.45
Cu	0.30	0.27	0.27	0.30
F	0.045	0.021	0.041	0.032
Fe	3.89	2.73	3.50	3.08
K	0.26	4.34	1.15	6.36
Mg	0.29	0.27	0.31	0.65
N(-3)	0.0053	0.0003	0	0
N(3)	0	0.149	0	0
N(5)	1.8	3.8	3.99	11.7
Na	0.85	0.78	0.42	0.54
P	0.72	0.22	0.005	0.92
Pb	0.31	0.42	0.44	3.08
S(6)	1.65	1.16	0.66	1.91
Zn	10.3	7.11	6	7.50

Phase	**Saturation index**			
Cupricferrite CuFe2O4	10.69	12.78	3.61	12.81
Cuprousferrite CuFeO2	9.23	10.22	4.15	10.25
IronIII hydroxide Fe(OH)3	2.53	3.02	0.02	3.04
Goethite FeOOH	5.23	5.72	2.72	5.74
Hematite Fe2O3	12.85	13.84	7.84	13.88
Magnetite Fe3O4	13.44	14.31	5.43	14.40
Pyromorphite Pb5(PO4)3Cl	8.70	11.49	-21.51	16.86
Strengite FePO4:2H2O	2.54	1.89	-5.62	2.56
Ionic strength	0.0011	0.0012	0.0005	0.0016
Charge imbalance	-44.30	-44.27	-99.62	-44.78

This simulation was performed with PHREEQC Interactive 3.0.6.7757; the data base used was minteq.v4.

Chapitre III : Effets d'alternances de saturation/désaturation et d'un apport de matière organique sur les cycles biogéochimiques de C, N, As et des métaux dans le sol de la Place-à-Gaz : Etude en mésocosme

La plateforme expérimentale LABBIO

Introduction au chapitre III

Effets d'alternance de saturation/désaturation et d'un apport de matière organique sur les cycles biogéochimiques du carbone, de l'azote, de l'arsenic et des métaux dans le sol de la Place-à-Gaz : Une étude en mésocosme

La partie précédente a permis de mettre en évidence la particularité du sol de la Place-à-Gaz en termes d'association minéralogique et de biogéochimie. Les conditions environnementales, en particulier les épisodes de saturation des sols et les dépôts de litière observés sur le site, sont susceptibles d'influencer la forme et la mobilité des contaminants. Afin de comprendre l'impact de ces phénomènes sur le comportement de l'arsenic et des métaux ainsi que de pouvoir prédire leur comportement sur le site, le sol de la Place-à-Gaz a été soumis à des cycles de périodes sèches et humides et à un apport de MO biodégradable, dans une expérience effectuée en mésocosme. L'étude des flux verticaux, dans cette colonne instrumentalisée, permettra d'appréhender les phénomènes liés aux écoulements, contraints sur le site par le substrat argileux. Ce chapitre, rédigé sous la forme d'un article soumis au journal *Science of the Total Environment* (STOTEN) en octobre 2016, décrit l'effet de ces changements de conditions environnementales sur les cycles biogéochimiques du carbone, de l'azote, de l'arsenic et des métaux. La description de la plateforme expérimentale, appelé LABBIO, et développée lors de cette thèse, précèdera l'article.

Résumé graphique :

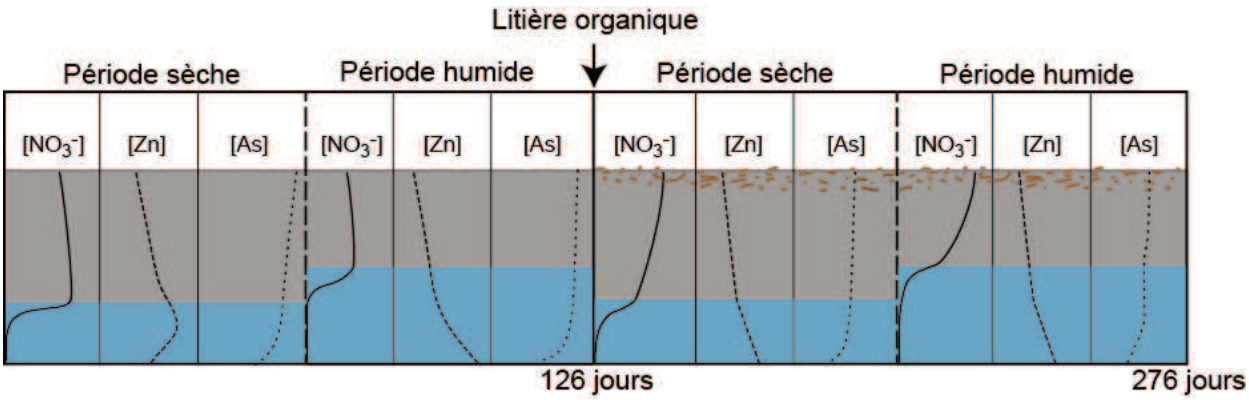

Résumé :

Afin d'évaluer l'impact d'épisodes de saturation en eau et de l'apport de matière organique sur les cycles biogéochimiques de C et N et sur le comportement de l'As et des métaux dans un sol fortement contaminé par la destruction d'obus arsénié, une étude en mésocosme a été

menée. Un mésocosme instrumenté de 1 m^3 a été rempli avec le sol contaminé échantillonné sur le site de la Place-à-Gaz. Quatre cycles de périodes sèches et humides, d'environ un mois chacune, ont été simulés pendant 276 jours. Après deux cycles sec/humide, la litière, échantillonnée sur le site, a été ajoutée à la surface du sol. Le mésocosme instrumenté permet notamment d'analyser les concentrations des principaux ions et métaux dans les solutions de sol à quatre profondeurs et à la sortie de colonne. Le cycle de l'azote a été le plus affecté par les alternances de saturation/désaturation, comme en témoigne la mise en évidence d'une dénitrification active dans les niveaux saturés. Les concentrations des deux polluants les plus mobiles, le zinc et l'arsenic, dans l'eau interstitielle, avoisinent respectivement 20-100 $mg.L^{-1}$ et 2-8 $mg.L^{-1}$. Après 8 mois d'expérience, environ 83 $g.m^{-3}$ de Zn et 3,5 $g.m^{-3}$ d'As ont été lessivés. Cependant, ces quantités importantes représentent moins de 1 % du stock d'As et de Zn présent dans la phase solide du sol. Les cycles sec/humide n'ont pas eu d'effet significatif sur la mobilité du Zn. Pour l'As, la saturation du sol a induit une immobilisation de l'As V, qui était la forme majoritaire d'As, néanmoins elle a favorisé la formation d'As III, plus mobile. Ces phénomènes ont été amplifiés par la présence de matière organique biodisponible, sa dégradation liée aux métabolismes microbiens conduisant au développement d'un milieu plus réducteur. Cette étude en mésocosme a montré que le dépôt naturel de la litière organique, permet la restauration d'une partie des fonctions biologiques du sol, mais a des conséquences antagonistes sur le transfert des contaminants inorganiques. Le principal danger de ce type de sites contaminés par des armes chimiques organo-arseniés concerne les stocks d'As présents dans le sol : en effet, l'arsenic pourrait être mobilisé et dispersé dans le milieu environnant pendant plusieurs centaines d'années.

La plateforme expérimentale LABBIO

A. Présentation globale

La plateforme instrumentale LABBIO (cofinancée par la Région Centre Val de Loire et le BRGM) (Fig.3.1) est un dispositif d'étude, développé par S. Dupraz, permettant de simuler des environnements biogéochimiques en conditions contrôlées (température, éclairage, humidité du sol, composition de l'atmosphère de la colonne). La plateforme LABBIO permet de manière automatisée de récupérer des prélèvements liquides et gazeux sur différentes profondeurs de sol, *via* des collecteurs et d'effectuer des analyses « on line ». La plateforme est équipée d'un panel d'instruments comprenant des sondes, un titrateur, une chromatographie ionique, une chromatographie gazeuse et un échantillonneur automatique permettant de récolter les échantillons afin d'effectuer des analyses non réalisables par la plateforme. L'ensemble des instruments est asservi par la plateforme afin d'automatiser les prélèvements et les analyses et ainsi disposer d'une plateforme « intelligente ». Le montage de cette plateforme et le développement du logiciel pilotant son fonctionnement ont fait partie à part entière des travaux présentés dans ce manuscrit.

Figure 3.1 : *La plateforme LABBIO*

B. Les instruments analytiques

B.1 Instrumentation de la colonne

La colonne est composée d'un module en acier inoxydable de 100 cm de haut et de 100 cm de diamètre, associé à un second module de 40 cm de hauteur comportant un fond incliné afin de faciliter l'écoulement de la solution vers la sortie de la colonne. L'eau est récoltée dans un bac de rétention dont le poids est mesuré par une balance. Un système situé en sortie de colonne permet de contrôler le niveau d'eau dans la colonne. La colonne est étanchement fermée par un couvercle en inox. Sous ce couvercle est fixé le système d'arrosage, composé de 12 buses et disposé en croix afin de disperser une quantité de précipitation homogène sur toute la surface du sol (Fig.3.2.B). Le système d'éclairage est composé de diodes électro luminescentes horticoles (5 spots) ayant un spectre adapté à la germination et la croissance de plante (Fig.3.2.B). L'éclairage par DEL a été préféré à d'autres systèmes d'éclairage, comme les ampoules au sodium, pour sa faible émission de chaleur, ainsi que pour son faible encombrement.

La température et l'humidité du sol peuvent être mesurées à quatre niveaux dans la colonne grâce à 4 sondes TDR (Time Domain Reflectometry, TRIME-PICO32, IMKO). Les sondes sont situées au centre de la colonne afin d'éviter les effets de bord que peuvent engendrer des écoulements préférentiels le long de la paroi (Fig.3.2.A). La mesure est basée sur la différence de permittivité électrique entre l'eau porale et les phases solides et gazeuses du sol. La sonde mesure l'humidité pour un volume > 250 mL, ce qui est adapté aux milieux hétérogènes. Pour chacun des niveaux, trois bougies poreuses disposées tous les 120° permettent de récolter l'eau porale du sol (Fig.3.2.A). L'échantillonnage de l'eau se réalise par une dépression dans la bougie supérieure, due à la succion du sol. Les corps des bougies poreuses sont fabriqués en polytétrafluoroéthylène (PTFE) et la partie poreuse est constituée de quartz afin d'éviter les interactions chimiques et biologiques avec le milieu. La porosité de la cellule de prélèvement est de 2 µm pour une surface de 33 cm^2.

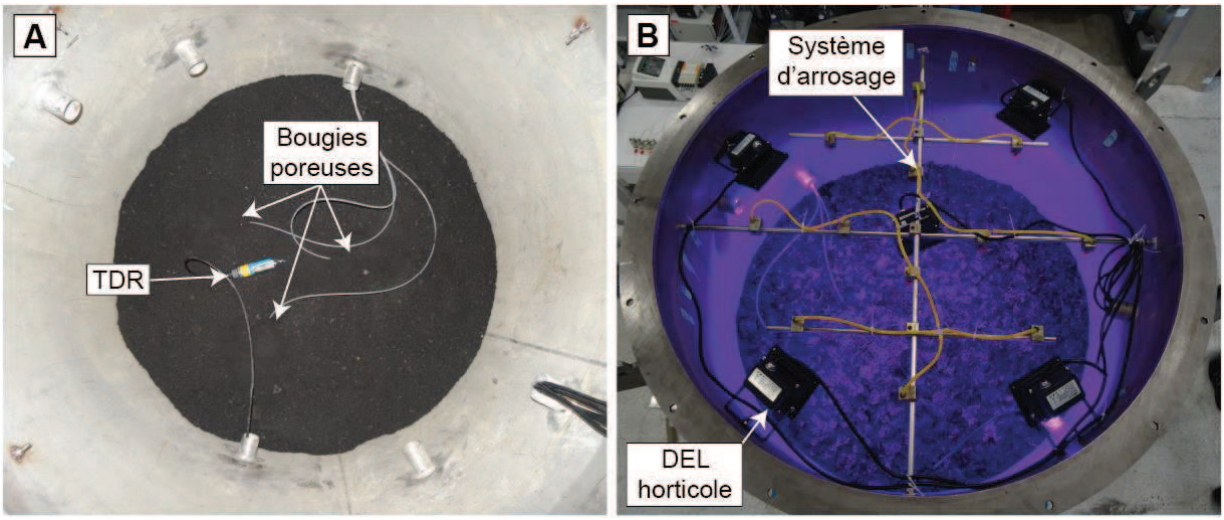

***Figure 3.2 : A** : Instrumentalisation avec une sonde TDR et trois bougies poreuses d'un niveau d'échantillonnage. **B :** Photo du système d'éclairage, composé de 5 DELs horticoles, et du système d'arrosage composé de 12 buses.*

B.2 Moniteur multiparamétrique et titrateur

Le pH, la conductivité, l'oxygène dissous, le potentiel d'oxydo-réduction et la température des solutions de sol sont mesurés à l'aide de quatre sondes : une électrode pH à électrolyte gélifiée (Fisherbrand), une sonde conductimétrique (Sentek), une sonde galvanique de mesure de l'oxygène (Fisherbrand) et une électrode RedOx gélifiée à pointe de platine (Fisherbrand). L'acquisition des résultats est effectuée par un enregistreur de données multi-canaux (multiparameter analyser C3040, Consort). Les sondes sont étalonnées toutes les semaines.

Un titrateur (848 Titrino plus, Metrohm) permet de mesurer l'alcalinité totale (AT) des solutions de sol. La solution de titration est de l'acide chlorhydrique (0.01N) et AT est calculée en évaluant les quantités nécessaires d'acide utilisé pour que l'échantillon atteigne le point d'équivalence du bicarbonate et de l'acide carbonique.

$$AT = \frac{1000 \,.\, Ep \,.\, C\alpha}{Ve}$$

Où :

- AT est l'alcalinitée total (mM).
- Ep est le volume de titrant HCl ajouté jusqu'au point d'équivalence du bicarbonate (mL).
- $C\alpha$ est la concentration du titrant ($C\alpha$= 0.01N).
- Ve est le volume d'échantillon titré (mL).

Le point d'équivalence est trouvé grâce à une sonde pH, et la méthode de titration utilisée est le titrage dynamique à point d'équivalence. L'ajout de titrant est effectué en ajoutant des volumes variables. Les incréments de volume varient en fonction de la pente de la courbe.

B.3 Chromatographie ionique

Une chromatographie ionique, 940 Professional IC Vario (Metrohm, Herisau, Switzerland ; Fig.3.3) équipée de conductimètres, est associée à la plateforme afin de mesurer indépendamment les concentrations en cations majeurs (Li^+, Na^+, NH_4^+, K^+, Ca^{2+}, Mg^{2+}) et anions majeurs (F^-, Cl^-, NO_2^-, Br^-, NO_3^-, SO_4^{2-}, PO_4^{2-}) des solutions de sol. Les anions sont séparés grâce à une résine échangeuse d'anions (groupement ammonium quaternaire) sur colonne Metrosep A Supp 16 (150 mm × 4 mm i.d.) associée à une colonne de garde Metrosep A Supp 4/5 Guard. La phase mobile est une solution de Na_2CO_3 (7,5 mM) et NaOH (0,75 mM) qui s'écoule à une vitesse de 0.8 $mL.min^{-1}$. La conductivité de la phase mobile est réduite par un suppresseur chimique (MSM model 833 suppressor unit) qui échange les ions sodium du Na_2CO_3 par des protons. Le suppresseur se compose de trois voies, la première est utilisée à la suppression, la deuxième est régénérée en parallèle par de l'acide sulfurique (5 mM) et la dernière est rincée avec de l'eau. A chaque nouvel échantillon, le suppresseur tourne de 120° afin de régénérer les trois voies. Les cations sont séparés avec une colonne échangeuse de cations Metrosep C6 (150 mm × 4 mm i.d.). L'éluant est une solution de HNO_3 (1,7 mM) et d'acide dipicolinique (1,7 mM), et circule à une vitesse de 0 ;9 $mL.min^{-1}$. L'échantillon est prélevé par une pompe péristaltique, puis filtré par un filtre tangentiel (0,2 µm) et stocké dans une boucle de 15 mL. L'échantillon peut ensuite être injecté indépendamment dans les boucles d'injection des voies anions et cations. Les boucles d'injection ont un volume de 250 µL.

Les calibrations ont été effectuées à partir de gamme de standards certifiés de 5 points adaptés à la concentration des ions de nos échantillons. La qualité des mesures a été vérifiée en analysant de l'eau déionisée afin de contrôler une éventuelle contamination.

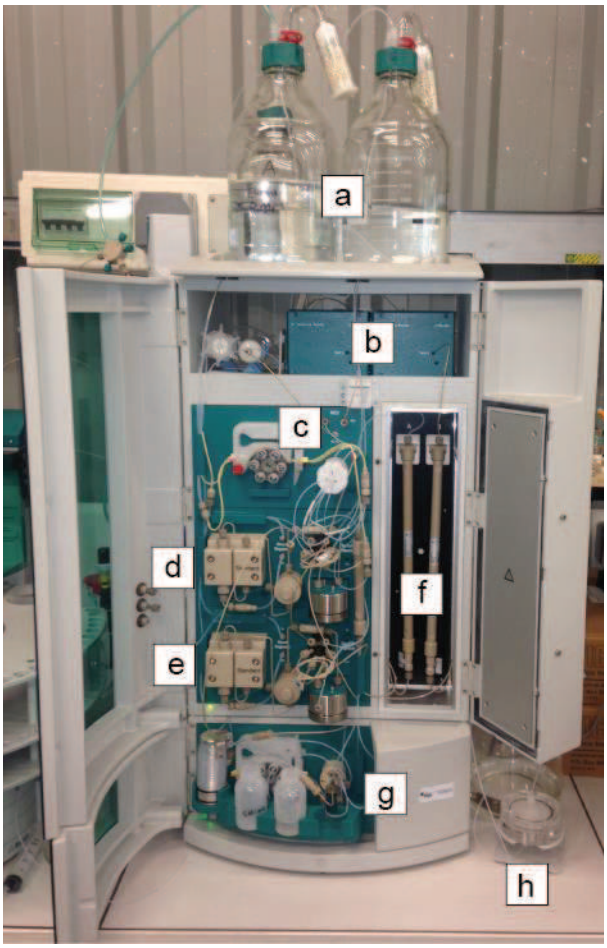

Figure 3.3 : *Photo de la chromatographie ionique 940 Professional (Metrohm). a) éluant ; b) conductimètres ; c) système de suppression chimique ; d) pompe et vanne d'injection de la voie d'analyse des anions ; e) pompe et vanne d'injection de la voie d'analyse des cations ; f) colonne de séparation des anions et colonne de séparation des cations ; g) module de prélèvement de l'échantillon ; h) filtre tangentiel affilié au module d'échantillonnage.*

B.4 Chromatographie en phase gazeuse

La chromatographie en phase gazeuse (Compact GC Interscience, CPG), utilisant l'hélium comme gaz vecteur, est équipée en parallèle de trois colonnes associées à trois détecteurs. La première colonne (Rt-Msieve 5A, 15 m × 0,32mm) permet de séparer à 45°C H_2, O_2, N_2, et CO. Les gaz sont ensuite analysés par un détecteur à conductivité thermique (DCT). CO_2, CH_4 et N_2O sont séparés à 45°C par une deuxième colonne (HayeSep D, 30 m × 0,32 mm) et analysés également par DCT. La troisième colonne (Stabilwax, 12 m × 0,32 mm) permet d'analyser les composés organiques volatils (COV) et les BTEX grâce à un détecteur à ionisation de flamme. Des standards externes ont été utilisés pour calibrer les trois détecteurs. La stabilité des résultats a été vérifiée en analysant régulièrement l'air de la pièce.

C. Automatisation

L'ensemble des instruments précédemment présentés, ainsi que les 3 pompes péristaltiques (Watson), les 30 électrovannes et les deux vannes sélecteur 8 voies (Valco), permettant le transfert des échantillons liquides et gazeux du sol vers les différents instruments analytiques sont tous asservis par la plateforme et pilotés par un logiciel (Fig.3.4). Le logiciel a été développé spécialement pour ce dispositif par la société RDPHYS sous LabVIEW (National Instrument). Il permet d'effectuer des mesures en continu ainsi que des actions de manière totalement autonome :

- L'acquisition des valeurs d'humidité et de température du sol des 4 niveaux de prélèvements est effectuée en continu avec un pas de temps d'enregistrement de 1h.
- L'eau sortant de la colonne est récoltée dans un bac de rétention et pesée par une balance. Cette dernière mesure les flux sortant de la colonne qui sont enregistrés toutes les heures par l'ordinateur. Lorsque le bac de rétention est plein, la vidange est effectuée par une pompe, tandis qu'une électrovanne ferme l'évacuation de la colonne.

Il permet également d'effectuer plusieurs actions ponctuelles:

- Les mesures des paramètres physico-chimiques : Cette fonction permet de prélever l'eau porale d'un niveau d'échantillonnage, via la pompe 1 voie (Fig.3.4). L'eau alimente les sondes mesurant le pH, l'Eh, la conductivité et l'oxygène dissous qui sont disposées en série et remplies en fin de ligne par un collecteur en téflon. L'eau est renouvelée pendant 15 minutes par la pompe. A la fin de cette période, le consort mesure les paramètres physico-chimiques, et ensuite la titration est lancée. Le volume d'échantillon titré présent dans le collecteur en téflon est fixé par un déversoir. Après la fin de la titration, les résultats sont envoyés à l'ordinateur et enregistrés. L'opération est renouvelée pour les autres niveaux de prélèvements.
- Le remplissage des collecteurs : Cette fonction permet de prélever l'eau d'alimentation, des 4 niveaux d'échantillonnages et de la sortie de colonne et de remplir les 6 collecteurs en téflon de 100 mL. Le prélèvement est permis par la pompe péristaltique 6 voies (Fig.3.4) qui remplit en parallèle les collecteurs. Des capteurs de niveaux permettent de contrôler le remplissage des collecteurs. Lorsqu'un collecteur est plein, une électrovanne permet de couper son remplissage. La méthode s'arrête lorsque toutes les voies de prélèvements ont atteint le niveau d'eau maximum dans le collecteur, ou une durée maximum (ces deux paramètres sont définis par l'utilisateur).

- L'analyse liquide : Elle consiste à l'analyse par chromatographie ionique et à l'échantillonnage par un collecteur automatique (Gilson) des différentes solutions de la colonne de sol. La première partie de cette fonction est similaire à la fonction de remplissage des collecteurs. Lorsque les collecteurs sont pleins une vanne sélecteur 8 voies (Valco) permet à la chromatographie ionique de prélever la solution correspondant à la solution de l'une des 6 voies d'échantillonnage. Parallèlement à l'analyse des ions, le surplus d'eau prélevé est échantillonné dans un collecteur de fractions pour la réalisation d'analyses complémentaires. Les résultats sont ensuite envoyés à l'ordinateur et le sélecteur change de voie afin de renouveler l'opération pour les solutions des autres niveaux de prélèvements.
- La vidange et le nettoyage des godets : cette fonction permet le nettoyage du système de remplissage par le passage d'éthanol (70 %), d'eau distillée et de gaz afin de ne pas avoir d'eau stagnante dans le réseau de tube.

D'autres fonctions n'ont pas pu être implémentées (mesure des gaz), et les mesures ont donc été effectuées manuellement.

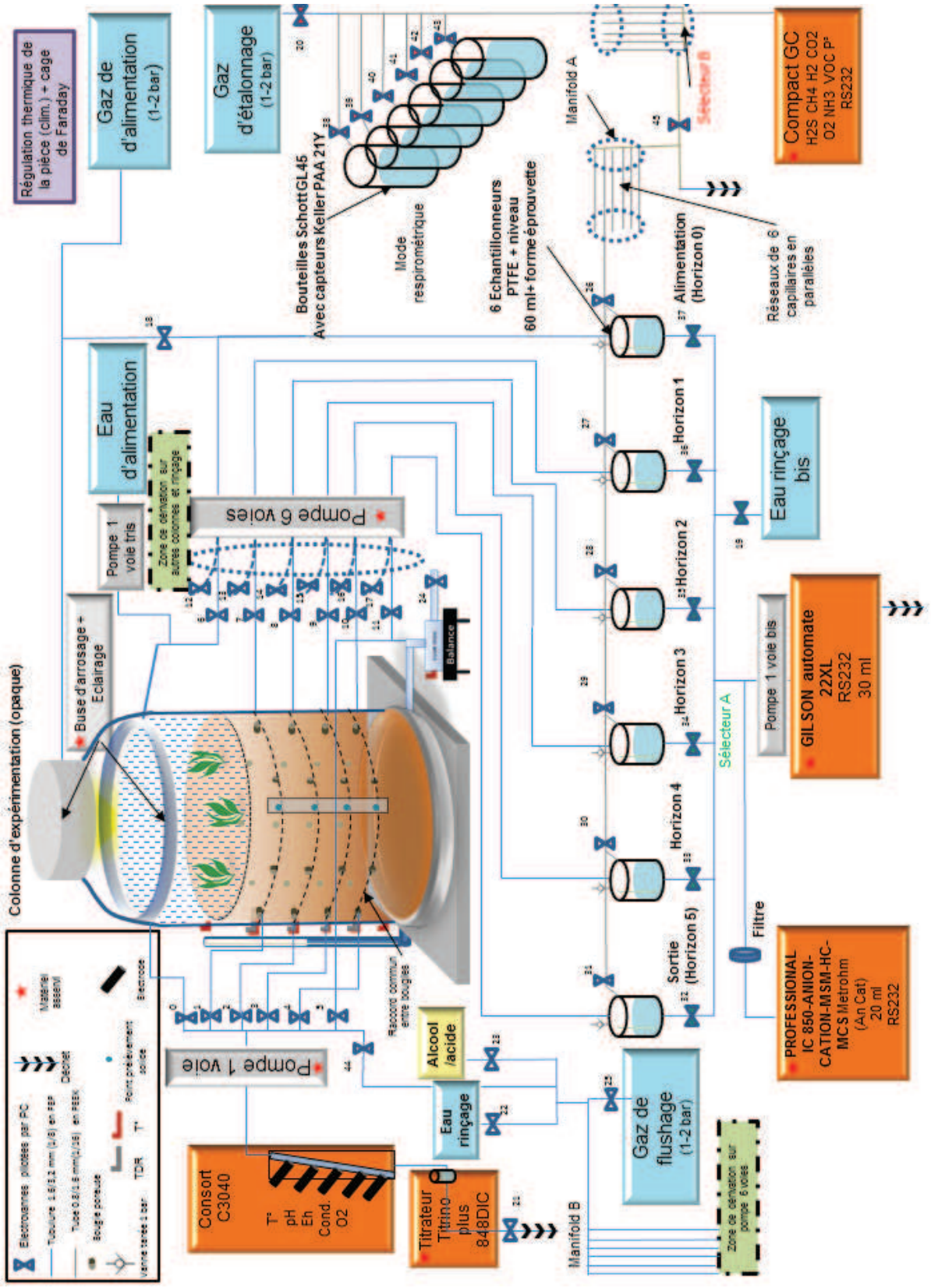

Figure 3.4 : *Schéma de la plateforme LABBIO.*

Chapitre III: Effect of saturation/desaturation cycles and input of natural organic matter on the biogeocycles of C, N, As and metals in a soil impacted by the burning of chemical warfare agents: a mesocosm study.

Hugues Thouin [a,b,c,d], Fabienne Battaglia-Brunet [a,b,c,d], Pascale Gautret [b,c,d], Lydie Le Forestier [b,c,d], Dominique Breeze [a], Fabienne Séby [e], Marie-Paule Norini [b,c,d], Sebastien Dupraz [a].

[a] BRGM, 3 avenue Claude Guillemin, 45060 Orléans, France

[b] Université d'Orléans, ISTO, UMR 7327, 45071 Orléans, France

[c] CNRS, ISTO, UMR 7327, 45071 Orléans, France

[d] BRGM, ISTO, UMR 7327, BP 36009, 45060 Orléans, France

[e] UT2A, Hélioparc Pau Pyrénées, 2 avenue du président Angot, 64053 Pau, France

Abstract

A mesocosm study was conducted to assess the impact of water saturation episodes and of the input of bioavailable organic matter on the biogeochemical cycles of C and N, and on the behavior of metal(loid)s in a soil highly contaminated by the destruction of arsenical shells. An instrumented mesocosm was filled with contaminated soil taken from the "Place-à-Gaz" site. Four cycles of dry and wet periods of about one month were simulated for 276 days. After two dry/wet cycles, organic litter sampled on the site was added above the topsoil. The nitrogen cycle was the most impacted by the wet/dry cycles, as evidenced by a denitrification microbial process in the saturated level. The concentrations of the two most mobile pollutants, Zn and As, in the soil water and in the mesocosm leachate were, respectively, in the 20–100 mg.L-1 and 2–8 mg.L-1 ranges. After 8 months of experiment, about 83 g.m-3 of Zn and 3.5 g.m-3 of As were leached from the soil. These important quantities represent less than 1 % of the solid stock of this contaminant. Dry/wet cycles had no major effect on Zn mobility. However, soil saturation induced the immobilization of As by trapping As V but enhanced As III mobility. These phenomena were amplified by the presence of bioavailable organic matter. The study showed that the natural deposition of forest organic litter allowed a part of the soil's biological function to be restored but did not immobilize all the Zn and As, and even contributed to transport of As III to the surrounding environment. The main hazard of this type of site, contaminated by organo-arsenic chemical weapons, is the constitution of a stock of As that may leach into the surrounding environment for several hundred years.

Keywords: mesocosm monitoring, metals, arsenic, nitrogen, organo-arsenic chemical weapons, soil saturation, organic matter

1. Introduction

Soil is a structurally porous and biologically active medium that fulfills a number of functions such as providing a habitat for organisms, climate regulation, cycling of elements and water purification. Soils contaminated by inorganic pollutants can lose some or all of these functions but they may also evolve under the influence of forcing factors such as climate, presence of organisms or human activity, and can spontaneously recover some functions when colonized by vegetation (Huot *et al*., 2015). Contaminated soils may contain large amounts of metals and metalloids whose fate is directly dependent on their evolution and function. The understanding of processes affecting and altering contaminated soils is essential to evaluating and predicting the behavior of pollutants.

Modern warfare is a source of habitat alteration and environmental pollution, and has been found to have highly negative effects on the structure and functioning of ecosystems (Lawrence *et al*., 2015). The First World War (Great War of 1914–1918) was the first modern conflict, with about 1 billion artillery shells fired by the belligerents and about 15 million tons of metal and explosive material buried on the frontline (Bausinger and Preuβ, 2005; Bausinger *et al*., 2007). Shells included chemical weapons containing nitroaromatic, chlorine, bromine and arsenical compounds, used on a massive scale. At the end of the Great War, the French military authorities faced the challenge of disposing of large amounts of unfired German chemical munitions. During the 1920–1928 period, 200,000 shells were broken down and open-burned near Verdun, on a site named “Place-à-Gaz”. The burning of Blue Cross shells – loaded with high explosives coating a glass bottle containing solid diphenylchloroarsine (CLARK 1) and diphenylcyanoarsine (CLARK 2) – resulted in locally intense soil contamination by arsenic and heavy metals and a lack of vegetation (Bausinger *et al*., 2007; Thouin *et al*., 2016).

The pollution of this site has already been characterized and detailed in two studies (Bausinger *et al*., 2007; Thouin *et al*., 2016). Their results demonstrated that the main As-carriers were amorphous materials composed of a blend of metals and arsenate minerals of Zn, Cu and Fe. On site, the most mobile contaminants were found to be Zn – whose behavior was mainly determined by pH – and As, whose behavior was correlated with the availability of iron sinks. The site is located in an oak forest and is therefore subject to natural deposition of litter that provides bioavailable organic matter (OM). In addition, the clayey formation beneath the contaminated soil severely limits the infiltration of rainwater and favors runoff of soluble inorganic pollutants from the site. Saturation of the lower part of the contaminated

layer was also observed during periods of high precipitation. The stability of the pollutants can therefore be altered by the evolution of environmental conditions.

The contaminated soil is rich in organic carbon (about 25%), due mainly to the presence of charcoal resulting from the use of firewood during destruction of the shells. However, the presence of biodegradable OM at the edge of the site was also demonstrated by Thouin *et al*. (2016). The two types of OM (charcoal and fresh OM) may influence the mobility of metals and metalloids, either because of the high adsorption capacity of the charcoal (Hua *et al*., 2009) or by chelation or methylation processes occurring in the presence of fresh organic compounds (Park *et al*., 2011; Huang *et al*., 2012). Bioavailable OM can also promote bacterial activity and change environmental conditions locally.

Saturation of the soil by water can influence the behavior of metals and metalloids in polluted soils as a result of the change in redox conditions. Many authors have observed that soil saturation increases As solubility because of the joint dissolution of iron oxides and reduction of AsV (Kumpiene *et al*., 2009; Weber et al., 2010; Couture et al., 2015). Soil saturation can also affect other biogeochemical cycles, such as those of nitrogen or carbon (Rey *et al*., 2005; Anderson *et al*., 2014) and, more generally, all reactions influenced by the redox conditions of the environment.

This study aimed to evaluate the effect of (i) water saturation episodes and (ii) input of bioavailable OM on the behavior of pollutants in a soil contaminated by burning of shells. To this end, an 8-month experiment was conducted with a 1 m^3 mesocosm. A mesocosm is an intermediate scale between full field scale and the laboratory microcosm. It is suitable for simulating environmental events in controlled conditions and for monitoring of contaminants in soil pore water. The composition of soil waters at different depths and in leachates provides information on the processes that can influence the fate of contaminants and the potential for transfer towards surrounding compartments.

2. Materials and methods

2.1. Study site and soil sampling

The study site, known as "Place-à-Gaz", is located in the Spincourt forest, 20 km northeast of Verdun, France (Bausinger *et al*., 2007; Thouin *et al*., 2016). On the site, there is a black layer of soil containing slag, coal ashes and ammunition residues resulting from the thermal destruction of arsenical shells (Bausinger *et al*., 2007; Thouin *et al*., 2016).

An instrumented mesocosm was filled with about 1 m^3 of material taken from the black layer (between 0 and 30 cm) with an excavator in October 2015. The material was excavated from the most contaminated part of the site. The biogeochemical characterization of the material had already been performed by Bausinger *et al*. (2007) and Thouin *et al*. (2016) and it was known to be severely contaminated with Zn, As, Cu and Pb. Organoarsenical and nitroaromatic compounds were also found (Bausinger *et al*., 2007). Oak organic litter was taken from the edge of the forest, close to the study site. The surface litter corresponding to the previous year's deposit was not sampled, only the thinner older organic litter was taken.

2.2. Instrumented mesocosm

The instrumented mesocosm (Fig.3.5) consisted of a closed stainless steel column (1 m in diameter and 120 cm high) filled with 610 kg of homogenized contaminated soil. A layer of inert gravel (centimetric quartz and flint particles) and a geotextile membrane were disposed at the bottom of the mesocosm to facilitate outflow drainage without loss of soil particles. During filling, the column was equipped at four depths (H1: 5 cm, H2: 20.5 cm, H3: 36 cm and H4: 48 cm, measured from the top) with time domain reflectometry (TDR) probes (TRIME-PICO32, IMKO), to measure soil moisture and temperature, and with inert PTFE/Quartz porous probes (pore size 2 µm, three probes for each sampling depth) to sample soil water. Five Horticultural LEDs at the top of the column simulated 12-hour day/night cycles. Rainfall was simulated by a sprinkler system connected to a water reservoir and fed by two pumps. The leachate was collected in a steel tank and quantified using a balance. Outflow weight and soil moisture and temperature at the four sampling levels (H1, H2, H3 and H4) were monitored continuously, with a frequency of one hour.

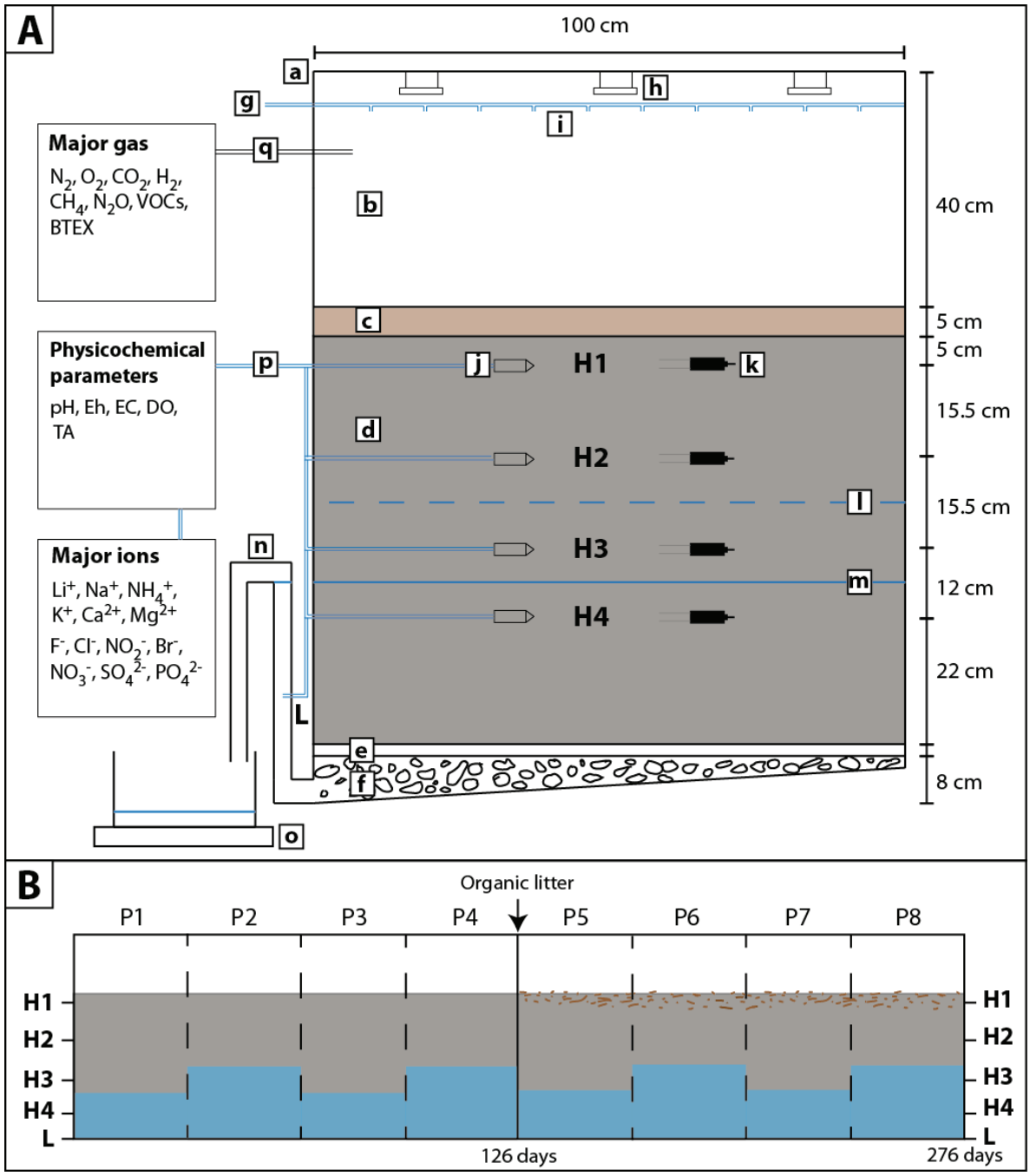

Figure 3.5: A. *Schematic of the mesocosm experiment. a: stainless steel column, b: controlled atmosphere, c: organic litter, d: contaminated soil, e: geotextile membrane, f: inert gravel, g: feedwater, h: LED lighting, i: watering system, j: porewater samplers, k: soil moisture and temperature probes, l: water table in wet condition, m: water table in dry condition, n: water level control, o: balance, p: FEP water tubing, q: gas tubing.* ***B.*** *Experiment design. P1, P3, P5, P7 were dry periods, P2, P4, P6, P8 wet. From the beginning of P5 forest litter was added at the top of the contaminated soil. H4 was permanently saturated; (blue) H2 and H1 were never saturated. The H3 level was not saturated in the dry period and saturated in the wet period. The leachate (L) was sampled at the outlet of the mesocosm.*

2.3. Experimental design

Water soil saturation effects were studied by simulation over around 8 months of cycles of dry/wet periods (P) of about one month each, referred to below as P1 to P8. The dry period was characterized by a saturation of the bottom of the mesocosm limited to the H4 level, and by the addition of around 12 L of Mont Roucous water once a week. This mineral water was used because of its chemical composition close to that of rainwater (pH = 6.38, electrical conductivity = 160 µS.cm^{-1}, Cl^- = 2 mg.L^{-1}, NO_3^- = 1.5 mg.L^{-1}, SO_4^{2-} = 1.5 mg.L^{-1}, Na^+ = 2.5 mg.L^{-1}, K^+ = 0.3 mg.L^{-1}, Ca^{2+} = 1 mg.L^{-1}, Mg^{2+} = 0.5 mg.L^{-1}). The wet period was characterized by elevation of the water table in order to saturate both H3 and H4 levels, and by the addition of 6 L of water every two days. After two dry-period/wet-period cycles (day 126), 24 kg of fresh organic litter taken from the "Place-à-Gaz" site was added above the topsoil in order to study the impact of a supply of fresh OM from the forest (under the mosses and lichens). The mesocosm atmosphere was controlled and renewed by wet compressed air (N_2 = 82.45 ± 0.15 %, O_2 = 22.68 ± 6.7 10^{-2} % and CO_2 = 0.053 ± 6.7 10^{-4}%) at a flow rate of 60 L.h^{-1} for the duration of the experiment.

2.4. Sampling and analyses of soil solution and leachate

Sampling of soil waters from levels H2, H3, H4 (not from H1 because this level did not contain enough water) and of the leachate L was performed twice a week via FEP tubing connected to a peristaltic pump. Major ions and physicochemical parameters of water samples were measured directly. Electrical conductivity (EC), redox potential (Eh), pH, dissolved oxygen (DO), and temperature were measured with a benchtop meter (multiparameter analyzer C3040, Consort) connected to an ORP sensor (Ref. Ag/AgCl) and oxygen probes (Fisherbrand), pH electrode (Fisherbrand) and conductivity probe (Sentek). Total alkalinity (TA) of the leachate was measured by titration, with the 848 Titrino plus (Metrohm).

Major ions (Li^+, Na^+, NH_4^+, K^+, Ca^{2+}, Mg^{2+}, F^-, Cl^-, NO_2^-, Br^-, NO_3^-, SO_4^{2-}, PO_4^{3-}) were detected and quantified by ion chromatography (IC) using a 940 Professional IC Vario instrument (Metrohm, Herisau, Switzerland) equipped with conductivity detectors. Anions were separated with a Metrosep A Supp 16 ionic resin column (150 mm × 4 mm i.d.) and cations with a Metrosep C6 (150 mm × 4 mm i.d.).

The soil waters were filtered at 0.45 µm once a week, to determine trace element concentrations (As, metals) and dissolved organic carbon (DOC). As speciation was performed immediately with an ion exchange method (Kim, 2001). Separation was performed

on anionic resin (AG 1-X8©, Biorad, Hercules, CA, USA). In these conditions (pH < 9.3), this method separates non charged species (AsIII-like) from anionic As species (AsV-like). A water sample was acidified for determination of total As, Fe, Cu, Zn and Pb. Arsenic and metals were quantified with an Atomic Absorption Spectrometry oven (AAS; Varian, Palo Alto, CA, USA). DOC concentration was measured using a TOC 5050/SSM 5000-A (Shimadzu) elemental analyzer.

As speciation in soil waters and in solutions obtained from gaseous traps was determined once a month by HPLC-ICP MS. Arsine gases, including arsine, monomethylarsine ($MeAsH_2$), dimethylarsine (Me_2AsH) and trimethyl arsine (TMAs), were quantified at the end of each period P using the method from Mestrot et al. (2009). Arsines were trapped on silver nitrate impregnated silica gel containing tubes connected to the outlet of the mesocosm for 3 days. Traps were eluted with 5 mL of boiling water. Concentrated hydrogen peroxide (100 µL) was added to the eluate in order to respectively oxidize TMAs to trimethylarsine oxide (TMAO), Me_2AsH to dimethylarsinic acid (DMAA), $MeAsH_2$ to monomethylarsonic acid (MMAA) and arsenite to arsenate, for further determination. Chromatographic separation was carried out with a Model 1100 HPLC pump (Agilent, Wilmington, DE, USA) as the delivery system. The exit of the column was connected directly to the Meinhard nebulizer (Glass Expansion, Romainmotier, Switzerland) of the ICP MS (Agilent 7500cx, Tokyo, Japan) via PEEK tubing. Injections were performed using a Rheodyne valve with a 100 µL loop. As species separation was performed using an anion exchange column (Hamilton PRP-X100 – 250 mm x 4.1 mm).

For soil waters, the mobile phase used was a carbonate based gradient at pH 8.9 (20 mM from 0 to 10 min and 50 mM from 10 to 25 min). This allowed determination of arsenobetaine, As(III), As(V) and methylated As species (DMAA and MMAA). Phenylated As compounds (courtesy of Lionel Lumet, Laboratoire de l'Environnement et de la Vendée, France) such as diphenylarsinic acid (DPAA), triphenylarsine oxide (TPAO) and triphenylarsine (TPA) were also injected but were not eluted from the column in these conditions. Solutions obtained from the gaseous traps were determined in the elution conditions given in Mestrot *et al*., 2009 using a phosphate buffer 10 mM pH 6.2 as mobile phase. These conditions allow the determination of TMAO, DMAA, MMAA and As(V) in solutions originally corresponding to the following gaseous arsines (TMAs, Me_2AsH, $MeAsH_2$ and AsH_3, respectively) after their oxidation . Concentration values and uncertainties found were calculated from a duplicate determination.

Nitroaromatic and aromatic arsenical compounds were identified and quantified in the mesocosm leachate at the end of the experiment (P8) by HPLC-DAD from a specialized laboratory (Envilytix, Wiesbaden, Germany).

2.5. Gas analyses of atmosphere and respiratory test

CO_2, O_2, H_2, N_2, N_2O, CO and CH_4 as well as light hydrocarbons in the atmosphere of the mesocosm were analyzed online, every week, using a gas chromatograph (Compact GC Interscience, CPG) equipped with three columns and detectors in parallel, with He as carrier gas. H_2, O_2, N_2, and CO were separated in an Rt-Msieve 5A column (5A, 15 m × 0.32 mm) and CO_2, CH_4 and N_2O were separated in a HayeSep D column (30 m × 0.32 mm). Gaseous species were analyzed by thermal conductivity detector (TCD). In the third column (Stabilwax, 12 m × 0.32 mm), volatile organic carbon (VOC) and BTEX were separated and analyzed by flame ionization detection (FID). The gas chromatograph was linked directly to the column atmosphere via 0.8–1.6 mm (1/16) PEEK capillary tubing.

The mineralization of CO_2 by the mesocosm was evaluated 6 times, at the end of each period with the exception of P1 and P2. The increase of CO_2 in the column atmosphere was measured in dark conditions and without input of atmospheric air. CO_2 concentrations were analyzed about every 7 minutes over 3 hours. Carbon mineralization rates were calculated from the linear increase of CO_2 concentration in the column over time.

2.6. Leaching tests

Leaching tests were performed to estimate the mobility of major compounds, metals and arsenic from the solid material. Two conditions were tested with solid/liquid ratios from 1 to 10 (wet solid equivalent to 10 g of dry weight, 100 mL of Mont Roucous water): polluted soil (similar to soil mesocosm, "Soil"), forest litter ("OM"). Tubes were rotated on a roller mixer for 24h at 20°C. All conditions were performed in triplicates. Chemical parameters, ions, metals and arsenic concentrations were measured by methods previously described.

2.7. Statistical analyses

All statistical tests were conducted in R 3.2.4 (www.r-project.org). To summarize temporal trends of element concentration, values were plotted with a smooth curve based on the loess function (ggplot 2 package). The Loess function is a smooth local regression for "geom_smooth" in the ggplot2 package for a small sample size; it is controlled by the "span" setting (Wickham, 2009) ranging from 0 (exceedingly "wiggly" smooth curve) to 1 (less

"wiggly" smooth curve). In this study, span was set between 0.3 and 0.4, depending on the variation of the temporal data.

Overall trends, without the effect of dry/wet cycles, were also statistically tested using the Seasonal Kendall (SK) test (Hirsch *et al*., 1982; Hirsch and Slack, 1984), which is a modified version of the non-parametric Mann Kendall test (Mann, 1945; Kendall, 1948) for monotonic trend. The SK test, which is robust to outliers and missing values, can be used considering inner dependence of data. The seasonal effect (here the shift between dry and wet periods) is reduced by making comparisons between data from a similar season (period). Kendall's tau (τ) measures the degree of correspondence between two variables. If $\tau = 0$ no correlation exists between the pairs, if τ is positive there is an upward trend and a negative τ is associated with a downward trend. The statistical significance of the trend is indicated by the corresponding *p*-value ($p \leq 0.05$ is considered significant).

Results from leaching tests were tested for homogeneity of variance and normality. One-way analysis of variance and Tukey tests were carried out to test for any differences between each treatment. For each treatment the number of observations was equal to 3, and a difference of 5% between means ($p \leq 0.05$) is considered significant.

3. Results

3.1. Composition of soil solution and leachate

3.1.1. Physicochemical parameters

The physicochemical parameters of water (pH, EC, Eh and DO) for the 3 levels of soil waters and leachate are shown in Figure 3.6. Soil waters and leachate were characterized by pH values between 5.5 and 6.0 at all of the different depths of soil water and throughout the experiment. Leachates were slightly more acid than the soil waters. Electrical conductivity ranged from 500 to 2,500 $\mu S.cm^{-1}$. EC increased with depth and was highest in the leachate. In the samples from each level, the maximum EC was measured in the first or second period and decreased until the end of the experiment. The redox potential (Eh) varied between 270 and 380 mV, indicating moderately oxidized soil waters and leachates. Eh was stable during the first 4 periods and then decreased, particularly in H4 and L. DO varied between 250 and 160 µM in H2 to 180 and 140 µM in H4. In H3 and H4, DO was lower in P6–P8 than in P1–P5 (about 180 to 140 µM). DO in the leachate fluctuated widely between 200 and 50 µM throughout the experiment.

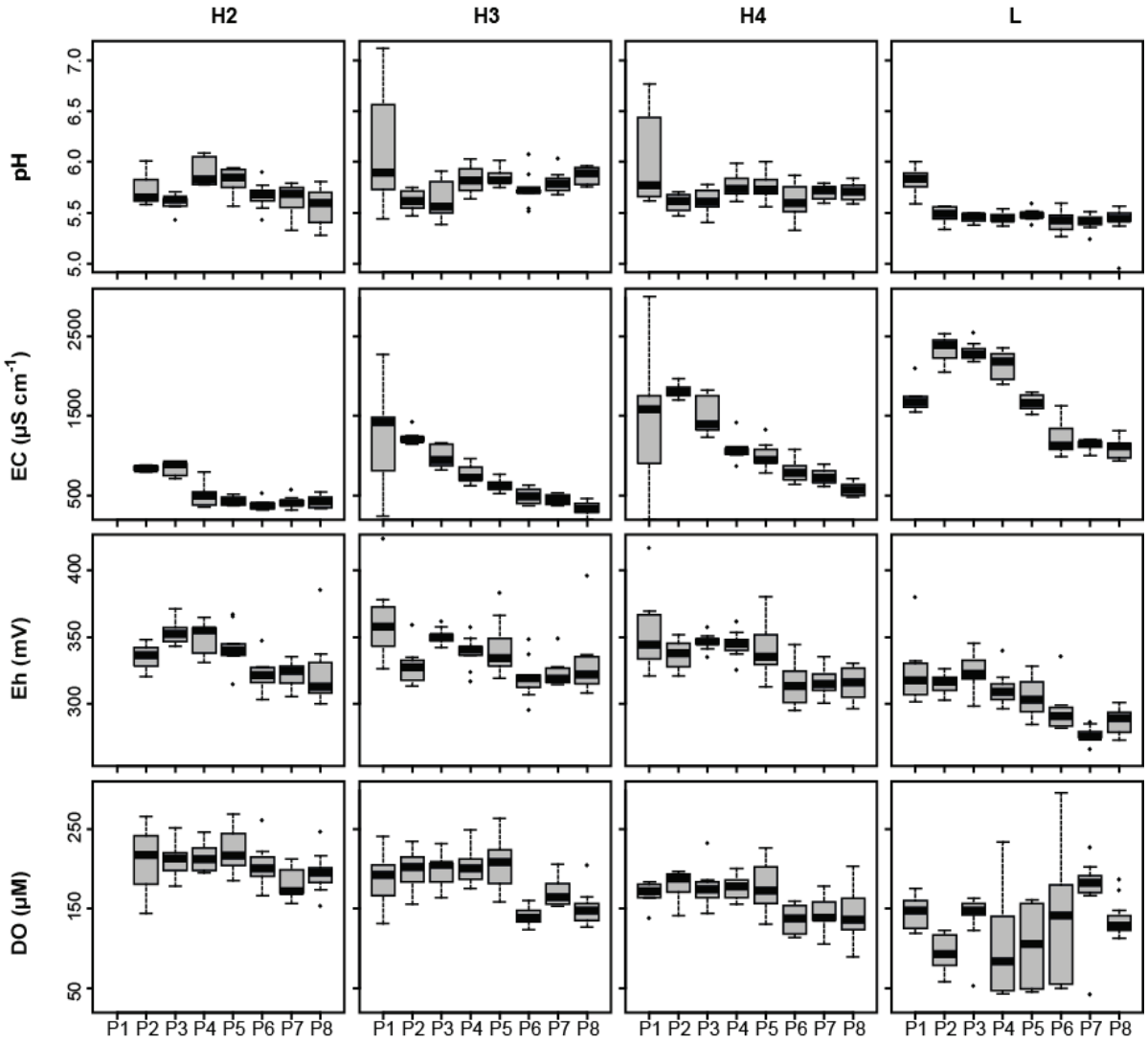

Figure 3.6 : *Evolution of physicochemical parameters in each sampling level. Boxplots represent the median, 25th percentile and the 75th percentile, error bars indicate 10th and 90th percentile. Data not included between the whiskers were plotted as an outlier. Each boxplot includes values of one period P (n = 5–10).*

3.1.2. Major ions concentrations

Major ions, with an average content greater than 1 mg.L^{-1}, were Cl^-, NO_3^-, SO_4^{2-}, K^+, Na^+, Ca^{2+} and Mg^{2+}. In order, their concentrations in soil waters were, respectively: $NO_3^- < Cl^- < SO_4^{2-}$ and $Ca^{2+} < Na^+ < K^+ < Mg^{2+}$. However, NO_3^- concentrations were lower (< 0.1 mg.L^{-1}) at the bottom of the mesocosm and in the leachate. Concentrations of most of the ions analyzed (Cl^-, SO_4^{2-}, K^+, Na^+, Ca^{2+}, Mg^{2+}) increased with depth and increased in the leachate in accordance with EC.

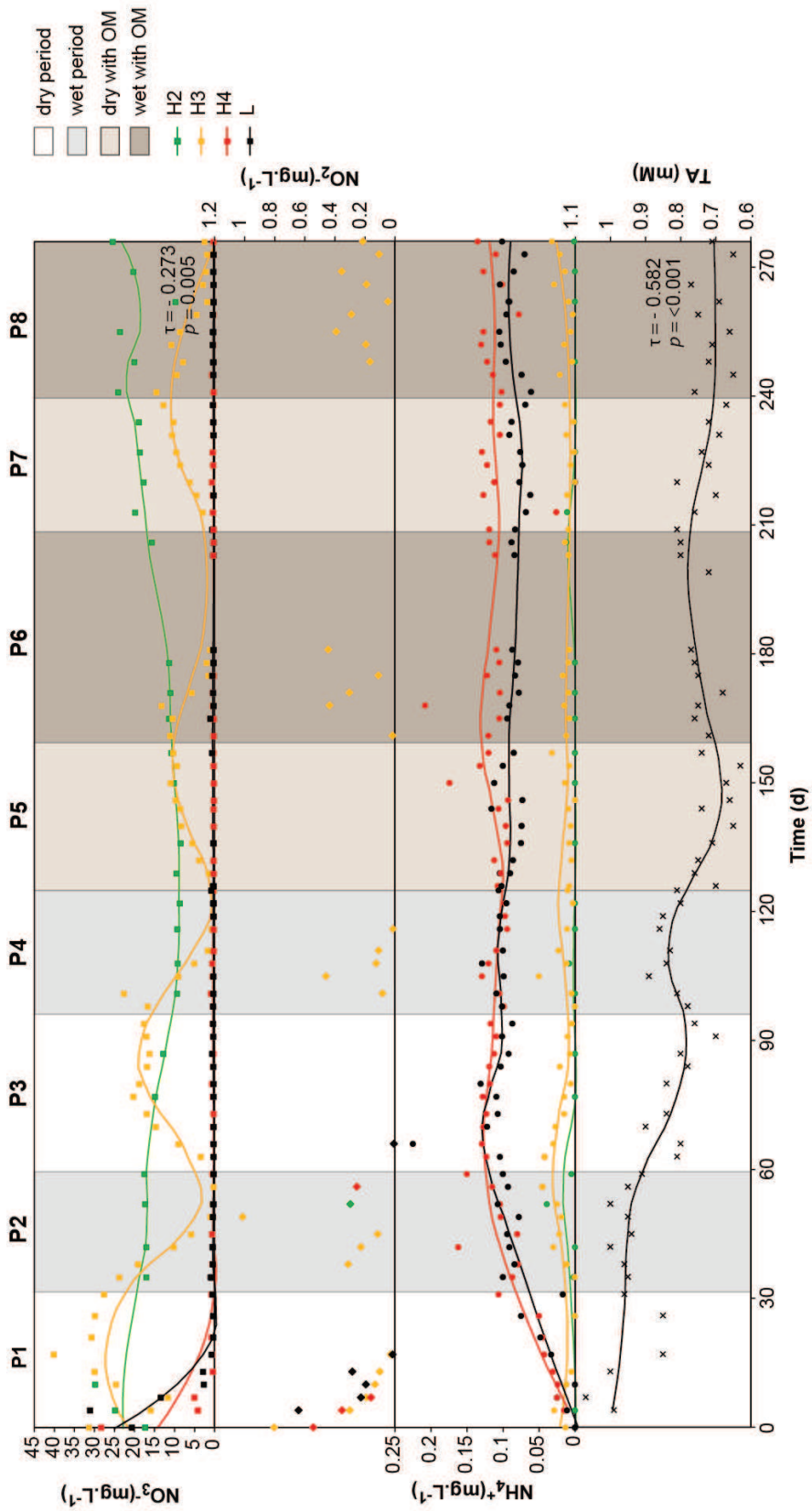

Figure 3.7: *Measured evolution of NO_3^- (square), NO_2^- (diamond), NH_4^+ (circle) and TA (cross) concentrations. Curves correspond to smooth local regression (span = 0.3). Kendall's tau (τ) and p-value were given for significant trends with SK test ($p < 0.05$).*

The evolution of NO_3^-, NO_2^- and NH_4^+ with depth (Fig.3.7) was different. At level H3, NO_3^- concentrations increased to reach a plateau in the dry periods then decreased until they disappeared in the wet periods. The maximum concentrations decreased from 30 $mg.L^{-1}$ during P1 to 15 $mg.L^{-1}$ at the end of P7. This significant trend for NO_3^- concentrations was found only in level H3 level (τ = -0.273, p = 0.005). Small amounts of NO_2^- were present in the water in H4 and L at the beginning of the experiment, and in H3 during each wet period. However, except for P1, no NO_2^- was detected during dry periods. NH_4^+ concentrations showed no significant trend, but two different behaviors. In H2 and H3, NH_4^+ concentrations were low (< 0.05 $mg.L^{-1}$) and constant, but in H4 and L concentrations increased until 0.1 $mg.L^{-1}$ during the two first periods and then remained constant.

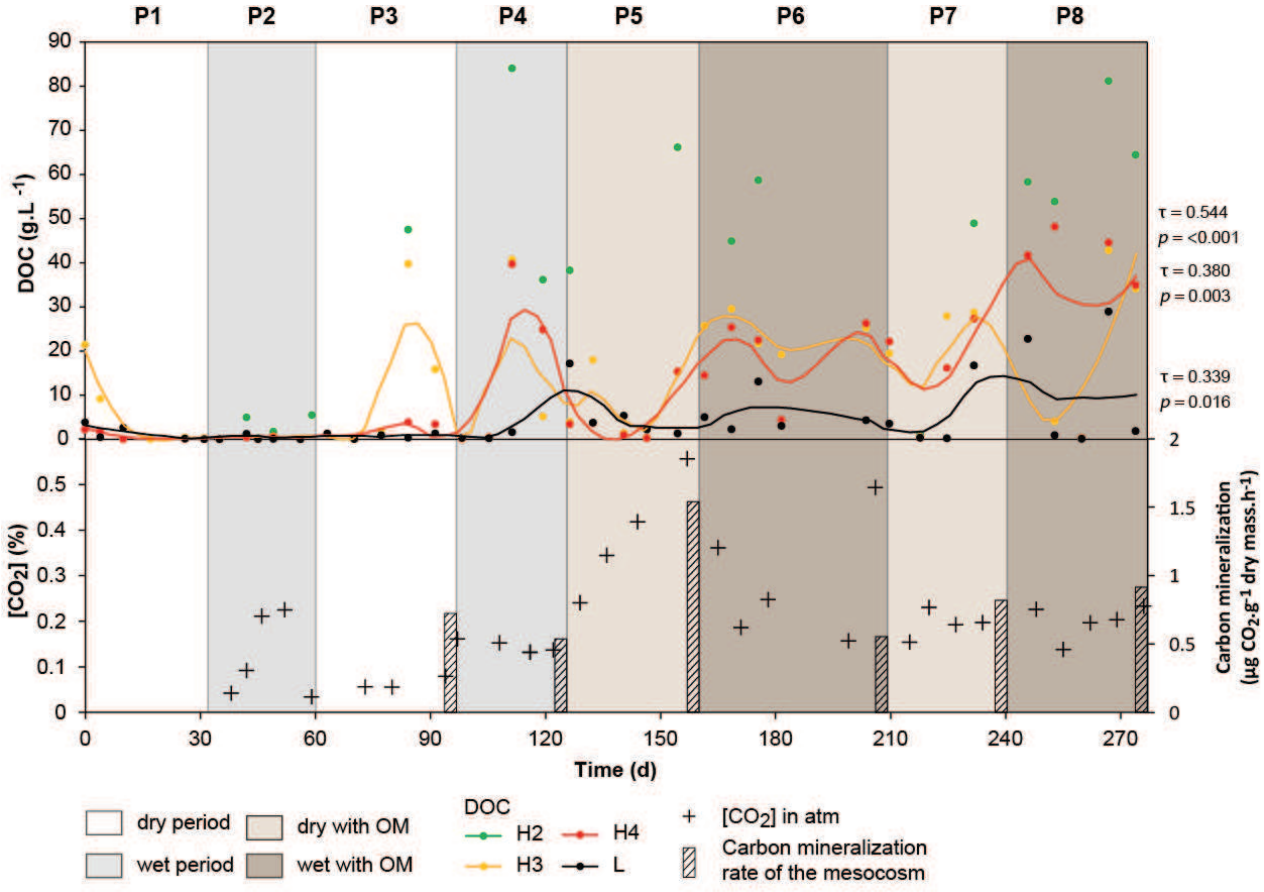

Figure 3.8: *Evolution of DOC (circle), gaseous CO_2 in mesocosm atmosphere (cross) and carbon mineralization rate of the mesocosm (bar), measured at the end of periods P3–P8. Curves correspond to smooth local regression (span = 0.4). For H2 level sampling no local regression was calculated because of the low frequency of measurement. Kendall's tau (τ) and p-value were given for significant trends with SK test ($p < 0.05$).*

Total alkalinity (TA) in the leachate decreased from 1 to 0.65 mM (Fig.3.7). This decrease was statistically significant based on the SK test (τ = - 0.582, p < 0.001). TA was subjected to monthly variability and therefore increased to a local maximum during wet periods (P2, P4 and P6) and decreased in dry periods (P1, P3 and P5). These variations were narrower in the last two periods, P7 and P8.

Dissolved organic carbon (DOC) concentrations were very high in the soil water at level H2 (> 30 g.L^{-1}) and decreased with depth (Fig.3.8). DOC was less concentrated before the addition of forest litter, but a few samples in H2, H3 and H4 revealed high concentration peaks. After the addition of organic litter to the top of the mesocosm, DOC concentrations increased in all the samples until the end of period P8. Despite the measurement of sporadic extreme values, monthly cyclic variations are visible at each sampling level. Focusing on seasonal variability induced by dry/wet periods revealed significant positive trends in H3 (τ = 0.544, p < 0.001), H4 (τ = 0.380, p = 0.003) and L (τ = 0.339, p = 0.016) (not calculated in H2 because of the low frequency of measurement).

3.1.3. Evolution of metals and arsenic concentrations

Zn was the metal with the highest concentration in soil water and leachate. Zn concentrations evolved in a similar manner at each sampling level, with an increase at the beginning of the experiment followed by a slight decrease (Fig.3.9). However, a lag time was observed with depth, with maximum concentration in P1 for H2 and H3, in P2 for H3, and in P4 in the leachate. Zn also became more concentrated with depth. It seems that dry/wet cycles have no major effect on the Zn concentrations in soil water but, following the addition of fresh OM, the Zn concentration in the output water decreased sharply from 90 mg.L^{-1} to 70 mg.L^{-1}.

Cu and Fe concentrations in solution were low, with maximum amounts of about 0.3 mg.L^{-1} and 2 mg.L^{-1}, respectively (Fig.3.9). Negative trends were observed in H2, H3 and L, with higher values before the addition of organic matter. In H4, Cu was mostly below the quantification limits (LQ = 0.1 mg.L^{-1}) from P1 to P4 but, after the addition of litter, Cu concentrations in H4 were higher than at other depths. Moreover, Cu concentrations at each sampling level stabilized to a constant value after the addition of organic litter. Fe concentration increased significantly in H3, H4 and L (τ = 0.298, p = 0.035; τ = 0.343, p = 0.011; τ = 0.519, p < 0.001), while negative trends were observed in H2 (τ = - 0.302, p = 0.047). Pb concentrations were below the quantification limits (LQ = 0.1 mg.L^{-1}) in the soil waters.

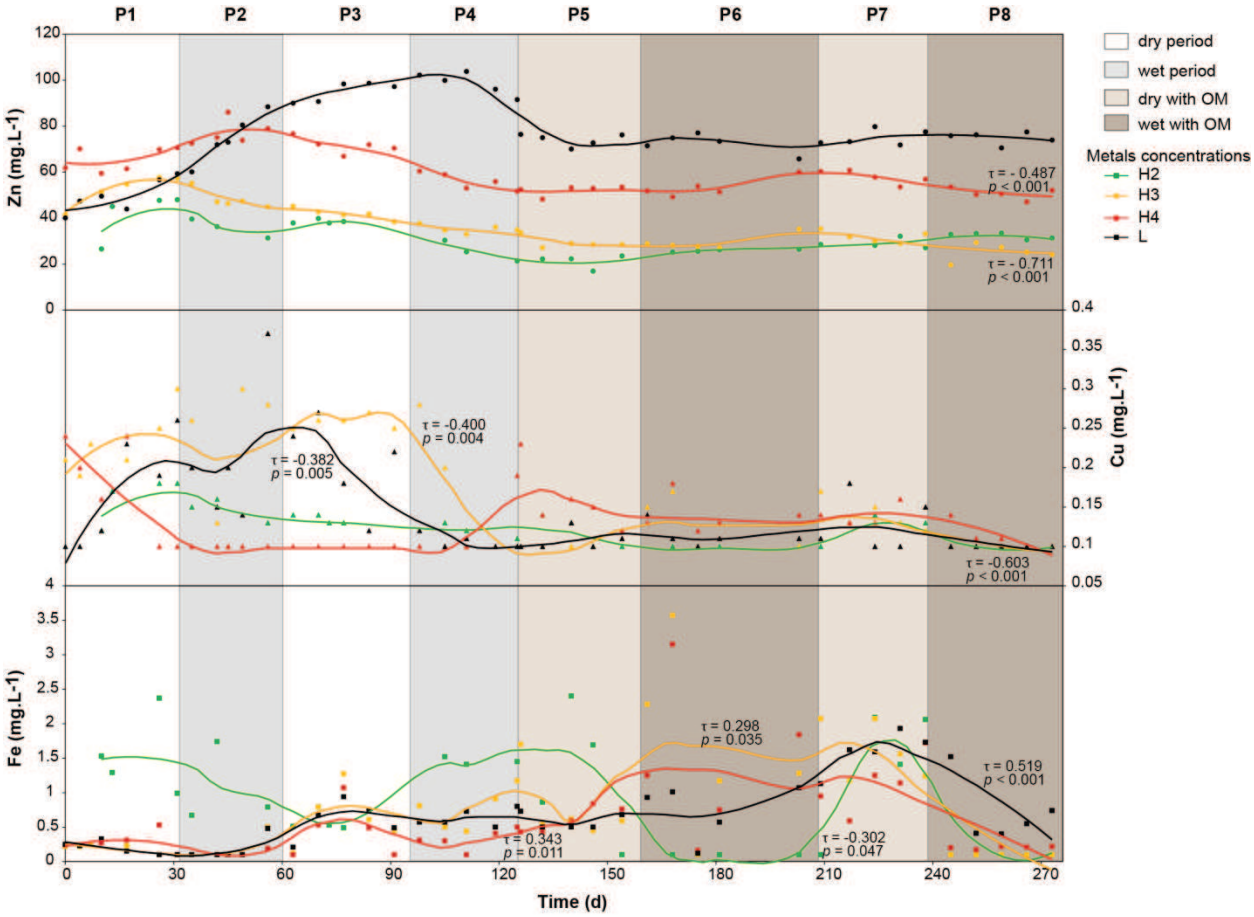

Figure 3.9: *Evolution of concentrations of Zn (circle), Cu (triangle) and Fe (square). For Cu and Fe concentration, measurements were plotted at 0.1 mg.L^{-1} when value was below the quantification limit (LQ = 0.1 mg.L^{-1}). Curves correspond to smooth local regression (span = 0.3). Kendall's tau (τ) and p-value were given for significant trends with SK test ($p < 0.05$).*

Together with Zn, As was a mobile inorganic contaminant throughout the experiment, although the evolution of As concentration was very different: As concentrations were globally higher in the H2 level and decreased with depth (Fig.3.10). No clear impact of dry/wet period was observed, even if monthly cycles are enhanced by the smooth curve of the data. Furthermore, the evolution of As $_{total}$ showed significant negative trends for H2 (τ = - 0.385, p = 0.033), H4 (τ = - 0.327, p = 0.012) and L (τ = - 0.380, p = 0.006), and it seems that, for soil waters, this trend was accentuated after the addition of OM and was visible after 140 days. The same evolution was observed with As V-like, which was the dominant As species in solution. At H4, however, As V-like decreased more significantly (τ = -0.450; p = 0.001) than As $_{total}$. As III-like increased significantly (independently of the cyclical variability) in level H4 (τ = 0.398, p = 0.003), especially after the addition of organic matter. In H2 and H3, As III-like concentration ranged from 300 to 700 µg.L^{-1}, with low amplitude of cyclic

variation, while the concentration in L ranged from 700 to 1,800 µg.L^{-1}, with a high amplitude of monthly variation.

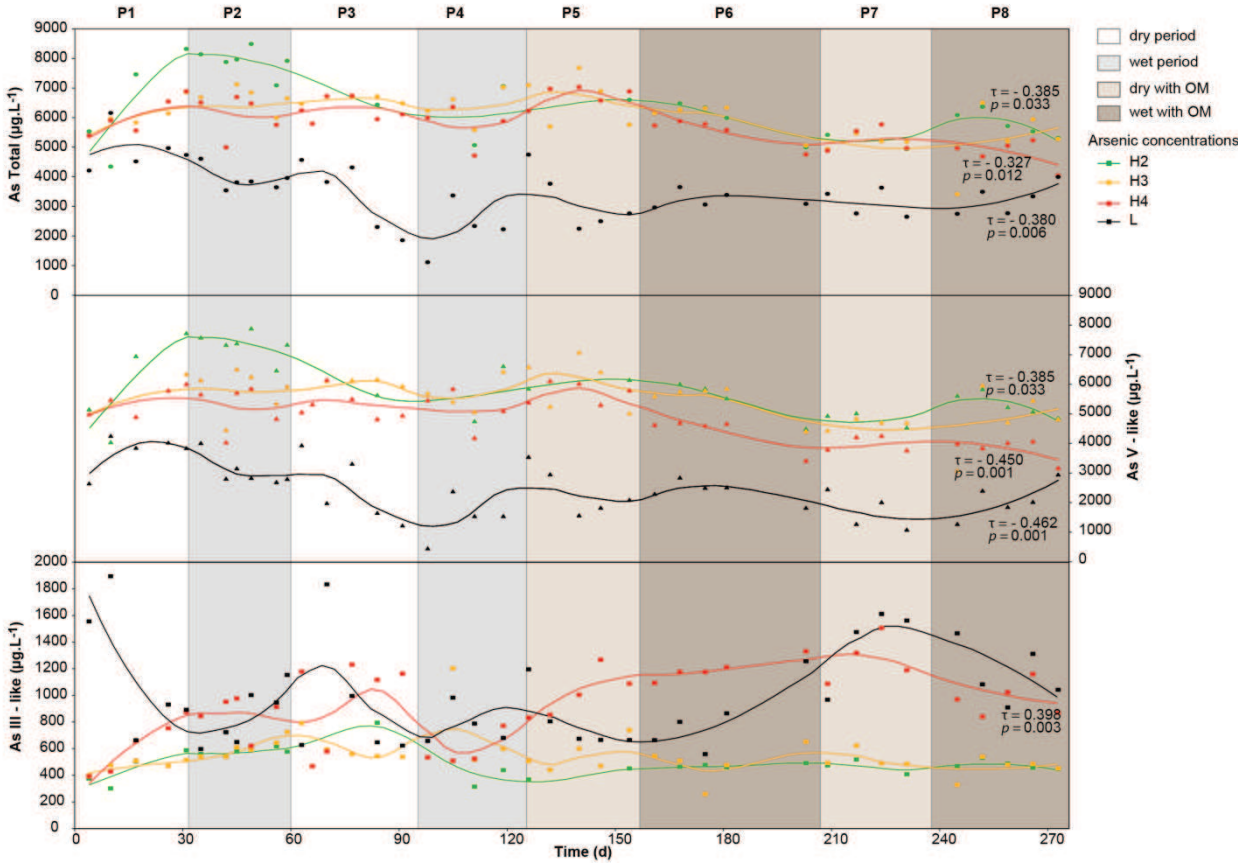

Figure 3.10: *Evolution of concentrations of total As (circle), As V-like (triangle) and As III-like (square) obtained by separation with resin and analyses by AAS. Curves correspond to smooth local regression (span = 0.3). Kendall's tau (τ) and p-value were given for significant trends with SK test ($p < 0.05$).*

Results of arsenic speciation obtained with HPLC-ICP MS in water from H2, H3 and H4 (Fig.3.11) show that As V concentration presents a distribution similar to that of As V measured as total As after separation on anionic resin. Conversely, As III concentrations measured with HPLC-ICP MS were lower. Four other As species were detected in soil water. Diphenylarsinic acid (DPAA) was identified and quantified in the mesocosm leachate at the end of the experiment (P8), its concentration reaching 30.6 µg.L^{-1} (SM.3.2). Three unknown species were also detected. Concentrations of the first unknown compound ranged from 150 to 200 µg.L^{-1} and were very homogeneous over all of the sampling levels and each of the periods. Unknown 1 was the third main arsenic species after As V and As III in terms of concentration. The second unknown compound was only detected in H4 and L, with

concentrations increasing from about 80 to 200 µg.L^{-1}, and in H3 during the wet periods (P2, P4, P6 and P8). A third unknown compound was detected in the leachate L and at all depths over the last four periods (P5–P8), with a range of 22 to 51 µg.$L^{-1.}$ Detection of this unknown arsenic species during the first four periods (P1-P4) was, however, compromised by the greater dilution of water sampling.

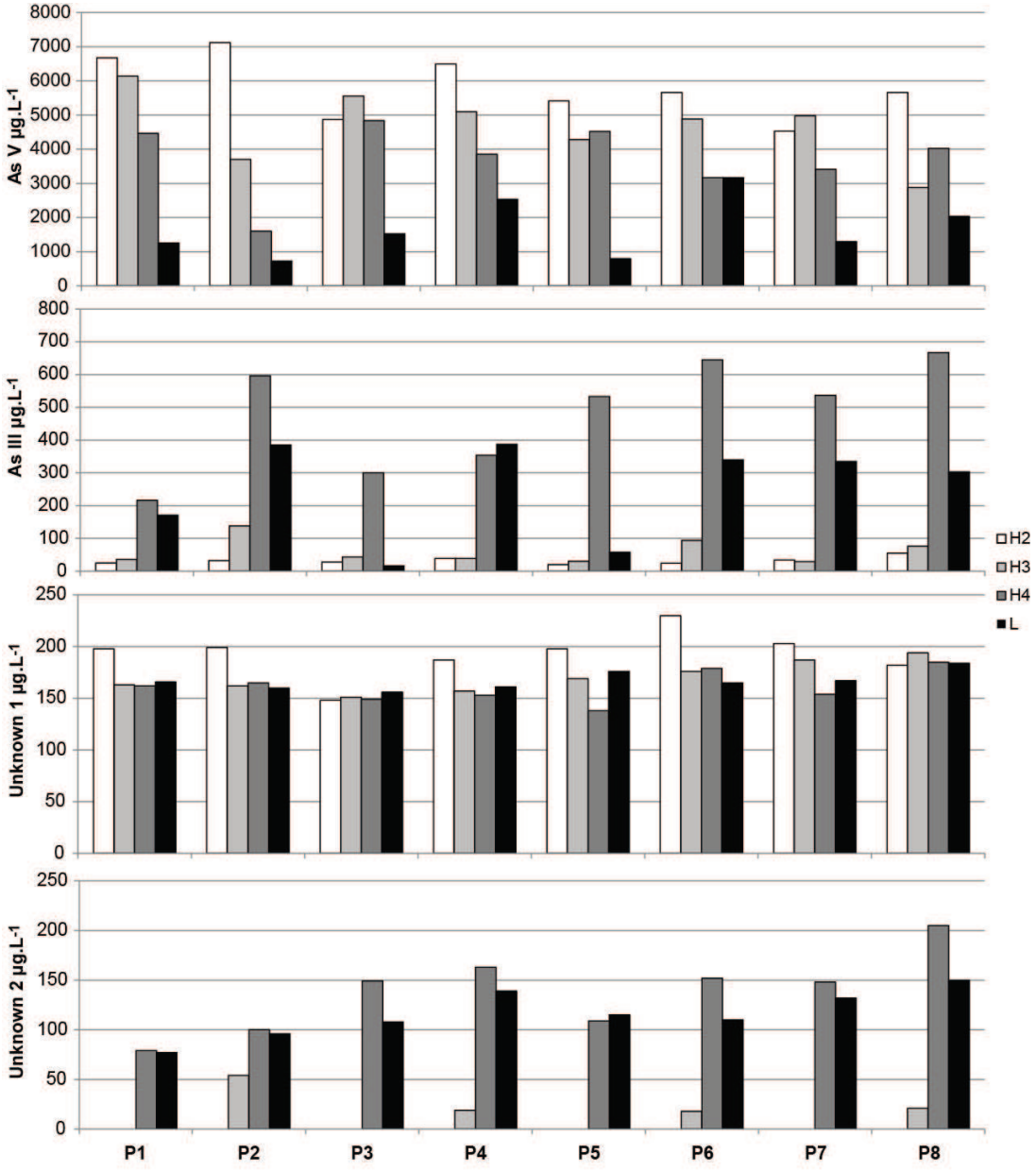

Figure 3.11 : *Arsenic speciation in soil water samples at the end of each period measured with HPLC-ICP MS. Unknown 1 and Unknown 2 were unknown As species. Their concentrations were evaluated from calibration of other species and are only indicative. (LQ = 0.1 µg.L^{-1} for As III and LQ = 0.5 µg.L^{-1} for the other species).*

3.2. Fluxes of solutes

Fluxes and total leaching of compounds were calculated for: the first four periods (P1–P4, 126 days) with a mean water flux of 2.65 $L.d^{-1}$; for the four periods after the addition of forest litter (P5–P8, 138 days) with a mean water flux of 2.01 $L.d^{-1}$; and for the whole experiment (Tab.3.1).

Table 3.1 : *Solute fluxes during the periods P1–P4 and P5–P8 (respectively before and after the addition of organic litter). Water leachate volume was measured with a balance. Total compound leaching was calculated by assuming that compound concentration in the leachate between two sampling operations was equal to the concentration measured in the last sample. Water fluxes were calculated by dividing the leachate volume by the total period duration and the elemental fluxes were calculated by dividing the amount of compound leached during the period by the total period duration.*

Period	P1-P4		P5-P8		Total	
Duration (day)	126		138		264	
Leachate volume (L)	334		278		612	
Water flux ($L.d^{-1}$)	2.65		2.01		2.32	
Major compounds	Flux ($mg.m^{-3}.d^{-1}$)	Total leaching ($g.m^{-3}$)	Flux ($mg.m^{-3}.d^{-1}$)	Total leaching ($g.m^{-3}$)	Flux ($mg.m^{-3}.d^{-1}$)	Total leaching ($g.m^{-3}$)
DOC	4959.1	624.8	30,626.3	4224.4	18,372.9	4849.2
TA	4.1	0.5	2.5	0.4	3.3	0.9
Cl^-	203.9	25.7	87.9	12.1	143.3	37.8
Br^-	2.7	0.3	1.0	0.1	1.8	0.5
SO_4^{2-}	134.3	16.9	65.8	9.1	98.5	26.0
K^+	8.1	1.0	4.5	0.6	6.2	1.6
Na^+	11.4	1.4	5.9	0.8	8.6	2.3
Ca^{2+}	162.1	20.4	72.9	10.1	115.5	30.5
Mg^{2+}	12.8	1.6	6.4	0.9	9.4	2.5
Metals and arsenic						
Fe	1.90	0.24	3.03	0.42	2.49	0.66
Zn	374.85	47.23	260.63	35.63	315.16	83.18
Cu	0.75	0.10	0.34	0.05	0.54	0.14
As $_{total}$	14.46	1.82	12.56	1.73	13.47	3.55
As III-like	4.45	0.56	3.62	0.50	4.01	1.06
As V-like	11.47	1.45	7.61	1.05	9.45	2.50

During P6, 12 days have been excluded from calculation because the monitoring was stopped and no water was input to the mesocosm.

After 276 days, the most leached compounds were DOC, Zn^{2+}, Cl^{-}, Ca^{2+}, SO_4^{2-} and, to a lesser extent, As, Mg^{2+}, Na^{+} and K^{+}. Among these compounds, Zn and As were the most mobile metal(loid)s, with, respectively, total amounts of 83.18 and 3.55 $g.m^{-3}$ leached, with about 30% of As III-like. Fluxes of DOC and Fe increased after the addition of OM, ranging from 4,959 to 30,626 $mg.m^{-3}.d^{-1}$ for DOC and 1.90 to 3.03 $mg.m^{-3}.d^{-1}$ for Fe. Between the first periods (P1-P4) and the periods following the addition of organic litter (P5–P8), the majority of the other compound fluxes were significantly halved, with the exception of As total flux which decreased less after the addition of OM (from 14.46 to 12.56 $mg.m^{-3}.d^{-1}$).

3.3. Gas composition and carbon mineralization

Among all the gases analyzed (i.e. CO_2, O_2, H_2, N_2, N_2O, CO, CH_4 and BTEX) only CO_2, O_2, H_2, N_2 were detected in the atmosphere of the mesocosm during the experiment. CO_2 was the only gas for which concentrations varied (Fig.3.8). The sum of the concentrations of CO_2, O_2, H_2 and N_2 was less than 100% because of the presence of water vapor in the mesocosm atmosphere. Prior to the addition of OM, the CO_2 concentrations seem to have been driven by the wet/dry periods, with higher concentration during the wet periods. CO_2 concentration was clearly affected by the addition of organic litter, with a strong increase from 0.137 to 0.556% during period P5. After this increase, the values dropped and stabilized at about 0.200%.

The rate of carbon mineralization in the mesocosm was evaluated at the end of periods P3, P4, P5, P6, P7 and P8 (Fig.3.8). It was highest at the end of P5, the first period following the addition of OM, at 1.54 µg $CO_2\,g^{-1}$ dry $mass.h^{-1}$. No major difference was observed in the other periods, but rates were slightly higher at the end of dry periods ($mean_{(P3,\ P5,\ P7)}$ = 1.03 ± 0.27 µg $CO_2.g^{-1}$ dry $mass.h^{-1}$) than wet periods ($mean_{(P4,\ P6,\ P8)}$ = 0.67 ± 0.12 µg $CO_2.g^{-1}$ dry $mass.h^{-1}$), and were also higher after the addition of OM ($mean_{(P3\text{-}P4)}$ = 0.63 ± 0.08 µg $CO_2.g^{-1}$ dry $mass.h^{-1}$, $mean_{(P5\text{-}P8)}$ = 0.95 ± 0.24 µg $CO_2.g^{-1}$ dry $mass.h^{-1}$).

As volatilization from the mesocosm was evaluated at the end of each period. Dimethylarsine, quantified as dimethylarsinic acid (DMAA), was detected in traps for all periods. The rate of dimethylarsine volatilization was between $2.44x10^{-3}$ and $8.97x10^{-3}$ $ng.kg^{-1}.d^{-1}$ for the first four periods and from $1.10x10^{-3}$ to $4.06x10^{-2}$ $ng.kg^{-1}.d^{-1}$ after the addition of forest litter. The maximum rate of dimethylarsine volatilization corresponded to period P5. No other volatile As species was detected in the traps.

3.4. Leaching test

The contribution of soil and litter to the composition of water from the mesocosm experiment was estimated by a leaching test with Mont Roucous water. The results for chemical parameters and quantities of major ions and metal(loid) compounds are presented in Table 3.2.

The pH of leaching tests ranged from 6.31 in the "Soil" test to 5.46 in the "OM" test. EC and DOC were significantly higher in the "OM" test. In the "Soil" leachate, Ca^{2+} and SO_4^{2-} were the most mobile ions, while Ca^{2+}, K^+ and NO_3^- were the dominant ions in the "OM" leachate. As indicated by EC, the "OM" leachate contained higher amounts of ions, especially Na^+, K^+, Mg^{2+}, NO_3^- and PO_4^{3-}. As, Fe, Pb and Cu were significantly more concentrated in leachate from the forest litter than from contaminated soil, up to seven times for As. DPAA was identified in the "Soil" leachate, with a concentration of 114 µg.L^{-1} (SM.3.2).

Table 3.2 : *Leaching test of the polluted soil (Soil) and the forest litter (OM).*

	Soil		OM	
Chemical parameters				
pH	6.31 ± 0.04	a	5.46 ± 0.42	b
EC (µS.cm^{-1})	329.67 ± 7.70	a	469.33 ± 122.78	b
DOC (mg.kg^{-1})	333.45 ± 3.95	a	3085.17 ± 120.78	b
Major ions (mg.kg^{-1})				
Na^+	23.05 ± 0.05	a	42.74 ± 0.87	b
K^+	9.00 ± 0.03	a	110.74 ± 0.22	b
Ca^{2+}	155.35 ± 0.68	a	149.18 ± 6.50	a
Mg^{2+}	9.91 ± 0.01	a	23.71 ± 0.80	b
Cl^-	24.78 ± 0.01	a	15.81 ± 1.23	a
Br^-	n.d.		3.60 ± 0.04	
NO_3^-	34.57 ± 0.25	a	183.49 ± 6.48	b
SO_4^{2-}	144.57 ± 0.13	a	43.60 ± 1.89	b
PO_4^{3-}	n.d.		58.61 ± 1.91	b
Meta(loid)s (mg.kg^{-1})				
As	47.75 ± 0.10	a	344.02 ± 4.07	b
Fe	< 0.1		10.91 ± 0.58	
Zn	134.18 ± 0.42	a	79.89 ± 2.77	b
Pb	1.30 ± 0.02	a	1.99 ± 0.05	b
Cu	< 0.1		0.23 ± 0.19	

Average values are expressed with their standard deviation (n=3). Values with different letters are significantly different ($p < 0.05$, ANOVA Tukey-HSD)

4. Discussion

4.1. Influence of saturation and OM on C and N cycles

Apart from the important concentration of metals and arsenic on the "Place-à-Gaz" site , this soil also contains a high amount of organic carbon (up to 25%, Thouin *et al*., 2016). As demonstrated in the previous study (Thouin *et a*l., 2016), two types of organic matter with very different biodegradabilities are present on the site: low degradable organic matter, inherited from the burning of firewood used during the destruction of ammunition (charcoal); and more biodegradable organic matter that comes from the forest litter. Charcoal accounts for most of the organic matter in the central part of the site. Wildfire-formed charcoals have the potential to greatly enhance soil fertility by enhancing N cycling (Berglund *et al*., 2004), and to provide habitat for microbial life (Pietikainen *et al*., 2000). However, the "Place-à-Gaz" site has been characterized by a lack of vegetation in its central part for almost a century. It is therefore obvious that charcoals, both bearing and mixed with high amounts of contaminants, have not promoted growth of vegetation on the site. Charcoals' stability and resistance to microbial degradation make them important long-term carbon sinks (Schmidt and Noack, 2000), meaning that most of the organic matter on the site is not bioavailable for the growth of microorganisms and vegetation. In the surrounding areas, close to the forest, three species have colonized the contaminated soil: a moss *Pohlia nutans* (Hedw.), a lichen *Cladonia fimbriata* (L.), and an herbaceous species *Holcus lanatus* (L.). The input of forest litter, which provides bioavailable nutrients, was certainly the cause of plants establishing themselves and then also influenced the site's carbon cycle.

The mesocosm experiment described here studied the modification of the carbon cycle induced by the input of oak forest litter. DOC concentrations in the mesocosm experiment were always higher than the common range of DOC concentration in soil water (Boyer *et al*., 1996, Clarke *et al*., 2005). A major part of the DOC in the mesocosm may be derived from the burned organic matter that might not have been entirely mineralized. Similar DOC concentrations, ranging from 300 to 90,000 $mg.L^{-1}$, were reported in leachates from disposal sites which contained municipal solid waste incineration residues (Seo *et al*., 2007). Here, the addition of forest litter induced a significant increase in DOC concentration in the soil water (Fig.3.8) and a very high flux of DOC during the periods following the input (Tab.3.1). The results of the leaching experiment – showing a significantly higher amount of organic carbon leached from the forest litter than from the contaminated soil (Tab.3.2) – underpin the impact of forest litter on DOC content in the soil water. DOC is the primary carbon source for

heterotrophic bacteria in soils (Metting, 1993, Horemans *et al*., 2013), so the increase in the carbon mineralization rate in the mesocosm after the addition of organic litter (Fig.3.8) seems to be directly linked to the biodegradation activity of microorganisms. The increase of CO_2 concentration in the mesocosm atmosphere during the period P5, from 0.137% to 0.556% (Fig.3.8), is another consequence of this high carbon mineralization activity.

The mineralization of organic matter by microbial metabolism is conditioned by the accessibility of terminal electron acceptors (TEA). Oxygen is the most efficient TEA available in the environment, and carbon mineralization consumes oxygen. Microbial respiration impacted the dissolved oxygen content and indirectly the redox potential, which decreased after the addition of organic matter (P6-P8). The reductive process, and hence the Eh decrease, was driven by the consumption/oxidation of DOC coupled with the reduction of the successive TEA's by the bacterial community. Dissolved oxygen also appeared to be determined by depth and by water saturation, even if it was not visible at level H3, alternately saturated and unsaturated.

However, denitrification was evident at level H3, and, globally, the nitrogen cycle was strongly affected by water saturation. During denitrification, nitrate and nitrite are reduced to N_2 gas by heterotrophic denitrifiers in the presence of OM as electron donor. Even though no significant variation of N_2 was observed in the atmosphere, the production of nitrite during each wet period and the variation of alkalinity were certainly the result of denitrification. In the saturated level (H4) and in the leachate, the rapid disappearance of nitrate concomitant with the appearance of nitrite and the increase in ammonium concentration attested to dissimilatory nitrate reduction to ammonium (DNRA). DNRA is a bacterial heterotrophic process occurring in anoxic environments with anaerobic or facultative anaerobic bacteria (Tiedje, 1988). DNRA activity is less sensitive than denitrification to an inhibitory effect by O_2 and equilibrium between denitrification and DNRA seems to be driven by bioavailable carbon (Fazzolari *et al*., 1998). Both mechanisms probably occurred simultaneously: denitrification was the dominant process, as ammonium concentration always remained an order of magnitude less than nitrate concentration, whereas the DNRA process only occurred during long term saturation.

The increase of nitrate concentration during dry periods at level H3 may have been the result of nitrification thanks to ammonium production from DNRA providing a source of NH_4^+ for nitrifying bacteria (Burgin and Hamilton, 2007). However, the small amount of

NH_4^+ in this level during the saturation periods, and the absence of nitrite simultaneously with the increase in nitrates during the dry periods, suggested that nitrification was not the main process inducing the increase of nitrate when soil was desaturated. The soil water from the surface of the mesocosm was rich in NO_3^- and the transport of nitrate down towards the H3 level may explain this phenomenon.

The origin of nitrogen present in the polluted soil could be linked to the degradation of nitroaromatic compounds and diphenylcyanoarsine which were mineralized by combustion. The resulting nitrate might have been adsorbed by charcoal and progressively released in the soil. No nitroaromatic compound was detected in the soil or solution water of the mesocosm. However some nitroaromatic compounds, and particularly 1,3-Dinitrobenzene, had been detected previously on the "Place-à-Gaz" site (Bausinger *et al*., 2007). Several studies have shown that microbial aerobic degradation of nitroaromatic compounds releases nitrogen as nitrite into the environment (Marvin-Sikkema and de Bont, 1994; Spain, 1995). The organic litter was also rich in leachable NO_3^- (Tab.3.2), arising mainly from the decomposition of plant OM. The increase in NO_3^- in level H2 following the addition of organic matter confirmed the supply of NO_3^- by the forest litter.

4.2. Behavior of metals and metalloids, and possible evolution of their mobility in the context of the changing site conditions

In line with the *in situ* observations of the "Place-à-Gaz" soil (Bausinger *et al*., 2007; Thouin *et al*., 2016), Zn and As were the most mobile metal(oid)s in the mesocosm. Zn concentration in the soil water showed a time related evolution with a delay in maximum concentration with depth. This particular evolution, also observed for Ca^{2+} and Mg^{2+} concentrations and EC, can be attributed to the leaching of Zn which was mobile in the pH range of 5–6. The initial concentrations of Zn at each depth and in the leachate were fairly similar and mobilization of Zn at the beginning of the experiment was thus comparable throughout the soil profile. However, after several periods, Zn mobility was greater in the saturated soil. The amount of Zn leached in saturated soils is commonly explained by a pH decreased cationic exchange capacity releasing the adsorbed Zn. However, in this case, the stability of pH during the experiment and throughout the soil profile suggests that desorption of easily exchangeable Zn is not the only phenomenon driving Zn mobility in water. Previous studies (Bausinger *et al*., 2007, Thouin *et al*., 2016) showed that the main carrier of Zn was an amorphous material that also contained large amounts of As, Pb, Cu and Fe. The dissolution of this amorphous material, whose conditions of stability are unknown, may release enough Zn to explain the

increase in Zn concentration in the saturated soil. However, the other metals present in this amorphous phase were not very abundant in the solution.

The pH of the soil water may explain the low solubility of Pb and Cu, as Bausinger *et al*. (2007) have shown that Pb and Cu were not mobile in the soil of the site at pH 5–6. Cu and Pb were probably adsorbed on soil grain surfaces or precipitated with the other ions present in solution. The oxidation-reduction potential (ORP) and pH conditions of the experiment were favorable to the precipitation of ferric oxides or hydrous ferric oxides (HFO). The precipitation of HFO allows the sorption of Cu and Pb onto their surface (Swallow *et al*., 1980; Morin *et al*., 2001), which explains their low solubility. Fe seemed to be the metal most impacted by dry/wet cycles, but the trend was not very clear even if the behavior of Fe in the top soil seems to be different from that in the saturated levels. In addition, the Fe concentration trends showed that Fe solubility decreased significantly in the unsaturated soil and increased significantly in soil levels that were alternately or permanently saturated. The addition of organic litter enhanced these trends and DOC seemed to have a greater impact on Fe mobility than dry/wet cycles.

The addition of forest litter at the top of the soil modified the behavior of Zn and Cu, which seemed to be stabilized. Conversely, a significant increase in Fe mobility was observed in the saturated soil during the three periods following the addition of this fresh organic litter. The presence of easily biodegradable organic matter was certainly the cause of this increase in Fe mobility, due to greater oxygen consumption and then to more reduced conditions.

Together with Zn, As was the major metal(loid) present in the soil water, with concentrations up to 800 times higher than the maximum level of 10 µg L^{-1} recommended by the WHO (2011). However, As behaved differently from Zn, with higher concentration at the top of the mesocosm and immobilization with increasing depth. Previous studies describing As behavior during redox oscillation (Parsons *et al*., 2013, Couture *et al*., 2015) have shown that the successive cycles of oxidizing and reducing conditions (between -300 and +500 mV) affect As mobility in relation with As speciation and sorption onto HFO. During oxidizing cycles, As is strongly associated with HFO; during reducing periods, the combination of reduction of Fe oxides and microbial reduction of As V to As III raises As solubility (Couture *et al*., 2015). Under the conditions of this experiment, dry/wet cycling did not induce reducing conditions, even in the permanently saturated level. Moreover, As V was always the major As species in solution and presented an evolution similar to total As. However, the decrease in As V

concentration with depth could be induced by the precipitation of HFO from Fe leached by the dissolution of the amorphous phase in the saturated level, as As V is more readily adsorbed onto HFO than As III at pH 5–6 (Dixit and Hering, 2003). Between H4 and L, As V concentration decreased by about 50% (Fig.3.10). This very large decrease may be linked to the precipitation of HFO or the growth of a biofilm from the soil, perhaps on the geotextile membrane. The precipitation of secondary arsenates as an explanation for the immobilization of As V in solution cannot be excluded.

As III seems to be affected by the wet/dry cycles: the higher As III concentration at the end of wet periods at all levels (Fig.3.11) was probably linked to less oxygenated water and decreased ORP. Also, the proportion of As III in water increased with depth, supporting the fact that As III behavior was driven by soil saturation. Inorganic As speciation can be altered by different bacterial mechanisms responsible for As III oxidation and As V reduction : the *ars* system, whose primary function is detoxification with As V being reduced by an arsenate reductase ArsC, potentially active in both aerobic and anaerobic conditions; the *aio* oxidation system through arsenite oxidase, mainly active in aerobic conditions; and the *arr* system of As V dissimilatory reduction in anaerobic conditions (Stolz *et al*., 2002, Inskeep et al., 2007). Biological As III oxidation activity had been detected previously in the soil of the "Place-à-Gaz" site under unsaturated conditions (Thouin *et al*., 2016). Less effective As III oxidation in saturated soil, caused by less favorable conditions and concomitant higher microbial As V reduction activity, may explain the increase in As III concentration with depth.

The excess of DOC after the addition of bioavailable OM promoted microbial respiration and Eh drop, but also enhanced Fe mobility. This process should have enhanced As mobility, but in fact immobilization of As, mainly as As V, was observed over the different depths. The addition of fresh organic matter may have contributed by providing adsorption sites enough to trap some As V. It also appears that more gaseous methylated arsenic was produced after input of OM. Even if the dimethylarsine concentration was too low to explain As decrease, it confirmed the influence of OM on the activity of As transforming microbes. The addition of OM also induced an increase in As III concentration in the saturated soil (Fig.3.10 and Fig.3.11). The organic carbon concentration influences the rate of microbial As III oxidation in soils, a decrease in oxidation rate being observed beyond 0.08 $g.L^{-1}$ of organic carbon (Lescure *et al*., 2016).

Among the soluble As species, DPAA (SM.3.2) and three unknown species were also detected (Fig.3.11). The sum of these compounds and As III and As V was approximately equal to total As, indicating that no other main As species was present. It also appears that the three unknown species were not in ionic form, since the sum of unknown 1, 2 and 3 and As III (Fig.3.11) was similar to the As III-like species concentration given by anionic resin separation (Fig.3.10). DPAA, the hydrolysis product of the chemical warfare agent (Clark I and Clark II), was detected in low concentration at the outlet of the mesocosm. This compound was identified in water from this contaminated soil for the first time, since aromatic arsenicals had not been detected previously on the site (Bausinger, *et al*., 2007). The bacterial degradation pathway of DPAA in soil may produce phenylarsonic acid (PAA; Harada *et al*., 2010) or phenylarsine oxide (PAO) in less oxidizing conditions (Daus *et al*., 2010). DPAA was not detected in the deeper zones of groundwater contaminated by a former ammunition deposit and chemical warfare agent filling station (Daus *et al*., 2010). This absence was concomitant with occurrence of PAO and with As III increase, while PAA was detected all along the depth profile. In our experiment, with similar redox and pH conditions, the unknown species 1, which was very stable independently of the changing conditions, might have been attributed to PAA, and unknown species 2, which only appeared in saturated conditions, to PAO, however the chromatographic conditions used did not allow their identification. The three unknown species could therefore be metabolites of DPAA, or may have resulted from the oxidation of Clark I and II during combustion with a more complex degradation pathway. Further investigation is required to identify these compounds and understand their origin.

With time, water soluble compounds, including metals and As, will be progressively leached from the soil profile. The 8-months mesocosm experiment represented about one year of precipitation on the "Place-à-Gaz" site with a succession of dry and wet periods simulating seasonal variations. If the fluxes leached from the soil during the mesocosm experiment are considered as being in the same range as on-site horizontal leaching fluxes, since the year 1928 (when the shells were destroyed), about 3,700 kg of Zn and 160 kg of As (including 50 kg of As III-like species) will have been leached from the site by runoff to the surrounding surface environment. The high concentration of soluble As and metals leached from the forest litter sampled from outside of the site attested to the important runoff of pollutants. The high concentration of soluble As and metals in the top layer of forest soil, and principally in the litter and humic horizon, can be very problematic for wildlife. Results also suggest that this

type of site may provide a stock of As from which leaching will continue for several hundred years.

5. Conclusion

For nearly one hundred years, the highly polluted site known as "Place-à-Gaz" has been submitted to: (i) water saturation during rainfall events, inducing the transfer of pollutants to the surrounding forest environment via surface runoff; and (ii) natural deposition of oak litter. In the mesocosm experiment described above, the soil was submitted to dry/wet cycles and to the addition of organic litter from the site in order to evaluate the influence of soil saturation levels and of bioavailable OM on the biogeocycles of C, N and metal(oid)s.

Organic carbon present on the site was mainly charcoal and did not provide bioavailable nutrients to restore the soil's biological functions. The addition of organic litter at the top of the contaminated soil increased microbial activity. The nitrogen cycle was clearly affected by the dry/wet cycles, with microbial denitrification occurring in saturated conditions. Nitroaromatic compounds and cyano-arsines were present as sources of nitrogen in the chemical shells subjected to burning, and the results have highlighted the persistent nature of nitrogen on this type of site.

As and Zn were the most mobile metal(oid)s but behaved differently as the experiment progressed. Zinc concentration in soil water increased with depth and was not affected by the dry/wet cycles nor by the addition of organic litter; arsenic was more concentrated in the unsaturated soil. Concentration of As V, the major As species in solution, decreased with depth, while the proportion of As III increased in saturated conditions and with increased bioavailability of OM. At the end of the experiment, the soil released less As but with a greater proportion of more toxic As III. Four other As species were also detected in solution in significant concentrations: DPAA, the hydrolysis product of the warfare agents, and three unknown species. Low concentration of Fe, Cu and Pb in solution was caused by the precipitation of HFO and/or the low solubility of Cu and Pb in these pH conditions.

The experiment underlined the high potential for Zn and As mobilization all around the site by surface water runoff, but also showed that the deposition of forest litter contributes to the immobilization of some As. However, the proportion of As III, the most toxic As species, is also enhanced. Furthermore, progressive growth of vegetation on the site, enabled by the bioavailable organic matter from litter, may modify the behavior of contaminants by changing

pH or releasing organics acids. To complete understanding of the fate of inorganic pollutants along with the evolution of environmental conditions on the site, the effects of the rhizosphere should be investigated. The instrumented mesocosm used in the present study, as an intermediate between field scale and a laboratory microcosm, proved to be a convenient experimental device to study the influence of environmental events on the behavior of contaminants.

Acknowledgments

This work was supported by Région Centre Val-de-Loire (convention 00087485) and the Labex Voltaire (ANR-10-LABX-100-01). The authors wish to thank Nathalie Lottier (ISTO) for DOC results and Tobias Bausinger (Envilytix) for the analyses of organoarsenical, and nitroaromatic compounds.

Supplementary materials

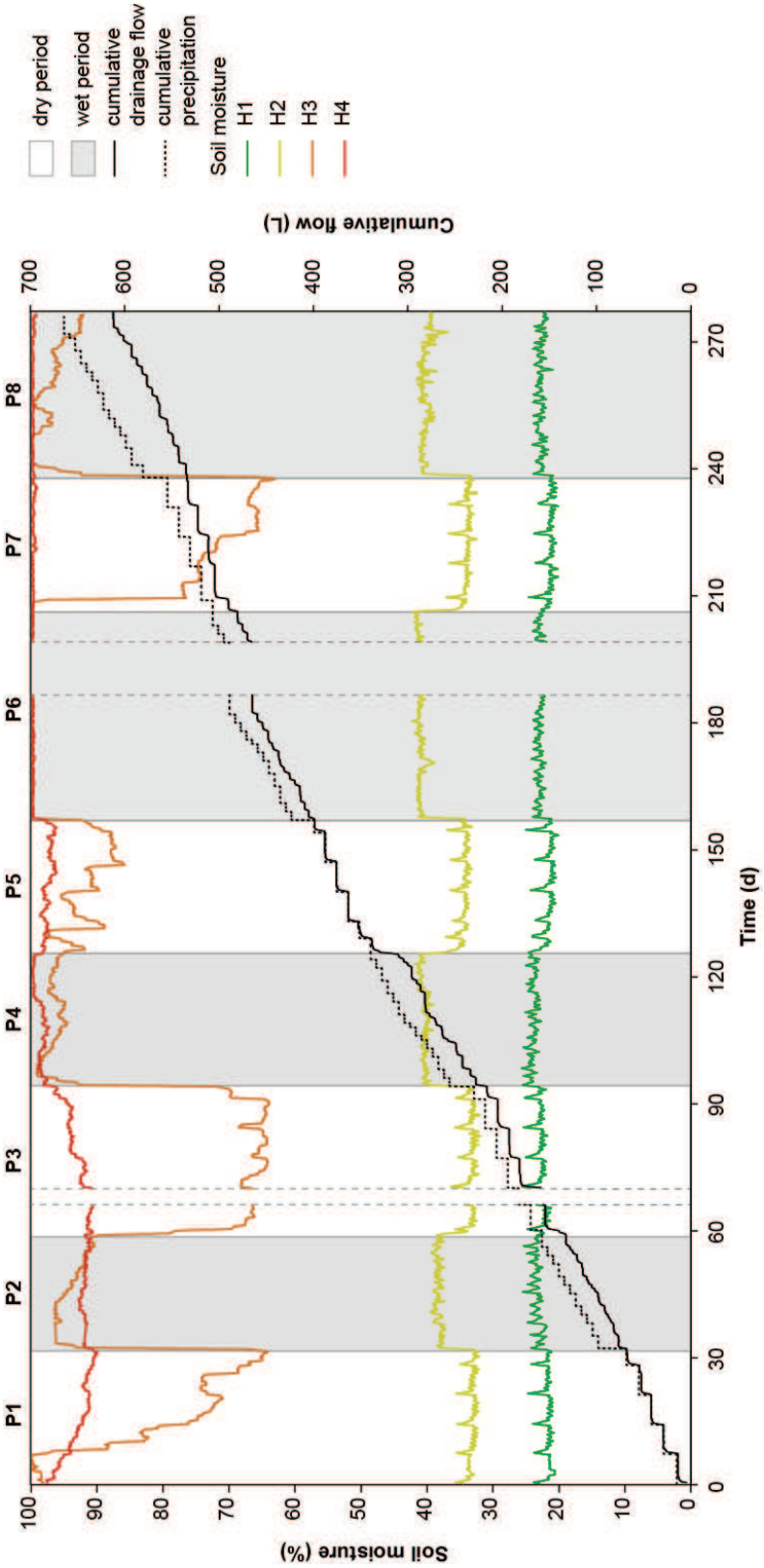

SM 3.1 : *Eight dry (white) and wet (grey) periods water balance and the soil moisture of the four sampling level. Dotted line periods represent a lack of data.*

SM 3.2: *Concentrations of nitroaromatic and aromatic arsenical compounds in water sample from leaching test of soil and from the leachate of the mesocosms at the end of P8. Diphenylarsinic acid was analyzed with HPLC-DAD. Cacodylic acid, clark I, clark II, triphenylarsine, 9-phenylarsafluorene were analyzed with GC-MS. (<LOQ: limit of quantification).*

#	Parameter	Test method	Sample	Unit	LOQ	Leaching test	Leachate at the end of P8
1	2-Amino-4,6-dinitrotoluene	DIN EN ISO 22478	water	µg/l	0,10	< LOQ	< LOQ
2	4-Amino-2,6-dinitrotoluene	DIN EN ISO 22478	water	µg/l	0,10	< LOQ	< LOQ
3	3,5-Dinitroaniline	DIN EN ISO 22478	water	µg/l	0,10	< LOQ	< LOQ
4	2,4-Dinitrotoluene	DIN EN ISO 22478	water	µg/l	0,10	< LOQ	< LOQ
5	2,6-Dinitrotoluene	DIN EN ISO 22478	water	µg/l	0,10	< LOQ	< LOQ
6	1,3,5-Trinitrobenzene	DIN EN ISO 22478	water	µg/l	0,10	< LOQ	< LOQ
7	2,4,6-Trinitrotoluene	DIN EN ISO 22478	water	µg/l	0,10	< LOQ	< LOQ
8	1,2-Dinitrobenzene	DIN EN ISO 22478	water	µg/l	0,10	< LOQ	< LOQ
9	1,3-Dinitrobenzene	DIN EN ISO 22478	water	µg/l	0,10	< LOQ	< LOQ
10	2-Nitroaniline	DIN EN ISO 22478	water	µg/l	0,10	< LOQ	< LOQ
11	3-Nitroaniline	DIN EN ISO 22478	water	µg/l	0,10	< LOQ	< LOQ
12	1-Nitronaphthalene	DIN EN ISO 22478	water	µg/l	0,10	< LOQ	< LOQ
13	2-Nitronaphthalene	DIN EN ISO 22478	water	µg/l	0,10	< LOQ	< LOQ
14	1,3-Dinitronaphthalene	DIN EN ISO 22478	water	µg/l	0,10	< LOQ	< LOQ
15	1,5-Dinitronaphthalene	DIN EN ISO 22478	water	µg/l	0,10	< LOQ	< LOQ
16	1,8-Dinitronaphthalene	DIN EN ISO 22478	water	µg/l	0,10	< LOQ	< LOQ
17	1,3,5-Trinitronaphthalene	DIN EN ISO 22478	water	µg/l	0,10	< LOQ	< LOQ
18	1,3,8-Trinitronaphthalene	DIN EN ISO 22478	water	µg/l	0,10	< LOQ	< LOQ
19	1,4,5-Trinitronaphthalene	DIN EN ISO 22478	water	µg/l	0,10	< LOQ	< LOQ
20	2-Amino-4,6-dinitrobenzoic acid	KORA-TV 5 (2008)	water	µg/l	0,10	< LOQ	< LOQ
21	4-Amino-2,6-dinitrobenzoic acid	KORA-TV 5 (2008)	water	µg/l	0,10	< LOQ	< LOQ
22	2,4-Dinitrobenzoic acid	KORA-TV 5 (2008)	water	µg/l	0,10	< LOQ	< LOQ
23	2,6-Dinitrobenzoic acid	KORA-TV 5 (2008)	water	µg/l	0,10	< LOQ	< LOQ
24	2,4,6-Trinitrophenol	KORA-TV 5 (2008)	water	µg/l	0,10	< LOQ	< LOQ
25	2,4,6-Trinitrobenzoic acid	KORA-TV 5 (2008)	water	µg/l	0,10	< LOQ	< LOQ
26	Diphenylarsinic acid	Envilytix GmbH	water	µg/l	0,25	**114**	**30,6**
27	Cacodylic acid	Envilytix GmbH	water	µg/l	0,25	< LOQ	< LOQ
28	Clark 1	Envilytix GmbH	water	µg/l	0,25	< LOQ	< LOQ
29	Clark 2	Envilytix GmbH	water	µg/l	0,25	< LOQ	< LOQ
30	Triphenylarsine	Envilytix GmbH	water	µg/l	0,25	< LOQ	< LOQ
31	9-Phenylarsafluorene	Envilytix GmbH	water	µg/l	0,25	< LOQ	< LOQ

SM 3.3: *Concentrations of nitroaromatic and aromatic arsenical compounds in the contaminated soil. Diphenylarsinic acid was analyzed with HPLC-DAD. Cacodylic acid, clark I, clark II, triphenylarsine, 9-phenylarsafluorene were analyzed with GC-MS. (<LOQ: limit of quantification).*

#	Parameter	Test method	Sample	Unit	LOQ	soil mesocosm
1	2-Amino-4,6-dinitrotoluene	DIN ISO 11916-1	soil	mg/kg DM	0,05	< LOQ
2	4-Amino-2,6-dinitrotoluene	DIN ISO 11916-1	soil	mg/kg DM	0,05	< LOQ
3	3,5-Dinitroaniline	DIN ISO 11916-1	soil	mg/kg DM	0,05	< LOQ
4	2,4-Dinitrotoluene	DIN ISO 11916-1	soil	mg/kg DM	0,05	< LOQ
5	2,6-Dinitrotoluene	DIN ISO 11916-1	soil	mg/kg DM	0,05	< LOQ
6	1,3,5-Trinitrobenzene	DIN ISO 11916-1	soil	mg/kg DM	0,05	< LOQ
7	2,4,6-Trinitrotoluene	DIN ISO 11916-1	soil	mg/kg DM	0,05	< LOQ
8	1,2-Dinitrobenzene	DIN ISO 11916-1	soil	mg/kg DM	0,05	< LOQ
9	1,3-Dinitrobenzene	DIN ISO 11916-1	soil	mg/kg DM	0,05	< LOQ
10	2-Nitroaniline	DIN ISO 11916-1	soil	mg/kg DM	0,05	< LOQ
11	3-Nitroaniline	DIN ISO 11916-1	soil	mg/kg DM	0,05	< LOQ
12	1-Nitronaphthalene	DIN ISO 11916-1	soil	mg/kg DM	0,05	< LOQ
13	2-Nitronaphthalene	DIN ISO 11916-1	soil	mg/kg DM	0,05	< LOQ
14	1,3-Dinitronaphthalene	DIN ISO 11916-1	soil	mg/kg DM	0,05	< LOQ
15	1,5-Dinitronaphthalene	DIN ISO 11916-1	soil	mg/kg DM	0,05	< LOQ
16	1,8-Dinitronaphthalene	DIN ISO 11916-1	soil	mg/kg DM	0,05	< LOQ
17	1,3,5-Trinitronaphthalene	DIN ISO 11916-1	soil	mg/kg DM	0,05	< LOQ
18	1,3,8-Trinitronaphthalene	DIN ISO 11916-1	soil	mg/kg DM	0,05	< LOQ
19	1,4,5-Trinitronaphthalene	DIN ISO 11916-1	soil	mg/kg DM	0,05	< LOQ
20	2-Amino-4,6-dinitrobenzoic acid	KORA-TV 5 (2008)	soil	mg/kg DM	0,05	< LOQ
21	4-Amino-2,6-dinitrobenzoic acid	KORA-TV 5 (2008)	soil	mg/kg DM	0,05	< LOQ
22	2,4-Dinitrobenzoic acid	KORA-TV 5 (2008)	soil	mg/kg DM	0,05	< LOQ
23	2,6-Dinitrobenzoic acid	KORA-TV 5 (2008)	soil	mg/kg DM	0,05	< LOQ
24	2,4,6-Trinitrophenol	KORA-TV 5 (2008)	soil	mg/kg DM	0,05	< LOQ
25	2,4,6-Trinitrobenzoic acid	KORA-TV 5 (2008)	soil	mg/kg DM	0,05	< LOQ
26	Diphenylarsinic acid	Envilytix GmbH	soil	mg/kg DM	0,25	< LOQ
27	Cacodylic acid	Envilytix GmbH	soil	mg/kg DM	0,25	< LOQ
28	Clark 1	Envilytix GmbH	soil	mg/kg DM	0,25	< LOQ
29	Clark 2	Envilytix GmbH	soil	mg/kg DM	0,05	< LOQ
30	Triphenylarsine	Envilytix GmbH	soil	mg/kg DM	0,05	< LOQ
31	9-Phenylarsafluorene	Envilytix GmbH	soil	mg/kg DM	0,10	< LOQ

SM 3.4: *Seasonal Kendall results*

Compounds	Sampling level	Kendall's Tau (τ)	S'	*p*-value	Interpretation
NO_3^-	H2	0.114	24.000	0.481	no trend
	H3	-0.273	-364.000	0.005	negative trend
	H4	-0.320	-772.000	0.051	no trend
	L	-0.226	-311.000	0.170	no trend
NH_4^+	H2	-0.065	-7.000	0.765	no trend
	H3	-0.108	-119.000	0.242	no trend
	H4	0.216	286.000	0.019	positive trend
	L	-0.062	-158.000	0.733	no trend
TA	L	-0.582	-680.000	< 0.001	negative trend
DOC	H2	0.288	38.000	0.059	no trend
	H3	0.380	130.000	0.003	positive trend
	H4	0.544	186.000	< 0.001	positive trend
	L	0.339	116.000	0.016	positive trend
Zn	H2	-0.171	-36.000	0.297	no trend
	H3	-0.711	-270.000	< 0.001	negative trend
	H4	-0.487	-185.000	< 0.001	negative trend
	L	0.126	48.000	0.361	no trend
Cu	H2	-0.603	-115.000	< 0.001	negative trend
	H3	-0.400	-141.000	0.004	negative trend
	H4	0.134	46.000	0.369	no trend
	L	-0.382	-133.000	0.005	negative trend
Fe	H2	-0.302	-60.000	0.047	negative trend
	H3	0.298	109.000	0.035	positive trend
	H4	0.343	128.000	0.011	positive trend
	L	0.519	195.000	0.000	positive trend
As	H2	-0.385	-60.000	0.033	negative trend
	H3	-0.228	-78.000	0.066	no trend
	H4	-0.327	-112.000	0.012	negative trend
	L	-0.380	-130.000	0.006	negative trend
As V	H2	-0.385	-60.000	0.033	negative trend
	H3	-0.234	-80.000	0.057	no trend
	H4	-0.450	-154.000	0.001	negative trend
	L	-0.462	-158.000	0.001	negative trend
As III	H2	-0.051	-8.000	0.783	no trend
	H3	-0.161	-55.000	0.209	no trend
	H4	0.398	136.000	0.003	positive trend
	L	0.181	62.000	0.178	no trend

Chapitre IV : Influence de changements environnementaux sur la minéralogie et les paramètres microbiens liés à la transformation de l'As : Etude en mésocosme

Image MEB de la phase amorphe porteuse de métaux

Introduction au chapitre IV

Influence de changements environnementaux sur la minéralogie et les paramètres microbiens liés à la transformation de l'As : Une étude en mésocosme

Ce chapitre, rédigé sous la forme d'un article qui va être soumis prochainement dans la revue scientifique *Journal of Hazardous Materials*, s'inscrit dans la continuité directe des travaux présentés dans le chapitre III. Il expose les résultats des analyses minéralogiques et biologiques des prélèvements solides effectués à trois étapes de l'expérience en mésocosme.

Résumé graphique :

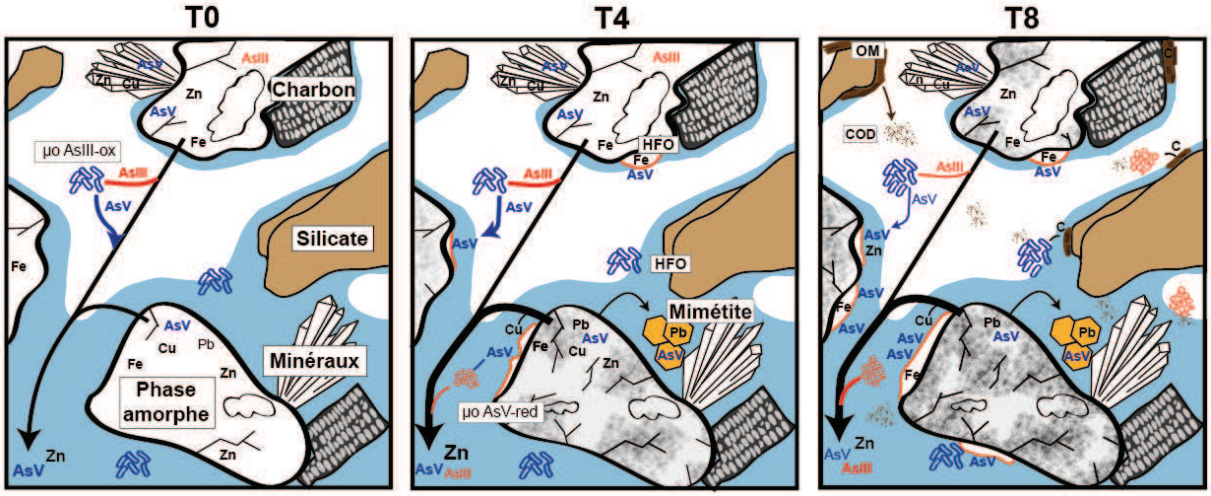

Résumé :

La destruction par brûlage de munitions chimiques de la Première Guerre Mondiale est à l'origine de la formation d'un matériel fortement contaminé qui montre une association minéralogique inédite et une microflore active pouvant oxyder l'As III. Afin d'évaluer l'impact des épisodes de saturation en eau et de l'apport de matière organique biodisponible sur la minéralogie et sur des paramètres microbiens liés à l'As, une étude en mésocosme a été menée. Pendant environ 8 mois, le sol contaminé a été soumis à des alternances de périodes sèches et humides. Après quatre mois, de la litière organique prélevée sur le site d'étude a été ajoutée au-dessus du sol contaminé. Des prélèvements solides ont été effectués par carottage de la colonne de sol, à trois pas de temps, au début de l'expérience, au bout de 4 mois (avant l'addition de MO), et à la fin de l'expérience. Les observations MEB-EDS ont montré que la phase amorphe, qui est le principal porteur des éléments As, Zn et Cu, est instable en

conditions saturées. L'altération de la surface de cette phase amorphe induit une libération de l'As et des métaux vers la solution du sol. Cependant, la précipitation de phases mal cristallisées riches en fer, certainement des oxy-hydroxydes, à proximité des phases amorphes altérées, semble avoir immobilisé une partie de ces contaminants. La précipitation d'un chlorure d'arséniate de plomb, la mimétite, dans la partie saturée du sol, a permis d'immobiliser de l'As et du Pb. La mimétite est un piège efficace pour ces éléments, en raison de son large domaine de stabilité. Cependant, cette réaction a été limitée par les faibles concentrations de Pb en solution et beaucoup d'As est resté mobile. La structure de la communauté bactérienne et l'évolution temporelle de sa diversité dans le mésocosme ont été évaluées par CE-t-RFLP. Les résultats ont montré une grande diversité de la communauté bactérienne, qui n'est pas affectée par les cycles sec/humide avant l'addition de MO. Cependant, l'ajout de MO biodisponible a modifié les communautés bactériennes et semble avoir favorisé des communautés différentes, en fonction du niveau de saturation du sol. La transformation microbienne de l'As est également affectée par l'addition de MO, induisant à la fois une augmentation de la concentration des microorganismes oxydant l'As III que des microorganismes réduisant l'As V. Néanmoins, un effet inhibiteur de la MO sur la vitesse d'oxydation de l'As III a été observé. Il pourrait être lié à une stimulation de l'activité de réduction de l'As V.

Chapitre IV: Influence of environmental changes on the mineralogy and As-related microbial parameters in a soil polluted by the destruction of chemical weapons: a mesocosm study

Hugues Thouin [a,b,c,d], Marie-Paule Norini [b,c,d], Fabienne Battaglia-Brunet [a,b,c,d], Lydie Le Forestier [b,c,d], Mickael Charron [a], Catherine Joulian [a], Sebastien Dupraz [a], Pascale Gautret [b,c,d]

[a] BRGM, 3 avenue Claude Guillemin, 45060 Orléans, France

[b] Université d'Orléans, ISTO, UMR 7327, 45071 Orléans, France

[c] CNRS, ISTO, UMR 7327, 45071 Orléans, France

[d] BRGM, ISTO, UMR 7327, BP 36009, 45060 Orléans, France

Abstract

The destruction by thermal treatment of chemical munitions from the World War I has caused the formation of heavily contaminated material which contain an unexpected mineral association and where microbial As III oxidation was detected. To assess the impact of water saturation episodes and the input of bioavailable organic matter on the mineralogy and the As-related microbial parameters, a mesocosm study was conducted. During about 8 month, the contaminated soil has been submitted to cycles of dry and wet period. After 4 month, fragmented litter from the study site was added above the top soil. Material have been sampling at three time step by coring, at the beginning of the experiment, after 4 months (before the addition of OM), at the end of the experiment. SEM-EDS observations showed that an amorphous phase, which was the main carrier of As, Zn and Cu, was instable in saturated conditions. Alteration process of the surface of amorphous phases release metal(loïd)s in solution but the precipitation of poorly crystalized hydrous ferric oxides near from these phases seems to immobilize a part of the contaminants. The precipitation of a lead arsenate chloride mineral, the mimetite, in the saturated soil promote the immobilization of As and Pb. Mimetite was a durable trap because of its large stability domain, however, this reaction was limited by the Pb concentration, and high amounts of As remained in solution. Bacterial community structure and diversity was assessed by CE-t-RFLP. Resulted show a high diversity of bacterial community which were not impacted by the dry/wet cycle before the addition of OM. However, the addition of bioavailable OM had modified the bacterial community and had promoted different community depending of water saturation. Microbial As transformation was also affected by the addition of OM, with the increasing of concentration of As III-oxidizing and As V-reducing microorganisms. An inhibitor effect of

OM on As III-oxidizing related to a decrease of the specific As III-oxidizing activity of bacteria and a stimulation of the As V-reducing activity was described.

Keywords: Arsenic, metal, mineral stability, microbial As III-oxidation, organic matter, dry/wet cycles, mesocosm study

1. Introduction

Chemical weapons were introduced during the First World War. Among these battle products, organo-arsenic compounds include diphenylchloroarsine (Clark I), diphenylcyanoarsine (Clark II), phenyldichloroarsine (Fiffikus), Lewisites, diphenylamine-chloroarsine (Adamsite) and their transformation products such as triphenylarsine and trichloroarsine (Marsite). Their introduction and degradation in environment induce the spreading of reaction sub-products, i.e. organic molecules and inorganic arsenic, which are mobile and toxic environmental contaminants (Karg, 2002). The site of the "Place-à-Gaz", located in northeast of Verdun (France), is one of many sites along the western front line of the First World War (1914-1918) where dangerous chemical weapons were destroyed after the end of the conflict. Between 1920 and 1928, about 200,000 shells containing organo-arsenical agents were submitted to a simple thermal treatment (Bausinger and Preuβ, 2005; Bausinger *et al*., 2007). The burnt ammunitions were mainly "blue cross shells" filled with Clark I and Clark II, and various parts of shells containing iron, zinc, copper and lead. The fire was supplied with explosive powders and firewood.

The thermal treatment resulted in a severe contamination by arsenic and heavy metals of the upper 40-10 cm of the topsoil of the site (Bausinger *et al*., 2007; Thouin *et al*., 2016). This superficial layer, which concentrates the inorganic contaminant, corresponds to the residues of the combustion of ammunitions. It is composed of slag, scoria, various elements of ammunition, and important amount of ash and charcoals resulting from the use of firewood that gives to this layer a black color (Bausinger *et al*., 2007; Thouin *et al*., 2016). The central part of the site was heavily contaminated in As, Zn, Cu and Pb whose concentrations respectively reached 72,820 $mg.kg^{-1}$, 90,190 $mg.kg^{-1}$, 9,113 $mg.kg^{-1}$ and 5,777 $mg.kg^{-1}$ (Thouin *et al*., 2016). The main part of organoarsenical agents has been oxidized during combustion resulting in the release of inorganic arsenic As_2O_3 and As_2O_5 (Bausinger *et al*., 2007). The previous study of Thouin *et al*. (2016) has shown that arsenic was principally in pentavalent form in solid (about 98 % of As V and 2 % of As III) and that several arsenate minerals crystallized during material cooling. An amorphous phase rich in Fe, Zn, Cu, and As with vitreous texture was also observed. This amorphous material was the principal carrier of As and metals but it stability was unknown.

Microorganisms actively contributing to metabolism of carbon and arsenic were observed on the site despite the low bioavailability of the organic matter (OM) (Thouin *et al*., 2016).

Microbial activities play a major role in As speciation in soils. Different bacterial mechanisms are responsible for As III oxidation or As V reduction (Battaglia-Brunet *et al*., 2002; Bachate *et al*., 2012; Zobrist *et al*., 2000; Stolz *et al*., 2002), thus altering As mobility, and bioavailability. Environmental conditions, such as modification of Eh or pH, are susceptible to modify this microbial activity. Moreover, the concentration and the composition of soil OM determines the biomass and diversity of microorganism (Tiedje *et al*., 1999) and can impact the bacterial activities of As transformation (Yamamura *et al*., 2009; Bachate *et al*., 2012; Lescure *et al*., 2016).

The contaminated soil of the "Place-à-Gaz" was submitted to partial saturation during periods of high precipitation because of the underlying clayey formation. Moreover, the site edge, near the oak forest, is exposed to natural deposition of litter that provides bioavailable OM. A 8-months experiment was performed in a 1 m^3 mesocosm filled with the contaminated material that was submitted to water saturation episodes and input of bioavailable OM. The monitoring of interstitial water compositions at different depths and in the leachate provided information on the processes that influence the fate of As and other inorganic contaminants and their transfer towards surrounding compartments (Thouin *et al*., *submitted*). The present study aimed to evaluate the behavior of minerals carriers of pollutants and their interactions with microorganisms in this soil. We focused our work on the evolution of the mineralogy, and on biogeochemistry of arsenic associated with solid phases during the mesocosm experiment.

2. Materials and methods

2.1. Experiment and soil sampling

The soil was collected in the site named "Place-à-Gaz" (Spincourt forest, 20 km of Verdun, France). This soil is characterized by Bausinger *et al*. (2007) and Thouin *et al*. (2016). It has a high Zn, As, Cu and Pb contamination and high organic content (slag, coal ashes and residues from ammunition). Soil samples used in this study come from the experimental device presented in Thouin *et al*., *submitted*.

The monitoring of water and solutes fluxes of polluted soil was performed for 276 days thanks to an instrumented mesocosm. This mesocosm was constituted of a closed stainless steel column (1 m diameter and 120 cm height), filled with 610 kg of homogenized contaminated soil. A layer of inert gravel (centimetric quartz and flint particles) and a geotextile membrane were disposed at the bottom of the mesocosm, in order to facilitate the

outflow evacuation without losing soil particles. Soil was submitted to dry/wet cycles (about 8 months) and to the addition of organic forest litter at the top of the surface soil after 4 months of analyses. Water rainfall was simulated by a sprinkler system connected to a water reservoir and fed by two pumps. The leachate was collected in a steel tank and quantified using a balance. Outflow weight and soil moisture and temperature at the four sampling levels (H1: 5 cm, H2: 20.5 cm, H3: 36 cm and H4: 48 cm, measured from the top) were monitored continuously with a one-hour frequency. H1 and H2 levels were always unsaturated, H4 level was always saturated and the level H3 was non saturated in the dry periods and saturated in wet periods. The coring was performed in the mesocosm with 5 cm diameters pipe, at three steps of the experiment: at the beginning (T0), before the addition of fragmented litter about 4 months after (T4) and at the end (T8). Each core was divided into four samples, H1 0-12.5 cm, H2 12.5-28 cm, H3 28-42 cm and H4 42-75 cm of depth; corresponding to the soil water sampling levels (Thouin *et al*., *submitted).*

2.2. Analytical techniques

For chemical analyses, soil samples were drying and ground to 70 µm. Total carbon and nitrogen hydrogen were quantified in powdered samples, by using an elemental flash pyrolyser analyser (Flash 2000, Thermo Fischer Scientific). Total organic carbon (TOC), hydrogen index (HI), oxygen index (OI) and temperature maximum of pyrolysable OM (T_{peak}) were determined by Rock-Eval pyrolysis (Rock-Eval 6 Turbo, Vinci Technologies). Total concentrations of As, Cu, Zn, Pb and Fe were determined using XL3t800 NITON© portable X-ray fluorescence field apparatus (pXRF).

The mineralogical composition of the bulk samples was determined by powder X-ray diffraction (XRD). XRD patterns were recorded using a INEL CPS120 diffractometer montage transmission (Debye-Scherrer geometry) equipped with a Co anode (Co $K\alpha_1$ = 1.78897 Å) and operating at 35 kV and 35 mA. Scans were recorded from 5° to 90° (2θ) with an angular steps of 0.03° and a total time acquisition of 210 min.

Scanning electron microscopy (SEM) and energy dispersive X-ray spectroscopy (EDS) were used to study the structure evolution of As and metal carrier phases during the experiment and to identify possible new precipitate phases. SEM was performed on a TM 3000 (Hitachi) and operated at 15 kV accelerating voltage. SEM was coupled to a SwiftED3000 X-Stream module (Hitachi). The acquisition time of EDS point analyses was 300 seconds.

2.3. As III-oxidizing activity tests and bacterial enumeration

Soil samples were incubated at 25°C for 72 h in order to activate the microflora before starting the As III-oxidizing activity tests and the As III-oxidizing and As V-reducing microorganisms enumeration. The As III-oxidizing tests were performed in triplicate in 250 mL Erlenmeyer flasks filled with 100 mL of CAsO1 medium (Battaglia-Brunet *et al*., 2002) supplemented with 1 mM As III and inoculated with a mass of material equivalent to 0.2 g of dry weight. Flasks were plugged with cotton to retain oxidizing conditions and were incubated at 25° under agitation (100 rpm). The samples taken to follow As III oxidation test were filtrated (0.45 µm) and stored at -20°C until analysis. As III and As V were separated with the PDC/MIBK method (Battaglia-Brunet *et al*., 2002), after the filtration at 45 µm. As V was then quantified by Flame Atomic Absorption Spectrometry (FAAS) (Varian, Palo Alto, CA, USA). As III-oxidizing rates were determined by linear regression fitting of the As V versus time line, during the reaction.

As III-oxidizing and As V-reducing microorganisms were enumerated by the Most Probable Number method (MPN). The method for As III-oxidizing microorganisms is detailed in Thouin *et al*. (2016). For As V-reducing, the fresh soil (equivalent to 0.2 g dry soil) was placed in a sterile, glass Erlenmeyer flask with 10 mL of sterile physiological saline (9 $g.L^{-1}$ NaCl in demineralized water), shaked for 30 min at 25°C, then sonicated 2 x 20 s at 45 kHz. Triplicate suspensions were prepared for each sample. Soil suspensions were diluted, in stages, in sterile physiological saline solution to a dilution of 10^{-6}. CAsO1 mineral medium (Battaglia-Brunet *et al*., 2002) was complemented with 20 mM lactic acid and As III was replaced by As V (100 $mg.L^{-1}$). The medium was distributed over Microtest TM Tissue culture plates (96 wells), 250 µL per well. Each well was inoculated with 25 µL of diluted soil suspension. Five wells were inoculated with each dilution. Culture plates were incubated at 25°C for 10 days in anaerobic jars. The presence of As III in the wells was revealed by the formation of As III-PyrrolidineDithioCarbamate (PDC), an insoluble white complex: 80 µL of 0.1 M acetate buffer (pH 5) and 40 µL PDC solution (5 $g.L^{-1}$) were added to each well. A white precipitate appeared when As III was present, i.e. when As V – reducing microorganisms were present (positive well). The number of positive wells for each dilution was determined, and the most probable number of bacteria in dilutions was given by Mc Grady table for five tubes.

2.4. Total DNA extraction, and bacterial communities diversity analysis

Nucleic acids were extracted in triplicate from 0.5 g of wet soil or litter directly after their sampling, using a FastDNA® Spin Kit for soil (MP Biomedicals) according to the manufacturer's instructions. The three replicates of each soil samples were pooled and purified using a Geneclean Turbo Kit (MP Biomedicals) according to the instructions of the manufacturer.

The diversity of the bacterial communities of the soil and of the organic litter was analyzed by Capillary Electrophoresis – terminal Restriction Fragment Length Polymorphism (CE-t-RFLP) of the 16S rRNA gene. Bacterial 16S rRNA genes were amplified with the FAM-labeled forward primer 8F-FAM (5′-AGAGTTTGATCCTGGCTCAG-3′) and the reverse primer 1406R (5′-ACGGGCGGTGTGTRC-3′) (Kumar and Khanna, 2010). PCR was performed in a 20 µL reaction mixture containing 1× PCR buffer (Promega), 1.5 mM $MgCl_2$, 0.2 mM of each deoxynucleotide triphosphate, 0.5 µM of each primer, 1 U of DNA polymerase (GoTaq® Flexi DNA polymerase, Promega) and 1 µL of a 1 ng/µL DNA-diluted template. PCR amplifications were carried out in a thermocycler with an initial denaturation at 95°C for 3 min, followed by 35 amplification cycles of 95 °C for 45 s, 57 °C for 45 s and 72 °C for 60 s followed by a final extension time at 72 °C for 10 min. The PCR products were purified using a PCR clean-up kit (NucleoSpin® ExtractII, Macherel-Nagel) according to the manufacturer's recommendations. 35 ng of each fluorescently labelled PCR product were digested with 2.5 U of *Hae*III (Promega) at 37 °C for 3 h in a 12 µL reaction. Fluorescently labelled t-RFs were resolved by capillary electrophoresis in an ABI 310 genetic analyser using an internal size standard (GeneScan™ 600 LIZ, Applied Biosystems).

T-RFLP profiles were analyzed using BioNumerics software (Applied Maths). The t-RFLP profiles were aligned to the internal standard and normalized. T-RFs between 60 and 480 pb and with a peak height > 0 fluorescent unit were included in the analysis. Richness (*S*) was determined by the presence or absence of t-RFs bands in the electrogram. Shannon index (*H'*) was determined using the formula $H' = -\sum p_i(\ln p_i)$ and Simpson index (*D'*) as ($D' = 1/\sum(p_i)^2$) with p_i the relative abundance of T-RFs. Hierarchical clustering dendrogram was performed on T-RFLP data using Euclidean distances and the Ward algorithm in order to determine dissimilarity between bacterial diversity of each samples.

2.5. Statistical analyses

Statistical test were carried out using R 3.2.4 (www.r-project.org). Pearson correlations were calculated with the four soil samples at three time steps *i.e*. 12 observations. Principal component analysis (PCA) was performed on biogeochemical parameters on the same observations.

3. Results and discussion

3.1. Stability of inorganic contaminants-bearing mineral phases

3.1.1. Relationship between inorganic contaminants

Metal and As concentrations given by pXRF method, were high in all soil samples, according to the following decreasing order As > Fe > Zn > Cu > Pb (Tab.4.1). As concentration varied between 102,380 and 150,360 $mg.kg^{-1}$, Zn concentration between 70,040 and 107,400 $mg.kg^{-1}$, Cu concentration between 13,450 and 20.790 $mg.kg^{-1}$ and Pb concentration between 3,490 and 6,030 $mg.kg^{-1}$. These inorganic contaminant concentrations were very important and in the same range than those measured in other soil samples from the same site (Bausinger *et al*., 2007; Thouin *et al*., 2016). Significant concentration differences were difficult to detect with depth and time because of the high heterogeneity of the soil. However at the end of the experiment (T8), metal(loid)s concentrations semm to be distributed in a pattern with higher values at the bottom of the mesocosm. Moreover, metals and As were less concentrated at the surface after 8 months than at the beginning of the experiment. These observations may be the result of the vertical transport of metals from top to bottom of the mesocosm and their immobilization in the saturated soil.

Table 4.1 : *Chemical analyses of soil samples determined by pXRF apparatus*

	Time	Fe	As	Zn	Cu	Pb
		$mg.kg^{-1}$	$mg.kg^{-1}$	$mg.kg^{-1}$	$mg.kg^{-1}$	$mg.kg^{-1}$
H1	T0	96,960	128,240	77,140	18,350	4 750
H2		97,860	122,930	77,150	15,830	4 240
H3		84,420	131,530	87,540	18,450	4 610
H4		89,380	147,070	107,400	20,790	5 530
H1	T4	102,640	145,330	82,010	17,840	6 030
H2		73,170	118,040	72,400	18,120	4 080
H3		102,710	102,380	64,680	13,990	3 490
H4		95,630	153,410	92,120	18,950	5 720
H1	T8	75,460	111,080	70,040	13,450	4 250
H2		81,560	126,890	83,030	17,250	4 220
H3		85,700	124,380	80,410	17,920	5 110
H4		96,810	150,360	99,390	20,740	5 180
Litter		21,260	8 060	29,050	3 440	2 440

However, the monitoring of metal(oid)s concentrations in the interstitial water (Thouin *et al*., *submitted*), showed that only As seemed to be immobilized in the bottom level of the mesocosm. Soluble Zn concentrations presented an opposite evolution, with its increasing with depth. However, the amounts of solubilized Zn and As were low compared with concentrations in solid. On the other hand, these results may be caused by the downward transport of fine particles, carrier of contaminants, during the experiment. However, the heterogeneity of the soil did not allow confirming this hypothesis.

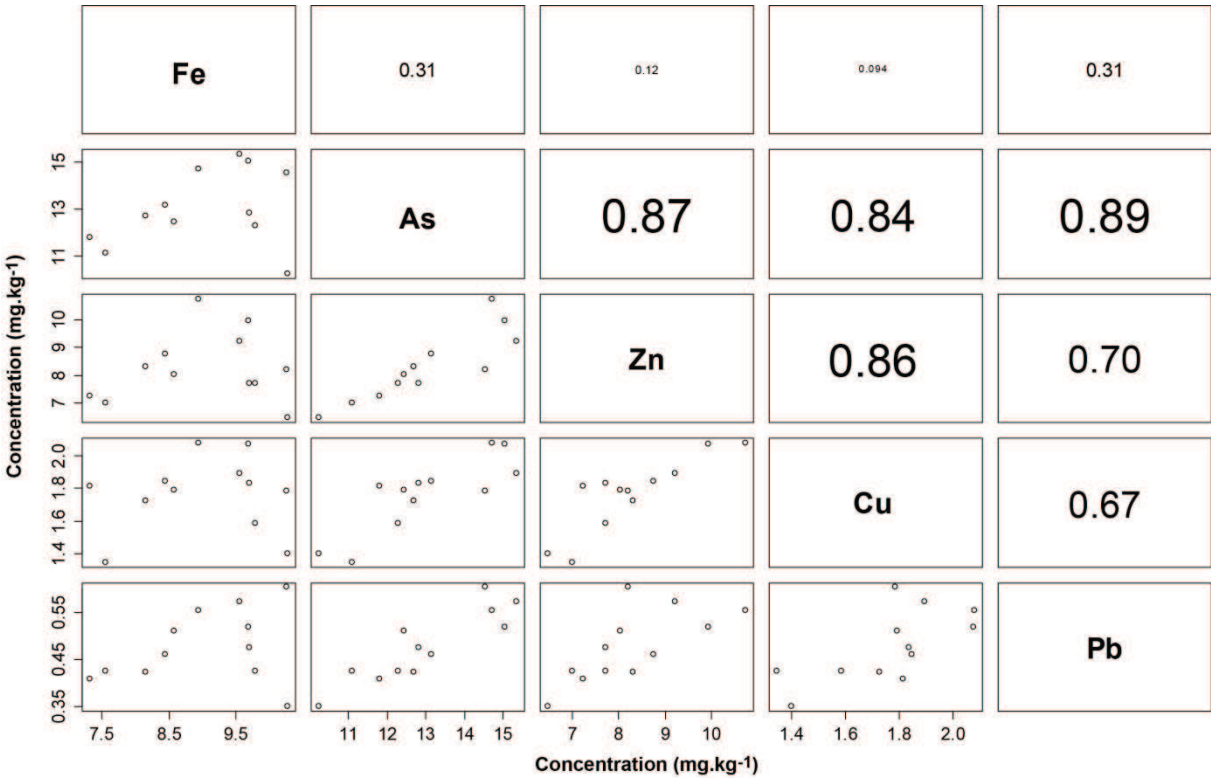

Figure 4.1: *Scatterplot matrix of metal(loid)s concentration. Co-plot in the lower panel and Pearson correlation of variables in upper panel (without litter observation). Size of Pearson index is proportional to correlation.*

The scatterplot and Pearson correlation matrix of the element concentrations presented above are given in figure 4.1. Results show that As, Zn, Cu and Pb concentrations were significantly inter-correlated, whereas iron concentration was not correlated with other metal(loid)s. These results showed that Zn, Cu, Pb and As were mainly link to the same solid phase in this soil, as previously shown (Bausinger *et al*., 2007; Thouin *et al*., 2016).

3.1.2. Stability of the amorphous phases

Thouin et al. (2016) highlighted amorphous phases containing high concentrations of iron, arsenic and metals. The evolution of the morphology of the amorphous phases was observed, by SEM, in the different samples in order to study their stability. Figure 4.2 shows the textural evolution of the vitrified amorphous phases in the water saturated soil. At the beginning of the experiment (Fig.4.2 (a)), this phase was characterized by a smooth texture, with micro-cracks, previously observed in site samples and attributed to the thermal process applied to destroy the weapons (Thouin *et al*., 2016). After 4 months of mesocosm experiment, the surface of the amorphous phases had changed and presented a rough texture (Fig.4.2 (b)).

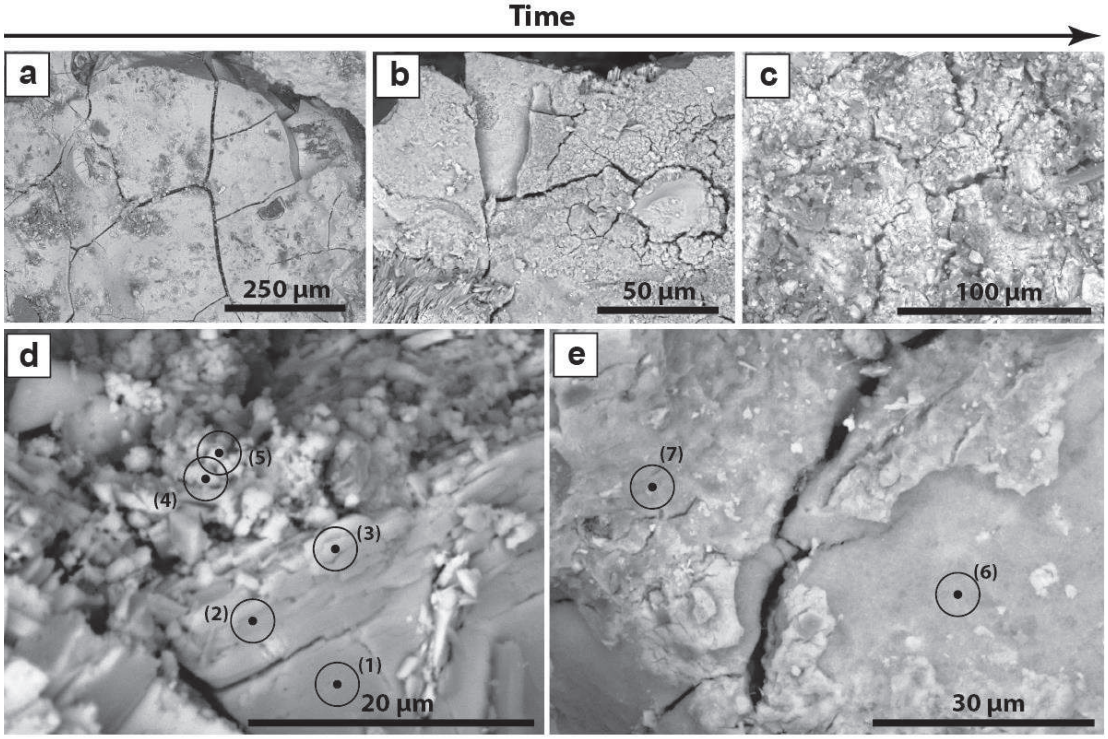

(%)	(1)	(2)	(3)	(4)	(5)	(6)	(7)
Fe	7.935	8.357	10.481	27.592	20.254	9.664	11.350
As	4.706	4.144	5.114	4.127	6.562	20.975	16.025
Cu	0.020	0.197	0.193	0.105	0.474	1.755	1.080
Zn	5.575	5.507	6.854	5.328	6.129	11.788	9.719
Pb	-	-	-	-	-	0.693	0.778

Figure 4.2: *Backscattered electron images and relative concentrations of metals (% weight) of amorphous phases in the saturated soil. (a), (b) and (c) illustration of three amorphous phases sampled in the H4 level at T0, T4 and T8 respectively. (d) SEM picture of amorphous phases, sampled in H4 at T4, showing dissolution figures at the surface (elemental analyses (1) to (3)) and reprecipitation of amorphous phases (analyses (4) and (5)). (e) Surface of amorphous phases, sampled in H3 at T8, (analysis (6)) covered with a granular layer (analysis (7)).*

The crack edges were altered and new networks of fissures appeared from the previous micro-crack. At the end of the experiment, after 276 days, the networks of fissures covered the entire surface of the amorphous phases which became very irregular (Fig.4.2 (c)). Similar observations were previously described during the alteration of a partially vitrified metallurgical waste (Seignez *et al*., 2007). These observations were consistent with the dissolution of the amorphous phases in the saturated soil, and then to the release in water of As, Zn, Cu, Pb and Fe, carried by these phases. However, metal(oid)s behaved differently in solution, with high As and Zn concentrations in opposition to Cu, Pb, Fe, that were not very mobile (Thouin *et al*., *submitted*).

Elemental composition of altered amorphous phases was investigated thanks to SEM-EDS analyses (Fig.4.2 (d) and (e)). Analyses were performed on amorphous phases presenting a gradient of weathering (Fig.4.2 (d)) and on the less altered part with granular layer covering its surface (Fig.4.2 (e)). Results showed that Fe proportion increased in the material from about 8 to 10.5 wt% following the degree of weathering. However, the proportion of the other inorganic contaminants did not increase in the same way as Fe. Tabular crumbling highlighted the action of surface processes (Fig.4.2 (d)). Close to this altered surface, a cluster of micrometric amorphous grains with higher concentration of Fe was observed. On the second example (Fig.4.2 (e)), the Fe concentration was less important (9.7 wt%) in the smooth amorphous phases than in the altered surface (11.3wt%). For the other metals and As, we observed an opposite relation with decrease from 21 wt% to 16 wt%. These results can be explained by the precipitation of amorphous and poorly crystallized hydrous ferric oxides (HFO) close to the amorphous phase, that can bind a part of As and metals. This hypothesis was consistent with the low concentrations of Fe in solution but also could explain the low mobility of Cu and Pb (Thouin *et al*., *submitted*), that can be adsorbed onto HFO (Swallow *et al*., 1980). As previously proposed (Thouin *et al*., 2016; Thouin *et al*., submitted) the precipitation of HFO, following the dissolution of the amorphous phases may explain the immobilization of some As V observed in the saturated part of the mesocosm. The high adsorption of AsV by amorphous HFO is a well-known phenomenon (Dixit and Hering, 2003).

3.1.3. Evolution of mineralogical association

The evolution of the mineralogy during the experiment was investigated by XRD analysis of soil samples from the different depths (Fig.4.3). Firstly, the important background of X-ray diffractograms confirms the importance of the amorphous phases in the soil. Quartz, potassium and sodium feldspars were identified in each sample with a relative intensity of peaks slightly evolving over time and depth. These silicates, already observed in natural site samples (Thouin *et al*., 2016), were attributed to the substrate, *i.e*. the clayey Woëvre formation.

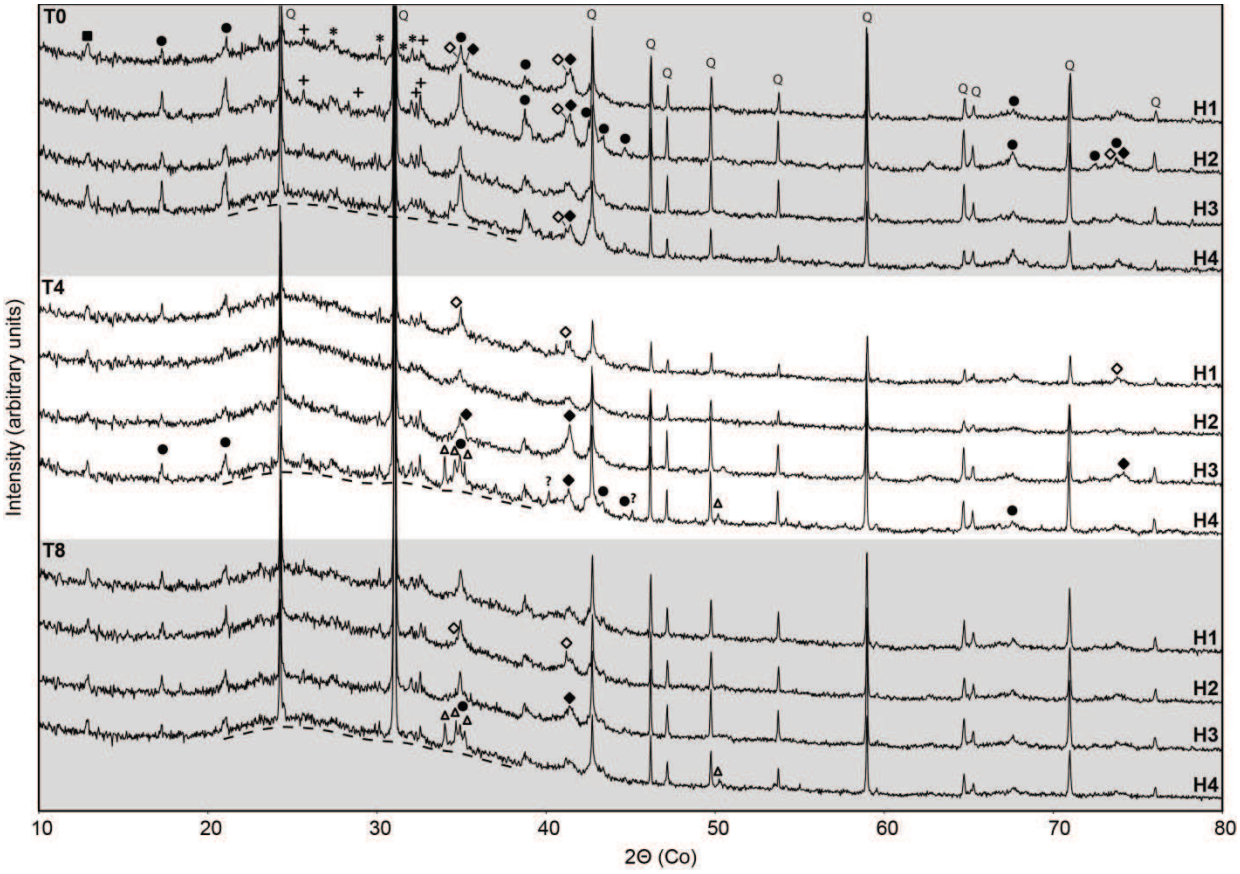

Figure 4.3: *X-ray diffractograms of bulk soil sample. Q: quartz (ICDD-1045); ✱: sodium feldspar (ICDD 19-1184); ✚: potassium feldspar (ICDD 31-0966); ●:adamite (ICDD 39-1354); ■: Na-Pharmacosiderite (ICDD 38-0388); ◆: magnetite (ICDD 19-0629); ◇: franklinite (ICDD 22-1012); ▲: mimetite (ICDD 19-0683); and ?: unknow mineral.*

Magnetite (Fe_3O_4) and franklinite ($ZnFe_2O_4$) were detected in most of the samples. Magnetite and franklinite exhibit spinel structure with similar lattice parameters resulting in an overlapping of their corresponding XRD peaks, so the presence of franklinite was difficult to

prove by XRD. However, the Zn concentration in solids and the large occurrence of magnetite-franklinite mineral association in metallurgical furnaces wastes (Pisciella *et al*., 2001; Julliot *et al*., 2003; Dutra *et al*., 2006; Puziewicz *et al*., 2007; Vereš, 2014) suggests that magnetite-franklinite solid solutions were present and inherited from the thermal process of destruction. The presence of zincite in site soil samples (Thouin *et al*., 2016), and in the metallurgical wastes together with magnetite and franklinite (Dutra *et al*., 2006; Puziewicz *et al*., 2007; Vereš, 2014), confirmed the inherited character of these minerals in this context. Although was not detected by XRD in soil of the mesocosm, zincite, as well as magnetite and franklinite, was most probably present in all samples but in insufficient amounts for an appropriate detection because of the soil heterogeneity. No significant effect of dry/wet cycles or addition of organic matter on the stability of these Fe and Zn minerals was detected.

The arsenates of Zn, Cu and Fe previously observed in this soil (Thouin *et al*., 2016), adamite ($Zn_2AsO_4(OH)$), olivenite ($Cu_2AsO_4(OH)$) and pharmacosiderite ($(K,Na,Ba)Fe_4(AsO_4)_3\,(OH)_5\,5H_2O$) were again identified in all samples (Fig.4.3). Adamite and olivenite are characterized by the same structure so they have similar XRD patterns, but SEM-EDS showed that crystals were mostly a solid solution of adamite and olivenite (Fig.4.4.a). Indeed, adamite-olivenite crystals were easily recognized with their prismatic and acicular texture (Fig.4.4.a), and can form large crystals may grow at the surface of grains. Pharmacosiderite with cubic structure was also observed (Fig.4.4.b). No evidence of weathering could be observed on these arsenate minerals, which were present all along the soil profile.

Mimetite ($Pb_5(AsO_4)_3Cl$), a lead arsenate chloride, was detected in the H4 level at T4 and T8 (Fig.4.3). Mimetite precipitation was proposed in soils treatment processes to remove arsenate ions from solution (Twidwell *et al*., 1994 ; Badja *et al*., 2006). Indeed, mimetite precipitates in conditions of low Pb and arsenate concentrations and presents a stability domain that covers the pH range of natural waters (Magalhães and Silva, 2003; Bajda, 2010). Arsenate and chloride ions, presenting high concentrations in the interstitial water all along the experiment, and the pH range of 5.5-6.0 (Thouin *et al*., *submitted*) were optimal for the precipitation of mimetite. The limiting factor of mimetite precipitation in the soil was the Pb concentration in solution. The precipitation of mimetite in the saturated part of the soil means that Pb was released in solution in these conditions and then confirms the hypothesis of progressive dissolution of the amorphous phases carrier of metals along the experiment. Mimetite was not observed with SEM, but micrometrics grains presenting high lead and other

metals concentrations were observed in the saturated depth level (Fig.4.4.c). This observation confirms that lead was released then re-precipitated. The precipitation of mimetite promoted by the soil saturation explained the previously described immobilization of Pb and AsV. Thanks to the large pH stability range of mimetite (until pH= 2 in the acidic domain), this mineral represents a durable trap for As and Pb in this soil. However, the very low concentration of Pb in solution limited the precipitation of mimetite and high amounts of As remained in solution.

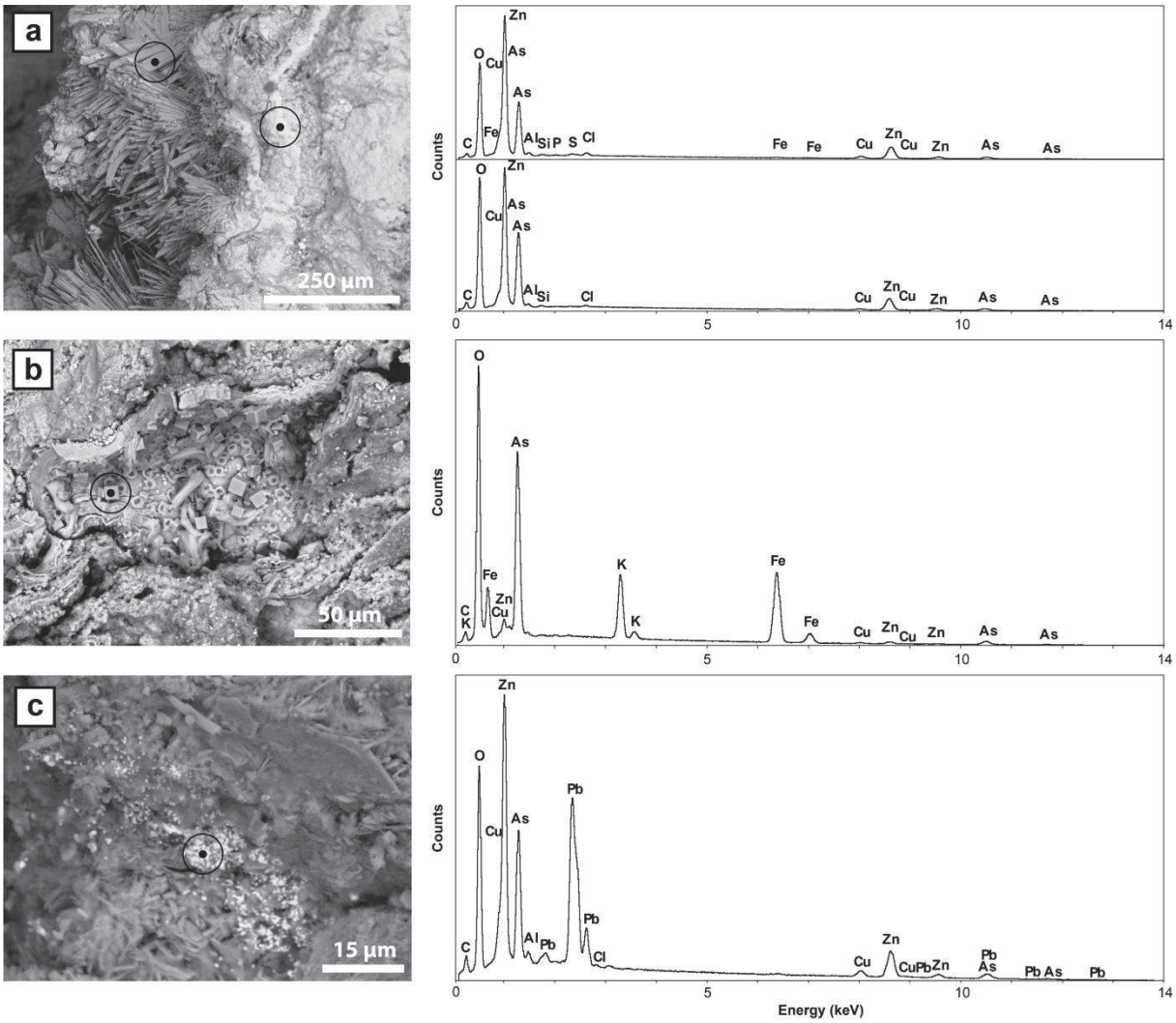

Figure 4.4: *SEM observations and EDS spectrum of mineral carrier of metal(oid)s. a: Growth of prismatic crystals carrier of As, Zn and Cu, at the surface of a grain. b: Cubic crystals composed of As, Fe and K. c: Amorphous micrometric grain carrier of Pb, As, Zn and Cu. The targets correspond to the location of EDS elemental analysis.*

3.2. Modification of the soil organic matter

The characterization of the soil OM from the mesocosm was performed using elemental flash pyrolyser analyser and Rock-Eval pyrolysis. Results are represented in table 4.2. Total carbon (C) ranged from 14.7 to 27.8 %, and total hydrogen varied between 1.6 and 2.4 % in the mesocosm soil. The N content of soil varied from 0.3 to 0.8 %. TOC ranged between 14.1 and 25.3 %. The hydrogen index HI is an indirect measurement for hydrocarbon content of soil OM (HI = S2/TOC, S2 being the amount of hydrocarbons produced during the thermal cracking of insoluble OM). Results were low for all mesocom samples (< 0.18 mg HC. g^{-1} TOC) except for the sample H1 – T8. The proportion of O containing OM (OI) ranged between 125 and 200 mg O_2. g^{-1} TOC. T_{peak} is the accurate temperature experienced by the sample when producing the maximum amount of hydrocarbons. T_{peak} values were higher than 440 °C and than 500 °C for two samples (H3 – T4 and H4 – T8). The high organic carbon content together with the HI and OI are not values expected in soil OM (Disnar *et al*., 2003), but rather presentchemical signatures of charcoals (Wolf *et al*., 2013; Saenger *et* al., 2015). These results were consistent with SEM observation and carbon mineralization rates of this soil (Thouin *et al*., 2016; Thouin *et al*., *submitted)*.

Table 4.2 : *Parameters related to OM*

	Time	C[a]	H[a]	N[a]	C/N[a]	TOC[b]	T_{peak}[b]	HI[b]	OI[b]	HI/OI[b]
		%	%	%		%	°C	mg HC. g^{-1} TOC	mg O_2. g^{-1} TOC	
H1	T0	21.1	1.8	0.6	36.3	16.1	441	13	161	0.08
H2		23.8	2.1	0.7	36.2	24.9	446	11	125	0.09
H3		25.9	2.3	0.7	36.6	18.5	443	17	161	0.11
H4		27.8	2.4	0.8	37.0	14.6	445	15	200	0.08
H1	T4	27.1	2.4	0.7	38.1	15.3	446	15	184	0.08
H2		25.9	2.2	0.6	40.5	18.3	452	16	147	0.11
H3		14.7	1.5	0.3	53.5	14.1	542	18	157	0.11
H4		15.1	1.6	0.3	45.8	19.4	440	14	147	0.10
H1	T8	27.8	2.4	0.8	37.0	25.3	439	37	169	0.22
H2		22.6	1.8	0.4	53.2	23.2	445	16	151	0.11
H3		22.8	1.7	0.5	49.5	22.8	446	18	150	0.12
H4		17.1	1.6	0.4	46.2	17.5	559	18	154	0.12
Litter		38.5	4.7	1.8	21.4	30.5	369	268	205	1.31

a : Flash pyrolyser analyser; b : Rock-Eval 6

Previous studies suggest that physical and chemical charcoal properties depend on fire temperature (Schneider *et al*., 2010; Wolf *et al*., 2013). The formation of charcoal begins with the loss of easily oxidizable OM (like aliphatic and carboxylic compounds), and with

increasing temperature organic compounds progressively aromatize. High temperature combustion (> 700°C) may cause a complete carbonization of OM and forms polyaromatic crystallites or graphite-like structure (Keiluweit *et al*., 2010). This restructuration of the OM is expressed by an increase of TOC and a decrease of OI and HI. Wolf *et al*. (2013) studied the relation between charcoal signature and burning conditions. According to their data, our OM signature (HI/OI, T_{peak}) would correspond to a temperature of fire ranging between 300 and 400 °C. However, this temperature seems to be relatively low to melt the metals (Fe, Cu, Zn, Pb) from the parts of shells, thus to form the amorphous phases. The wood was placed on the top of shells dumps during their destruction. Probably, the temperature was higher in the central parts of the fire, thus explaining the non representativity of the fire temperature signal of charcoal compared to the total range temperature reached during the combustion.

The organic litter added at T4 has a signal very different than that of the soil. It contains higher organic carbon (30.5 %), and nitrogen (1.8 %) content, higher HI (268 mg HC. g^{-1} TOC) and OI (205 mg O_2. g^{-1} TOC) and has a lower T_{peak} (369 °C). Disnar *et al*. (2003) determined that fresh or fragmented litter normally presents high TOC values (10-40%) and HI values higher than 300 mg HC. g^{-1} TOC. The T_{peak} at 360-370 °C is mostly attributed to cellulose and /or lignin, two major components of woody tissues frequently observed in litters. These results confirmed the immature character of the organic litter added on the top soil of the mesocosm.

The intrinsic OM of the “Place-à-Gaz” soil, with high C/N and low HI/OI ratio presented recalcitrant nature (Fig.4.5), not adapted for the development of an active microflora and vegetation. However, addition of the fragmented litter has enhanced the proportion of biodegradable OM in the top soil. The effect of litter was visible on the surface soil sample H1 – T8 with higher carbon organic content (25.3 %) and higher HI/OI ratio (0.22; Fig.4.5), but did not increase the C/N ratio. Previous study (Thouin *et al*., *submitted*) showed that addition of organic litter increased DOC in soil solution and carbon mineralization rate, then we supposed that microbial activities was impacted by the addition of litter.

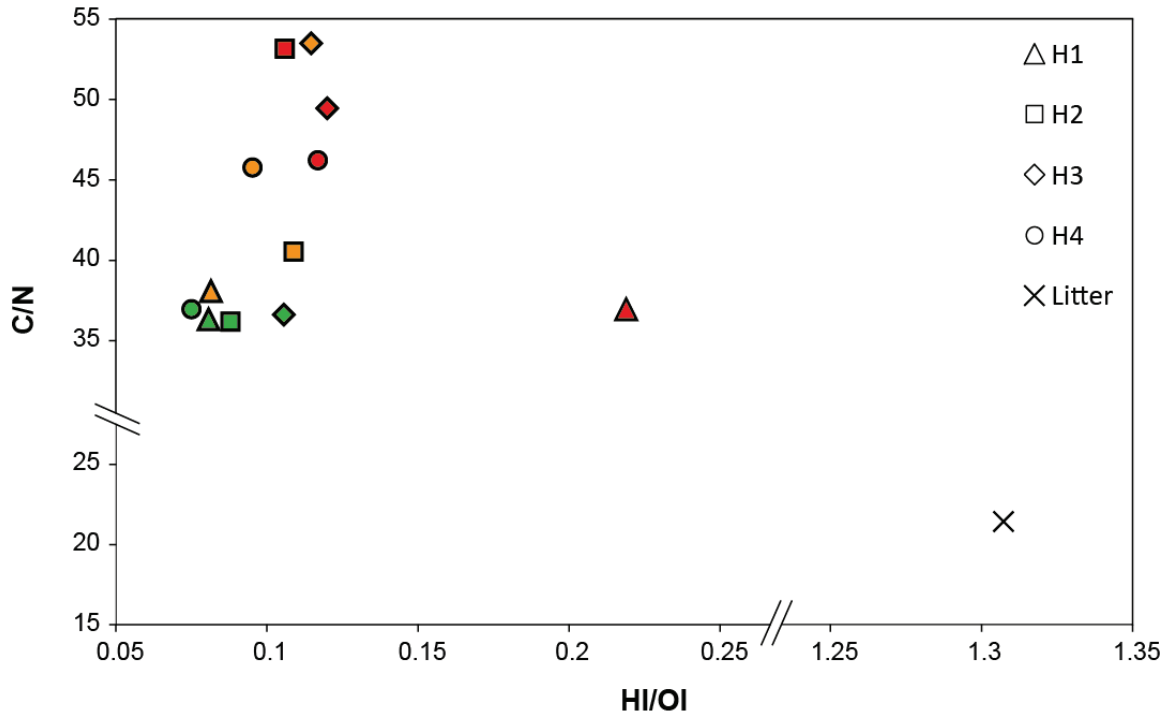

Figure 4.5 : *HI/OI vs C/N diagram. (T0: green; T4: orange, T8: red)*

3.3. Evolution of the bacterial community structure and As transformation activities

3.3.1. Bacterial community structure

T-RFLP was used to assess the spatial and temporal evolution of bacterial diversity in soil from the mesocosm. Hierarchical clustering of t-RFLP profiles allows evaluating the dissimilarity of bacterial community structure of each sample. First of all, all t-RFLP profiles were very similar (SM.1) with maximum level of dissimilarity of 4.3 %, but modification of bacterial community was observable (Fig.4.6.a). Hierarchical clustering allows to group bacterial community structure of T4 samples with two samples from T0 (H2 and H4) and one sample from T8 (H2). Other samples were all dissimilar from this group, and particularly samples H1 and H3 at T0. In all samples, a large bacterial diversity was detected. Richness (*S*) ranged between 61 and 122 t-RFs (Fig.4.6.b). Each time, *S* values were lower in H3 samples than in other samples. Diversity index of Shannon *H'* and Simpson *D'* presented high values and close results. However, bacterial diversity seemed to increase with time in the upper level of soil and, between T4 and T8, to decrease in the levels H3 and H4.

Despite the low bioavailable organic matter and non-favorable C/N ratio of the soil, bacterial diversity was important even before the addition of organic litter. At T0, the bacterial community structure was non homogenous in the mesocosm with high dissimilarity of t-RFLP patterns and *S*, *D'*, *H'* very different between each samples. This observation may be

attributed to a priming effect and enhanced by an incomplete stabilization of the soil in the mesocosm, also characterized by the dispersion of pH, Eh, conductivity, DOC values, during the first month of experiment (Thouin *et al*., *submitted*). After 4 months, bacterial community seemed to be more homogeneous throughout the mesocosm (Fig.4.6.b), suggesting that bacterial community structure was nearly similar in the unsaturated soil and in soil that was always saturated. The previous study showed that the physico-chemical parameters (pH, Eh, dissolved oxygen and DOC), driving the metabolism of soil microflora, were not affected by the wet/dry cycles before the addition of fragmented litter (Thouin *et al*., *submitted*). These homogeneous conditions, independent of depth and soil moisture, can explain the bacterial community structure at T4. Fierer *et al*. (2003), studied the effect of drying-rewetting cycles on bacterial community structure of a soil covered by grass and oak. They observed that the cycles had an impact on the bacteria residing in oak soil but not in grass soil. They attributed the modification of diversity in oak soil to the low frequency of moisture exposure compared with grass soil. The "Place-à-Gaz" soil was submitted to frequent rainfall events, and to saturation during periods of high precipitation. Autochthonous bacterial community is thus probably adapted to variable soil moistures conditions and this may explain that bacterial community composition was not affected by the wet/dry cycles in the mesocosm, before the addition of litter.

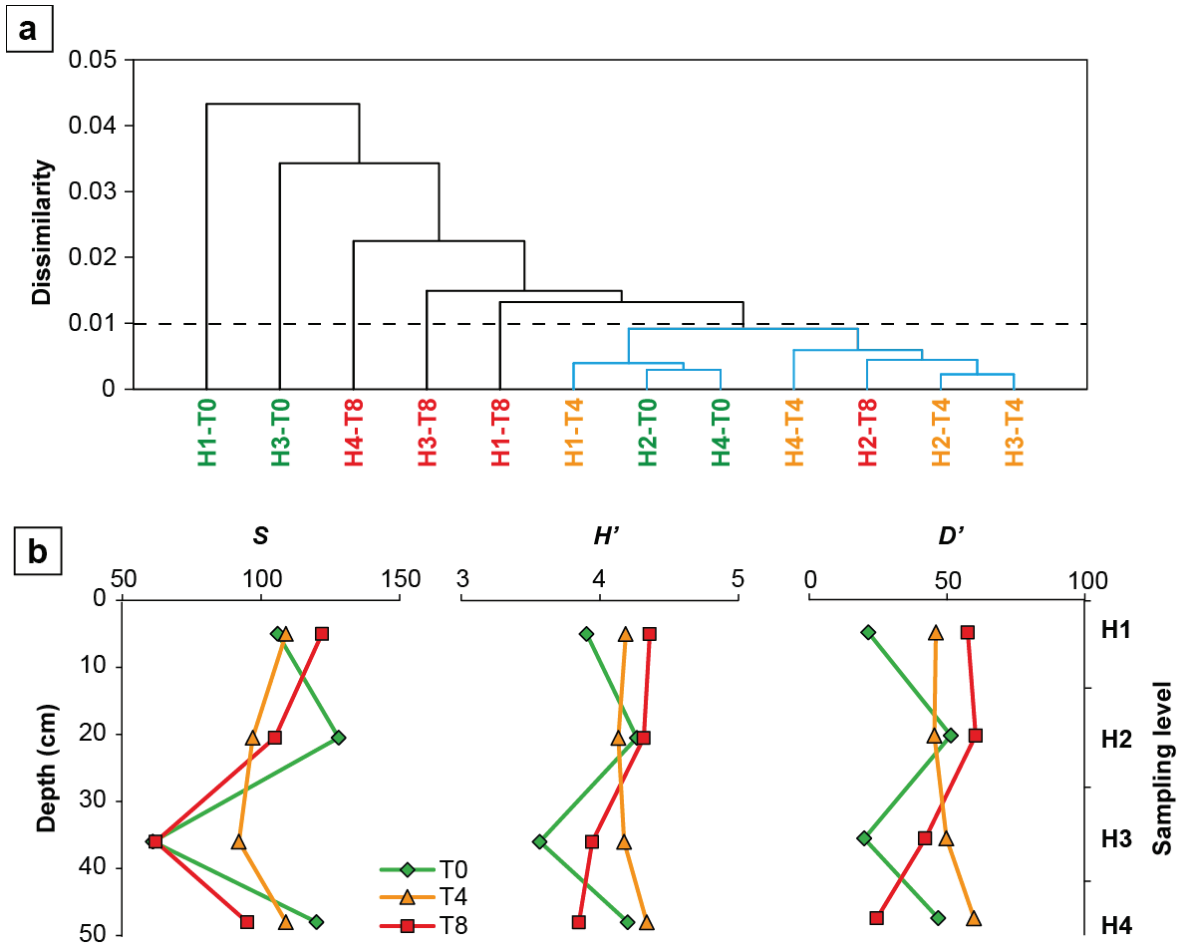

Figure 4.6: *Diversity analysis of bacterial community for the four samples (H1 unsaturated, H2 unsaturated, H3alternatively unsaturated/saturated and H4 saturated) at T0, T4 and T8. a: Ward cluster dendrogram based on Euclidian distance of bacterial t-RPLF profiles. b: Evolution of richness (S), Shannon index (H') and Simpson index (D') with depth and time.*

The addition of bioavailable OM after T4 seems to have impacted the bacterial diversity. Community structure at T8 seemed to be influenced by depth. In H2, bacterial community at T8 was close to that at the same level at T4, but for the other depths the community structures differed from T4 to T8, the greatest divergence being observed with H4 and H3 (Fig.4.6.a). Richness and diversity indexes suggested that the addition of organic matter enhanced the bacterial diversity on the upper part of the soil. The modification of bacterial community composition together with the increase of diversity in H1 seems to be directly linked to the addition of litter because (i) a distinct bacterial community was provided with the litter and (ii) bioavailable OM provided electron donor sources and carbon substrates which promoted the growth of specific bacteria (Gomez *et al.*, 2006). Indeed, the different types of OM from litter were major factors that control soil community composition (Tiedje *et al.*, 1999). The diversity and complexity of the organic amendments could promote specific groups of

microorganisms, which could best utilize the added substrates (Pérez-de-Mora *et al*., 2006). Here, bacteria capable to use substrates derived from lignin and cellulose were certainly promoted.

In H3 and H4 levels, bacterial community composition was changed after the addition of litter and diversity declined. The mineralization of biodegradable OM consumed dissolved oxygen in the saturated soil, leading to a decrease of redox potential in these levels (Thouin *et al*., *submitted*). The modification of bacterial community may have been caused by these environmental changes. Lundmann *et al*. (2000) observe spatial changes in the bacterial community structure correlated to the depletion of oxygen in a flooded soil. The obligate aerobic bacteria were disadvantaged compared with facultative anaerobic bacteria thus inducing the modification of bacterial community structure in these levels. The decrease of bacterial diversity can also be caused by the enhanced mobility of As III during the last period of the experiment in the saturated soil.

3.3.2. Microbial As transformation

The potential of microbial As III oxidation during the experiment was evaluated by As III-oxidizing activity tests (Fig.4.7). At T0, As III oxidation began between 70 and 90 hours. With time, the As III oxidation started earlier, particularly in the saturated soil. At T8, the As III oxidation kinetics of each sample were well temporally separated, with the complete As III oxidation reached according to the following order: H4<H3<H2<H1. The rate of microbial As III oxidation was globally higher in saturated or alternatively saturated/unsaturated levels H4 and H3 than in the unsaturated levels H1 and H2 (except for H3 T0) (Fig.4.7.b). The efficiency of As III oxidation decreased with time, mostly in H1 and H4 whose values decrease respectively from 1.31 and 2.16 mg of As $V.mL^{-1}.h^{-1}$ at T0 to 0.76 and 1.28 mg of $AsV.mL^{-1}.h^{-1}$ at T8. The concentrations of As III-oxidizing and As V-reducing microorganisms were evaluated by MPN (Fig.4.7.b). Between T0 and T4, As III-oxidizing microorganism concentrations were stable with higher values in H2 and lower in H3. After the addition of fragmented litter, the concentration of As III-oxidizing microorganisms increased in all levels, and particularly in H1. As V-reducing microorganisms were significantly less abundant than As III-oxidizing microorganisms (one order less). At T0, no or very low concentrations, < 100 As V-reducing microorganisms by gram of dry soil, were observed. After 4 months of experiment, As V-reducing microorganism concentrations increased in saturated and alternatively saturated/unsaturated levels. At T8, the concentration

of AsV-reducing microorganisms increased in H1 and H2, decreased in H3 and remained constant in H4. As previously discussed, the litter brought to the surface soil levels (H1 and H2) new microorganisms, probably including As V-reducing ones.

The results of microbial As III oxidation activity tests at T0 were consistent with the results previously obtained with soil sampled in the most polluted zone of the "Place-à-Gaz" site (Thouin *et al*., 2016), with identical latency of about 100 h A shorter latency was observed in the less contaminated soil at the periphery of the "Place-à-Gaz" site containing higher concentrations of bioavailable OM and As III-oxidizing microorganisms (Thouin *et al*., 2016). Our results seem to confirm that the latency before the beginning of As III oxidation was driven by the initial amount of As III-oxidizing microorganisms of the soil. This phenomenon was particularly observable in H4 sample between T4 and T8 with the increase of As III-oxidizing microorganisms together with the decrease of latency.

The concentration in As III-oxidizing microorganisms impacted also the As III oxidation rate (Fig.4.7). Indeed, at T8, As III oxidation rates decreased in all levels despite the higher concentration in As III-oxidizing microorganisms. Similar results were observed in soil sample of the study site and were associated to a selective pressure of the toxic elements concentrations on the microbial communities, resulting in more efficient As-III oxidizing microorganisms even present in lower concentration. Thus, the As III-oxidation rate doesn't seem to be linked to initial concentration in As III-oxidizing bacteria. The increase of microbial As V-reducing activity can also reduce the efficiency of As III oxidation. The increase of As III in soil solution (Thouin *et al*., *submitted*) together with the increase of As V-reducing microorganisms concentrations seems to indicate an increase of As V-reducing activity in the saturated levels H3 and H4. This As V-reducing activity may have negatively impacted the As III oxidation rate, in relation with the concentration and composition of organic substrates.

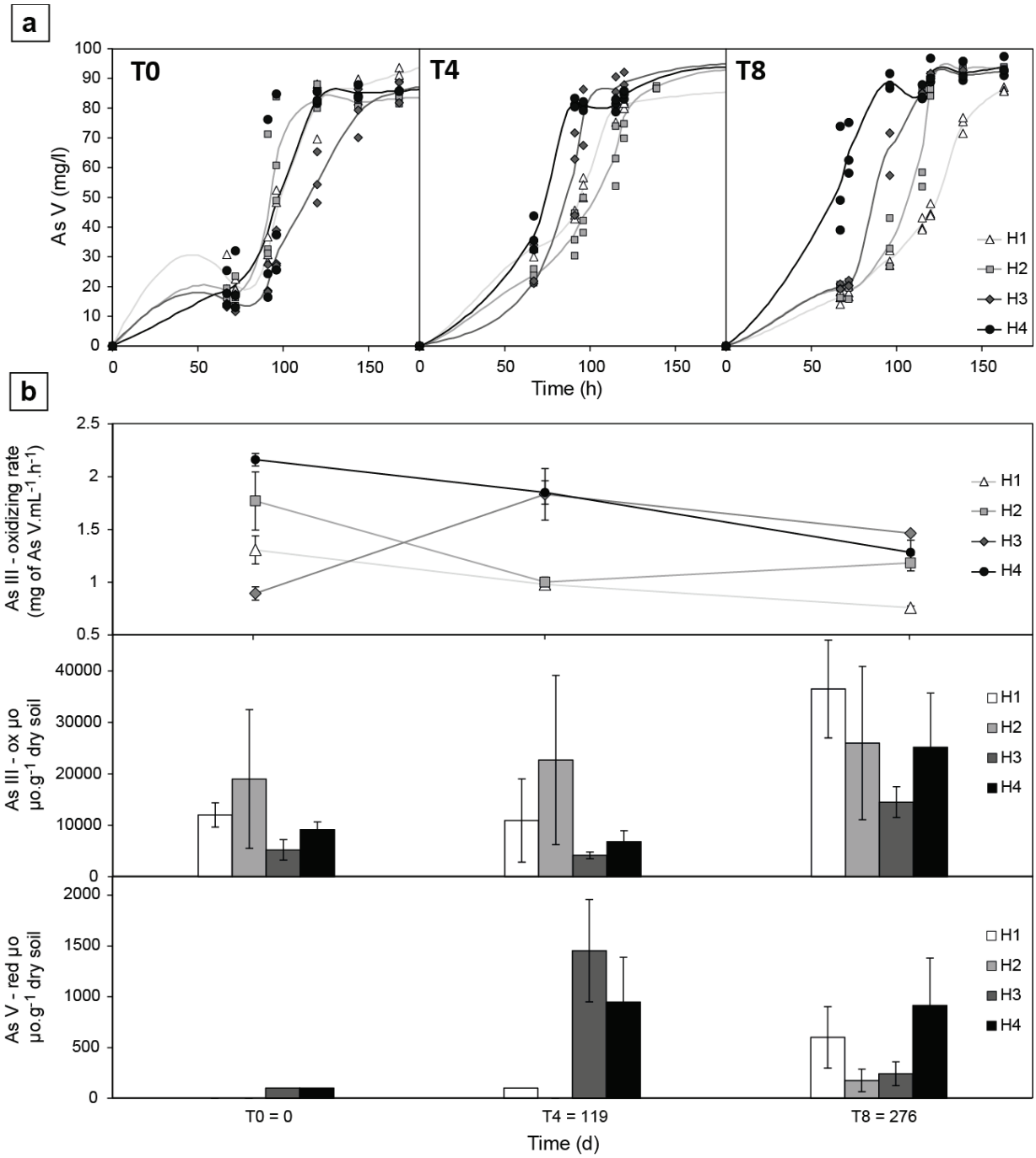

Figure 4.7: *Microbial As III-oxidizing and As V-reducing activities. a: Evolution of As V concentration during the As III-oxidizing activity test for the four soil samples at T0, T4 and T8. b: Plot of As III oxidation rates corresponding to the previous activity tests. Concentration of As III-oxidizing and As V-reducing microorganisms measured by MPN. Errors bars represent the standard deviation of the mean of three replicates for the four soil samples. For As V-reducing microorganisms a lack of value means that results from the two or three replicates were < 50 µo.g^{-1} dry soil. (ox: oxidizing; red: reducing; µo: microorganisms).*

As a fact, the As III oxidation rate results from the global activity of all microorganisms involved in As speciation, as microbial As III oxidation and As V reduction can occur simultaneously, even in aerobic condition. In order to observe the impact of the OM on this microbial communities able to transformed As, a PCA including variables describing OM quantities and qualities (TOC, DOC, HI/OI, C/N), microbial diversity and As transformation parameters (*D'*, As II-oxidation rate, As III-oxidizing microorganisms, As V-reducing microorganisms), As speciation and mobility in the interstitial water ([As], [As III], [As V]) and physicochemical parameters of water (pH, Eh) was built (Fig.4.8).

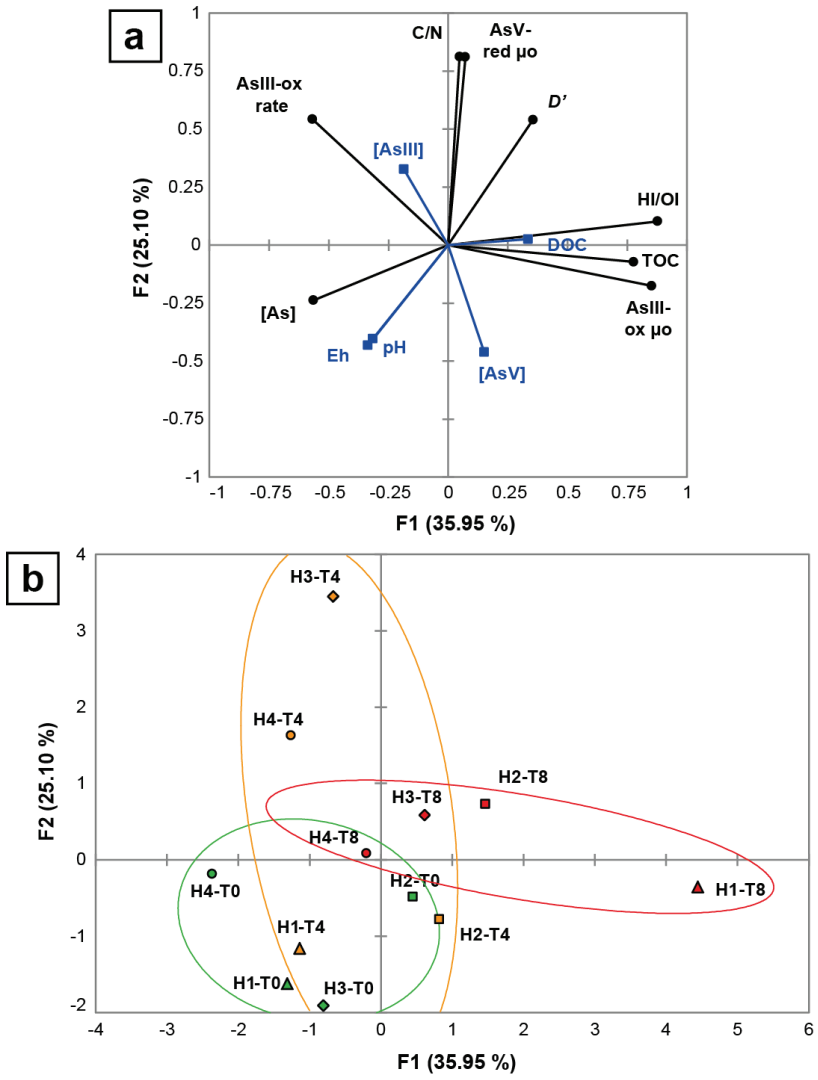

Figure 4.8: *PCA using biogeochemical parameters of soil samples (black) with geochemical parameters of soil solutions as supplementary data (blue). a: Correlation circle showing variable relationships. b: Factorial plan showing samples. Ellipses represent 90 % confidence limits of sample time step. (ox: oxidizing; red: reducing; µo: microorganisms). Pearson correlation matrix was presented in supplementary material 4.2.*

As previously observed, As III-oxidizing microorganisms concentrations were anti-correlated with As III oxidation rate while they were correlated with DOC, TOC and HI/OI (Fig.4.8). All As III-oxidizing bacteria isolated from soils were heterotrophs or facultative autotrophs (Inskeep *et al*., 2007; Bachate *et al*., 2012; Bahar *et al*., 2013; Dong *et al*., 2014). The increasing amount of OM and of its quality therefore promoted the growth of As III-oxidizing microorganisms. However, several studies showed that important concentrations of bioavailable organic matter negatively impact the efficiency of the As III-oxidizing bacterial activity (Challan-Belval *et al*., 2009; Bachate *et al*., 2012; Lescure *et al*., 2016). A similar inhibiting effect of the OM on the microbial As III oxidation rate seems to be observed in this soil submitted to an addition of fragmented litter.

The bioavailable organic matter may also stimulate the As V-reducing activity of soil microorganisms in aerobic conditions (Yamamura et al., 2009), because the As V-reducing mechanism liked to ARS resistance system consumes energy. In our study, concentrations in As V-reducing microorganisms increased in the non-saturated soil after addition of fragmented litter. However, As V-reducing microorganisms were correlated to C/N ratio (Fig.4.8) but not to the organic matter concentrations (DOC, TOC). The relation between As V-reducing microorganisms concentrations in the soil and OM qualities and quantities cannot be confirmed here. Finally, the correlation of As V-reducing microorganisms numbers with As III concentrations of in soil interstitial water suggests that microbial As V-reducing activity play an major role in the speciation and mobility of As in this soil, and particularly in saturated conditions.

4. Conclusion

This study provided important information about the mineralogical evolution and stability of the carriers of arsenic and heavy metals in the soils of the “Place-à-Gaz” submitted to environmental changes. The amorphous phases, identified as main As, Cu and Zn carrier, were altered in saturated conditions. This alteration caused the release of their constituents in the environment. The low concentration of Fe in soil solution and the observation of Fe-rich clusters of micrometric amorphous grains, in the vicinity of the altered amorphous phases, were corroborated by the precipitation of poorly crystalized hydrous ferric oxides. This result was also consistent with low concentration of Pb and Cu in soil solution and the immobilization of As V, observed in the previous study (Thouin *et al*., *submitted)*.

The mineralogical association didn't seem to be impacted by the environmental changes. Indeed, no traces of alteration were observed on the arsenate minerals present in the soil at the beginning of the experiment. However, in the saturated part, the appearance of mimetite, a lead arsenate chloride mineral, was detected. Its precipitation contributed to the As V and Pb immobilization but this reaction was limited by the low Pb concentration in soil solution.

The improvement of OM quality, caused by the addition of fragmented litter, significantly modified the bacterial community structure. The bacterial diversity was also affected by the addition of OM and decreased in saturated soil. The present study highlighted the active contribution of microorganisms to the arsenic dynamics. The input of OM contributed to the growth of As III-oxidizing microorganisms, however efficiency of As III oxidation decreased. High concentrations of organic substrates seemed to inhibit microbial As III-oxidizing activities, and enhanced the aerobic As V-reducing activity of soil microorganisms.

The saturation of soil of the "Place-à-Gaz", during high precipitation episodes, promotes the release of Zn and As in solution. Microbial As III oxidation, adsorption of As V on HFO and precipitation of mimetite, resulting in a global immobilization of As. However, the addition of OM caused increasing As III concentrations, by inhibited As III-oxidizing activity and enhanced As V-reducing.

Acknowledgments

This work was supported by Région Centre Val-de-Loire (convention 00087485) and the Labex Voltaire (ANR-10-LABX-100-01). The authors wish to thank Philippe Penhoud, Marielle Hatton and Rachel Boscardin (ISTO) for XRD, CHNS and Rock-Eval results, and Pascal Auger (BRGM) for Niton analyses.

Supplementary Material

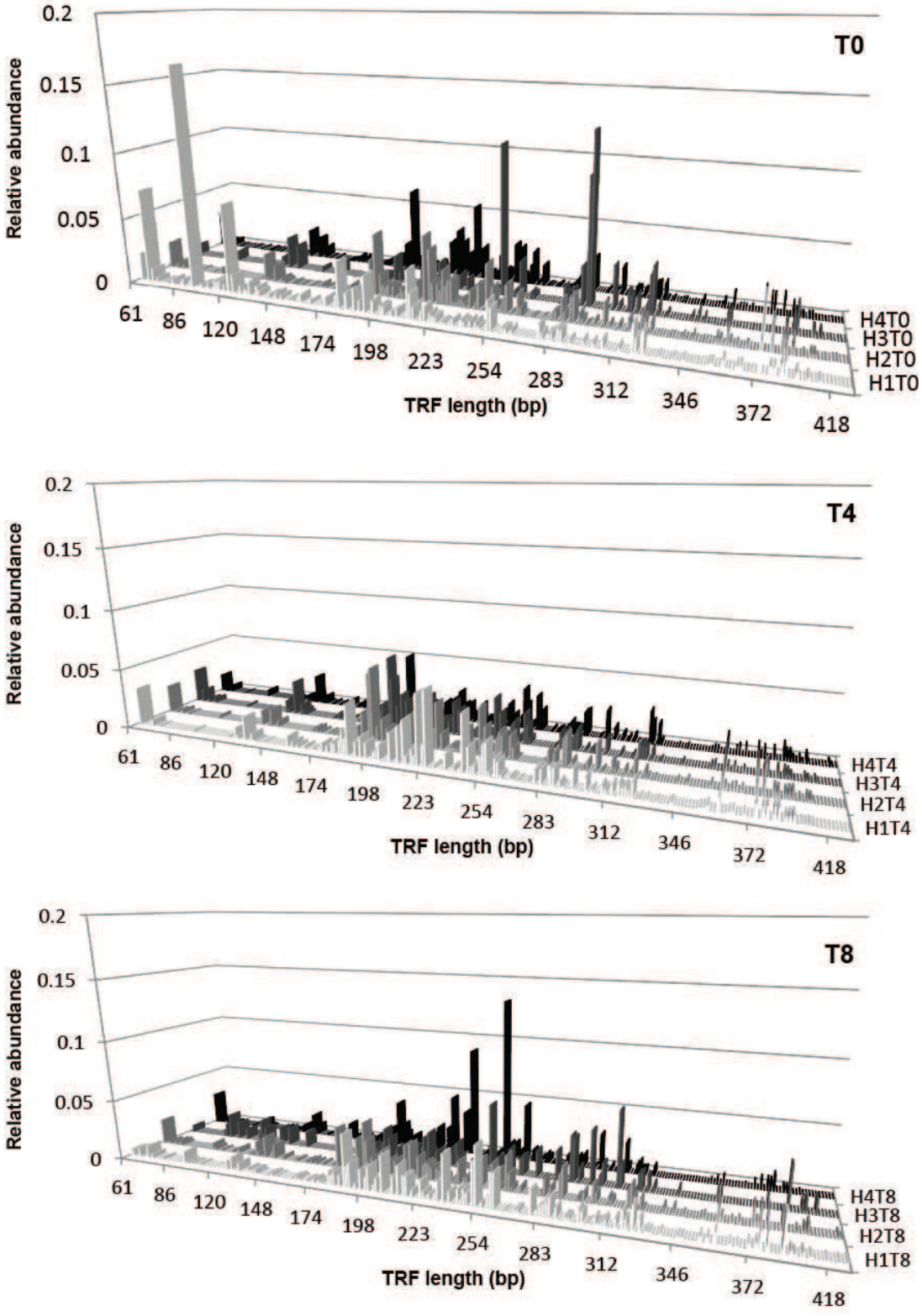

SM 4.1: *Relative abundances of t-RFs obtained from samples of each sampling level at T0, T4 and T8.*

SM 4.2: *Pearson correlation coefficients matrix of PCA variables*.

Variables	C/N	TOC	HI/OI	[As]	AsIII-ox rate	AsIII-ox µo	AsV-red µo	D'	DOC	[As V]	[As III]	pH	Eh
C/N	**1**	0.016	0.042	-0.176	0.214	-0.037	**0.591**	0.314	0.574	-0.505	0.300	**-0.739**	**-0.746**
TOC	0.016	**1**	0.535	-0.284	-0.266	**0.651**	-0.181	0.407	0.379	0.311	-0.522	-0.348	-0.400
HI/OI	0.042	0.535	**1**	-0.488	-0.495	**0.677**	0.320	0.250	0.486	-0.281	0.207	-0.425	-0.556
[As]	-0.176	-0.284	-0.488	**1**	0.213	-0.237	-0.149	-0.184	0.075	-0.282	0.455	0.165	0.280
AsIII-ox rate	0.214	-0.266	-0.495	0.213	**1**	-0.504	0.268	0.246	-0.534	-0.371	0.246	0.148	0.051
AsIII-ox µo	-0.037	**0.651**	**0.677**	-0.237	-0.504	**1**	-0.102	0.256	**0.684**	0.296	-0.003	-0.515	-0.543
AsV-red µo	**0.591**	-0.181	0.320	-0.149	0.268	-0.102	**1**	0.191	-0.091	-0.586	**0.762**	-0.353	-0.416
D'	0.314	0.407	0.250	-0.184	0.246	0.256	0.191	**1**	0.198	-0.166	-0.199	-0.583	-0.418
DOC	0.574	0.379	0.486	0.075	-0.534	**0.684**	-0.091	0.198	**1**	-0.131	0.004	**-0.738**	-0.572
[As V]	-0.505	0.311	-0.281	-0.282	-0.371	0.296	-0.586	-0.166	-0.131	**1**	-0.556	0.242	0.277
[As III]	0.300	-0.522	0.207	0.455	0.246	-0.003	**0.762**	-0.199	0.004	-0.556	**1**	-0.182	-0.255
pH	**-0.739**	-0.348	-0.425	0.165	0.148	-0.515	-0.353	-0.583	**-0.738**	0.242	-0.182	**1**	**0.887**
Eh	**-0.746**	-0.400	-0.556	0.280	0.051	-0.543	-0.416	-0.418	-0.572	0.277	-0.255	**0.887**	**1**

Conclusions générales et perspectives

L'objectif de la présente étude était de caractériser les mécanismes de transfert de polluants des sols vers les eaux souterraines ou de surface, en lien avec le couplage des cycles biogéochimiques du carbone et des polluants inorganiques dans un sol pollué. Dans cette perspective, les travaux réalisés se sont focalisés sur l'étude de l'effet d'un apport de matière organique naturelle complexe, sur l'évolution biogéochimique d'un sol pollué par des métaux et métalloïdes, soumis à des conditions redox variables. Le site de la Place-à-Gaz, présentant une pollution intense mais localisée en contaminants inorganiques a été choisi comme pour cette étude. La contamination de cette zone est liée à la destruction par pyrolyse d'armes organo-arséniées de la Première Guerre Mondiale, en 1928. Il s'agit du deuxième site de ce genre à avoir fait l'objet d'études, avec celui localisé à Poeklapellen, en Belgique (Bausinger et Preuβ, 2005), néanmoins, à ce jour d'autres lieux de destructions similaires ont été trouvés le long de l'ancienne ligne de front (localisation confidentielle). Les principaux contaminants de ces sites sont l'arsenic, le cuivre, le plomb et le zinc. Ces éléments peuvent localement présenter des concentrations très rarement observées dans la littérature (> 100 g/kg). Des contaminants organiques, liés à la dégradation des agents explosifs et chimiques contenus dans les obus, ont également été détectés sur les sites. L'acide diphénylearsénique, issu de l'oxydation des composés Clark I (chlorure de diphénylarsine) et Clark II (cyanure de diphénylarsine), ainsi que des composés nitroaromatiques, des perchlorates, des dioxines, et des hydrocarbures aromatiques polycycliques, issus de agents explosifs, ont été observés sur le site de la Place-à-Gaz (Bausinger *et al*., 2007). Néanmoins, et contrairement à la contamination inorganique, cette contamination organique est d'une importance mineure. Bausinger *et al*. (2007) proposent que la méthode de destruction des munitions, par pyrolyse, ait conduit à une minéralisation presque complète des agents de guerres explosifs et chimiques. Nos travaux ont ainsi essentiellement porté sur le comportement des contaminants inorganiques. Cependant, sur ce genre de site, cette contamination organique ne peut pas être laissée de côté lors d'un diagnostic environnemental complet visant à vérifier l'état des milieux.

La première partie de ces travaux présente une caractérisation complète de la contamination inorganique du site, avec la localisation, à l'échelle du site et des phases du sol, des métaux et de l'arsenic, ainsi que l'étude de leur mobilité, et une évaluation de l'activité des microorganismes du site. La mesure *in situ* des métaux dans le sol a confirmé la faible

étendue de la contamination. Les contaminants sont essentiellement situés dans une couche noire composée des résidus de la pyrolyse (morceaux de munition, charbons, scories, cendres). Cette couche s'étend sur environ 2000 m^2, et son épaisseur varie entre 40 et 5 cm. Au centre de la Place-à-gaz, les concentrations les plus importantes ont été détectées, As = 124 $g.kg^{-1}$, Zn = 152 $g.kg^{-1}$, Cu = 28 $g.kg^{-1}$, Pb = 5 $g.kg^{-1}$. Ces concentrations diminuent de façon concentrique en s'éloignant du centre. L'étendue de la contamination est observable par ses conséquence sur la végétation. Dans la partie centrale, aucune végétation de c'est implantée depuis près d'un siècle. Lorsque l'intensité de la contamination diminue, certaines espèces végétales parviennent à se développer ; enfin, la limite de la couche noire est soulignée par la lisière de la forêt. L'absence de végétation et la très faible diversité de la flore présente sur ce site, et son caractère tolérant aux métaux et à l'As, soulignent le caractère polluant de cette couche noire et la perte de certaines fonctions de ce sol.

L'étude de la localisation des contaminants inorganiques dans les différentes phases du sol a confirmé l'impact du traitement thermique, suggérée par Bausinger *et al*. (2007), sur la spéciation des contaminants inorganiques. Le matériel pollué est composé d'argiles (héritées du sol naturel), de grandes quantités de charbons (issus de l'utilisation de bois pendant la combustion), de morceaux d'obus, et enfin de minéraux et phases secondaires porteuses de métaux et d'arsenic. Du fait du protocole de destruction des munitions par traitement thermique, la majorité des métaux se retrouve aujourd'hui sous forme d'une phase amorphe riche en Fe, Cu, Zn et As à l'aspect vitreux. Des minéraux secondaires porteurs d'arsenic ont également été observés dans l'échantillon le plus pollué : deux minéraux composés d'arséniates de zinc et de cuivre (adamite et olivénite) ainsi que deux hydroxy-arséniates de fer (pharmacosidérites). L'assemblage minéralogique retrouvé dans ce sol est très particulier puisque ces arséniates sont généralement retrouvés dans des contextes miniers, issus de l'altération de minéraux précurseur comme l'arsénopyrite (Morin *et al*., 2002 ; Morin et Calas, 2006 ; Drahota et Filippi, 2009 ; Haffert *et al*., 2010). A notre connaissance, c'est la première fois qu'une association minéralogique similaire, liée à une activité d'incinération de matériaux dangereux, est observée.

Le sol de la Place-à-Gaz n'est pas pauvre en matière organique puisque les concentrations en carbone organique atteignent 250 $g.kg^{-1}$. Néanmoins cette étude a montré que celle-ci était peu biodégradable. Dans la partie centrale du site, ce carbone organique est lié aux quantités importantes de charbons. Cependant, une proportion faible de métaux et d'arsenic est adsorbée à la surface de ces charbons. L'absence de matière organique biodisponible,

conjointement aux concentrations en contaminants inorganiques, ont limité le développement de la microflore du sol. Ces conditions particulières ont exercé une pression sélective sur les communautés microbiennes, augmentant la proportion de microorganismes capables d'oxyder l'As III. Ces microorganismes contribuent à maintenir une forte proportion d'As V dans le sol.

Sur le site, la couche superficielle polluée peut être affectée par des changements de conditions environnementales, telles que des cycles de saturation. En effet, pendant les épisodes pluvieux, le sol du site est saturé en raison de la présence d'un substrat argileux sous-jacent imperméable. La présence de zones humides permanentes a également été observée à la périphérie du site. La couche noire est également affectée par des apports de matière organique biodégradable issue des feuilles mortes et débris végétaux déposés par la forêt. La suite des travaux a donc été orientée vers l'étude de l'impact d'épisodes de saturation en eau et de l'apport de matière organique sur les cycles biogéochimiques du carbone et des contaminants inorganiques, et en particulier sur leur mobilisation dans l'eau interstitielle du sol.

Pour étudier ces phénomènes, une étude en mésocosme, offrant une échelle intermédiaire entre les observations de terrain et les caractérisations en petit volumes, et permettant un contrôle des conditions environnementales et un suivit des contaminants dans les différents compartiments du sol, a été menée. Une colonne instrumentalisée (1 m^3), nommée LABBIO, a été remplie avec le sol contaminé échantillonné dans la partie centrale de la Place-à-Gaz. Afin d'étudier l'effet de la saturation du sol en eau, des cycles de périodes sèches et humides d'un mois ont été simulés pendant 8 mois. Après deux cycles sec/humide, de la litière organique, échantillonnées à la périphérie du site, a été ajoutée à la surface du sol, afin d'étudier l'effet de la matière organique biodisponible sur le comportement des polluants inorganiques.

Après 8 mois de suivi, des tendances particulières ont pu être observées. Tout d'abord, les conditions environnementales imposées n'ont pas eu d'effet très marqué sur les paramètres pH et potentiel redox du milieu. Malgré la mise en évidence de concentrations très élevées en carbone organique dissous (COD), le potentiel redox n'a pas beaucoup diminué dans les zones saturées du mésocosme. Cette observation est cohérente avec la série d'espèces chimiques potentiellement utilisables par les microorganismes comme accepteurs d'électrons, dont la spéciation et la concentration a pu être affectée au cours de l'expérience, dans les

niveaux saturés : l'oxygène dissous, le nitrate, l'arsenic. Les principaux cycles biogéochimiques affectés par les conditions environnementales imposées ont donc été ceux du carbone, de l'azote et de l'arsenic. Le COD était peu biodégradable, puisque qu'il n'a pas entraîné une diminution du potentiel redox suffisante pour induire une respiration du fer. Le cycle de l'azote, élément lié à la composition des explosifs, et certainement minéralisé pendant leur combustion, est le plus affecté par les cycles de saturation/désaturation. En effet dans le niveau alternativement saturé ou désaturé, un processus de dénitrification a pu être mis en évidence. Dans les niveaux qui sont restés saturés, une réduction dissimilatrice du nitrate en ammonium semble contribuer également à la disparition du nitrate.

Comme observé sur le site et lors de la phase de caractérisation préliminaire, le Zn et l'As sont les contaminants les plus mobiles dans le mésocosme. La concentration en Zn dans l'eau augmente avec la profondeur : elle s'élève à 30 $mg.L^{-1}$ à la surface, et jusqu'à 80 $mg.L^{-1}$ en sortie de colonne. Les cycles sec/humide n'ont pas d'effet important sur sa mobilité, néanmoins, les quantités de zinc mobilisé dans la partie saturée du sol semblent plus importantes. Cette augmentation du Zn mobilisé dans la partie saturée du sol peut être expliquée par l'altération de la phase amorphe, entrainant un relargage en solution des contaminants entrant dans sa composition. Cependant, les autres éléments n'ont pas le même comportement, et sont moins mobiles que le Zn dans l'eau interstitielle. Les concentrations en Fe en solution, et l'observation de phase précipitée enrichie en fer à la périphérie des phases amorphes altérées, semble être en accord avec la re-précipitation d'oxyhydroxyde de fer mal cristallisé. La précipitation de ces phases a très probablement induit une immobilisation du Cu, du Pb et de l'AsV.

Contrairement, aux éléments Cu et Pb, beaucoup d'As reste en solution. Les concentrations en As sont globalement plus faibles dans la partie inférieure du mésocosme (4 $mg.L^{-1}$) par rapport aux niveaux supérieurs (6 $mg.L^{-1}$). L'As V est l'espèce la plus abondante, cependant la proportion d'As III augmente avec la profondeur. En sortie de colonne elle représente près de 20% de l'As total. L'apport de matière organique a eu pour conséquence de diminuer les concentrations en As V dans tous les niveaux de prélèvements, et d'augmenter les concentrations en As III dans le niveau saturé. L'immobilisation de l'As V dans les niveaux les plus profonds peut être liée à leur adsorption sur les oxyhydroxydes de fer, mais également à la précipitation de la mimétite, un chloroarséniate de plomb. La mimétite précipite facilement à partir d'As V, de Cl^- et de très faible quantité de Pb^{2+}, conditions réunies dans notre sol. La précipitation de la mimétite, qui est stable jusqu'à pH 2, permet d'immobiliser

une partie de l'As V de la solution, néanmoins ce processus est limité par les très faibles concentrations de Pb en solution.

Les concentrations en As V sont également contrôlées par l'activité bactérienne. En effet, des tests ont pu montrer une activité d'oxydation microbienne de l'As III active dans le sol, contribuant à la prédominance de l'As V. Néanmoins, cette activité microbienne, tout comme la structure des communautés bactériennes du sol, ont été affectées par l'apport de matière organique biodisponible. En effet, la présence de matière organique a favorisé le développement des microorganismes effectuant l'oxydation de l'As III, cependant cela ne s'est pas traduit par une amélioration de la vitesse d'oxydation de l'As III. La matière organique semble avoir un effet inhibiteur, lorsque qu'elle est trop concentrée, et le développement de microorganismes As V - réducteurs a contribué à la diminution de la vitesse d'oxydation de l'As III. Il résulte de ces processus une augmentation significative de la concentration en As III en solution dans la partie saturée du mésocosme à la fin de l'étude, malgré la diminution globale de la quantité d'As lessivé.

Des espèces d'arsenic organiques ont également été détectées dans la solution du mésocosme, dont l'acide diphenylarsénique et trois molécules inconnues. Les concentrations de ces molécules inconnues ne sont pas négligeables, et l'une d'elle n'apparait que lorsque le sol est saturé. Ces espèces ne semblent pas être les métabolites habituels de l'acide diphénylarsénique, ni des espèces méthylées. Leur identification serait très utile dans la perspective du développement de stratégies de suivi et de remédiation des sites impactés par les armes chimiques. Ce verrou scientifique représente un véritable enjeu à l'échelle internationale. En effet, peu de données existent sur les voies et cinétiques de dégradations, ainsi que sur la toxicité et l'écotoxicité de ces molécules organo-arséniées.

Les résultats de la présente thèse apportent des connaissances nouvelles sur les processus ayant affecté et affectant aujourd'hui encore la mobilité des contaminants sur le site de la Place-à-Gaz, et permettent d'appréhender les flux d'éléments transférés du sol contaminé vers les compartiments environnants par lessivage et ruissellement. Nos conditions environnementales simulées correspondent à environ 1 an de précipitations sur le site de la Place-à-Gaz, avec les cycles sec/humide simulant les variations saisonnières. On considère également que les écoulements étudié en mésocosmes sont représentatifs des écoulements sur site, avec dans la partie haute du mésocosme (i) : les écoulements verticaux ayant lieu dans la partie insaturé de la couche pollué et dans la partie basse du mésocosme(ii) : les écoulements

horizontaux ayant lieu dans la partie saturé de la couche pollué (Fig.5.1) Ainsi si les flux lessivés pendant l'expérience en mésocosme sont représentatifs des flux horizontaux induits sur le site par la présence du substrat argileux imperméable, alors on peut estimer à 3 700 kg de Zn et 160 kg d'As les quantités de ces éléments transférées à partir de ce site par ruissèlement, depuis 1928. La proportion d'As III, espèce plus toxique et plus mobile que l'As V, représente environ 30 % de l'arsenic total, et peut être encore augmentée par des apports plus importants de MO. Les quantités importantes d'As et de métaux lessivées à partir de la litière organique échantillonnée en marge du site attestent de l'important transfert horizontal de ces contaminants inorganiques vers l'environnement proche.

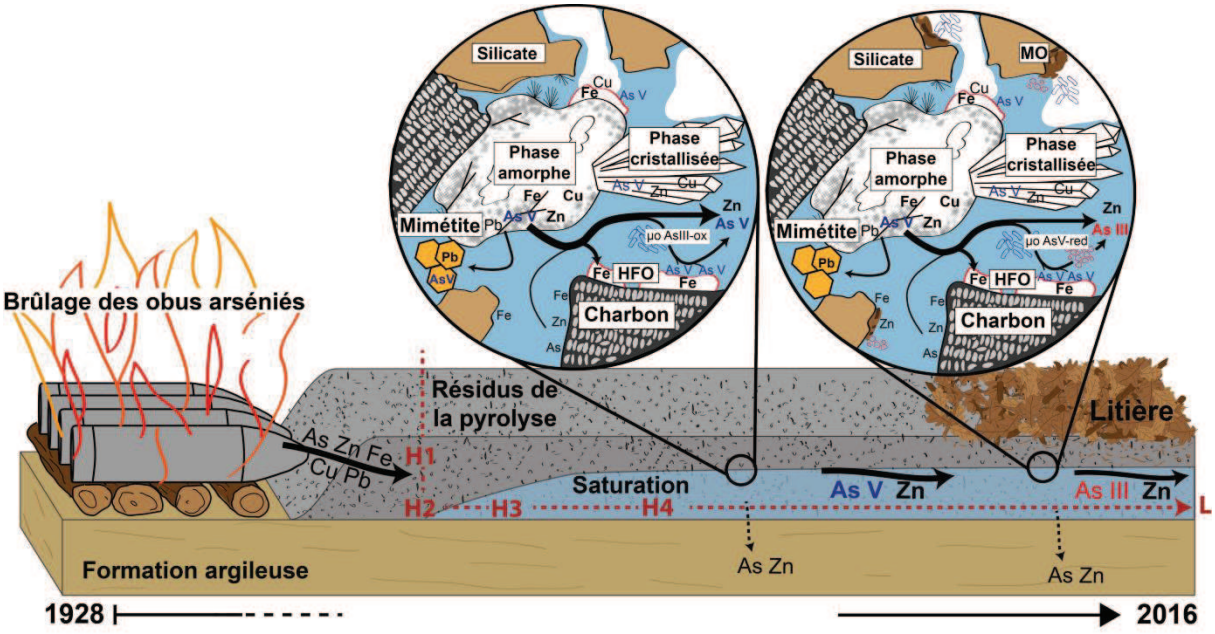

Figure 5.1 : *Transposition du comportement des métaux dans le sol du mésosocosme, soumis à des alternances de saturation en eau et d'un apport de MO, aux conditions environnementales du site de la Place-à-Gaz. En rouge, le transfert verticale étudié dans le mésocosme transposé aux écoulements sur site.*

Les travaux présentés dans ce manuscrit, ne prennent pas en compte l'impact rhizosphérique lié à l'implantation de la houlque laineuse dans les parties les moins contaminées du site, soumises à des dépôts de litières. L'activité de cette herbacée et des microorganismes qui lui sont associés peuvent influencer leur environnement proche, par la formation d'exsudats racinaires (Jones, 1998), et la minéralisation de la MO. Ces activités seraient susceptible de modifier de manière directe (précipitation, complexation, adsorption) ou indirecte (modification du pH et Eh, dissolution, précipitation de minéraux,…) le comportement des

contaminants inorganiques (McGrath *et al*., 2001). De la houlque laineuse a été semée dans le mésocosme après les 8 premiers mois d'expérience présentés dans ce manuscrit. Le développement de ces herbacées n'a pas été optimale, et seulement quelques plants ont survécu. Les premiers résultats ont cependant montré une augmentation importante de la minéralisation de carbone organique dans le mésocosme et un développement de biomasse microbienne capable de transformer l'As (microorganismes As III oxydant et As V réducteur) dans le sol rhizosphérique. Le sol et la solution rhizosphérique sont en cours d'analyse afin d'étudier l'effet du développement des plantes sur le comportement des métaux.

L'apport de litière a augmenté la complexité de la MO du sol de la Place-à-Gaz, modifiant par la même occasion le cycle de l'azote et du carbone sur le site. La biodisponibilité de l'azote et de substrats organiques facilement biodégradables sont des facteurs qui peuvent favoriser le développement des communautés bactériennes ou fongiques (Meier et Bowman, 2010 ; Strickland et Rousk, 2010 ; Koranda *et al*., 2014). L'apport de litière dans notre mésocosme a modifié la diversité bactérienne du sol dans les niveaux proches de la surface, mais a certainement également modifié la structure des communautés fongiques ainsi que leur biomasse. Afin d'étudier ces paramètres, des analyses de l'abondance des gènes (par réaction en chaîne par polymérase en temps réel, PCR quantitative) codant l'ARN ribosomique 16S (commun au domaine des *Eubacteria*) et 18S (commun au règne des *Fungi*), et l'identification des microorganismes présents dans le sol (par séquençage haut débit) seront effectués. Ces résultats, au même titre que ceux liés à l'étude de la rhizosphère, seront valorisés.

Certaines des observations et des résultats originaux présentés dans ce manuscrit sont spécifiques aux sites de brûlage d'obus chimiques, néanmoins cette étude apporte des réponses plus globales sur l'impact environnemental des activités liées aux conflits à l'échelle internationale, des sites de stockage et d'enfouissement étant disséminés sur plusieurs continents. Il est probable que des cocktails de contaminants inorganiques identiques, des associations minéralogiques similaires, des communautés microbiennes très spécifiques soient observés sur les autres sites de brûlage connus. Des diagnostics de ces sites permettraient d'autre part d'évaluer l'ampleur de leur empreinte environnementale. Aujourd'hui les séquelles environnementales de la Grande Guerre sont encore difficile à évaluer, il est néanmoins sûr que près de 100 ans après la fin des conflits, le réservoir chimique disséminé dans les sols et les lacs des champs de batailles n'est pas épuisé.

Au-delà de cette problématique, la présente thèse a généré des informations nouvelles concernant l'effet de la matière organique sur les communautés microbiennes contribuant au cycle de l'arsenic, en termes d'impacts sur leur concentration dans le sol, et sur la cinétique globale d'oxydation de l'As III par la microflore. Des connaissances plus poussées concernant les interactions entre le cycle de l'arsenic et celui du carbone sont ainsi disponibles, et ces résultats sont transposables à différents types de sites pollués par des activités minières, métallurgiques ou industrielles, sur lesquels des stratégies de phyto-management sont envisagées. Le mésocosme LABBIO s'est révélé être un dispositif adapté à l'étude de l'effet d'un apport de MO végétale sur la mobilité des polluants du compartiment « sol pollué » vers les compartiments « eau » et « gaz ». La mise en œuvre de tels mésocosmes permet de générer de nombreuses données sur les différents compartiments, en conditions environnementales imposées et contrôlées. Les nombreuses données acquises au cours de la présente thèse, au niveau de la géochimie des eaux, pourront être utilisées pour modéliser les processus identifiés. Ainsi, les résultats de la présente thèse seront potentiellement utiles, à court et moyen terme dans les domaines de la connaissance du cycle biogéochimique de l'arsenic, du diagnostic d'impact des sites pollués, à travers les mécanismes identifiés et le développement méthodologique de la plateforme qui sera transposable à d'autres types de sols. Enfin, à plus long terme, cette thèse apporte des éléments de compréhension des interactions entre MO et métaux, qui seront utiles dans le domaine de la remédiation de sites par différentes techniques de phytomanagement, impliquant le développement de végétaux et des amendements de matière organique.

Références bibliographiques

A

Achour-Rokbani, A., Bauda, P., and Billard, P. (2007). Diversity of arsenite transporter genes from arsenic-resistant soil bacteria. Research in Microbiology *158*, 128–137.

Achour-Rokbani, A., Cordi, A., Poupin, P., Bauda, P., and Billard, P. (2010). Characterization of the ars gene cluster from extremely arsenic-resistant microbacterium sp. Strain A33. Applied and Environmental Microbiology *76*, 948–955.

Ahmann, D., Roberts, A.L., Krumholz, L.R., and Morel, F.M.M. (1994). Microbe grows by reducing arsenic. Nature *371*, 750–750.

Altmann, R. S., and Bourg, A. C. (1997). Cadmium mobilisation under conditions simulating anaerobic to aerobic transition in a landfill leachate-polluted aquifer.Water, Air, and Soil Pollution, *94*(3-4), 385-392.

Anderson, T.R., Goodale, C.L., Groffman, P.M., and Walter, M.T. (2014). Assessing denitrification from seasonally saturated soils in an agricultural landscape: A farm-scale mass-balance approach. Agriculture, Ecosystems and Environment *189*, 60–69.

Andrieu, S., and Müller, P. (2012). Les surfaces solides: concepts et méthodes. EDP Sciences.

Ashworth, D.J., and Alloway, B.J. (2008). Influence of dissolved organic matter on the solubility of heavy metals in sewage-sludge-amended soils. Communications in Soil Science and Plant Analysis *39*, 538–550.

Auffan, M., Rose, J., Bottero, J.-Y., Lowry, G.V., Jolivet, J.-P., and Wiesner, M.R. (2009). Towards a definition of inorganic nanoparticles from an environmental, health and safety perspective. Nature Nanotechnology *4*, 634–641.

B

Baba, K., Arao, T., Maejima, Y., Watanabe, E., Eun, H., and Ishizaka, M. (2008). Arsenic speciation in rice and soil containing related compounds of chemical warfare agents. Analytical Chemistry *80*, 5768–5775.

Bachate, S.P., Khapare, R.M., and Kodam, K.M. (2012). Oxidation of arsenite by two β-proteobacteria isolated from soil. Applied Microbiology and Biotechnology *93*, 2135–2145.

Bahar, M.M., Megharaj, M., and Naidu, R. (2013). Kinetics of arsenite oxidation by Variovorax sp. MM-1 isolated from a soil and identification of arsenite oxidase gene. Journal of Hazardous Materials *262*, 997–1003.

Baize, D. (1997). Teneurs totales en éléments traces métalliques dans les sols (France): Références et stratégies d'interprétation. Programme ASPITET. Editions Quae.

Bajda, T., Szmit, E., and Manecki, M. (2006). Removal of As (V) from solutions by precipitations of mimetite Pb5 (AsO4) 3Cl. Environmental Engineering, 119-124.

Bajda, T. (2010). Solubility of mimetite $Pb_5(AsO_4)_3Cl$ at 5–55°C. Environmental Chemistry *7*, 268.

Battaglia-Brunet, F., Dictor, M.-C., Garrido, F., Crouzet, C., Morin, D., Dekeyser, K., Clarens, M., and Baranger, P. (2002). An arsenic(III)-oxidizing bacterial population: selection, characterization, and performance in reactors. Journal of Applied Microbiology *93*, 656–667.

Battaglia-Brunet, F., Joulian, C., Garrido, F., Dictor, M.-C., Morin, D., Coupland, K., Barrie Johnson, D., Hallberg, K.B., and Baranger, P. (2006). Oxidation of arsenite by Thiomonas strains and characterization of Thiomonas arsenivorans sp. nov. Antonie van Leeuwenhoek *89*, 99–108.

Baubron J. C. (2004) Tests analytiques d'un sol contaminé par des résidus de munitions au sud de Verdun (Meuse). BRGM/LOR04N849.

Baur, W.H. (2012). Rigid frameworks of zeolite-like compounds of the pharmacosiderite structure-type. Microporous and Mesoporous Materials *151*, 13–25.

Bausinger, T., and Preuβ, J. (2005). Environmental remnants of the First World War: Soil contamination of a burning ground for arsenical Ammunition. Bulletin of Environmental Contamination and Toxicology *74*, 1045–1053.

Bausinger, T., Bonnaire, E., and Preuß, J. (2007). Exposure assessment of a burning ground for chemical ammunition on the Great War battlefields of Verdun. Science of The Total Environment *382*, 259–271.

Bentley, R., and Chasteen, T.G. (2002). Microbial methylation of metalloids: arsenic, antimony, and bismuth. Microbiology and Molecular Biology Reviews *66*, 250–271.

Berglund, L.M., DeLuca, T.H., and Zackrisson, O. (2004). Activated carbon amendments to soil alters nitrification rates in Scots pine forests. Soil Biology and Biochemistry *36*, 2067–2073.

Bertrand, H., Poly, F., Van, V.T., Lombard, N., Nalin, R., Vogel, T.M., and Simonet, P. (2005). High molecular weight DNA recovery from soils prerequisite for biotechnological metagenomic library construction. Journal of Microbiological Methods *62*, 1–11.

Blum, J.S., Han, S., Lanoil, B., Saltikov, C., Witte, B., Tabita, F.R., Langley, S., Beveridge, T.J., Jahnke, L., and Oremland, R.S. (2009). Ecophysiology of "Halarsenatibacter

silvermanii" Strain SLAS-1T, gen. nov., sp. nov., a facultative chemoautotrophic arsenate respirer from salt-saturated Searles Lake, California. Applied and Environmental Microbiology *75*, 1950–1960.

Bodénan, F., Baranger, P., Piantone, P., Lassin, A., Azaroual, M., Gaucher, E., and Braibant, G. (2004). Arsenic behaviour in gold-ore mill tailings, Massif Central, France: hydrogeochemical study and investigation of in situ redox signatures. Applied Geochemistry *19*, 1785–1800.

Bradl, H.B. (2004). Adsorption of heavy metal ions on soils and soils constituents. Journal of Colloid and Interface Science *277*, 1–18.

Buschmann, J., Kappeler, A., Lindauer, U., Kistler, D., Berg, M., and Sigg, L. (2006). Arsenite and arsenate binding to dissolved humic acids: Influence of pH, type of humic acid, and aluminum. Environmental Science and Technology,*40*(19), 6015-6020.

Bunnet J. F., Mikolajczyk M. (1998) Arsenic and Old Mustard : Chemical problems in the desctruction of old arsenical and « Mustard » munitions ; NATO ASI Series 1. Disarmament Technology; Springer: Berlin 1998, Vol. 19.

Burgin, A. J., and Hamilton, S. K. (2007). Have we overemphasized the role of denitrification in aquatic ecosystems? A review of nitrate removal pathways. Frontiers in Ecology and the Environment, *5*(2), 89-96.

C

Catrouillet, C., Davranche, M., Dia, A., Bouhnik-Le Coz, M., Marsac, R., Pourret, O., and Gruau, G. (2014). Geochemical modeling of Fe(II) binding to humic and fulvic acids. Chemical Geology *372*, 109–118.

Catrouillet, C., Davranche, M., Dia, A., Bouhnik-Le Coz, M., Pédrot, M., Marsac, R., and Gruau, G. (2015). Thiol groups controls on arsenite binding by organic matter: New experimental and modeling evidence. Journal of Colloid and Interface Science *460*, 310–320.

Catrouillet, C., Davranche, M., Dia, A., Bouhnik-Le Coz, M., Demangeat, E., and Gruau, G. (2016). Does As III interact with Fe(II), Fe(III) and organic matter through ternary complexes? Journal of Colloid and Interface Science *470*, 153–161.

Certini, G., Scalenghe, R., and Woods, W.I. (2013). The impact of warfare on the soil environment. Earth-Science Reviews *127*, 1–15.

Challan-Belval, S., Garnier, F., Michel, C., Chautard, S., Breeze, D., and Garrido, F. (2009). Enhancing pozzolana colonization by As III-oxidizing bacteria for bioremediation purposes. Applied Microbiology and Biotechnology *84*, 565–573.

Chow, A.T., Tanji, K.K., Gao, S., and Dahlgren, R.A. (2006). Temperature, water content and wet–dry cycle effects on DOC production and carbon mineralization in agricultural peat soils. Soil Biology and Biochemistry *38*, 477–488.

Contin, M., Mondini, C., Leita, L., and De Nobili, M. (2007). Enhanced soil toxic metal fixation in iron (hydr) oxides by redox cycles. Geoderma, *140*(1), 164-175.

Couture, R.-M., Charlet, L., Markelova, E., Madé, B., and Parsons, C.T. (2015). On–off mobilization of contaminants in soils during redox oscillations. Environmental Science and Technology *49*, 3015–3023.

Cullen, W.R., and Reimer, K.J. (1989). Arsenic speciation in the environment. Chemical Reviews *89*, 713–764.

D

Daus, B., Hempel, M., Wennrich, R., and Weiss, H. (2010). Concentrations and speciation of arsenic in groundwater polluted by warfare agents. Environmental Pollution *158*, 3439–3444.

Davis, J. A. (1984). Complexation of trace metals by adsorbed natural organic matter. Geochimica et Cosmochimica Acta, *48*(4), 679-691.

Davis, J.A., and Leckie, J.O. (1978). Effect of adsorbed complexing ligands on trace metal uptake by hydrous oxides. Environmental Science & Technology *12*, 1309–1315.

Disnar, J.R., Guillet, B., Keravis, D., Di-Giovanni, C., and Sebag, D. (2003). Soil organic matter (SOM) characterization by Rock-Eval pyrolysis: scope and limitations. Organic Geochemistry *34*, 327–343.

Dixit, S., and Hering, J.G. (2003). Comparison of arsenic(V) and arsenic(III) sorption onto iron oxide minerals: implications for arsenic mobility. Environmental Science and Technology *37*, 4182–4189.

Dombrowski, P.M., Long, W., Farley, K.J., Mahony, J.D., Capitani, J.F., and Di Toro, D.M. (2005). Thermodynamic analysis of arsenic methylation. Environmental Science & Technology *39*, 2169–2176.

Dong, D., Ohtsuka, T., Dong, D.T., and Amachi, S. (2014). Arsenite oxidation by a facultative chemolithoautotrophic *Sinorhizobium* sp. KGO-5 isolated from arsenic-contaminated soil. Bioscience, Biotechnology, and Biochemistry *78*, 1963–1970.

Drahota, P., and Filippi, M. (2009). Secondary arsenic minerals in the environment: A review. Environment International *35*, 1243–1255.

Dutra, A.J.B., Paiva, P.R.P., and Tavares, L.M. (2006). Alkaline leaching of zinc from electric arc furnace steel dust. Minerals Engineering *19*, 478–485.

E

Egli, M., Sartori, G., Mirabella, A., Giaccai, D., Favilli, F., Scherrer, D., Krebs, R., and Delbos, E. (2010). The influence of weathering and organic matter on heavy metals lability in silicatic, Alpine soils. Science of The Total Environment *408*, 931–946.

F

Farrell, M., and Jones, D.L. (2010). Use of composts in the remediation of heavy metal contaminated soil. Journal of Hazardous Materials *175*, 575–582.

Fazzolari, É., Nicolardot, B., and Germon, J.C. (1998). Simultaneous effects of increasing levels of glucose and oxygen partial pressures on denitrification and dissimilatory nitrate reduction to ammonium in repacked soil cores. European Journal of Soil Biology *34*, 47–52.

Fierer, N., and Schimel, J.P. (2002). Effects of drying–rewetting frequency on soil carbon and nitrogen transformations. Soil Biology and Biochemistry *34*, 777–787.

Fierer, N., Schimel, J.P., and Holden, P.A. (2003). Influence of drying-rewetting frequency on soil bacterial community structure. Microbial Ecology *45*, 63–71.

Fisher, G.L., Prentice, B.A., Silberman, D., Ondov, J.M., Biermann, A.H., Ragaini, R.C., and McFarland, A.R. (1978). Physical and morphological studies of size-classified coal fly ash. Environmental Science and Technology *12*, 447–451.

Flemming, C. A., and Trevors, J. T. (1989). Copper toxicity and chemistry in the environment: a review. Water, Air, & Soil Pollution *44*, 143-158.

Förstner, U., 1985. Chemicals forms and reactivities of metals in sediments. In: Chemical methods for assessing bioavailable metals in sludges and soil. Lescher, R., Davis, R.D., L'Hermite, P., CEC, Elsevier Applied Science publishers, 1-30.

Franz, A., Burgstaller, W., and Schinner, F. (1991). Leaching with Penicillium simplicissimum: influence of metals and buffers on proton extrusion and citric acid production. Applied and Environmental Microbiology, *57*(3), 769-774.

G

Gadd, G.M., and White, C. (1985). Copper uptake by Penicillium ochro-chloron: Influence of ph on toxicity and demonstration of energy-dependent copper influx using protoplasts. Microbiology *131*, 1875–1879.

Garnaga, G., Wyse, E., Azemard, S., Stankevičius, A., and de Mora, S. (2006). Arsenic in sediments from the southeastern Baltic Sea. Environmental Pollution *144*, 855–861.

Gihring, T.M., and Banfield, J.F. (2001). Arsenite oxidation and arsenate respiration by a new Thermus isolate. FEMS Microbiology Letters *204*, 335–340.

Gomez, E., Ferreras, L., and Toresani, S. (2006). Soil bacterial functional diversity as influenced by organic amendment application. Bioresource Technology *97*, 1484–1489.

Griffith, S. M., and Schnitzer, M. (1976). The alkaline cupric oxide oxidation of humic and fulvic acids extracted from tropical volcanic soils. Soil Science,*122*(4), 191-201.

Grybos, M., Davranche, M., Gruau, G., and Petitjean, P. (2007). Is trace metal release in wetland soils controlled by organic matter mobility or Fe-oxyhydroxides reduction? Journal of Colloid and Interface Science *314*, 490–501.

Gupta, V.K., Saini, V.K., and Jain, N. (2005). Adsorption of As III from aqueous solutions by iron oxide-coated sand. Journal of Colloid and Interface Science *288*, 55–60.

H

Haffert, L., Craw, D., and Pope, J. (2010). Climatic and compositional controls on secondary arsenic mineral formation in high-arsenic mine wastes, South Island, New Zealand. New Zealand Journal of Geology and Geophysics *53*, 91–101.

Hall, G.E.M., Vaive, J.E., Beer, R., and Hoashi, M. (1996). Selective leaches revisited, with emphasis on the amorphous Fe oxyhydroxide phase extraction. Journal of Geochemical Exploration *56*, 59–78.

Hantke, K. (2005). Bacterial zinc uptake and regulators. Current Opinion in Microbiology *8*, 196–202.

Harada, N., Takagi, K., Baba, K., Fujii, K., and Iwasaki, A. (2010). Biodegradation of diphenylarsinic acid to arsenic acid by novel soil bacteria isolated from contaminated soil. Biodegradation *21*, 491–499.

Hattab, N., Motelica-Heino, M., Faure, O., and Bouchardon, J.-L. (2015). Effect of fresh and mature organic amendments on the phytoremediation of technosols contaminated with high concentrations of trace elements. Journal of Environmental Management *159*, 37–47.

Hirsch, R.M., Slack, J.R., and Smith, R.A. (1982). Techniques of trend analysis for monthly water quality data. Water Resources Research *18*, 107–121.

Hirsch, R.M., and Slack, J.R. (1984). A nonparametric trend test for seasonal data with serial dependence. Water Resources Research *20*, 727–732.

Hoeft, S.E., Blum, J.S., Stolz, J.F., Tabita, F.R., Witte, B., King, G.M., Santini, J.M., and Oremland, R.S. (2007). Alkalilimnicola ehrlichii sp. nov., a novel, arsenite-oxidizing

haloalkaliphilic gammaproteobacterium capable of chemoautotrophic or heterotrophic growth with nitrate or oxygen as the electron acceptor. International Journal of Systematic and Evolutionary Microbiology *57*, 504–512.

Hoffmann, M., Mikutta, C., and Kretzschmar, R. (2013). Arsenite binding to natural organic matter: Spectroscopic evidence for ligand exchange and ternary complex formation. Environmental Science and Technology *47*, 12165–12173.

Horemans, B., Vandermaesen, J., Smolders, E., and Springael, D. (2013). Cooperative dissolved organic carbon assimilation by a linuron-degrading bacterial consortium. FEMS Microbiology Ecology *84*, 35–46.

Hua, L., Wu, W., Liu, Y., McBride, M.B., and Chen, Y. (2009). Reduction of nitrogen loss and Cu and Zn mobility during sludge composting with bamboo charcoal amendment. Environmental Science and Pollution Research *16*, 1–9.

Huang, H., Jia, Y., Sun, G.-X., and Zhu, Y.-G. (2012). Arsenic speciation and volatilization from flooded paddy soils amended with different organic matters. Environmental Science and Technology *46*, 2163–2168.

Hubé, D. (2013). Potentialités d'un marquage des eaux souterraines par des substances pyrotechniques en relation avec les zones de combats de la première guerre mondiale – Le cas des perchlorates. Rapport final. BRGM/RP-62008-FR. 26p.

Hubé, D. (2016,). Sur les traces d'un secret enfoui : Enquête sur l'héritage toxique de la Grande Guerre, Michallon.

Huot, H., Séré, G., Charbonnier, P., Simonnot, M.-O., and Morel, J.L. (2015). Lysimeter monitoring as assessment of the potential for revegetation to manage former iron industry settling ponds. Science of The Total Environment *526*, 29–40.

Hupy, J.P., and Schaetzl, R.J. (2008). Soil development on the WWI battlefield of Verdun, France. Geoderma *145*, 37–49.

I

Inskeep, W. P., Macur, R. E., Hamamura, N. H., Warelow, T. P., Ward, S. A., Santini, J. M. (2007). Detection, diversity and expression of aerobic bacterial arsenite oxidase genes. Environmental Microbiology *9*, 934-943.

J

Johnson, D.B., Ghauri, M.A., and McGinness, S. (1993). Biogeochemical cycling of iron and sulphur in leaching environments. FEMS Microbiology Reviews *11*, 63–70.

Jones, D. L. (1998). Organic acids in the rhizosphere–a critical review. Plant and soil, *205*(1), 25-44.

Jong, T., and Parry, D.L. (2003). Removal of sulfate and heavy metals by sulfate reducing bacteria in short-term bench scale upflow anaerobic packed bed reactor runs. Water Research *37*, 3379–3389.

Juillot, F. (1998). Localisation et spéciation de l'arsenic, du plomb et du zinc dans des sites et sols contaminés. Comparaison avec un sol développé sur une anomalie géochimique naturelle en plomb (Doctoral dissertation).

Juillot, F., Morin, G., Ildefonse, P., Trainor, T.P., Benedetti, M., Galoisy, L., Calas, G., and Brown, G.E. (2003). Occurrence of Zn/Al hydrotalcite in smelter-impacted soils from northern France: Evidence from EXAFS spectroscopy and chemical extractions. American Mineralogist *88*, 509–526.

K

Kabata-Pendias, A. (2010). Trace elements in soils and plants. CRC press.

Karg, F. (2002). Sites pollués par les armes chimiques : Impact des contaminations graves oubliées et redécouvertes. Environnement & Technique *219*, 27–32.

Keiluweit, M., Nico, P.S., Johnson, M.G., and Kleber, M. (2010). Dynamic molecular structure of plant biomass-derived black carbon (biochar). Environmental Science & Technology *44*, 1247–1253.

Kendall M. G., Rank Correlation Methods, Griffin, London (1948).

Kim, M.-J. (2001). Separation of inorganic arsenic species in groundwater using ion exchange method. Bulletin of Environmental Contamination and Toxicology *67*, 0046–0051.

Koranda, M., Kaiser, C., Fuchslueger, L., Kitzler, B., Sessitsch, A., Zechmeister-Boltenstern, S., and Richter, A. (2014). Fungal and bacterial utilization of organic substrates depends on substrate complexity and N availability. FEMS Microbiology Ecology *87*, 142–152.

Kumar, M., and Khanna, S. (2010). Diversity of 16S rRNA and dioxygenase genes detected in coal-tar-contaminated site undergoing active bioremediation. Journal of Applied Microbiology *108*, 1252–1262.

Kumar, N., Millot, R., Battaglia-Brunet, F., Négrel, P., Diels, L., Rose, J., and Bastiaens, L. (2013). Sulfur and oxygen isotope tracing in zero valent iron based In situ remediation system for metal contaminants. Chemosphere *90*, 1366–1371.

Kumpiene, J., Ragnvaldsson, D., Lövgren, L., Tesfalidet, S., Gustavsson, B., Lättström, A., Leffler, P., and Maurice, C. (2009). Impact of water saturation level on arsenic and metal mobility in the Fe-amended soil. Chemosphere *74*, 206–215.

L

Lawrence, M.J., Stemberger, H.L.J., Zolderdo, A.J., Struthers, D.P., and Cooke, S.J. (2015). The effects of modern war and military activities on biodiversity and the environment. Environmental Reviews *23*, 443–460.

Le Forestier, L., and Libourel, G. (1998) Characterization of flue gas residues from municipal solid waste combustors. Environmental Science and Technology *32*, 2250-2256.

Lescure, T., Moreau, J., Charles, C., Ben Ali Saanda, T., Thouin, H., Pillas, N., Bauda, P., Lamy, I., and Battaglia-Brunet, F. (2016). Influence of organic matters on AsIII oxidation by the microflora of polluted soils. Environmental Geochemistry and Health *38*, 911–925.

Ludemann, H., Arth, I., and Liesack, W. (2000). Spatial changes in the bacterial community structure along a vertical oxygen gradient in flooded paddy soil cores. Applied and Environmental Microbiology *66*, 754–762.

Lundquist, E., Jackson, L., and Scow, K. (1999a). Wet–dry cycles affect dissolved organic carbon in two California agricultural soils. Soil Biology and Biochemistry *31*, 1031–1038.

Lundquist, E.., Scow, K.., Jackson, L.., Uesugi, S.., and Johnson, C.. (1999b). Rapid response of soil microbial communities from conventional, low input, and organic farming systems to a wet/dry cycle. Soil Biology and Biochemistry *31*, 1661–1675.

M

Macy, J.M., Nunan, K., Hagen, K.D., Dixon, D.R., Harbour, P.J., Cahill, M., and Sly, L.I. (1996). Chrysiogenes arsenatis gen. nov., sp. nov., a new arsenate-respiring bacterium isolated from gold mine wastewater. International Journal of Systematic Bacteriology *46*, 1153–1157.

Macy, J.M., Santini, J.M., Pauling, B.V., O'Neill, A.H., and Sly, L.I. (2000). Two new arsenate/sulfate-reducing bacteria: mechanisms of arsenate reduction. Archives of Microbiology *173*, 49–57.

Maejima, Y., Arao, T., and Baba, K. (2011). Transformation of diphenylarsinic acid in agricultural soils. Journal of Environment Quality *40*, 76.

Magalhâces, M.C.F., Pedrosa De Jesus, J.D., and Williams, P.A. (1988). The chemistry of formation of some secondary arsenate minerals of Cu(II), Zn(II) and Pb(II). Mineralogical Magazine *52*, 679-690.

Magalhães, M.C.F., and Silva, M.C.M. (2003). Stability of lead(II) arsenates. Monatshefte Für Chemie / Chemical Monthly *134*, 735–743.

Malasarn, D., Keeffe, J.R., and Newman, D.K. (2008). Characterization of the arsenate respiratory reductase from shewanella sp. Strain ANA-3. Journal of Bacteriology *190*, 135–142.

Mamindy-Pajany, Y., Bataillard, P., Séby, F., Crouzet, C., Moulin, A., Guezennec, A.-G., Hurel, C., Marmier, N., and Battaglia-Brunet, F. (2013). Arsenic in marina sediments from the mediterranean coast: speciation in the solid phase and occurrence of thioarsenates. Soil and Sediment Contamination: An International Journal *22*, 984–1002.

Manceau, A., Marcus, M. A., and Tamura, N. (2002). Quantitative speciation of heavy metals in soils and sediments by synchrotron X-ray techniques.Reviews in Mineralogy and Geochemistry, 49(1), 341-428.

Mann H.B. (1945) Nonparametric tests against trend, Econometrica *13*, 245–259

Marvin-Sikkema, F.D., and de Bont, J.A.M. (1994). Degradation of nitroaromatic compounds by microorganisms. Applied Microbiology and Biotechnology *42*, 499–507.

Masscheleyn, P.H., Delaune, R.D., and Patrick, W.H. (1991). Effect of redox potential and pH on arsenic speciation and solubility in a contaminated soil. Environmental Science and Technology *25*, 1414–1419.

Matousek J. (1997) Chemical weapon production in former Czechoslovakia. In T. Stock and K. Lohs (Eds) The Challenge of old chemical munitions and toxic armaments wastes. Oxford University Press.

McBride, M.B. (2003). Toxic metals in sewage sludge-amended soils: has promotion of beneficial use discounted the risks? Advances in Environmental Research *8*, 5–19.

McGrath, S. P., Zhao, F. J., and Lombi, E. (2001). Plant and rhizosphere processes involved in phytoremediation of metal-contaminated soils. Plant and soil, *232*(1-2), 207-214.

Meerschman, E., Cockx, L., Islam, M.M., Meeuws, F., and Van Meirvenne, M. (2011). Geostatistical assessment of the impact of World War I on the spatial occurrence of soil heavy metals. AMBIO *40*, 417–424.

Meier, C.L., and Bowman, W.D. (2010). Chemical composition and diversity influence non-additive effects of litter mixtures on soil carbon and nitrogen cycling: Implications for plant species loss. Soil Biology and Biochemistry *42*, 1447–1454.

Merritt, K.A., and Erich, M.S. (2003). Influence of organic matter decomposition on soluble carbon and its copper-binding capacity. Journal of Environment Quality *32*, 2122.

Mestrot, A., Uroic, M.K., Plantevin, T., Islam, M.R., Krupp, E.M., Feldmann, J., and Meharg, A.A. (2009). Quantitative and qualitative trapping of arsines deployed to assess loss of

volatile arsenic from paddy Soil. Environmental Science & Technology *43*, 8270–8275.

Metting, F. B., *(ed) (*1993*)* Structure and physiological ecology of soil microbial communities. Soil Microbial Ecology - Application in Agricultural and Environmental Management. pp. 3–24. Marcel Dekker, New York.

Mikha, M.M., Rice, C.W., and Milliken, G.A. (2005). Carbon and nitrogen mineralization as affected by drying and wetting cycles. Soil Biology and Biochemistry *37*, 339–347.

Moldrup, P., Olesen, T., Komatsu, T., Schjønning, P., and Rolston, D.E. (2001). Tortuosity, diffusivity, and permeability in the soil liquid and gaseous phases. Soil Science Society of America Journal *65*, 613.

Morin, G., Juillot, F., Ildefonse, P., Calas, G., Samama, J.-C., Chevallier, P., and Brown, G.E. (2001). Mineralogy of lead in a soil developed on a Pb-mineralized sandstone (Largentière, France). American Mineralogist *86*, 92–104.

Morin, G., Lecocq, D., Juillot, F., Calas, G., Ildefonse, P., Belin, S., and Borensztajn, S. (2002). EXAFS evidence of sorbed arsenic V and pharmacosiderite in a soil overlying the Echassières geochemical anomaly, Allier, France. Bulletin de la Société Géologique de France *173*, 281-291.

Morin, G., and Calas, G. (2006). Arsenic in soils, mine tailings, and former industrial sites. Elements *2*, 97–101.

Moyano, F.E., Manzoni, S., and Chenu, C. (2013). Responses of soil heterotrophic respiration to moisture availability: An exploration of processes and models. Soil Biology and Biochemistry *59*, 72–85.

Murayama, N., Yamamoto, H., and Shibata, J. (2002). Mechanism of zeolite synthesis from coal fly ash by alkali hydrothermal reaction. International Journal of Mineral Processing *64*, 1–17.

N

Nakamiya, K., Nakayama, T., Ito, H., Edmonds, J.S., Shibata, Y., and Morita, M. (2007). Degradation of arylarsenic compounds by microorganisms. FEMS Microbiology Letters *274*, 184–188.

O

Ona-Nguema, G., Morin, G., Juillot, F., Calas, G., and Brown, G.E. (2005). EXAFS analysis of arsenite adsorption onto two-line ferrihydrite, hematite, goethite, and lepidocrocite. Environmental Science & Technology *39*, 9147–9155.

P

Park, J.H., Lamb, D., Paneerselvam, P., Choppala, G., Bolan, N., and Chung, J.-W. (2011). Role of organic amendments on enhanced bioremediation of heavy metal(loid) contaminated soils. Journal of Hazardous Materials *185*, 549–574.

Parsons, C.T., Couture, R.-M., Omoregie, E.O., Bardelli, F., Greneche, J.-M., Roman-Ross, G., and Charlet, L. (2013). The impact of oscillating redox conditions: Arsenic immobilisation in contaminated calcareous floodplain soils. Environmental Pollution *178*, 254–263.

Pérez-de-Mora, A., Burgos, P., Madejón, E., Cabrera, F., Jaeckel, P., and Schloter, M. (2006). Microbial community structure and function in a soil contaminated by heavy metals: effects of plant growth and different amendments. Soil Biology and Biochemistry *38*, 327–341.

Pierce, M.L., and Moore, C.B. (1982). Adsorption of arsenite and arsenate on amorphous iron hydroxide. Water Research *16*, 1247–1253.

Pietikainen, J., Kiikkila, O., and Fritze, H. (2000). Charcoal as a habitat for microbes and its effect on the microbial community of the underlying humus. Oikos *89*, 231–242.

Pisciella, P., Crisucci, S., Karamanov, A., and Pelino, M. (2001). Chemical durability of glasses obtained by vitrification of industrial wastes. Waste Management *21*, 1–9.

Puziewicz, J., Zainoun, K., and Bril, H. (2007). Primary phases in pyrometallurgical slags from a zinc-smelting waste dump, swietochlowice, upper silesia, poland. The Canadian Mineralogist *45*, 1189–1200.

Q

Quéméneur, M., Cebron, A., Billard, P., Battaglia-Brunet, F., Garrido, F., Leyval, C., and Joulian, C. (2010). Population structure and abundance of arsenite-oxidizing bacteria along an arsenic pollution gradient in waters of the upper Isle river basin, France. Applied and Environmental Microbiology *76*, 4566–4570.

Querol, X., Moreno, N., Umaña, J., Alastuey, A., Hernández, E., López-Soler, A., and Plana, F. (2002). Synthesis of zeolites from coal fly ash: an overview. International Journal of Coal Geology *50*, 413–423.

R

Radu, T., Subacz, J.L., Phillippi, J.M., and Barnett, M.O. (2005). Effects of dissolved carbonate on arsenic adsorption and mobility. Environmental Science and Technology *39*, 7875–7882.

Redman, A.D., Macalady, D.L., and Ahmann, D. (2002). Natural organic matter affects arsenic speciation and sorption onto hematite. Environmental Science and Technology *36*, 2889–2896.

Rey, A., Petsikos, C., Jarvis, P.G., and Grace, J. (2005). Effect of temperature and moisture on rates of carbon mineralization in a Mediterranean oak forest soil under controlled and field conditions. European Journal of Soil Science *56*, 589–599.

S

Saada, A., Breeze, D., Crouzet, C., Cornu, S., and Baranger, P. (2003). Adsorption of arsenic V on kaolinite and on kaolinite–humic acid complexes. Chemosphere *51*, 757–763.

Saenger, A., Cécillon, L., Poulenard, J., Bureau, F., De Daniéli, S., Gonzalez, J.-M., and Brun, J.-J. (2015). Surveying the carbon pools of mountain soils: A comparison of physical fractionation and Rock-Eval pyrolysis. Geoderma *241–242*, 279–288.

Santini, J.M., Sly, L.I., Schnagl, R.D., and Macy, J.M. (2000). A new chemolithoautotrophic arsenite-oxidizing bacterium isolated from a gold mine: phylogenetic, physiological, and preliminary biochemical studies. Applied and Environmental Microbiology *66*, 92–97.

Santini, J.M., and vanden Hoven, R.N. (2004). Molybdenum-Containing Arsenite Oxidase of the Chemolithoautotrophic Arsenite Oxidizer NT-26. Journal of Bacteriology *186*, 1614–1619.

Sauvé, S., McBride, M.B., and Hendershot, W.H. (1997). Speciation of lead in contaminated soils. Environmental Pollution *98*, 149–155.

Sayer, J.A., Cotter-Howells, J.D., Watson, C., Hillier, S., and Gadd, G.M. (1999). Lead mineral transformation by fungi. Current Biology *9*, 691–694.

Schmidt, M. W., and Noack, A. G. (2000). Black carbon in soils and sediments: analysis, distribution, implications, and current challenges. Global biogeochemical cycles, *14*(3), 777-793.

Schneider, M.P.W., Hilf, M., Vogt, U.F., and Schmidt, M.W.I. (2010). The benzene polycarboxylic acid (BPCA) pattern of wood pyrolyzed between 200°C and 1000°C. Organic Geochemistry *41*, 1082–1088.

Schwab, P., Zhu, D., and Banks, M.K. (2007). Heavy metal leaching from mine tailings as affected by organic amendments. Bioresource Technology *98*, 2935–2941.

Seignez, N., Gauthier, A., Bulteel, D., Buatier, M., Recourt, P., Damidot, D., and Potdevin, J.L. (2007). Effect of Pb-rich and Fe-rich entities during alteration of a partially vitrified metallurgical waste. Journal of Hazardous Materials *149*, 418–431.

Shibu, M.E., Leffelaar, P.A., Van Keulen, H., and Aggarwal, P.K. (2006). Quantitative description of soil organic matter dynamics—A review of approaches with reference to rice-based cropping systems. Geoderma *137*, 1–18.

Shigemoto, N., Hayashi, H., and Miyaura, K. (1993). Selective formation of Na-X zeolite from coal fly ash by fusion with sodium hydroxide prior to hydrothermal reaction. Journal of Materials Science *28*, 4781–4786.

Sidenko, N., Gieré, R., Bortnikova, S., Cottard, F., and Pal'chik, N. (2001). Mobility of heavy metals in self-burning waste heaps of the zinc smelting plant in Belovo (Kemerovo Region, Russia). Journal of Geochemical Exploration *74*, 109–125.

Silver, S. (1996). Bacterial resistances to toxic metal ions - a review. Gene *179*, 9–19.

Smedley, P., and Kinniburgh, D. (2002). A review of the source, behaviour and distribution of arsenic in natural waters. Applied Geochemistry *17*, 517–568.

Smith, A. H., Hopenhayn-Rich, C., Bates, M. N., Goeden, H. M., Hertz-Picciotto, I., Duggan, H. M., and Smith, M. T. (1992). Cancer risks from arsenic in drinking water. Environmental health perspectives, *97*, 259.

Smith, A.S., and Jacinthe, P.-A. (2014). A mesocosm study of the effects of wet–dry cycles on nutrient release from constructed wetlands in agricultural landscapes. Environ. Sci.: Processes Impacts *16*, 106–115.

Spain, J.C. (1995). Bacterial degradation of nitroaromatic compounds under aerobic conditions. In Biodegradation of Nitroaromatic Compounds, J.C. Spain, ed. (Boston, MA: Springer US), pp. 19–35.

Sposito, G., Skipper, N.T., Sutton, R., Park, S. -h., Soper, A.K., and Greathouse, J.A. (1999). Surface geochemistry of the clay minerals. Proceedings of the National Academy of Sciences *96*, 3358–3364.

Stolz, J., Basu, P., and Oremland, R. (2002). Microbial transformation of elements: the case of arsenic and selenium. International Microbiology *5*, 201–207.

Strickland, M.S., and Rousk, J. (2010). Considering fungal:bacterial dominance in soils – Methods, controls, and ecosystem implications. Soil Biology and Biochemistry *42*, 1385–1395.

Swallow, K.C., Hume, D.N., and Morel, F.M.M. (1980). Sorption of copper and lead by hydrous ferric oxide. Environmental Science and Technology *14*, 1326–1331.

T

Takeno, N. (2005). Atlas of Eh-pH diagrams. Geological survey of Japan open file report, 419, 102.

Tebo, B.M., and Obraztsova, A.Y. (1998). Sulfate-reducing bacterium grows with Cr(VI), U(VI), Mn(IV), and Fe(III) as electron acceptors. FEMS Microbiology Letters *162*, 193–198.

Thouin, H., Le Forestier, L., Gautret, P., Hube, D., Laperche, V., Dupraz, S., and Battaglia-Brunet, F. (2016). Characterization and mobility of arsenic and heavy metals in soils polluted by the destruction of arsenic-containing shells from the Great War. Science of The Total Environment *550*, 658–669.

Thouin, H., Battaglia-Brunet, F., Gautret, P., Le Forestier, L., Breeze, D., Seby, F., Norini, M.P., and Dupraz, S. Effect of saturation/desaturation cycles and input of natural organic matter on C, N, As and metal biogeocycles in a chemical warfare agents burning impacted soil: a mesocosm study. Submitted.

Tiedje, J. M. (1988). Ecology of denitrification and dissimilatory nitrate reduction to ammonium. Biology of anaerobic microorganisms, *717*, 179-244.

Tiedje, J.M., Asuming-Brempong, S., Nüsslein, K., Marsh, T.L., and Flynn, S.J. (1999). Opening the black box of soil microbial diversity. Applied Soil Ecology *13*, 109–122.

Tipping, E. (1998). Humic ion-binding model VI: an improved description of the interactions of protons and metal ions with humic substances. Aquatic geochemistry, *4*(1), 3-47.

Tsutsuki, K., and Kuwatsuka, S. (1978). Chemical studies on soil humic acids: II. Composition of oxygen-containing functional groups of humic acids. Soil Science and Plant Nutrition *24*, 547–560.

Tucker, M.D., Barton, L.L., and Thomson, B.M. (1998). Reduction of Cr, Mo, Se and U by Desulfovibrio desulfuricans immobilized in polyacrylamide gels. Journal of Industrial Microbiology and Biotechnology *20*, 13–19.

Tufano, K.J., Reyes, C., Saltikov, C.W., and Fendorf, S. (2008). Reductive processes controlling arsenic retention: revealing the relative importance of iron and arsenic reduction. Environmental Science and Technology *42*, 8283–8289.

Twidwell, L.G., Plessas, K.O., Comba, P.G., and Dahnke, D.R. (1994). Removal of arsenic from wastewaters and stabilization of arsenic bearing waste solids: Summary of experimental studies. Journal of Hazardous Materials *36*, 69–80.

V

Van Meirvenne, M., Meklit, T., Verstraete, S., De Boever, M., and Tack, F. (2008). Could shelling in the First World War have increased copper concentrations in the soil around Ypres? European Journal of Soil Science *59*, 372–379.

Vega, F.A., Covelo, E.F., VÁZquez, J.J., and Andrade, L. (2007). Influence of mineral and organic components on copper, lead, and zinc sorption by acid soils. Journal of Environmental Science and Health, Part A *42*, 2167–2173.

Vereš, J. (2014). Determination of zinc speciation in metallurgical wastes by various analytical methods. International Journal, *5*(5).

Violante, A., and Pigna, M. (2002). Competitive sorption of arsenate and phosphate on different clay minerals and soils. Soil Science Society of America Journal *66*, 1788.

Vodyanitskii, Y. N. (2010). Zinc forms in soils (Review of publications). Eurasian Soil Science, *43*(3), 269-277.

Vulkan, R., Zhao, F., Barbosa-Jefferson, V., Preston, S., Paton, G.I., Tipping, E., and McGrath, S.P. (2000). Copper speciation and impacts on bacterial biosensors in the pore water of copper-contaminated soils. Environmental Science and Technology *34*, 5115–5121.

W

Wang, C.-H., Hsiao, C.K., Chen, C.-L., Hsu, L.-I., Chiou, H.-Y., Chen, S.-Y., Hsueh, Y.-M., Wu, M.-M., and Chen, C.-J. (2007). A review of the epidemiologic literature on the role of environmental arsenic exposure and cardiovascular diseases. Toxicology and Applied Pharmacology *222*, 315–326.

Weber, F.-A., Hofacker, A.F., Voegelin, A., and Kretzschmar, R. (2010). Temperature dependence and coupling of iron and arsenic reduction and release during flooding of a contaminated soil. Environmental Science and Technology *44*, 116–122.

Wershaw, R. L., Leenheer, J. A., Kennedy, K. R., and Noyes, T. I. (1996). Use of 13c nmr and ftir for elucidation of degradation pathways during natural litter decomposition and composting i. Early stage leaf degradation. Soil science, *161*(10), 667-679.

Wickham, H. (2009). ggplot2: elegant graphics for data analysis. Springer Science & Business Media.

Wolf, M., Lehndorff, E., Wiesenberg, G.L.B., Stockhausen, M., Schwark, L., and Amelung, W. (2013). Towards reconstruction of past fire regimes from geochemical analysis of charcoal. Organic Geochemistry *55*, 11–21.

World Health Organization (1993) Guidelines for drinking water quality. World Health Organization. Geneva. P-41

World Health Organization. (2011). Guidelines for drinking-water quality. World health organization, Geneva, p.135.

Y

Yamamura, S., Watanabe, M., Yamamoto, N., Sei, K., and Ike, M. (2009). Potential for microbially mediated redox transformations and mobilization of arsenic in uncontaminated soils. Chemosphere *77*, 169–174.

Yang, J.Y., Yang, X.E., He, Z.L., Li, T.Q., Shentu, J.L., and Stoffella, P.J. (2006). Effects of pH, organic acids, and inorganic ions on lead desorption from soils. Environmental Pollution *143*, 9–15.

Z

Zobrist, J., Dowdle, P.R., Davis, J.A., and Oremland, R.S. (2000). Mobilization of arsenite by dissimilatory reduction of adsorbed arsenate. Environmental Science and Technology *34*, 4747–4753.

Liste des Figures

Liste des tables et tableaux

Valorisation scientifique des travaux

Article dans un journal avec comité de lecture

Lescure, T., Moreau, J., Charles, C., Ben Ali Saanda, T., Thouin, H., Pillas, N., Bauda, P., Lamy, I., et Battaglia-Brunet, F. (2016). Influence of organic matters on AsIII oxidation by the microflora of polluted soils. Environmental Geochemistry and Health *38*, 911–925.

Thouin, H., Le Forestier, L., Gautret, P., Hube, D., Laperche, V., Dupraz, S., et Battaglia-Brunet, F. (2016). Characterization and mobility of arsenic and heavy metals in soils polluted by the destruction of arsenic-containing shells from the Great War. Science of The Total Environment *550*, 658–669.

Communications en congrès

Thouin, H., Lescure, T., Gautret, P., Joulian, C., Le Milbeau, C., & Battaglia-Brunet, F. (2014, June). Influence of organic matter and microbial activities on the mobility of arsenic and metals in polluted soils. In *Biogeochemical Processes at Air-Soil-Water Interfaces and Environmental Protection*. (communication orale)

Thouin, H., Lescure, T., Gautret, P., Joulian, C., Le Milbeau, C., Dupraz, S., & Battaglia-Brunet, F. (2014, October). Influence de la matière organique et de l'activité bactérienne sur la mobilité de l'arsenic et des métaux dans des sols pollués. In *24ème Réunion des Sciences de la Terre*. (communication orale)

Thouin, H., Battaglia-Brunet, F., Le Forestier, L., Hube, D., Dupraz, S., et Gautret, P. (2015, September). Arsenic speciation related to mineral and microbial context in a soil polluted by the destruction of arsenical shells from the Great War. In *22nd International Symposium on Environmental Biogeochemistry*. (communication orale)

Thouin, H., Le Forestier, L., Gautret, P., Dupraz, S., Hube, D., & Battaglia-Brunet, F. (2016, June). Detection and quantification of As (III)-oxidizing microbes in soils highly polluted by breaking-down of old chemical ammunition during inter-war. In *Arsenic Research and Global Sustainability: Proceedings of the Sixth International Congress on Arsenic in the Environment (As2016), June 19-23, 2016, Stockholm, Sweden* (p. 111). CRC Press. (communication orale)

Annexe 1

Science of the Total Environment 550 (2016) 658–669

Contents lists available at ScienceDirect

Science of the Total Environment

journal homepage: www.elsevier.com/locate/scitotenv

Characterization and mobility of arsenic and heavy metals in soils polluted by the destruction of arsenic-containing shells from the Great War

Hugues Thouin [a,b,c,d,*], Lydie Le Forestier [b,c,d], Pascale Gautret [b,c,d], Daniel Hube [a], Valérie Laperche [a], Sebastien Dupraz [a], Fabienne Battaglia-Brunet [a,b,c,d]

[a] BRGM, 3 avenue Claude Guillemin, 45060 Orléans, France
[b] Université d'Orléans, ISTO, UMR 7327, 45071 Orléans, France
[c] CNRS, ISTO, UMR 7327, 45071 Orléans, France
[d] BRGM, ISTO, UMR 7327, BP 36009, 45060 Orléans, France

HIGHLIGHTS

- Examination of the complex legacy of chemical shell destruction
- Amorphous phase identified as main As, Cu and Zn carrier
- Unexpected mineralogical association observed
- Potential for bacterial As(III) oxidation detected
- As stability driven mainly by adsorption to hydrous ferric oxides (HFO)

GRAPHICAL ABSTRACT

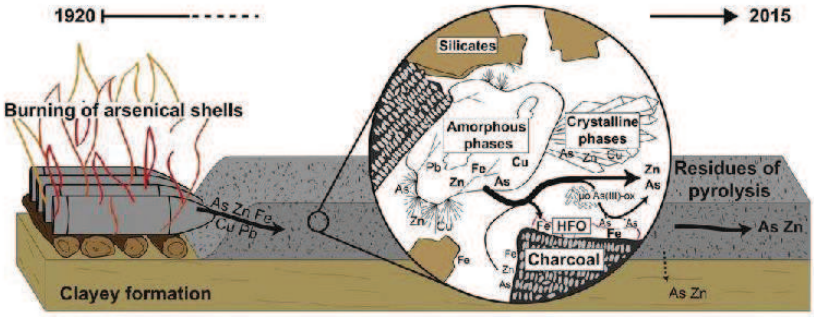

ARTICLE INFO

Article history:
Received 24 December 2015
Accepted 18 January 2016
Available online 2 February 2016

Editor: F.M. Tack

Keywords:
Chemical ammunition destruction
Soil contamination
Metals
Arsenates
Microbial As(III)-oxidation

ABSTRACT

Destruction of chemical munitions from World War I has caused extensive local top soil contamination by arsenic and heavy metals. The biogeochemical behavior of toxic elements is poorly documented in this type of environment. Four soils were sampled presenting different levels of contamination. The range of As concentrations in the samples was 1937–72,820 mg/kg. Concentrations of Zn, Cu and Pb reached 90,190 mg/kg, 9113 mg/kg and 5777 mg/kg, respectively. The high clay content of the subsoil and large amounts of charcoal from the use of firewood during the burning process constitute an ample reservoir of metals and As-binding materials. However, SEM–EDS observations showed different forms of association for metals and As. In metal-rich grains, several phases were identified: crystalline phases, where arsenate secondary minerals were detected, and an amorphous phase rich in Fe, Zn, Cu, and As. The secondary arsenate minerals, identified by XRD, were adamite and olivenite (zinc and copper arsenates, respectively) and two pharmacosiderites. The amorphous material was the principal carrier of As and metals in the central part of the site. This singular mineral assemblage probably resulted from the heat treatment of arsenic-containing shells. Microbial characterization included total cell counts, respiration, and determination of As(III)-oxidizing activities. Results showed the presence of microorganisms actively contributing to metabolism of carbon and arsenic, even in the most polluted soil, thereby influencing the fate of bioavailable As on the site. However, the mobility of As correlated mainly with the availability of iron sinks.

© 2016 Elsevier B.V. All rights reserved.

* Corresponding author at: BRGM, 3 avenue Claude Guillemin, 45060 Orléans, France.

http://dx.doi.org/10.1016/j.scitotenv.2016.01.111
0048-9697/© 2016 Elsevier B.V. All rights reserved.

1. Introduction

Almost 100 years after the end of the First World War the scars of battle can still be observed along the front line. Hupy and Schaetzl (2008) have studied the effect of shelling on soil structure and landscape recovery after the conflict. The First World War was the first incidence of major warfare that made massive use of chemical weapons. However, very little information is available on the chemical impacts of the conflict on soil, groundwater or wildlife. High concentrations of metals in living organisms and the presence of perchlorate in groundwater along the red zone nevertheless reflect a real impact of this war on the environment (Hube, 2013; Prefectoral decree, Pas de Calais, 25 October 2012).

In the early 2000s, several sites where First World War chemical weapons were destroyed were found to be contaminated by inorganic pollutants. Only two of these were investigated: the first is located in Belgium (Bausinger and Preuβ, 2005) and the second is northeast of Verdun, in France (Bausinger et al., 2007). Chemical shells were disposed of by burning on both of these sites during the 1920s. The munitions destroyed were mainly "blue cross shells" containing organoarsenic warfare agents. The Belgian burning ground has since been used for agriculture (Bausinger and Preuβ, 2005) but the French site, named "Place-à-Gaz", has been unaffected by human activities and undisturbed since destruction of the shells.

Bausinger et al. (2007) showed that the "Place-à-Gaz" had locally limited but severe soil contamination by arsenic, zinc, copper and lead, with concentrations reaching respectively 150 g/kg, 130 g/kg, 15 g/kg and 25 g/kg. The metals came from various parts of the munitions. Shells contained mainly iron, while fuses, driving bands and shell casings were made from copper or zinc. Lead was used for shrapnel balls, primary explosives and chemical warfare equipment. "Blue cross shells" were filled with diphenylchloroarsine (Clark I) and diphenylcyanoarsine (Clark II). These organoarsenic molecules were probably oxidized during the combustion, releasing huge amounts of inorganic arsenic into the surrounding environment. Bausinger et al. (2007) estimated that, over a century, most of the arsenic oxides have been transformed into arsenates or sorbed onto iron oxides or clays, abundant in the inherited soil.

The primary factor influencing mobility of heavy metals in these soils appeared to be pH (Bausinger et al., 2007). Under the site conditions, the soil pH varied from 5 to 6, which favored Cu and Pb fixation in soil, while Zn was more mobile and leached. Arsenic was less affected by pH and behaved differently from metals. However, As concentrations in interstitial waters (c_{mean} = 838 μg/L) were significantly higher than the maximum contaminant level (MCL) of arsenic in drinking water as recommended by the World Health Organization (WHO, 1993) in 1993, i.e. 10 μg/L. The mobility of As on the site thus required further investigation.

Arsenic is mainly found in the environment as inorganic species, arsenate As(V) and arsenite As(III) (Cullen and Reimer, 1989). Microbial activities play a major role in As speciation in soil. Different bacterial mechanisms are responsible for As(III) oxidation or As(V) reduction (Santini et al., 2000; Stolz et al., 2002), thus altering As mobility, toxicity and bioavailability (Pierce and Moore, 1982; Masscheleyn et al., 1991). The bacterial activity on former ammunition destruction sites has not been documented to date, but biogeochemistry may explain As speciation and mobility in such environments.

Organic matter, which can have high concentrations in soil (up to 25%), may drive the mobility of metals and arsenic on the site (Bausinger et al., 2007). Indeed, the organic compounds may contain adsorption or complexation sites or induce methylation of metals and metalloids (Saada et al., 2003; Park et al., 2011; Huang et al., 2012). The presence of organic matter also affects bacterial activity. A recent study has shown that As(III)-oxidizing activity in polluted soil can be influenced by the amount of bioavailable organic matter (Lescure et al., in press).

Bausinger et al. (2007) explored the mobility of inorganic pollutants in the "Place-à-Gaz" ground material by sequential extractions. These experiments provided indirect information on the carrier phases but no direct information was available on the mineralogy of soil materials. Moreover, arsenic speciation was not directly determined and no data were available on the activity of microorganisms in this type of heavily polluted soil. Our work focused on the mineralogy, particle size and the geochemistry of the "Place-à-Gaz" surface soils, in order to better understand the behavior of inorganic pollutants on sites polluted by the destruction of chemical weapons. These data were also linked with the mobility of pollutants and biogeochemical parameters.

2. Materials and methods

2.1. Study site

The study site, known as "Place-à-Gaz", is located in the Spincourt forest, 20 km northeast of Verdun, France (Bausinger et al., 2007). At the end of the First World War large amounts of shells and ammunition were stored in the region. In 1920, the Pickett and Fils company was commissioned by the French Ministry of War to destroy these munitions. 200,000 German chemical shells were opened and burned in piles at the center of this area in 1928. The fire was fueled by wood covered with explosive materials.

2.2. Chemical characterization and soil sampling

Total concentrations of As, Cu, Zn and Pb were determined in situ using XL3t800 NITON© portable X-ray fluorescence field apparatus (pXRF), in order to define the metal(loid)s distribution and to target the soil sampling. The signals were calibrated with the chemical analyzes of the soil samples and considered the soil moisture. Maps of As, Cu, Zn and Pb concentrations were drawn by interpolating data by kriging (ArcGIS©).

Four soils were sampled in the surface, non-saturated black layer (0–10 cm) in zones with contrasting vegetation cover. The soils were sieved at 2 mm through sterile sieves, placed in sterile glass jars and stored at 5 °C. Their water content was determined by drying at 105 °C for 24 h. In order to study the chemical composition of different particle size fractions, soil sub-samples were separated into three fractions by mechanical sieve shaker: coarse sand (>200 μm), fine sand (50–200 μm) and loam and clay (<50 μm).

2.3. Soil chemistry and mineralogy

For chemical and mineralogical analyses, the raw soils and particle fractions were ground to 70 μm. Major elements were determined by inductively coupled plasma (ICP) atomic emission spectroscopy (AES) using a Thermo Fischer ICap 6500; trace elements were determined by ICP-mass spectrometry (MS) on a Siex Perkin-Elmer Elan 5000a, both analyses being conducted at the Service d'Analyses des Roches et des Minéraux (SARM — rock and minerals analysis unit of the CRPG-CNRS National Research Institutes). Prior to analysis, the samples were fused with $LiBO_2$ and dissolved in a mixture of 1 N HNO_3, H_2O_2 and glycerol. Organic carbon (C_{org}) and total S were also determined at the SARM center, by carbon and sulfur determination on a Leco SC144 DRPC (SARM, CRPG-CNRS). The mineralogical composition was determined by X-ray diffraction (XRD). XRD patterns were recorded between 0° and 90° (2θ) at a scan rate of 0.3° 2θ cm^{-1} using an INEL CPS120 diffractometer equipped with a Co anode (Co $K\alpha_1$ = 1.78897 Å).

Scanning electron microscopy (SEM) and energy dispersive X-ray spectroscopy (EDS) were performed to explore the composition and distribution of metals and As in the four soils. SEM was performed on a TM 3000 accompanied by a SwiftED3000 X-Stream module (Hitachi),

and operated at 15 kV accelerating voltage. The acquisition time of EDS analyses was 300 s per sample.

2.4. Leaching and percolation tests

Leaching tests provide information about the mobility of metals and As from soil towards the water phase. The four wet soil samples were mixed with ultrapure water, with a solid/liquid ratio of 1 to 10 (wet soil equivalent to 25 g dry soil, 250 mL of ultrapure water), and the tubes were rotated on a roller mixer for 24 h. The leaching solutions were filtered at 0.45 μm then acidified with 10% of HNO_3. Fe, Cu, Zn and Pb concentrations were determined using an atomic absorption spectrophotometer (AAS, Varian, Palo Alto, CA, USA).

The leaching test was not suitable for evaluation of the speciation of soluble As, because some As(III) may be oxidized during the 24 h leaching test. A percolation test was performed to determine the speciation of soluble As in conditions close to those of the site. The soil (as wet soil equivalent to 1 g dry soil) was placed in a 5 mL syringe (diameter 13 mm) equipped with a rock wool stopper, without packing. Percolation experiments were performed in triplicate for each soil. 25 mL of a weakly mineralized spring water (Mont Roucous, pH 5.85; 3.1 $mg \cdot L^{-1}$ Na^+; 2.4 Ca^{2+}; 0.5 Mg^{2+}; 2.0 SO_4^{2-}; 6.3 HCO_3^-; 3 NO_3^-), used to simulate rain water, was fed in drops onto the surface of the soil in the syringe. Percolation water was recovered and filtered at 0.2 μm. As(III) and As(V) were immediately separated using an ion exchange method (Kim, 2001). Separation was performed on anionic resin (AG 1-X8©, Biorad, Hercules, CA, USA). A sample of percolation water filtered at 0.2 μm was acidified for total As determination. Arsenic was quantified with an AAS oven (Varian, Palo Alto, CA, USA).

A specific leaching test was applied to particles coated with materials in the amorphous phase. Soil particles, previously observed by SEM, were incubated in 0.25 M hydroxylammonium chloride and 0.25 M HCl for 10 min. The particles were observed again by SEM after the leaching step.

2.5. Bacterial enumeration

Total bacteria were extracted from soils using a Nycodenz gradient separation method (Bertrand et al., 2005) and enumerated after fluorescent DAPI staining, as described in Kumar et al. (2013).

As(III)-oxidizing bacteria were enumerated by the Most Probable Number method. The soil (as wet soil, equivalent to 0.2 g dry soil) was placed in a sterile, glass Erlenmeyer flask with 10 mL of sterile physiological saline (9 $g \cdot L^{-1}$ NaCl in demineralized water), agitated for 30 min at 25 °C, then sonicated 2×20 s at 45 kHz. Triplicate suspensions were prepared for each soil. The soil suspension was diluted in stages in sterile physiological saline to a dilution of 10^{-7}. CAsO1 mineral medium (Battaglia-Brunet et al., 2002) containing 100 $mg \cdot L^{-1}$ As(III) was distributed over Microtest TM Tissue culture plates (96 wells), 250 μL per well. Each well was inoculated with 25 μL of diluted soil suspension. Five wells were inoculated with each dilution. Culture plates were incubated at 25 °C for 10 days. The presence of As(III) in the wells was revealed by the formation of As(III)-PyrrolidineDithioCarbamate (PDC), an insoluble white complex: 150 μL of 0.1 M acetate buffer (pH 5) and 100 μL PDC solution (5 $g \cdot L^{-1}$) were added to each cell. A white precipitate appeared when As(III) was present, i.e. when As(III)-oxidizing bacteria were absent (negative well). Non-inoculated wells served as negative blanks while wells containing CAsO1 medium with 100 $mg \cdot L^{-1}$ As(V) provided a positive reference. The number of positive wells for each dilution was determined, and the most probable number of bacteria in dilutions was given by Mc Grady table for five tubes.

2.6. As(III)-oxidizing activity tests

The four samples were incubated at 25 °C for 72 h before starting the tests. The As(III) oxidizing tests were performed in 250 mL Erlenmeyer flasks filled with 100 mL of CAsO1 medium (Battaglia-Brunet et al., 2002) supplemented with 1 mM As(III) and inoculated with a mass of material equivalent to 0.2 g of dry weight. Flasks were plugged with cotton to retain oxidizing conditions and were incubated at 25° under agitation (100 rpm). The flasks were sampled each day, and twice a day during As(III) oxidation. Samples were filtered at 45 μm and frozen at −20 °C until As(III)/As(V) separation was performed. Tests were performed in triplicate. As(V) was quantified by flame AAS (Varian, Palo Alto, CA, USA), after As(III)/As(V) separation with the PDC/MIBK method (Battaglia-Brunet et al., 2002). First order As(III) oxidizing rate constants were determined by linear regression fitting of the As(V) versus time line, during the reaction.

2.7. Mineralization of biological carbon

The biodegradability of intrinsic organic matter was studied via CO_2 emission (soil respiration), as per Rey et al. (2005). The equivalent of 100 g of dry weight, adjusted to 80% of water holding capacity, was placed in 250 mL serum flasks. Samples were incubated at 25 °C. After one week of stabilization, flasks were sealed hermetically with rubber stoppers and gas samples were taken weekly for 5 weeks via the septum with a double-needle blood collection tube and a vacuum tube (Vacuette®, Greiner Bio-one). The soil moisture was kept constant by adjusting the water content to the initial mass each week. CO_2 concentration in the gas phase was analyzed with a Varian 3400 gas chromatograph using thermal conductivity detection.

Carbon mineralization rates were calculated from the linear increase of CO_2 concentration in flasks over time. The specific carbon mineralization rate was calculated as the carbon mineralization rate/total soil organic carbon ratio.

2.8. Statistical tests

Statistical analyses were performed using the XLSTAT (Addinsoft) software. Data were tested for homogeneity of variance and normal distribution. One-way analysis of variance (ANOVA) and Tukey HSD (Honestly Significantly Different) tests were carried out to test for any significant differences between the means. Differences between means at the 5% level ($P < 0.05$) were considered significant.

3. Results

3.1. Site characterization

The "Place-à-Gaz" has a surface area of 2000 m^2 (Fig. 1.a.1). The soil surface is covered by a black layer containing slag, coal, ash and residues from the pyrolysis of munitions (Fig. 1.a.2). The thickness of this layer varies from a few centimeters at the edge of the zone to around 40 cm at the center of the site (Fig. 1.a.3). The substrate beneath the black layer is a clayey Woëvre formation (Callovian age) with a thickness of around 200 m. These clays seriously limit the infiltration of rainwater, which will tend to run off to wetlands in low-lying areas at the periphery of the site (Fig. 1.a). The height of annual precipitation in the study area is 758 mm and the annual average temperature is 10.7 °C (data from Météo France, Metz station).

The central part of the site has not been colonized by plants (Fig. 1.a and c). The first colonizing species was *Pohlia nutans* mosses. A species of lichen, *Cladonia fimbriata*, and an herbaceous plant, *Holcus lanatus*, are implanted on the outer areas, growing on mosses. The surface area of the bare zone seems to have declined since the Bausinger et al. (2007) study, indicating progressive revegetation of the site.

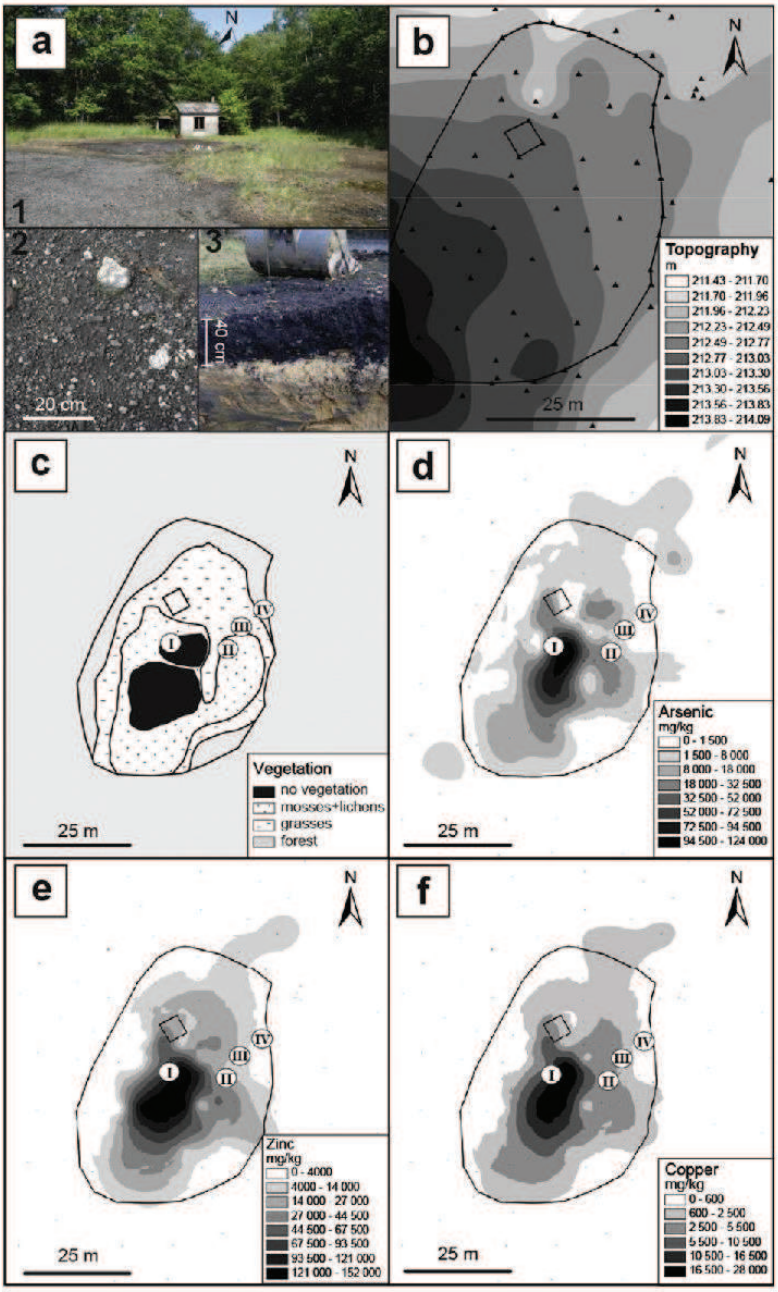

Fig. 1. Situation and contamination of the study site (a.1): Overview of the "Place-à-Gaz"; (a.2): black layer surface; and (a.3): soil profile with black layer overlying Woëvre formation clays. (b): topography of the study area. (c): implantation of vegetation. Roman numerals represent soil sample locations. (d, e, f): maps of concentrations of As, Zn and Cu at the soil surface, measured with pXRF.

The central part of the burned area was heavily contaminated by zinc, copper and arsenic. Intensity of contamination decreased progressively towards the edge of the forest, as shown by As, Cu and Zn maps (Fig. 1.d, e and f). For Pb mapping (given in SM.1) the interpolating kriging was conducted with five high-Pb-concentration measuring points in the northeast of the site, at the extremity of the sampling fields, which induced a nugget effect. These high Pb concentrations were measured in a peripheral deposit of shell fragments; however, the pollution gradient was still observable in the burned ground.

3.2. General soil characteristics and elemental composition

The four soil samples studied were taken from zones with contrasting pollution levels and different vegetation cover (Fig. 1.c, d, e and f):

soil I, with no vegetation, was the most contaminated; soil II, covered by mosses and lichens, was less contaminated; soil III was covered by grasses; and soil IV, covered by forest vegetation and humus, was the least contaminated.

All four soils contained 25–40% of fine sand (SM.2) but soil IV had a different texture with a lower proportion of coarse sand and a higher proportion of fine particles (clay and loam). The lowest proportion of fine particles was found in soil I. Electrical conductivity was similar for all soils (around 10 $mS \cdot cm^{-1}$) but the pH of soil I (5.3) was lower than that of the others (5.8–5.9).

Concentrations of elements in the surface material samples are given in Table 1. Contamination of the soils by As, Zn and Cu decreased in the following order: sample I < sample II < sample III < sample IV. Concentrations of As vary between 72,820 and 1937 mg/kg, Zn concentrations between 90,190 and 10,660 mg/kg and Cu concentrations between 9113 and 1451 mg/kg. Lead behaved differently, with a greater concentration in sample II: 5777 mg/kg. Metals and arsenic were found mainly in the coarse and fine sand fractions, while Si, Al and K were most present in the loam and clay fraction. An important concentration of organic carbon was measured in sample I: 25.87%.

3.3. Textural characterization, microscopic observation and EDS analysis

Several types of grains were observed in the four soils. Millimetric to micrometric grains with tabular structure were observed in all soils, as well as aggregates of the smallest grains (Fig. 2.a). These grains, present in greater proportions in soils III and IV, were identified as potassic and sodic aluminosilicate phases. No traces of metal(loid)s, except Fe, were detected by EDS analyses. Black grains, mainly in soils I and II, presented a wood structure with cell porosity, and high carbon contents (Fig. 3b). These grains were identified as charcoals. Many micrometric particles were present at the charcoal surfaces, and may be composed by a mixture of Si, Al and Cl, associated with small amounts of metal(loid)s (Fe, Zn, As).

White and/or green-blue crystalline materials were observed in the macroporosity of soil I, and were characterized by a prismatic texture (Fig. 3.a and b), on an acicular texture (Fig. 3.c and d). As revealed by SEM/EDS analyses, the prismatic crystals mainly contained O, Zn and As (Fig. 4.a), whereas acicular minerals were composed of an assemblage of O with Zn, As and Cu (Fig. 4.b). The soil I was also characterized by large amorphous phases (Fig. 3.e, f, g and h), with contrasting colors (yellow, red, white), covering diverse soil particles (charcoal, silicates, metallic fragments of shells), and forming aggregates. The surface of the amorphous phases presented semi-spherical nodules and microcracks (Fig. 3.f). The agglomerates of micrometric spheres were also observed in the porosity (Fig. 4.c), and are composed by a blend of Fe, As, Zn, Cu and Al (Fig. 4.c). Incubation of grains, from soil sample I, in hydroxylammonium chloride and HCl resulted in the total or partial dissolution of the amorphous material (Fig. 5).

3.4. Soil mineralogy

The crystallized phases from the four samples were investigated by XRD analysis for the different size fractions (Fig. 6). Quartz, a ubiquitous mineral, was present in the four soils. Potassium and sodium feldspars were detected in samples from soils II, III and IV. Clays were detected in soil IV, particularly in its fine fraction, however the mineralogy of the clay could not be defined. In soil I, four secondary arsenic minerals were identified: adamite ($Zn_2AsO_4(OH)$), olivenite ($Cu_2AsO_4(OH)$), Na-pharmacosiderite ($NaFe_4(AsO_4)_3\ (OH)_5\ 5H2O$) and Ba-pharmacosiderite ($BaFe_4(AsO_4)_3(OH)_5\ 5H_2O$). The zinc and copper arsenates were more abundant in the coarse sands fraction. The pharmacosiderite minerals were mainly present in the silts and clays fraction. A zinc oxide, zincite (ZnO), was also identified in the bulk and coarse sand fraction. Soil I also gave a significant XRD background signal, suggesting an important amorphous phase.

3.5. Mobility of contaminants

The mobility of As, Zn, Cu, Pb and Fe was assessed by leaching with water in batch systems (Table 2). Concerning the absolute quantities of leached elements, As solubility was significantly higher in soil I than in the other soils and As was less leachable in soils III and IV. The concentrations of soluble Cu and Pb were similar in all soils and the mobility of Zn was higher in soil I than in the other soils. Focusing on the proportion (%) of each leached element compared to its total concentration in the solids, the mobility in closed (batch) systems was overall low (<1.5%), however it was higher in all cases for soils III and IV than for soils I and II.

A different tendency was revealed by the percolation experiment (Table 3): with this open and short-term system, mobile As concentration decreased from 2202 μ/L in soil I to 28 μg/L in soil IV; the proportion of mobile As was highest in soil II and lowest in soil IV.

As(V) was the main As species in all soils (Table 3). Despite significant differences in absolute As(III) and As(V) concentrations in the four soils, the proportion of As(III) was constant at around 2%. Another species of arsenic was detected in all soils but did not correspond to monomethylarsonate, dimethylarsinate or arsenobetaine. As(V) was also the dominant form (Table 3) in aqueous phases of percolation tests. The proportion of mobile As(III) was low (less than 5%), but significantly higher in soil I compared to soil II.

Table 1
Chemical analyses of the four soil samples. CS: coarse sand. FS: fine sand. L&C: loam and clay.

		Major (%)										Trace (mg/kg)							
Sample	Particle size fractions	SiO_2	Al_2O_3	Fe_2O_3	CaO	K_2O	P_2O_5	MnO	MgO	Corg	S total	As	Cu	Pb	Zn	Ba	Cd	Cr	Sn
I	Bulk	13.62	2.29	11.13	0.61	0.42	0.38	0.10	0.15	25.87	0.13	72,820	9113	3830	90,190	743.4	158.9	57.6	308.1
	CS	6.65	1.86	14.87	0.51	0.23	0.35	0.09	0.11	21.58	0.14	74,870	12,680	4331	152,200	448.4	224	40.6	324.3
	FS	16.16	2.64	11.97	0.6	0.5	0.44	0.10	0.18	21.12	0.12	83,090	8929	4526	84,520	779.1	127.3	56.3	318
	L&C	26.06	3.09	10.17	0.59	0.71	0.39	0.09	0.20	19.89	0.1	67,270	7331	3661	68,330	993.4	109.1	104.6	323.6
II	Bulk	50.15	4.83	6.19	0.64	1.22	0.29	0.06	0.28	12.26	0.11	30,840	5082	5777	37,310	453.4	76.8	77.1	138.8
	CS	18.24	3.39	12.26	1.1	0.56	0.4	0.09	0.29	23.33	0.21	57,840	8736	9325	61,730	477.8	136	58.5	219.7
	FS	42.57	4.54	6.92	0.72	1.11	0.34	0.08	0.29	14.39	0.14	41,900	6501	8012	40,210	502.9	95.9	69.5	175.5
	L&C	66.17	5.48	4.08	0.49	1.52	0.21	0.04	0.29	5.63	0.07	21,310	3106	3927	23,610	465.1	48.1	98.7	109.1
III	Bulk	69.61	6.72	4.99	0.45	1.75	0.18	0.07	0.42	3.69	0.04	6253	1591	2528	10,660	296.1	18	84.4	45.9
	CS	61.11	6.7	10.66	0.79	1.64	0.21	0.12	0.46	4.03	0.06	9793	3009	4379	19,550	395.2	30.5	94.5	71.9
	FS	69.19	6.52	4.53	0.44	1.76	0.2	0.07	0.41	4.26	0.05	8480	1863	3620	12,610	380.2	23.9	97.1	56.6
	L&C	75.85	6.8	2.9	0.38	1.83	0.15	0.04	0.40	2.55	0.03	4055	1078	2102	7257	345.3	12.9	120.1	34.9
IV	Bulk	58.85	7.2	4.08	0.62	1.73	0.27	0.15	0.53	8.44	0.07	1937	1451	968	13,270	312.5	26.2	97.3	43.6
	CS	36.41	5.77	7.63	0.88	1.2	0.4	0.32	0.47	17.3	0.1	3612	2795	2007	24,540	262.9	49.7	79.8	59.7
	FS	52.89	7.13	4.34	0.64	1.65	0.33	0.22	0.55	10.64	0.08	8469	2042	1427	12,670	354.3	30.1	89.7	48.4
	L&C	67.57	7.5	3.42	0.47	1.88	0.21	0.07	0.52	5.3	0.05	1436	992	646	9284	321.8	17.6	111.8	39.2

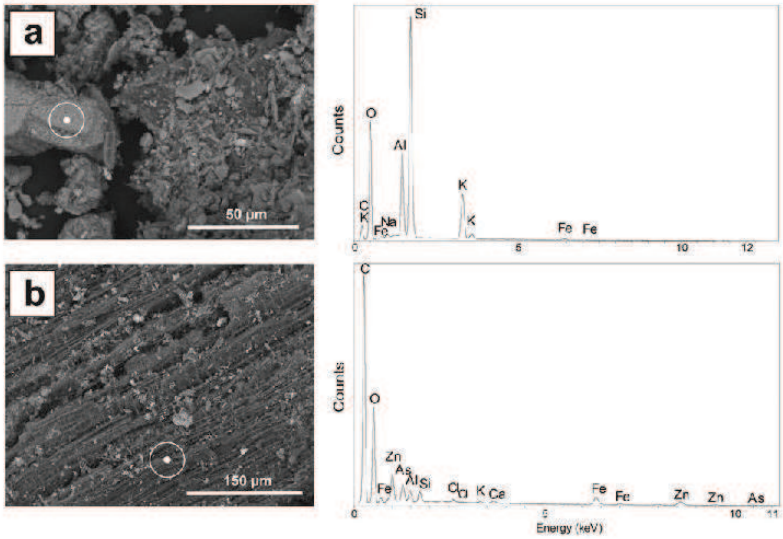

Fig. 2. Observation and composition of inherited silicates and charcoals from black layer (a): Backscattered electron images and EDS spectrum of a silicate mineral from soil sample IV. This grain was mainly composed of Si, Al and O. K and Na were also detected. The only metal(loid) detected was Fe. (b): SEM picture and EDS analysis of a charcoal grain from soil sample I. These grains were identifiable by their woody structure, and contain carbon associated with. The EDS spectrum indicated charcoal containing many small quantities of elements, particularly Fe, Zn and As. The targets correspond to the location of EDS elemental analysis.

3.6. Biogeochemical parameters

Although microbial As(III) oxidation began earlier in the less polluted soils III and IV (Fig. 7a), the As(III)-oxidation rate was significantly higher in the most polluted soils I and II (Fig. 7b). The total bacterial concentration was significantly higher in soils III and IV than in soils I and II. Whereas the absolute concentration in As(III)-oxidizing bacteria was in the same range for the four soils, the percentage of active As(III)-oxidizing bacteria, in the whole bacterial community, was higher in the most polluted soil I (Table 3).

Carbon mineralization was significantly more rapid in soil IV (25.17 ± 2.07 µg C-CO_2 g^{-1}dry mass day^{-1}) and in soil I (19.01 ± 0.52 µg CO_2 g^{-1}dry mass day^{-1}) than in the two other samples (Fig. 8a). Rates measured for II and III soils were about five times lower. However, as the intrinsic carbon content varied greatly from one soil to another, the data were also expressed as specific mineralization rates (Fig. 8b). The specific carbon mineralization rate was therefore not significantly different in soils I and II (73 ± 2 µg CO_2 g^{-1}Corg day^{-1} and 58 ± 1 µg CO_2 g^{-1}Corg day^{-1}, respectively). Specific carbon mineralization of soil IV remained the highest.

4. Discussion

4.1. Environmental contamination caused specifically by the thermal treatment of gas shells

The "Place-à-Gaz" was mainly contaminated by arsenic, copper, zinc and lead. The different parts of the containers of chemical shells probably constitute the sources of the heavy metals Cu, Zn and Pb. As contamination, on the other hand, was derived from the oxidation of diphenylarsines contained in "blue cross shells" during the combustion process. Besides the considerable amount of contaminants, the samples of the surface black layer contained high concentrations of organic carbon (Table 1). Bausinger et al. (2007) have suggested that organic carbon had two origins; the humic matter provided by the forest and the charcoal resulting from the use of firewood during the thermal treatment. Here, the carbon mineralization rates confirm the presence of two types of organic matter (Fig. 8): bioavailable organic matter in the less polluted soil, which can be attributed to humic matter; and less bioavailable organic matter in the central part, corresponding to charcoal.

The subsoil of the Woëvre-plain (Fig. 1.a.3) is formed from clay and other silicates. The concentrations of Si, Al and K, mainly present in the fine fraction of the four soils (Table 1), and the detection of Na and K feldspars and clays in soil V (Fig. 6) confirmed the presence of inherited silicates in the black layer. During and after the incineration treatment, metals and metalloids were released into an environment rich in iron, clay and charcoal, three substances known for their capacity to bind inorganic contaminants (Bradl, 2004). The spatial and mineralogical relationships between these substances and contaminants were investigated in the four soils.

Traces of As, Zn and Fe were detected in the charcoal fragments (Fig. 2.b). However, the results of SEM–EDS analyses performed on different grains of the four soils attested that As and heavy metals were not principally bound to charcoals or silicates. The observations of crystalline and amorphous materials containing large quantities of metals and arsenic suggested common carriers for inorganic contaminants. The white and blue crystallized materials with prismatic structures with radial intergrowths (Figs. 3,a–d and 4.a,b) certainly correspond to minerals of the adamite–olivenite series ($(Zn–Cu)_2AsO_4(OH)$) detected by XRD (Fig. 6). Two other arsenates were identified in the most contaminated soil: Na-pharmacosiderite ($NaFe_4(AsO_4)_3(OH)_5$, 5H2O) and the Ba-pharmacosiderite ($BaFe_4(AsO_4)_3(OH)_5$ $5H_2O$). These arsenic carrier minerals are usually found as secondary minerals resulting from the alteration of primary minerals such as arsenopyrite and have been observed most frequently in post-mining environments (Morin et al., 2002; Drahota and Filippi, 2009; Haffert et al., 2010). To our knowledge, the present study is the first to reveal such a mineral association in a context of incineration of hazardous materials. However, the sequential extraction performed by Bausinger et al. (2007) showed that most of the As, Zn, Cu and Pb were not hosted by crystallized fractions yet, in the central part of the site, the majority of As, Cu, Pb and Zn were leached by hydroxylammonium chloride and HCl. This leached fraction was attributed to species bound to amorphous

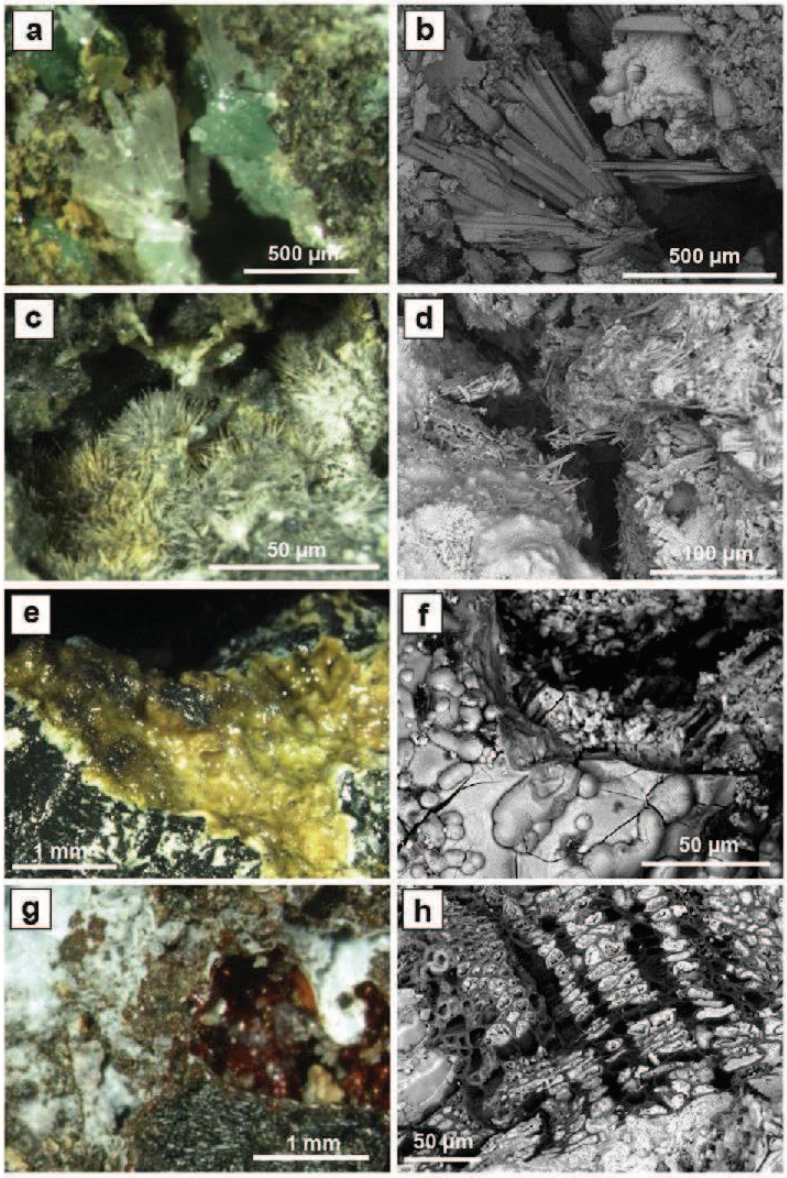

Fig. 3. Microscopic pictures of crystalline and amorphous phases of soil sample I. On the left, (a, c, e and g) binocular magnifier pictures, and on the right (b, d, f and h) SEM pictures. (a) and (b): white prismatic crystals and green-blue crystals formed in the porosity. (c) and (d): white acicular crystals with radial intergrowth. (e): grain of charcoal covered with yellow amorphous phase. Its surface was smooth. (f): SEM view of surface of the amorphous phases. This one is covered by semi-spherical nodules and micro-cracks. (g): white and red amorphous phases close to a charcoal grain whose porosity was filled by white amorphous phases. (h): high-resolution image of this wood charcoal.

Fe-oxyhydroxides (Hall et al., 1996). DRX and SEM–EDS results highlighted the presence of amorphous material composed mainly of Fe but also containing important amounts of As, Cu and Zn. Moreover, this amorphous phase was leached by hydroxylammonium chloride and HCl (Fig. 5) and can thus be attributed to the amorphous Fe-oxyhydroxides fraction mentioned by Bausinger et al. (2007) as a major carrier of pollutants, detected indirectly by a selective extraction procedure. Consequently, the amorphous phase observed directly here was probably the principal carrier of arsenic and metals in the central parts of the "Place-à-Gaz".

Several indices suggested that the nature of the carrier phases was directly related to the incineration of chemical shells. The structure of the amorphous phase was the first sign that a significant high temperature was reached during destruction. The micro-cracks, observed on the surface (Fig. 2.f), were certainly formed as the material cooled. Moreover, the small spherical particles in soil pores (Fig. 4.c) present similar morphology as particles observed in fly ashes produced by incinerators (Fisher et al., 1978; Le Forestier and Libourel, 1998). In addition, pharmacosiderite has a zeolite structure (Baur, 2012) and many authors have detected zeolite forms in incineration ashes (Shigemoto et al., 1993; Murayama et al., 2002; Querol et al., 2002). Zincite (ZnO) indentified in the soil I is a synthetic mineral found typically in metallurgical furnace residues. Sidenko et al. (2001) have observed the presence of zincite in the self-combusting waste heaps of a zinc smelting plant.

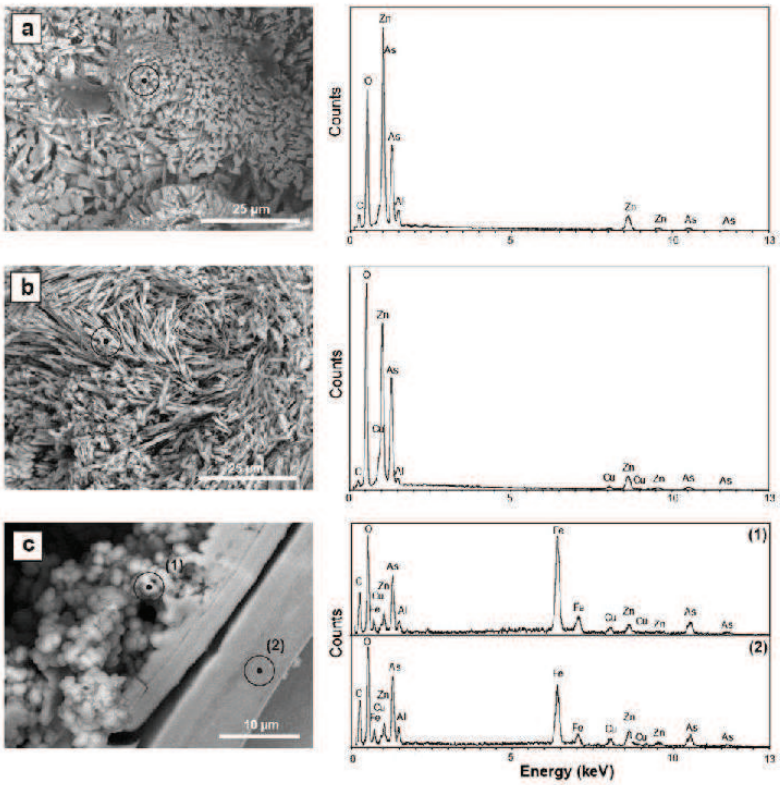

Fig. 4. Observation and composition of crystallized mineral and amorphous phase carriers of metal(loid)s Soil sample I SEM images with elemental spectra of As carrier crystallized minerals with Zn (a) and Zn + Cu (b). (c): iron-rich amorphous phases with spheres, carrier of As, Cu and Zn. The targets correspond to the location of EDS elemental analysis.

The presence of amorphous materials, small spherical particles, zeolite-like structures of pharmacosiderite and zincite therefore suggested that the mineralogical associations in the polluted soil were driven by the incineration of shells. First, the combustion oxidized organoarsenic molecules and smelted metals from shell containers, resulting in the formation of an iron and oxygen-rich amorphous phase covering grains of the inherited soil. This amorphous material was the main carrier of As, Cu, and Zn. Then, during cooling, the secondary arsenate minerals (adamite, olivenite and pharmacosiderite) and zincite crystallized in the material pores. Furthermore, the presence of iron in the amorphous phase can be used to estimate that the maximum combustion temperature was above the melting point of iron, i.e. 1538 °C. Such an amorphous mineral phase, mainly composed of iron, oxygen, arsenic and heavy metals, had never been observed before this study.

4.2. Mobility of contaminants

Contamination of the site by As, Cu, Pb and Zn was significant but very localized. As, Cu and Zn (and to a lesser extent Pb) were distributed along a concentration gradient from the center of the site, devoid of vegetation, towards the forest (Fig. 1.c–f). In June 2014, during the sampling campaign, wetland zones were observed in the periphery of the "Place-à-Gaz", resulting from meteoritic water accumulation at low topographic points, because of the very low permeability of the Woëvre

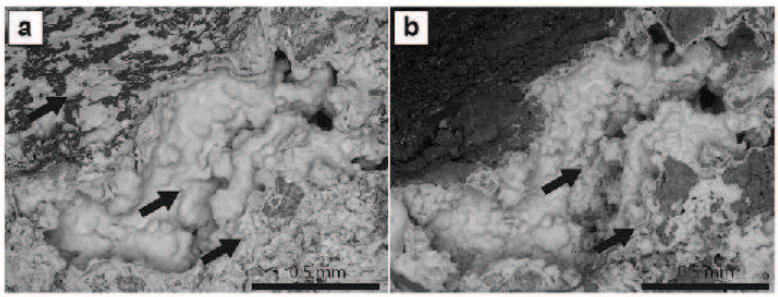

Fig. 5. SEM pictures showing effect of hydroxylammonium chloride and HCl on amorphous phases of soil sample I. (a): Grain of soil covered by amorphous phase. (b): the same sample after 10 min in 0.25 M hydroxylammonuim chloride + 0.25 HCl solution. The amorphous phases that covered charcoal (top arrow) and silicate grains (bottom arrow) were totally dissolved. The surface of the thicker amorphous phase covering the cavity (middle arrow) was partially dissolved.

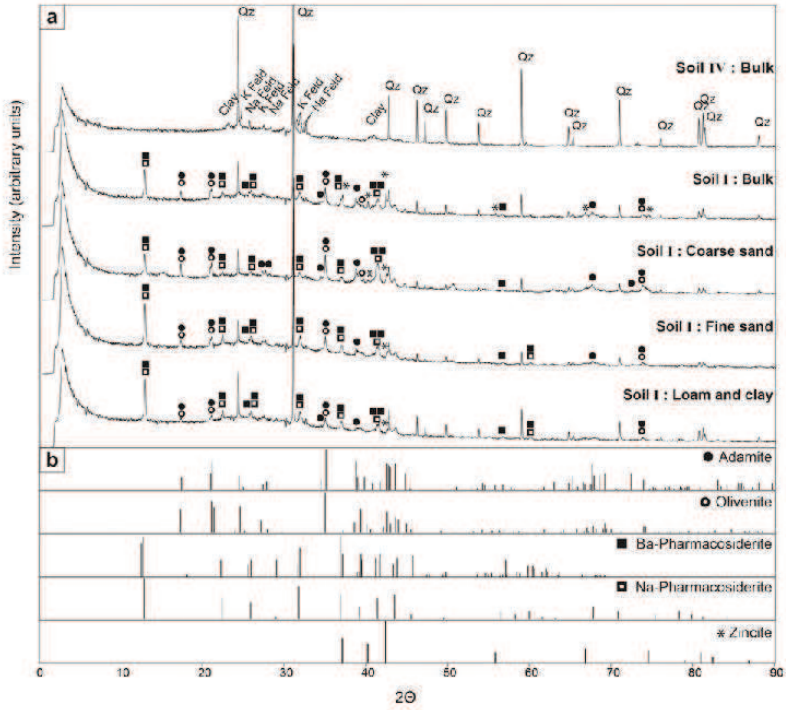

Fig. 6. Mineralogy of soils sample I and IV (a): X-ray diffractograms of bulk sample of soil IV and of each particle size fraction of soil sample I: Qz = quartz (ICDD 46-1045); Na Feld = sodium feldspar (ICDD 19-1184); K Feld = potassium feldspar (ICDD 31-0966). (b): standard XRD patterns of the five reference mineral carriers of metals and As detected in soil I: adamite (ICDD 39-1354); olivenite (ICDD 42-1353); Ba-Pharmacosiderite (ICDD 34-0154); Na-Pharmacosiderite (ICDD 38-0388); zincite (ICDD 36-1451).

formation clays. This formation, beneath the heavily contaminated black layer, limited the vertical transfer of metals and As, forming a natural barrier to infiltration of rainwater. The higher pH (above pH 7), in the clay horizon also formed a chemical barrier to the mobility of metals, especially Zn (Bausinger et al., 2007). Transfer of contaminants on the site was therefore mainly driven by runoff water at the base of the highly permeable black layer. The contaminated area at the northern low topographic point of the site, outside the burning zone, showed this horizontal transfer (Fig. 1.b and d–f).

The solubility of the main carrier phases of metals and arsenic was difficult to predict since, while the solubility constants of adamite and olivenite are documented (K_{sp} equal to 5.71 for adamite and 2.39 for olivenite, Magalhâces et al., 1988), no solubility or thermodynamic data are available for pharmacosiderite minerals (Drahota and Filippi, 2009). Moreover, the stability of the amorphous phase was unknown. The potential mobility of metals and arsenic was first evaluated by leaching tests (Table 2). Leached Cu and Pb values seemed to reach a threshold independently of the original ground level pollution (Table 2). The percentages of leached pollutants were very low (below 2%), however they revealed that a higher proportion of pollutants were mobilized from the less contaminated soil. These observations can be explained by the saturation of these elements in the aqueous phase of the leaching batch systems, which would induce their re-precipitation. In order to evaluate the mobility of metals and arsenic in these conditions, the geochemical PHREEQCi 3.0.6.7757 code together with the minteq.v4 thermodynamic database was used by integrating the complete chemistry of the leached water (SM3). In these acid ($5 < pH < 6$) and oxidizing conditions, the PHREEQCi simulation, integrating the chemical parameters and concentrations of major and trace chemical species of the leached water, highlighted that hydroxides and oxides containing Cu, Pb and Fe should precipitate (SM.3). This could explain the low mobility of Cu and Pb in the environmental conditions of the site. Conversely, according to the PHREEQCi simulation, no mineral containing arsenic or zinc should precipitate but iron minerals known to efficiently adsorb As (ferrihydrite, goethite) should precipitate. Where the behavior of zinc is concerned, these results are consistent with the Bausinger et al. (2007) study concluding that the moderately acidic soil pH allowed mobilization of considerable amounts

Table 2
Leaching test. Solubility of metal(loid) contaminants of samples after 24 h batch leaching tests with ultrapure wat. Amounts of leached elements were expressed as milligrams per kilogram of dry soil. The proportion of leached pollutants was expressed as percentage of total pollutant concentrations in the soils.

	As			Fe			Cu			Pb			Zn		
Sample	mg/kg		%	mg/kg		%	mg/kg		%	mg/kg		%	mg/kg		%
I	77.2	a	0.11	39.1	a	0.04	3.0	a	0.03	2.9	a	0.08	103.9	a	0.12
II	40.5	b	0.13	27.2	b	0.04	2.8	a	0.05	4.6	a	0.08	70.8	ab	0.19
III	21.8	c	0.35	35.1	ab	0.07	2.8	a	0.17	4.2	a	0.17	59.9	b	0.56
IV	26.3	c	1.36	30.6	ab	0.07	3.0	a	0.21	2.2	a	0.22	74.5	ab	0.56

Values are the means (n = 3). Values with different letters are significantly different ($P < 0.05$, ANOVA, Tukey-HSD).

Table 3
Parameters related to As speciation. Arsenic speciation in the solid phases of the four bulk soils (solid), speciation in water from percolation tests (liquid), and enumeration of specific As(III)-oxidizing micro-organisms (μo) (bacteria).

			I		II		III		IV	
Solid	$As(III)_{total}$	mg/kg	1577	a	852	b	191	c	29	c
	$As(V)_{total}$	mg/kg	70,178	a	36,846	b	7355	c	1954	c
	Ratio of $As(III)_{total}$	%	2.25	a	2.33	a	2.41	a	1.48	a
	As_{total}/Fe_{total}	mol As/mol Fe	0.48		0.37		0.09		0.04	
Liquid*	As_p	μg/L	2202	a	1627	b	141	c	28	c
	$As(III)_p$	μg/L	97	a	39	b	<10		<10	
	$As(V)_p$	μg/L	2106	a	1588	b	134	c	25	c
	Ratio of As $total_p$	%	0.075		0.13		0.056		0.036	
	Ratio of $As(III)_p$	%	4.5	a	2.5	b	–		–	
	pH		5.34		5.95		5.84		5.92	
Bacteria**	As(III)-ox μo	Bact/g dry soil × 10^3	1.93	a	1.47	a	10.35	a	5.92	a
	Ratio of As(III)-ox μo***	‰	0.165	a	0.049	ab	0.043	ab	0.012	b

Values are the means (n = 3). Values with different letters are significantly different (P < 0.05, ANOVA, Tukey-HSD). (*) percolation tests. (**) in the bulk soils, (***) ratio specific As(III)-oxidizing μo / total μo.

of Zn. However, Bausinger et al., 2007 did not explain the behavior of arsenic, as no simple correlation between As mobility and pH could be found.

Arsenic concentrations in water obtained with the percolation test (Table 3) were in the same range than those measured by Bausinger et al. (2007) in soil interstitial water samples (mean value of 838 μg/L and maximum value of 2377 μg/L). The proportion of As(III) in the percolation water of the most polluted soil was greater than the proportion of As(III) in the corresponding solid. This can be explained by the high mobility of arsenite which has no charge at this pH range, unlike the arsenate (Smedley and Kinniburgh, 2002). However, in soil II the proportion of As(III) in the percolating water was not higher than in the solid phase. This result can be explained by the difference of pH between soils I (5.3) and soil II (5.9), as differential As(III) and As(V) adsorption behavior is very sensitive to pH in this range. At pH 5–6, As(V) sorbs more readily to amorphous hydrous ferric oxides (HFO) than does As(III) (Dixit and Hering, 2003). However, adsorption of As(III) increases with pH, while adsorption of As(V) shows an opposing trend This may explain why more As(III) was released by soil I than by soil II.

Biological As(III) oxidation may decrease the proportion of As(III). As(III)-oxidizing tests (Fig. 7) and enumeration of specific As(III)-oxidizing organisms (Table 2) revealed the potential for bacterial As(III) oxidation in all soils. However, the longer time lapse in As(III)-oxidizing activity tests in soil I than in other soils shows that this activity may be inhibited because of the high concentrations of toxic elements. This toxicity clearly influenced the total bacterial concentration and microbial activities (i.e. organic matter mineralization; Fig. 8) that were significantly lower in soils I and II than in soils III and IV. The High Cu concentration in soil I may explain the lower microbial numbers and the lower microbial activities involved in C-mineralization process (Flemming and Trevors, 1989). Thus, the relative inhibition of microbial As(III) oxidizing activity may have contributed to the higher proportion of As(III) released from soil I compared to soil II.

However, the elevated toxic element concentrations seemed to have exerted a selective pressure on the microbial communities, as suggested by the high As(III)-oxidizing rates observed with microbial populations from soils I and II (Fig. 7) and by the highest proportion of As(III)-oxidizing microorganisms compared to the total bacterial concentration in soil I (Table 2).

Concerning total As mobility, the batch leaching test (Table 2) resulted in a higher mobility from soils III and IV, contrary to the percolation experiment (Table 3), which indicated a maximum As mobility in soil II. This apparent contradiction can be explained by the difference in experimental procedure. In the batch leaching test, the contact time between water and soils allowed the leaching and re-precipitation of iron that induced As removal through adsorption on fresh HFO, the absolute iron concentration being higher in soils I and II than in soils III and IV

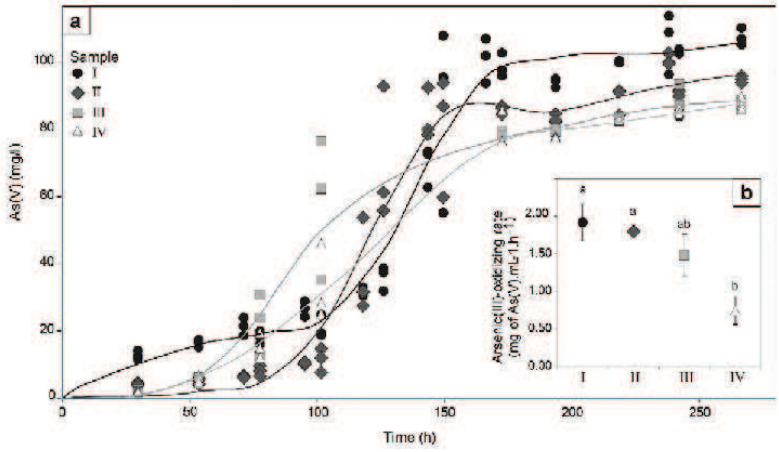

Fig. 7. Bacterial As-III oxidizing activities (a): Evolution of As(V) concentration during the As(III)-oxidizing activity tests performed with triplicates on the four soils. (b): As(III) oxidation rates corresponding to the previous activity tests. Error bars represent the standard deviation of the mean of three replicates. Different letters denote significant difference between samples (P < 0.05, ANOVA, Tukey-HSD).

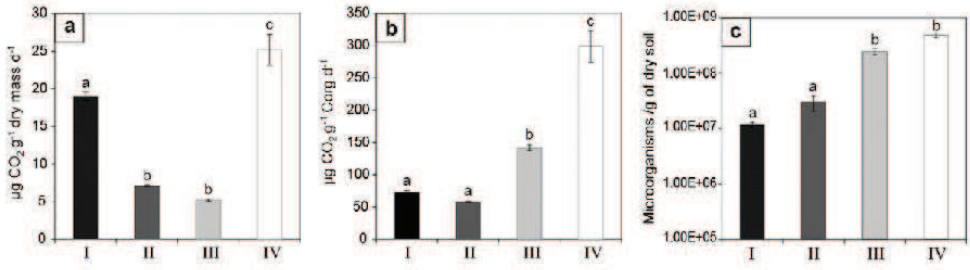

Fig. 8. Biological carbon mineralization (a): Carbon mineralization rates of the four contaminated soils. (b): specific carbon mineralization rates (carbon mineralization rate/organic carbon concentration ratio). (c): total microorganisms concentration. Error bars represent the standard deviation of the mean of three replicates; Letters denote significant difference between samples ($P < 0.05$, ANOVA, Tukey-HSD).

(Table 1). This phenomenon explains why in batch leaching tests the percentage of final soluble As was higher with soils III and IV. Conversely, the percolation test was rapid (less than 1 h), and the percolating water was immediately filtered and acidified; re-precipitation of solubilized iron was, therefore, probably limited. In the percolation conditions, the mobility of As was most probably governed by the molar ratio As/Fe and pH of the soils.

Dixit and Hering (2003) gave values of site density for As adsorption on HFO: between 0.2 and 0.3 mol sites per mol Fe. The molar ratio As/Fe in the center of the "Place-à-Gaz" was greater than 0.3 (Table 3), suggesting that the adsorption sites for As in the soils I and II were saturated. Thus, As should be more mobile in soils I and II than in soils III and IV. Lastly, the higher mobility of As from soil II than from soil I in percolation tests may be explained by soil pH: soil I was more acidic than soil II, yet As(V) adsorption onto iron oxides continuously decreases when pH increases between 3.5 and 10 (Dixit and Hering, 2003). Thus, As(V) was less strongly adsorbed onto Fe-rich particles in soil II than in soil I.

Then, the adsorption of As onto the HFO in the most contaminated part of the site was not enough to immobilize the whole amount of arsenic. At the periphery of the site, where the As/Fe ratio was less than 0.2, a significant decrease of mobile arsenic was detected in the percolating water. Batch leaching and percolation experiments yielded different and complementary information concerning As mobility in the soils: percolation testing represents the short-term mobility occurring when rainwater passes rapidly through the permeable surface soil, whereas the leaching test mimics the phenomena that probably occur in the stagnant water retained in the saturated areas. On the whole, these results suggest that bacterial As(III) oxidation contributes to reduce the proportion of As(III) in soil pore water but that the adsorption of As onto HFO was the major phenomenon driving the short-term mobility of As.

5. Conclusion

The present study has provided new information about the carriers of arsenic and heavy metals in soils strongly polluted by the historical incineration of chemical weapons.

Nearly one century after the polluting event, arsenic speciation shown by SEM–EDS and XRD was proven to be directly linked to the incineration of shells. Indeed, the two main As-carriers were identified as amorphous materials composed of a blend of metals and secondary arsenate minerals that were formed in the pores of the material as it cooled. Such amorphous carriers of arsenic and heavy metals, with high iron content and no silica but presenting a glass-like morphology, were observed here for the first time.

The soils of the "Place-à-Gaz" site were strongly contaminated by As, Zn, Cu and Pb, the more mobile of these pollutants being Zn and As. The mobility of Zn was probably governed primarily by pH, whereas As behavior seems to be related to pH, As/Fe ratio, Fe dissolution/precipitation processes and microbial activities.

The long-term exposure to high levels of toxicity in soils I and II, and particularly in soil I, exerted a selective pressure on the microbial communities that probably tended to select organisms with high As(III)-oxidizing efficiency and increased the proportion of As(III)-oxidizing bacteria in the global community. Thus, microbes can contribute to maintaining of a high proportion of AsV on site. However, the microbial activity studied, i.e. organic matter mineralization and As(III) oxidation, are less active in the most polluted soils compared to those with lower concentrations in inorganic pollutants, suggesting that the inorganic pollutants still exert an inhibiting effect on biogeochemical cycles in the most polluted part of the site.

Supplementary data to this article can be found online at http://dx.doi.org/10.1016/j.scitotenv.2016.01.111.

Acknowledgments

This work was supported by the Région Centre Val de Loire (convention 00087485) and the Labex Voltaire (ANR-10-LABX-100-01).

References

Battaglia-Brunet, F., Dictor, M.-C., Garrido, F., Crouzet, C., Morin, D., Dekeyser, K., Clarens, M., Baranger, P., 2002. An arsenic(III)-oxidizing bacterial population: selection, characterization, and performance in reactors. J. Appl. Microbiol. 93, 656–667. http://dx.doi.org/10.1046/j.1365-2672.2002.01726.x.

Baur, W.H., 2012. Rigid frameworks of zeolite-like compounds of the pharmacosiderite structure-type. Microporous Mesoporous Mater. 151, 13–25. http://dx.doi.org/10.1016/j.micromeso.2011.11.021.

Bausinger, T., Preuß, J., 2005. Environmental remnants of the first world war: soil contamination of a burning ground for arsenical ammunition. Bull. Environ. Contam. Toxicol. 74, 1045–1053. http://dx.doi.org/10.1007/s00128-005-0686-z.

Bausinger, T., Bonnaire, E., Preuß, J., 2007. Exposure assessment of a burning ground for chemical ammunition on the Great War battlefields of Verdun. Sci. Total Environ. 382, 259–271. http://dx.doi.org/10.1016/j.scitotenv.2007.04.029.

Bertrand, H., Poly, F., Van, V.T., Lombard, N., Nalin, R., Vogel, T.M., Simonet, P., 2005. High molecular weight DNA recovery from soils prerequisite for biotechnological metagenomic library construction. J. Microbiol. Methods 62, 1–11. http://dx.doi.org/10.1016/j.mimet.2005.01.003.

Bradl, H.B., 2004. Adsorption of heavy metal ions on soils and soils constituents. J. Colloid Interface Sci. 277, 1–18. http://dx.doi.org/10.1016/j.jcis.2004.04.005.

Cullen, W.R., Reimer, K.J., 1989. Arsenic speciation in the environment. Chem. Rev. 89, 713–764. http://dx.doi.org/10.1021/cr00094a002.

Dixit, S., Hering, J.G., 2003. Comparison of arsenic(v) and arsenic(iii) sorption onto iron oxide minerals: implications for arsenic mobility. Environ. Sci. Technol. 37, 4182–4189. http://dx.doi.org/10.1021/es030309t.

Drahota, P., Filippi, M., 2009. Secondary arsenic minerals in the environment: a review. Environ. Int. 35, 1243–1255. http://dx.doi.org/10.1016/j.envint.2009.07.004.

Fisher, G.L., Prentice, B.A., Silberman, D., Ondov, J.M., Biermann, A.H., Ragaini, R.C., McFarland, A.R., 1978. Physical and morphological studies of size-classified coal fly ash. Environ. Sci. Technol. 12, 447–451. http://dx.doi.org/10.1021/es60140a008.

Flemming, C.A., Trevors, J.T., 1989. Copper toxicity and chemistry in the environment: a review. Water Air Soil Pollut. 44, 143–158. http://dx.doi.org/10.1007/BF00228784.

Haffert, L., Craw, D., Pope, J., 2010. Climatic and compositional controls on secondary arsenic mineral formation in high-arsenic mine wastes, South Island, New Zealand. N. Z. J. Geol. Geophys. 53, 91–101. http://dx.doi.org/10.1080/00288306.2010.498403.

Hall, G.E.M., Vaive, J.E., Beer, R., Hoashi, M., 1996. Selective leaches revisited, with emphasis on the amorphous Fe oxyhydroxide phase extraction. J. Geochem. Explor. 56, 59–78. http://dx.doi.org/10.1016/0375-6742(95)00050-X.
Huang, H., Jia, Y., Sun, G.-X., Zhu, Y.-G., 2012. Arsenic speciation and volatilization from flooded paddy soils amended with different organic matters. Environ. Sci. Technol. 46, 2163–2168. http://dx.doi.org/10.1021/es203635s.
Hube, D., 2013. Potentialités d'un marquage des eaux souterraines par des substances pyrotechniques en relation avec les zones de combats de la première guerre mondiale – Le cas des perchlorates. Rapport final. BRGM/RP-62008-FR (26pp.).
Hupy, J.P., Schaetzl, R.J., 2008. Soil development on the WWI battlefield of Verdun, France. Geoderma 145, 37–49. http://dx.doi.org/10.1016/j.geoderma.2008.01.024.
Kim, M.-J., 2001. Separation of inorganic arsenic species in groundwater using ion exchange method. Bull. Environ. Contam. Toxicol. 67, 0046–0051. http://dx.doi.org/10.1007/s00128-001-0089-8.
Kumar, N., Millot, R., Battaglia-Brunet, F., Négrel, P., Diels, L., Rose, J., Bastiaens, L., 2013. Sulfur and oxygen isotope tracing in zero valent iron based in situ remediation system for metal contaminants. Chemosphere 90, 1366–1371. http://dx.doi.org/10.1016/j.chemosphere.2012.07.060.
Le Forestier, L., Libourel, G., 1998. Characterization of flue gas residues from municipal solid waste combustors. Environ. Sci. Technol. 32, 2250–2256. http://dx.doi.org/10.1021/es980100t.
Lescure, T., Moreau, J., Charles, C., Ben Ali Saanda, T., Thouin, H., Pillas, N., Bauda, P., Lamy, I., Battaglia-Brunet, F., 2016. Influence of organic matters on As(III) oxidation by the microflora of polluted soils. Environ. Geochem. Health http://dx.doi.org/10.1007/s10653-015-9771-3 (in press).
Magalhães, M.C.F., Pedrosa De Jesus, J.D., Williams, P.A., 1988. The chemistry of formation of some secondary arsenate minerals of Cu(II), Zn(II) and Pb(II). Mineral. Mag. 52, 679–690.
Masscheleyn, P.H., Delaune, R.D., Patrick, W.H., 1991. Effect of redox potential and pH on arsenic speciation and solubility in a contaminated soil. Environ. Sci. Technol. 25, 1414–1419. http://dx.doi.org/10.1021/es00020a008.
Morin, G., Lecocq, D., Juillot, F., Calas, G., Ildefonse, P., Belin, S., Borensztajn, S., 2002. EXAFS evidence of sorbed arsenic (V) and pharmacosiderite in a soil overlying the Echassières geochemical anomaly, Allier, France. Bull. Soc. Géol. Fr. 173, 281–291. http://dx.doi.org/10.2113/173.3.281.
Murayama, N., Yamamoto, H., Shibata, J., 2002. Mechanism of zeolite synthesis from coal fly ash by alkali hydrothermal reaction. Int. J. Miner. Process. 64, 1–17. http://dx.doi.org/10.1016/S0301-7516(01)00046-1.
Park, J.H., Lamb, D., Paneerselvam, P., Choppala, G., Bolan, N., Chung, J.-W., 2011. Role of organic amendments on enhanced bioremediation of heavy metal(loid) contaminated soils. J. Hazard. Mater. 185, 549–574. http://dx.doi.org/10.1016/j.jhazmat.2010.09.082.
Pierce, M.L., Moore, C.B., 1982. Adsorption of arsenite and arsenate on amorphous iron hydroxide. Water Res. 16, 1247–1253. http://dx.doi.org/10.1016/0043-1354(82)90143-9.
Querol, X., Moreno, N., Umaña, J., Alastuey, A., Hernández, E., López-Soler, A., Plana, F., 2002. Synthesis of zeolites from coal fly ash: an overview. Int. J. Coal Geol. 50, 413–423. http://dx.doi.org/10.1016/S0166-5162(02)00124-6.
Rey, A., Petsikos, C., Jarvis, P.G., Grace, J., 2005. Effect of temperature and moisture on rates of carbon mineralization in a Mediterranean oak forest soil under controlled and field conditions. Eur. J. Soil Sci. 56, 589–599. http://dx.doi.org/10.1111/j.1365-2389.2004.00699.x.
Saada, A., Breeze, D., Crouzet, C., Cornu, S., Baranger, P., 2003. Adsorption of arsenic (V) on kaolinite and on kaolinite–humic acid complexes. Chemosphere 51, 757–763. http://dx.doi.org/10.1016/S0045-6535(03)00219-4.
Santini, J.M., Sly, L.I., Schnagl, R.D., Macy, J.M., 2000. A new chemolithoautotrophic arsenite-oxidizing bacterium isolated from a gold mine: phylogenetic, physiological, and preliminary biochemical studies. Appl. Environ. Microbiol. 66, 92–97. http://dx.doi.org/10.1128/AEM.66.1.92-97.2000.
Shigemoto, N., Hayashi, H., Miyaura, K., 1993. Selective formation of Na-X zeolite from coal fly ash by fusion with sodium hydroxide prior to hydrothermal reaction. J. Mater. Sci. 28, 4781–4786. http://dx.doi.org/10.1007/BF00414272.
Sidenko, N., Gieré, R., Bortnikova, S., Cottard, F., Pal'chik, N., 2001. Mobility of heavy metals in self-burning waste heaps of the zinc smelting plant in Belovo (Kemerovo Region, Russia). J. Geochem. Explor. 74, 109–125. http://dx.doi.org/10.1016/S0375-6742(01)00178-9.
Smedley, P., Kinniburgh, D., 2002. A review of the source, behaviour and distribution of arsenic in natural waters. Appl. Geochem. 17, 517–568. http://dx.doi.org/10.1016/S0883-2927(02)00018-5.
Stolz, J., Basu, P., Oremland, R., 2002. Microbial transformation of elements: the case of arsenic and selenium. Int. Microbiol. 5, 201–207. http://dx.doi.org/10.1007/s10123-002-0091-y.
WHO, 1993. Guidelines for drinking water quality. World Health Organization, Geneva, p. 41.

Annexe 2

Detection and quantification of As(III)-oxidizing microbes in soils highly polluted by breaking-down of old chemical ammunition during inter-war

H. Thouin, L. Le Forestier, P. Gautret
Université d'Orléans, CNRS, BRGM, ISTO, UMR 7327, Orléans, France

S. Dupraz, D. Hube, F. Battaglia-Brunet
BRGM, ISTO, UMR 7327, 45060 Orléans, France

SUMMARY: The open-burning of organo-arsenical compounds present in chemical ammunitions from the First World War was responsible for locally high concentrations of arsenic in top-soil of a highly polluted site from the region of Verdun (France). In order to understand the biogeochemistry of arsenic in this type of environment, quantitative and qualitative characteristics of microbial communities were determined in soil samples with differing As pollution levels. The total concentration of micro-organisms was negatively affected by the pollution level. However the proportion of heterotrophic As(III)-oxidizing organisms and the As(III)-oxidizing rate were higher in the most contaminated than in the less contaminated samples. These results suggest that pollutants, including arsenic, exerted a selective pressure on composition and/or activity of microbial communities.

1 INTRODUCTION

After the Great War, the French military authority was challenged with disposal of large amounts of German chemical ammunitions that had not been fired or when fired, had not detonated. Open burning is one way to break these projectiles down. The burning of Blue Cross shells loaded with solid vomiting and emetic warfare agents, diphenylchloroarsine and diphenylcyanoarsine, resulted in locally intense soil contamination by arsenic and heavy metals. Biogeochemical behavior of arsenic is poorly documented in this type of environment. In the framework of the extended characterization of a highly polluted soil from the region of Verdun (France), characteristics of the microbial communities of samples presenting variable As concentration were examined.

2 METHODS

2.1 *Sampling and analyses*

The study site known as "Place-à-gaz" is located in the Spincourt forest 20 km northeast of Verdun. Between 1926 and 1928, more than 200,000 German chemical shells (especially Blue Cross shells) were open-burned in tranches and rows in the center of this area [1] following a method developed by M. Kostevitch, operating for the British company Pickett & Fils. The severe contamination of this area is visible because of the lack of vegetation. Total concentrations of As, Pb, Cu and Zn were determined in situ using a X-ray fluorescence field portable apparatus, NITON©. Four soils presenting a gradient of contamination were sampled from the surface, non-saturated black layer (0-10 cm). After size separation at 70 µm, the raw soils were analyzed by ICP-OES for major elements and ICP-MS for trace elements.

2.2 *Microbiological analyses*

Total bacteria were extracted from soils using a Nycodenz gradient separation method. Total microbes were enumerated after fluorescent DAPI staining. Arsenic(III)-oxidizing oligotrophic organisms were enumerated by the Most Probable Number method (MPN). The soil (as wet soil, equivalent to 0.2 g dry soil) was placed in a sterile glass erlenmeyer flask with 10 mL of sterile physiologic water, agitated for 30 min at 25°C, then sonicated 2 x 20 s at 45 kHz. The soil suspension was serially diluted in sterile physiologic water. Mineral medium containing 100 mg/L As(III) was distributed in Microtest TM Tissue culture plates (96 wells), 250 µL by well. Each well was inoculated with 25 µL of soil suspension dilution. Five wells were inoculated with each dilution. Culture plates were incubated at 25°C for 10 days. The presence of As(III) in the wells was revealed by the formation of the insoluble white complex AsIII-PyrrolidineDithioCarbamate (PDC). The same method but with 1 g/L yeast extract was applied to determine the MPN of copiotrophic As(III)-oxidizing microbes. The MPN of copiotrophic microbes able to grow in the presence of 100 mg/L As(III) was revealed by the development of turbidity in the wells. As(III)-oxidizing activities were determined as detailed in [2].

3 RESULTS AND DISCUSSION

3.1 *Concentrations in heavy metals and As*

The level of As, Cu and Pb pollution decreased from soil 1 to soil 4 (Table 1). Soils 1 and 2 were characterized by particularly high concentrations in As and Zn (more than 3%). Copper concentration was also close to 1% in soil 1.

Table 1. ICP-MS analyses of the four samples of polluted soils.

Soils	As (%)	Pb (%)	Cu (%)	Zn (%)
1	7.28	0.38	0.91	9.02
2	3.08	0.58	0.52	3.73
3	0.63	0.25	0.16	1.07
4	0.19	0.098	0.15	1.33

3.2 *Microbial concentrations*

The total microbes concentration was significantly lower in the most polluted soils 1 and 2 (10X less) than in the less polluted soils 3 and 4 (Fig. 1).

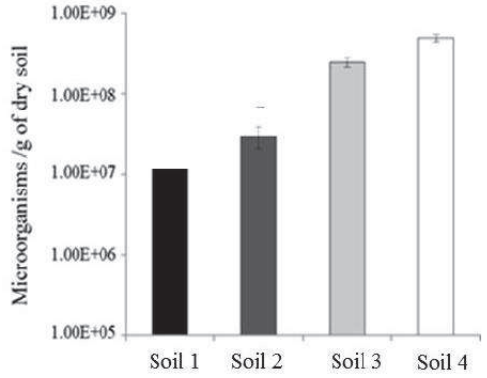

Figure 1: Concentrations of total microorganisms in the four soil samples

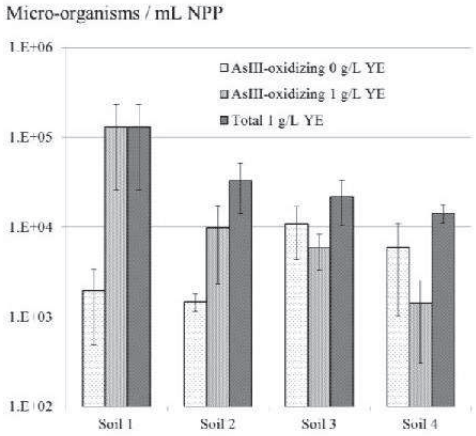

Figure 2: Concentrations of living microorganisms in the four soil samples.

The concentration of oligotrophic As(III)-oxidizing microbes (growing in mineral medium without yeast extract) was lower in the most polluted soils 1 and 2 than in the less polluted soils 3 and 4 (Fig. 2). This result may be linked to a protective effect of yeast extract against toxicity of pollutants. Conversely, the concentration of microbes oxidizing arsenic in presence of 1 g/L yeast extract was the highest in the most polluted soil 1. Remarkably, the same tendency was observed with total microbes concentration growing in presence of both As(III) at 100 mg/L and yeast extract at 1 g/L. Moreover, in the most polluted soil 1, As(III) oxidation was observed in all wells where microbial growth was detected: the concentration in copiotrophic As(III)-oxidizing microbes was equivalent to that of total microbes growing in presence of both As(III) and yeast extract.

3.3 *As(III) oxidizing activities*

The rates of microbial As(III) oxidation were in the range 0.5 to 2 mg/L/h. The highest rates, close to 2 mg/L/h, was obtained with the most polluted soil 1, whereas the lowest rate, close to 0.5 mg/L/h, was observed with the lowest polluted soil 4.

4 CONCLUSIONS

The presence of As and heavy metals in high concentrations seems to exert a strong selective pressure on the microbial communities of soils polluted by the destruction of chemical weapons from the First World War. The high level of As and metals concentration negatively affected the total microbial concentration, but induced an increase of copiotrophic As(III)-oxidizing microbes concentration. The proportion of As(III)-oxidizing bacteria in the global community and the As(III)-oxidizing activities were clearly positively influenced by the pollution level. These results support the hypothesis of the adaptation of the microbial community, with increased proportions and efficiency of organisms involved in the cycle of arsenic, in highly polluted soils.

ACKNOWLEDGEMENTS

This work was supported by the Région Centre Val de Loire (convention 00087485) and the Labex Voltaire (ANR-10-LABX-100-01).

REFERENCES

Bausinger, T., Bonnaire, E., Preuß, J. 2007. Exposure assessment of a burning ground for chemical ammunition on the Great War battlefields of Verdun. *Sci. Total Environ.* 382: 259–271.

Lescure, T., Moreau, J., Charles, C., Ben Ali Saanda, T., Thouin, H., Pillas, N., Bauda, P., Lamy, I., Battaglia-Brunet, F. 2015. Influence of organic matters on As(III) oxidation by the microflora of polluted soils. *Environ. Geochem. Hlth.* (doi: 10.1007/s10653-015-9771-3).

Hugues THOUIN

Transfert de polluants inorganiques dans un technosol de brûlage d'armes organo-arséniées soumis à un apport de matière organique et à des cycles de saturation/désaturation : Expérimentation en mésocosme.

La destruction par brûlage de munitions chimiques de la Première Guerre Mondiale a provoqué une contamination importante de la partie supérieure du sol du site de la Place-à-Gaz par l'arsenic, le zinc, le cuivre et le plomb. Le traitement thermique a eu pour effet de minéraliser l'As des agents de guerre organoarséniés, et de former un assemblage minéral inattendu composé d'arséniates de Zn, Cu et Fe, et d'une phase amorphe riche en Fe, As, Zn, Cu et Pb. Ce matériel amorphe est la principale phase porteuse de l'As et des métaux dans la zone la plus polluée. Le site est sujet à des changements environnementaux pouvant affecter la stabilité des contaminants inorganiques. Afin d'évaluer l'impact d'épisodes de saturation en eau et de l'apport de matière organique sur les cycles biogéochimiques des métaux et de l'As, une étude en mésocosme a été menée. Les résultats montrent que la phase amorphe est instable en conditions saturées, et libère des contaminants dans l'eau interstitielle du sol. Comme sur le site, les contaminants les plus mobiles sont le Zn et l'As. L'addition de matière organique a induit une immobilisation de l'As, par piégeage de l'As V sur les oxyhydroxydes de fer, dans la partie saturée du sol. La caractérisation du compartiment microbien a été effectuée *via* des dénombrements, une analyse de la diversité bactérienne et des tests d'activités d'oxydation de l'As III et de respiration et. Les résultats montrent que les microorganismes ont contribué activement au métabolisme du C et de l'As. L'apport de matière organique a promu la croissance des microorganismes As III-oxydants et As V-réducteurs et modifié la structure des communautés bactériennes. Cependant, un effet négatif de la matière organique sur la vitesse d'oxydation de l'As III a été observé, entrainant une augmentation des concentrations d'As III en solution. Cette étude en mésocosme a montré que le dépôt naturel de litière organique a des conséquences antagonistes sur le transfert des contaminants inorganiques. Ces résultats fournissent de plus amples informations sur l'impact environnemental de la Grande Guerre et, de façon plus générale, sur les processus biogéochimiques contrôlant le comportement des métaux/métalloïdes sur les sites pollués.

Mots clés : destruction de munitions chimiques, sol, arsenic, métaux, matière organique, cycles sec/humide, transformation microbienne de l'As, mésocosme

Transfer of inorganic pollutants in a burning ground for organo-arsenical ammunition submitted to an input of organic matter and to saturation/desaturation cycles: A mesocosm study.

The thermal destruction of chemical munitions from World War I, on the site of "Place-à-Gaz", induced intense local top soil contamination by arsenic and heavy metals. The heat treatment mineralized As from organoarsenic warfare agents, resulting in a singular mineral assemblage, composed of Zn, Cu and Fe arsenates and of an amorphous phase rich in Fe, As, Zn, Cu and Pb. The amorphous material was the principal carrier of As and metals in the central part of the site. The site undergoes environmental changes which may alter the stability of inorganic contaminants. To assess the impact of water saturation episodes and input of bioavailable organic matter on the biogeochemical cycles of metal(loid)s, a mesocosm study was conducted. Results showed that amorphous phase was instable in saturated conditions, and released contaminants in soil water. As previously observed on site, the most mobile contaminants were Zn and As. The addition of organic matter induced the immobilization of As by trapping of As V onto hydrous ferric oxides in the saturated soil. Microbial characterizations including counting, bacterial community structure, respiration, and determination of As III-oxidizing activities were performed. Results showed that microorganisms actively contribute to the metabolisms of C and As.The addition of organic matter induced the increase of As III-oxidizing and As V-reducing microorganisms concentrations and modified the bacterial diversity. However, a negative effect of organic matter on the activity of As III oxidation was observed resulting in higher As III concentration in soil water. This study showed that the natural deposition of forest organic litter on the site, induced antagonist effects on the transfer of inorganic pollutants did not immobilize all the Zn and As and even contributed to As III transport to the surrounding environment. These results provide more information about the environmental impact of the Great War and more generally about the processes driving the behavior of metals/metalloids on polluted sites.

Keywords: chemical ammunition destruction, soil, arsenic, heavy metals, organic matter, dry/wet cycles, microbial As transformation, mesocosm monitoring

Institut des Science de la Terre d'Orléans

CNRS/INSU, ISTO, UMR 7327, 45071 Orléans, France